Parameters Interpretability in Phenomenological-Based Semiphysical Models. A Human Glucose Homeostasis Model

Laura Lema Pérez
Bioengineer, M.Sc.

Universidad Nacional de Colombia
Facultad de Minas
Departamento de Procesos y Energía
Medellín
2018

Parameters Interpretability in Phenomenological-Based Semiphysical Models. A Human Glucose Homeostasis Model

Laura Lema Pérez
Bioengineer, M.Sc.

Dissertation presented for the degree of
Doctor en Ingeniería

Advisor
Hernán Alvarez, Ph.D. Ingeniero Químico, M.Sc., Doctor en Ingeniería

Coadvisor
José F. García - Tirado, Ph.D. Ingeniero de Control, M.Sc., Doctor en Ingeniería

Adviser
Carlos Esteban Builes Montaño, M.D. Médico Internista, Endocrinólogo

Research group
Grupo de Investigación en Procesos Dinámicos, KALMAN

Universidad Nacional de Colombia
Facultad de Minas
Departamento de Procesos y Energía
Medellín
2018

Title in English

Parameters Interpretability in Phenomenological-Based Semi-physical Models. A Human Glucose Homeostasis Model

Abstract: In this thesis, the structure of a phenomenological-based semi-physical model (PBSM) of the glucose homeostasis in the human body was deduced such that its descriptive ability can be compared with the existent physiological models or maximal-like models. The PBSM of the glucose homeostasis has gathered the available physiological insight about such homeostasis by means of a systematic application of mass, energy, and momentum balances over the process systems of interest. To get a whole mathematical model of the glucose homeostasis, a model of each organ involved in such mechanism was developed like a sub-model. Once the main model structure was achieved, the specific transference mechanisms were determined according to the human physiology, providing what is known as constitutive and assessment equations, allowing to write the mathematical model in terms of the main variables in the homeostasis. Finally, a degree of freedom analysis over each mathematical model provided the information about which parameters of the model need to be identified by means of data-based or statistical procedures reported in the available literature. The sub-models give information about the clinical experimentation needed to make the mathematical model usable for real-life applications. Such a complex model deduction is seized to construct a conceptual framework about parameters interpretability to allow a particular model definition in terms of parameters with physical or physiological meaning. In this regard, a conceptual framework from a qualitative point of view was proposed to analyze and endow interpretability the parameters of the model. The concepts proposed were based on the identifiability concept reported in the literature.

Keywords: Interpretability, phenomenological-based semi-physical models, modeling, glucose homeostasis

Dedicatory

A mi papá por permanecer en mi.
A mi mamá por ser mi mayor motivación.

Acknowledgements

Creo que Dios ha sido el mayor guía de mi vida y quien permitió que esta tesis fuera posible, por eso a Dios gracias. Gracias a Jose, por su confianza y por haber pensado en mi cuando tenía este proyecto en sus planes, gracias por convencer a Hernán para que me dirigiera, pues no pude haber caído en mejores manos. Gracias Hernán por tanta humanidad y profesionalismo, gracias por trabajar con el corazón, y gracias infinitas por aceptarme sin conocerme. Eres una persona admirable y un gran ejemplo para mi, gracias por enseñarme tanto. Gracias a Carlos, por ser un médico de mente abierta y haber aceptado el reto de acompañarnos en este camino de combinar la medicina con la ingeniería. Además, le agradezco los ánimos que tiene para que esto no muera aquí sino que se proyecte y llegue mas lejos. A los estudiantes de ingenieria química que se atrevieron a lanzarse a este mundo de la ingeniería aplicada al cuerpo humano. Gracias a mis ahora colegas en ingenieria biomédica: Jessica, Estefania, y mi Angela, quien además de ser colega ha sido mi compañera de vida. A todos ellos gracias por el esfuerzo, la constancia y por permitirme aprender al lado de ustedes. Gracias a los participantes del grupo de investigación Kalman, estudiantes y profesores, por moldear en cada reunión este trabajo. Gracias a los compañeros de postgrado con los que compartí ánimos y desánimos, ustedes también fueron parte importante de este proceso doctoral. A Rafael, por aceptar recibirme en su grupo de investigación en Francia y guiar mi trabajo durante la pasantía. A Colciencias por su absoluto apoyo económico.

A pesar de la impotencia que siento por tu ausencia, mi corazón siempre guarda una gratitud infinita contigo papá, pues tu fuiste quien me proyectó, creíste siempre en lo que llegaría a ser, porque esto no se trata de lograr metas materiales ni de hacer, sino de ser. Yo soy tu creación, soy lo que imaginaste que sería, y espero seguir siendo lo que querías que fuera. Confiaste en mi, entonces espero seguir caminando la vida pensando en que la decisión que tome y lo que yo sea te hagan sentir satisfecho allá donde existes. Gracias por ponerme en esta ruta, gracias por convencerme de que el conocimiento es la mejor herramienta para defenderse en este mundo, gracias por estar en mi y conmigo. Continuando con este relato, debo confesar que también siento impotencia con la vida por dejar a mi mamá con diabetes. Sin embargo, ella se convirtió en la motivación mas grande para decirle sí a esta oportunidad. Por ella quisiera que esto no muriera aquí y seguir soñando que todo lo que se trabaja con esfuerzo es posible. Gracias de nuevo a Angela, porque a pesar de que no soy tan mayor para ser su ejemplo, me motiva a automoldearme y autoevaluarme, porque es la única persona en la que puedo ver el reflejo de la eduación que recibí de mis padres, porque ha sido mi compañera de vida y la persona con la que siempre he soñado llegar lejos. A mis raices: mi abuela y mis tios maternos, porque sin ellos seguramente el trayecto de mi vida habría sido mucho mas difícil, porque cada dia

me enseñan con su simple existencia que la familia es de lo mas valioso que se tiene. A Cata por su amistad incondicional, por hacerme creer que la confianza en otros es posible, por transmitirme tanta sabiduría para vivir y por animarme cada que sentía que esto no valía la pena. A Fede, gracias por no sólo poner mariposas en mi estómago, sino por llenar de paz mi corazón.

Contents

List of Tables

List of Figures

1

Introduction

Diabetes mellitus is a group of metabolic diseases characterized by blood glucose levels unregulated resulting from defects in insulin secretion, insulin action, or both. Traditional linear control theory and mathematical models of glucose-insulin dynamics are currently used to regulate blood glucose levels. However, blood glucose control using these methods is limited due to the complexity of the biological system. In addition, the existent mathematical models to describe glucose dynamic or to build control systems are not based on the phenomena and lack parameters interpretability. Interpretability is still a fuzzy concept in the literature. Few authors have tried to use the concept mainly referring to models instead of parameters. Additionally, this concept has been used in empirical models but has not been explored in phenomenological-based semi-physical models. This topic has not a definition in pure phenomenological models (first principles models) because in these white box models each parameter has origin in theories, laws, or principles. Therefore, the parameters of a phenomenological model are all interpretable. Instead, for empirical models the parameters interpretability is a hot research topic since the simultaneous identification of parameters from data obscures the parameter meaning. In this sense, phenomenological-based semi-physical models preserve the structure from first-principles models but somehow the parameters interpretability can be lost due to an excess on the use of statistical-based fitting strategies for parameter representation.

In the case of glucose homeostasis, there exist evidence indicating a lack of parametric interpretability in the existing models implying the application of cumbersome parameter identification strategies for each patient, which in practice is not desirable. In addition, needed clinic studies may not be easily deduced from model parameters to be identified for a given patient due to the absence of interpretability of those parameters in the models available nowadays.

From the review of state of the art presented in this thesis, it is clear that both black box models and models from mass balances containing semi-mechanistic aspects have been developed to describe the main features of the glucose homeostasis. However, to the best of the author's knowledge, there are no evidences of physiologically based models of glucose homeostasis by exploiting the natural interconnection among organs through a plantwide view. In other words, it is not evident the use of mass balances for interesting components at each organ maintaining their interconnection by blood flows and considering processes performed by organs as task of the body as a whole. Moreover, the reviewed models have a limited number or no parameters with interpretability due possibly to strong assumptions on the proposed model structure during its construction.

With respect to diabetes, it is known that is a widespread disease affecting many people around the world. Regarding only to the conventional treatment to type 1 diabetes mellitus (T1DM), it involves regular injections of genetically engineered insulin. Some patients with T1DM measure their blood glucose concentration by using a personal external meter and then they calculate the dose of insulin to be injected. This required insulin dosage does not only depend on the measured blood glucose levels, but also on the amount of carbohydrates to be ingested and on the time elapsed since the last insulin injection. A more recent treatment involves continuous glucose measurements (CGM) in the interstitial tissue and a continuous dosage of insulin from an insulin pump. Although the life quality of patients is significantly improved by using both the CGM and the insulin pump, still patients and clinicians should manage the pump in order to dose the correct amount of insulin based on a stated schedule. In this context, a significant effort for the construction of a closed-loop glucose controller, known elsewhere as artificial pancreas, is being done by some research groups around the world. However, since most of the control developments are being performed upon a model based control strategy, a reliable process model is needed to guarantee the desired closed-loop performance. The model developed in this thesis is a reliable process model due to its parameter interpretability property, provided that individualization of the model in a specific patient be done before designing a control strategy.

Using the above ideas, the research problem to be addressed in this thesis is: "There is no a phenomenological-based semiphysical model (PSBM) describing the glucose homeostasis in the human being obtained by exploring the natural interaction among the organs and substances involved in such a homeostasis, and also, guaranteeing the interpretability of the model parameters with respect to the human physiology and looking for an adjustable model to a individual parametric identification."

In this thesis, a conceptual framework of parameters interpretability was addressed from a qualitative point of view. The construction of the formalism of interepretability was built upon the identifiability concept. Identifiability property is also tackled, but from a quantitative point of view, in an inspiring way to build concepts of parameters interpretability. However, the identifiability property is not within the objective of this thesis. It is expected that in the future, interpretability property could be addressed not only from a qualitative point of view but also from a quantitative point of view. In addition, a deducted PSBM of glucose homeostasis is used here to demonstrate the usefulness of the theoretical construction around interpretability.

The human body and the blood glucose system exhibit a high degree of structural and behavioral complexity. The construction of a PBSM for the glucose homeostasis in the human body could be used to obtain a better understanding of parts of the system and, in a long term it may help to generate new physiological theories that can be applied in adjacent physiological systems. Moreover, a complete mathematical model of the glucose homeostasis mechanism in humans will allow having virtual patients available to perform *in silico* clinical tests, since *in vivo* clinical tests are both time consuming and expensive. In general, *in silico* experiments are less expensive, easier to perform and are not limited by ethical constraints. The model constructed in this thesis is based on conservation principles. Moreover, the knowledge about the nature of the phenomena reflects a correct qualitative and quantitative behavior of the glucose in the bloodstream and this could avoid confusion, misunderstandings, and wasted efforts. Likewise, the use of a phenomenological-based mathematical model to describe the blood glucose concentration in the human body can be a useful tool to carry out clinical tests in a specific patient

and to do a parametric identification in an easier way. Thus, an on-line parametric identification is expected to be easier to do in a phenomenological-based semiphysical model (PBSM) with guaranteed parameter interpretability.

This doctoral thesis is organized as follows: Chapter 2 presents concepts about process modeling, with a special attention to phenomenological-based semi-physical models and its application to physiological processes. Chapter 3 gives a general background about glucose homeostasis in humans, including a description of the role of the main organs involved in this natural mechanism. Mathematical models of main organs involved in glucose homeostasis are reported in Chapter 4, in which a process analysis using plantwide view is carried out. In Chapter 5, the core of this thesis is presented, i.e., a conceptual framework of parameters interpretability is proposed along with its application to the case study. Finally, conclusions and future work are given in Chapter 6.

2

Process Modeling

This chapter presents the basic concepts commonly used in the literature about process modeling, including modeling of physiological processes in the human body. Also, some new concepts about how a mathematical model is composed are introduced. There is a specific section devoted to discuss about Phenomenological-Based Semi-physical Modeling (PBSM) due to the importance to develop the main theoretical construction of this dissertation. Finally, an approach to represent physiological systems from PBSM is included.

2.1 Model definition

A model is a representation of the reality [107]. That representation can be graphic, verbal, conceptual, physical, mathematical or a combination of them. Mathematics is the universal language used in engineering to represent the world and for that reason mathematical models are the most used representation to perform design, control, validations, and development of new products [99]. Mathematical models make easier the prediction of the reality, present the knowledge in a usable form, and make possible to do tests without risking the production process or a person's life [81]. On the other hand, process modeling is the action and effect of approaching to a model, which is a theoretical scheme that simplifies a real object or complex reality with the aim of improving its understanding of making predictions about how that real object will behave [104]. The process term is used here to qualify the modeling task emphasizing on a process as the main real object characteristic [223]. The similitude between the concepts of process and system is used to convert the interesting part of the real object into a system in accordance to its role into the real object as a whole [28]. Using a systemic view, the study object can be modeled easier than the complete real object. Thanks to models the real object can be better explained, controlled, simulated, predicted, and even improved [16; 88].

The development of reliable and comprehensive models is the main objective in process modeling [46]. In few words, a model is an imitation of reality and a mathematical model is a particular form of representation. During model building, the real object is translated into an equivalent mathematical object in order to gain insight into the original real world situation [107]. Due to the enormous complexity of any real object it is even partitioned in order to facilitate its study. In this sense, a model focuses on a part of that complex real object called study object. The final aim when a real object is modeled is to group several particular models each one focused over one study object looking for an integrated view of the real object, when these particular models are solved as a whole [41].

A model can be used to perform experiments which are expensive or considered difficult or dangerous. Therefore, a model should be as similar as possible to the real object in terms of its important properties for the model intended use. In other words, the mathematical model should describe or reflect the real object properties relevant to the modeling goal [107]. On the other hand, models are never identical to the real object. They should be substantially less complex and hence much cheaper and easier to handle in mathematical format so that the analysis can be carried out in a convenient way. The reduced complexity of the model relative to the real object is usually achieved by its partition in study objects. Additionally, the use of modeling assumptions to describe the specific knowledge currently available about the real object and each one of the study objects parts taken by subjective partition.

2.2 Model families

Models can be classified in many ways [162; 223], for instance with respect to the cause-effect analysis, the variables dependency of the spatial position, the application of the superposition principle, the derivation from phenomena or data, etc. Each way leads to a variety of model characteristics which have an impact on the model solution techniques as well as on the potential application areas of the model. According to the source of information of the models, these are classified in three big model families: black box models, white box models, and grey box models [107].

2.2.1 Black box models

Black box models are also referred to as empirical models or correlation models. These models are the result of adjusting pre-existing mathematical structures to experiments and observations from the real object. Empirical models do not rely on the knowledge of the basic principles and mechanisms which are present in the study object being modeled. In other words, the black box modeling is performed entirely from data without the use of a priori knowledge and considering a no preset mathematical structure. They employ essentially equation fitting where the parameters have little or no physical meaning [155; 158]. It follows that the use of these models is basically predictive only. Using these models, it is only possible to determine how the system would respond to stimuli or changes occurring within the range indicated by the experimental observations used to tune the model. Empirical models are efficiently used where the actual underlying phenomena are not known or understood. The name of black box models reflects the fact that little or none is known about the internal real mechanism of the processes taken place in the study object. In these models all parameters, structural and functional, must be identified from available data. Therefore parameters interpretability in a black box model is not immediate nor easily obtained.

2.2.2 White box models

White box models, also termed as mechanistic models or pure phenomenological models, have their basic derivation from phenomena taking place in the real object and use information regarding the structure and function of the metabolic system, the basic chemical and physical laws applicable, and quantitative data about dimensions, material properties,

process rates, and the like. In the literature, first-principles models or physical models are also widely used to refer to the same type of models. White box models are derived from a knowledge of the underlying mechanism of the process by using a suitable mathematical scheme to represent it [33]. A mechanistic model holds its phenomenological characteristic as long as it does not include any empirical relationship. White box models explain the relations between the several features of the system structure and process behavior in terms of theories, laws, and principles established for the phenomena taken place in the process. In a white box model, all mathematical parts have meaning from the phenomena producing the processes occurring in the real object. Due to this restrictive condition, the number of phenomenological models currently available is extremely low. In these kind of models, all parameters, structural and functional, must be formulated from theories, laws and principles of phenomena taking place into the process. This fact gives to white box parameters, either structural or functional, to be inherently interpretable.

2.2.3 Gray box models

In process engineering practice, the most common type of model combines mechanistic and empirical parts and is commonly termed as gray box models or semi-physical models. In this approach, certain processes from the real object present at study object are modeled considering prior knowledge [148]. The unknown or less understood phenomena are modeled with black box procedures using data driven model identification. This involves the definition of kinetic and transport mechanisms, the estimation of key kinetic and transport parameters and the validation of the model against with respect to performance specifications. With this approach, a better balance between reliability and comprehensibility is attained.

Semi-physical models give the possibility of using either a first-principles structure or a empirical structure. The origin of gray box model structure establishes a crucial difference between the following two subfamilies: *i*) phenomenological-based semi-physical models and *ii*) empirical based semi-physical models. Both inherit their main characteristics from its structure generator model. In this sense, any empirical structure restricts the prediction ability of the model to the data from which the model structure was fitted. In other words, empirical structures have, in most cases, problems with generalization of the modeled phenomena. Therefore, empirical based semi-physical models are not frequently found in process engineering practice. The other family is most used due to its versatility and generality inherited from the phenomenological-base structure.

2.3 Phenomenological-Based Semi-physical Models - PBSM

2.3.1 What is a PBSM?

This subfamily, included in the gray box family, results to be the most useful among all possible models when the process of interest has at least one underlying known phenomenon. As its name indicates, a Phenomenological-Based Semi-physical Model (PBSM) is not a white-box model. It shares, however, the basic model structure from the mechanistic approach, which gives to PBSMs the ability to generalize and to be constructed in incremental mode. In this type of models, the structure is divided into a basic and an extended structure [147]. The parameters of the basic structure, from now structural

parameters, are formulated from theories, laws, and principles of the phenomena taking place in the process, but at least one of the parameters of the extended structure, from now functional parameters, is identified using available data from the real process operation or represented by an empirical submodel. In this sense, structural parameters have direct interpretability from their phenomenological origin but functional parameters interpretability is not necessarily guaranteed. The uncommon terms previously mentioned are discussed in detail later.

The origin of the PBSM name is as follows. It is said that a model is phenomenologically based when its structure is developed in similar way that it is done for a phenomenological model, by applying conservation principles over mass, energy, and momentum balances basically, but with the option of using other balances. It can also be said that a model is semi-physical when empirical formulations for one or more parameters are used as a part of the model. In this sense, the mixture of those concepts produces the full name Phenomenological-Based Semi-physical Model. This family of models, specifically using lumped parameters, have been commonly used in process analysis, design, and control [10]. In this sense, and looking for clarifying the model presentation, a ten steps procedure to obtain a PBSM was presented in [9], which supposed that the modeled problem can be formulated with the following algorithmic problem statement [107]:

Given:

- A process system
- A modeling goal
- A validation criteria

Find:

- A mathematical model

Subject to:

- Fulfilling the modeling goals and a validation criteria for the model.

One of the key elements during the model construction is to establish an appropriate modeling hypothesis. When a PBSM is being constructed, some description about the phenomena taking place must be formulated. Then, model assumptions are stated. In addition, there are a group of considerations useful to fix the values of some parameters of the process given some a priori information. The above elements constitute the modeling hypothesis. Such a hypothesis is based on one or more abstraction of the current phenomena into pre-stated phenomena, easily linked to but simpler than current process phenomena [216]. This abstraction suggests to create a mental image conformed by enough pre-stated phenomena in order to cover interesting characteristics of the process and to write a description of real process behavior using that abstraction. In this way, the final representation seems like the real process and give the opportunity of simulating real behaviors using supposed pre-stated behaviors [184]. However, the interpretability of the model is affected if the abstractions are not related to the current phenomena, as it will be discussed in Chapter 5.

A PBSM can be developed as a hierarchical grouping of submodels in aggregative mode. In other words, any PBSM can be formulated as a multiscale model being the first level of that scale the phenomenological-based model structure obtained from the application of the conservation principles. The second level of the scale is dedicated to formulate a submodel for each parameter of the first level of model equations. A third level is dedicated to formulate submodels for secondary parameters used into the second level formulation. Successive levels, each one more deep, can be stated in a PBSM. Those mentioned levels are related to the specification level no necessarily linked to detail (size) level. Several levels of detail exist in a PBSM but only the level at which the Process Systems (PSs) were determined gives the level of detail of the model as a whole. Therefore, it can be defined that the level of detail of the model is that stated for the PSs partition.

2.3.2 Parts of a PBSM

Any mathematical model is composed of mathematical structure, linear operators, and terms. The mathematical structure reflects the way the terms are related among them. Linear operators (taken in the most simple sense of linear characteristics as $+, -, =, <$, or $>$), connect the terms in one way or another. A term, in turn, is composed of variables, constants, parameters, and nonlinear operators (i.e., product, division, exponents, logarithm, etc.). A variable is a numerical value only determined after the model solution. Some authors call them internal variables or state variables, some of them being possibly measured by sensors. A constant is a numerical value that is universally accepted or its value is fixed by the modeler in the context of the model. Finally, a parameter is a symbol used for fine tuning the model to reach the desired description of the observations. As such, it may take many or infinite feasible values [1] that changes whether to prove its influence (called by some authors input variable) or should be calculated by using a parametric identification technique from data. Figure 2.1 shows how a mathematical model is made up. Details on the classification of the parameters in structural and functional, and the levels of interpretability of the functional parameters are given at the end of this section.

As mentioned before, the structure of a PBSM is composed of a basic and an extended structure. An example of how a model may evolve as the basic structure is extended is given in Figure 2.2. In this type of models, the basic structure comes out from applying balances (conservation law) over the real object. In turn, the extended structure appears once constitutive and assessment equations are used to replace or calculate structural parameters. In addition, the extended structure deals directly with two additional levels: level of detail and level of specification. The level of detail is related to the size at which a partition of the real object is done to determine a functional parameter. Thus, additional levels of detail can be stated referring to the used scale, i.e., macroscopic, mesoscopic, microscopic, colloidal, macro-molecular, molecular-atomistic [117]. However, a deeper level of detail appears as long as a parameter needs a further description. This fact implies that any model has at least two levels of detail mentioned in the general description, the level of detail related to the model structure (due to the partitions), and a lower level of detail used probably in at least one model parameters. When a functional parameter is identified through a constitutive or assessment equation located in a scale of size smaller

[1] For PBSM is better to use the symbol instead a numerical value because the symbol keeps the interpretability unlike the number, which has not interpretability by itself. This will be discussed later in Chapter 5.

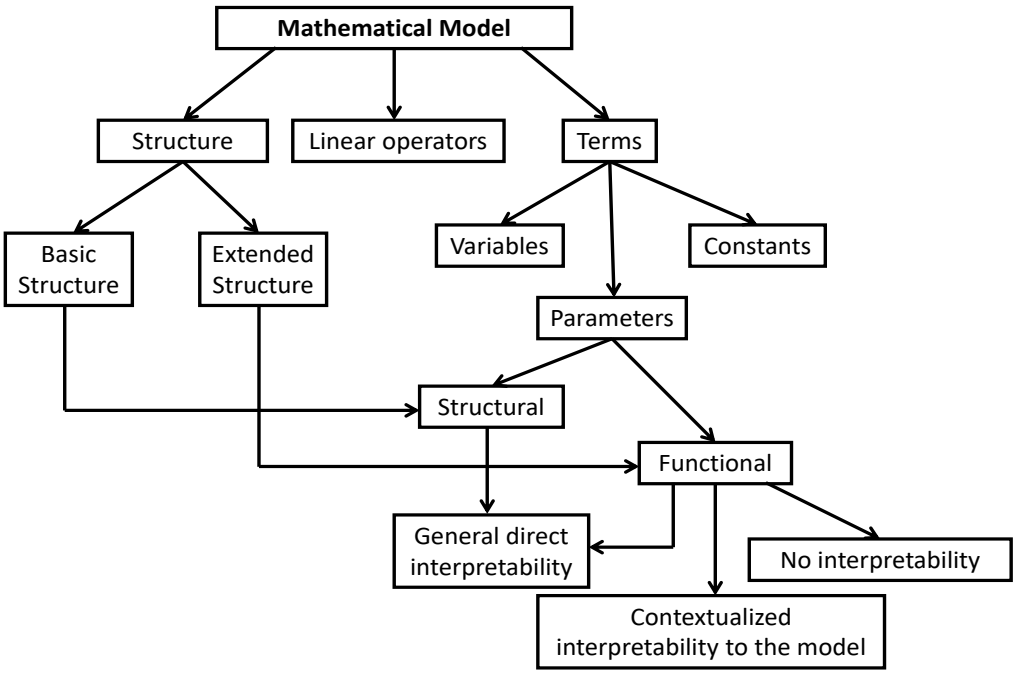

FIGURE 2.1. Scheme representing the parts of a mathematical model.

than detail level of the model, likewise a new level in the model, called specification level, is opened. A formal definition of these two concepts are presented as follow.

Definition 2.1. ***Level of detail.*** *The position of the current partition in a scale of sizes of fragments or parts of something. That scale begins at gross detail, which indicates the real object as a whole (only separated from the rest of the world), and finishes at the possible minimum physical size. The level of detail is determined by a set of assumptions and decisions that are aimed at meeting the model goal. This set supports the development of a PBSM.*

Definition 2.2. ***Level of specification.*** *Is the position of the current demarcation of an object or any of its parts in a scale of information contents of mathematical determinations. That scale begins at minimal information contents, consist on a number without unit of measure, and finishes at the explainable information consisting on a Law or Theory.*

Definition 2.3. ***Scale.*** *Size of each partition. The real object is analyzed to different scales looking to obtain additional information increasing the knowledge about the object.*

Constitutive and assessment equations of the extended structure are modeler dependent because each equation can be stated at different level of detail in accordance with the specific modeler preferences or knowledge.

Model construction requires a balance between simplicity (i.e., coarse-grained) and elaboration (i.e., fine-detailed) [109]. A model should be as coarse-grained as possible, but as fine-detailed as necessary [152]. The level of detail of a model should be determined by its use [155], looking for the level that best fits the purpose of the model [149]. Regarding

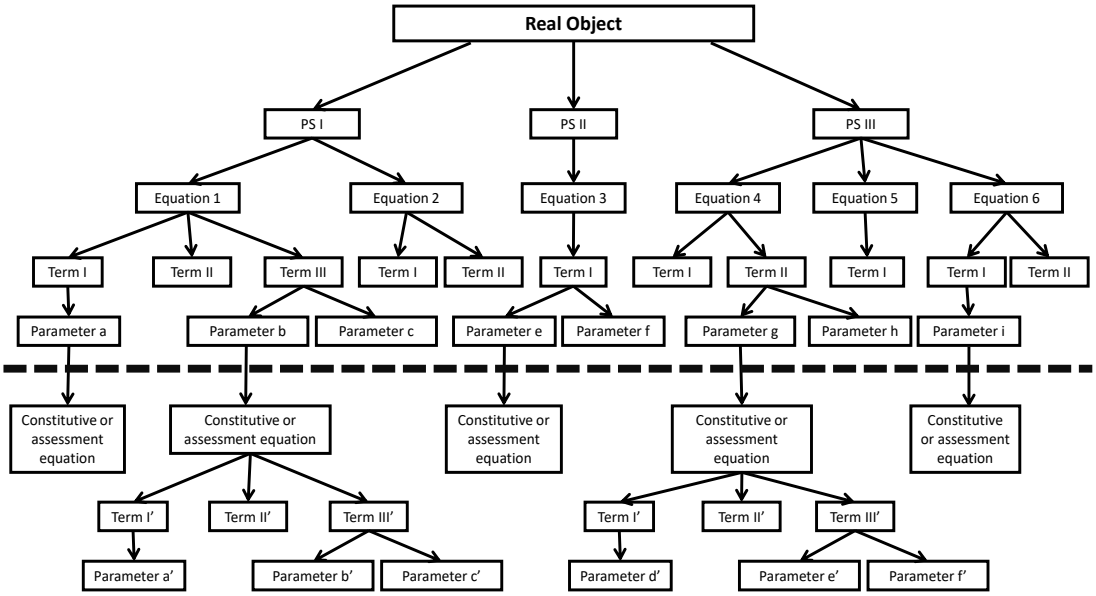

FIGURE 2.2. Model structure of a PBSM. The PS acronym is for Process System.

the theory of modeling and simulation, which provides a fundamental and rigorous mathematical formalism for representing dynamical systems, degree of system specification or merely specification degree is an instance at which the behavior of each new subsystem can be described along with the mechanisms that make it works [260]. Such specification degree requires a partition of the real object producing subsystems with lower (at least equal) size each time. After that, a submodel is generated at a the different level of detail. In this situation, the differences in size of each partition generate a scale in the produced subsystems. However, the real object can be partitioned in several levels of detail, either with different scales or with the same scale. Each partition or subsystem can offer new characteristics, which are described through specification degrees. Alternatively, a model can be seen like a set of layers, in which all layers are related to each other and provide useful information to produce the output of the model. Moreover, it is not necessary to consider a model hierarchically organized or a multilevel model. It is just important to know the underlying phenomena at every layer. An approach about partition of systems can be observed in Figure 2.3, when a real object of interest is considered to be represented by a PBSM. The real object is divided into four study objects according to its physical natural partitions and the model aim. This first partition is the level of detail of the model. Each study object generates balance equations and each set of mathematical equations is considered a submodel of the real object. The separation of each term of each equation generates a layer, and also the break down of each term into constants and parameters can be regarded as a new layer. However, when a new mathematical equation is used to define a parameter, a new specification level appears, generating new parameters and new layers in the model. In other words, a level of detail is related to the physical partition of the real object, and the level of specification is related to the new equations used to define the unknown parameters, and the layers are related to the parts of a mathematical equation.

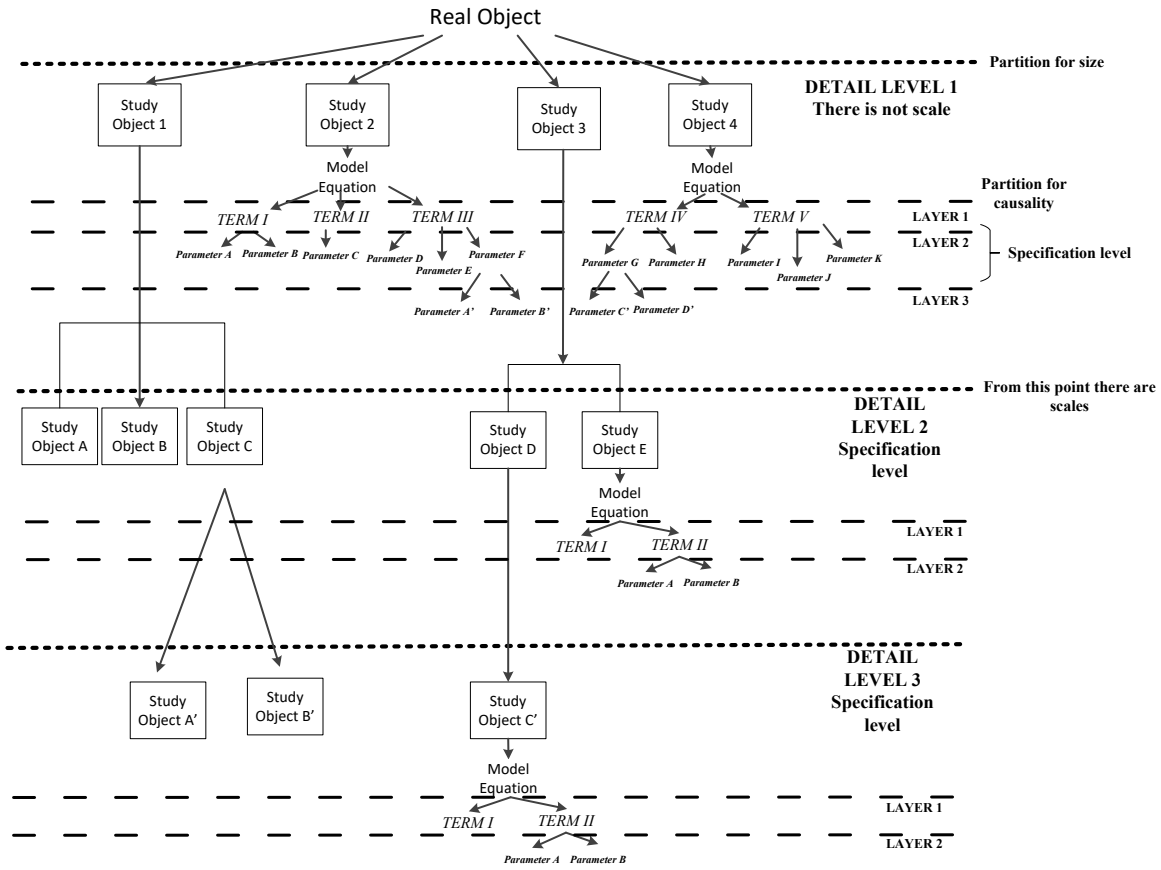

FIGURE 2.3. An approach about partition of systems.

Previously some concepts, maybe uncommon in the literature, have been mentioned. However, to continue with the discussion about PBSMs it is necessary to give a formal definition to the following concepts, used throughout the thesis:

Definition 2.4. ***Variable.*** *Quantity to be solved by the model.*

Definition 2.5. ***Basic structure.*** *Set of equations obtained after the application of the conservation law. At this level, the functions that represent the phenomena taking place in the study object are not detailed mathematically. Instead, they are represented by symbols.*

Definition 2.6. ***Extended structure.*** *Set of equations allowing to specify the parameters of the model. The extended structure results from defining the symbols of the mathematical equations of the basic structure. Some of these equations are trivial, i.e., they imply only the assignment of a numerical value to a parameter.*

Definition 2.7. ***Model structure.*** *Set of equations encompassing both basic and extended structures.*

Definition 2.8. ***Constitutive or assessment equation.*** *Equation used in the extended structure of the model acting as a mathematical specification of a parameter.*

Definition 2.9. ***Structural parameter.*** *Parameter belonging to the basic structure of the model. The structural parameter represents either a quantity that varies in time or a given scalar.*

Definition 2.10. ***Functional parameter.*** *Parameter belonging to a constitutive or assessment equation. It is categorized in coupled parameter, no coupled parameter or scalar parameter.*

All parameters presented as a symbol in the balance equations that form the basic model structure are called structural parameters. Structural parameters change both the output and the structure of the model in a dramatical way. They can be associated with a numerical value or a constitutive or assessment equation describing each one of them. Also, its interpretability is inherent because the basic structure is developed with the knowledge of the process phenomena. The remaining parameters of the mathematical model are called functional parameters because they are inside a constitutive or assessment equations, though its effect over the system response is not as steep as the one observed with structural parameters. They are symbols that can be linked to a numerical value or a constitutive or assessment equation that describes a structural parameter or a functional parameter of a lower level of specification. Functional parameters can also be: i) inherently interpretable, i.e., inherent physical meaning, ii) interpretable according to its context into a specific mathematical model, iii) non-interpretable. Definitions introduced above will be complemented in Chapter 5 with detailed and broader information about interpretability.

2.3.3 Properties of a PBSM

The PBSMs have a particular mathematical structure that makes them different from other types of models, providing to PBSMs some properties useful to analyze the modeled process. The properties are shortly described as follows because three of them (uniqueness and modularity of the basic structure, and combinations of levels of detail) are not the focus of this thesis.

2.3.3.1 Uniqueness of the basic structure

The equations that appear when the conservation law is applied (balance equations) form the basic structure of the model. Balance equations coming from an analogy of the real object may not be a unique representation of such a real object since every analogy may represent a different modeler viewpoint. Otherwise, if the conservation principle is applied directly to the study object without using an analogy, the PBSM has a unique basic structure. The uniqueness of the model basic structure allows reproducing a set of processes that shares their its basic phenomenology. This property is very interesting due to several processes with similar features can be described with the same basic mathematical structure, being the constitutive and assessment equations the ones that change because they are defined by the modeler. For this reason, constitutive and assessment equations are not considered within the basic structure of the model, i.e. if they are replaced in the balance equations, the uniqueness of the basic structure of a PBSM is partitioned.

2.3.3.2 Modularity of the basic structure

The modularity of a PBSM means the ability to expand from a initial model that considers only a part of the process to a model considering a larger layout. A way to model many processes or the whole system is to build phenomenological-based semi-physical submodels (sub-PBSM) and then link them. In complex processes, partitioning always helps to

manage the entire problem. After using the PBSM modeling methodology for subsystems, its further interconnection becomes a natural step. This property is interesting because allows modeling the system under different conditions but using the same partition. In addition, this property is useful to enlarge an existing PBSM, either by integrating new process systems or by expressing functional parameters using sub-PBSMs (combining levels of detail).

2.3.3.3 Combinations of levels of detail

PBSMs have the advantage of combining levels of detail or size partitions to obtain accurate information at the highest level of the model. The highest level of detail is at macroscopic scale and the lowest one is at the atomic scale [117]. A PSBM has minimum two levels of detail: one issued from the partition of the real object in process systems (level of detail of the model), and one used to calculate at least model parameter [8]. On the other hand, combination of specification levels in a PBSM is natural because that appears when a parameter, be structural or functional, needs to be calculated by a constitutive or assessment equation. The first specification level arises when constitutive or assessment equations are used to determine a structural parameter and they are associated with functions and not with scalars. Thus, functional parameters appear. If some functional parameters must be expressed by other constitutive or assessment equations, a second specification level is generated, and so on, until to have all constitutive or assessment equations formulated in terms of known constants, variables, and parameters. A lower level of specification may require information about the state of the system which is determined at a higher level, while at the same time the upper specification level requires parametric and structural information of the system obtained at the lower levels [117]. This property is interesting because the different levels considered to build the PBSM can exchange phenomena and information between them, providing to the model users additional knowledge of the process.

2.3.3.4 Parameter interpretability

This is the property discussed in detail in this thesis. Interpretability is a property of the parameters but not of the model, due to interpretability of the models comes from model structure which is not analyzed here. The basic structure of a PBSM comes from the phenomena of the process and for that reason, its parameter interpretability is guaranteed, that is, all structural parameters are inherently interpretable. Empirical models, however, do not enjoy this property. A parameter is said to be interpretable if it has a physical meaning within the process being modeled. A parameter can be considered interpretable if, when integrated into the model, it provides additional knowledge if compared to the one when only its numerical value is considered. In this way, a PBSM allows giving interpretability to the functional parameters through specification and detail levels. The interpretability of the functional parameters depends on the selected constitutive and assessment equations. Therefore, it is important to consider phenomenological mathematical expressions whenever possible to preserve the phenomenological model description. This property is very interesting when the modeler wants to get more knowledge about the process being modeled. Also, it is a characteristic of the phenomenological-based semi-physical models, but limited for empirical models. The core of this thesis is parameter interpretability, then this property will be widely discussed in Chapter 5.

2.3.4 Methodology to build a PBSM

The construction of a model may be linked to a form of art. This subjective character explain the existence of several methodologies for building PBSMs [20; 21; 72; 104; 107; 114; 162; 169; 188; 239; 257]. In our research group in dynamic processes KALMAN of the Universidad Nacional de Colombia, several studies have been carried out [9; 123; 192] to propose the following methodology, described in 10 steps.

1. **Process description and model aim:** a verbal description of the process is performed including a process flow diagram as a graphic representation. Also, the model aim made explicit through the question to be answered by the model.

2. **Model hypothesis and level of detail:** a hypothesis or analogy about the behavior of the real process may be proposed. If the modeled process takes place in a specific area of the engineering in which the phenomena of the process are known, there is no need to state an analogy and the model hypothesis is the description of such phenomena. Otherwise, the process may be strategically related to a known process, an analogy is of paramount importance, and a set of assumptions is fixed. Moreover, this type of models are built applying the balance equations on the partition or study object arose from the real object. The position of such partition into all possible partitions for the process is the level of detail of the model. Steps 1 and 2 are iterated until reaching both steps completely.

3. **Definition of the process systems:** a process system is an abstraction of a part of the process seen like a system. Each process system is a partition of the real process, and this partition must be as real as possible, that is, physical distinctions, changes in the phases or characteristics marking spatial differences in the process need to be considered for partitioning.

4. **Application of the conservation law:** the conservation law is applied to each process system defined in step 3 for the interest substances. The equations obtained contribute to the basic structure of the model.

5. **Determination of the basic structure of the model:** among the balance equations emerged in the last step, indicate those with valuable information to answer the question in step 1 and to achieve the model aim.

6. **Identification of the variables, structural parameters and structural constants:** make a list of variables, structural parameters, and structural constants. Variables are quantities whose values result from the solution of the model equations. Contrary, the parameters are values that need to be defined beforehand to solve the model. They can be known values or must be identified. Finally, the constants are fixed values either because it is an universal value like gravity constant.

7. **Definition of constitutive and assessment equations and functional parameters:** constitutive and assessment equations are proposed to calculate the largest number of unknown parameters of every process system. The set of constitutive and assessment equations are selected according to the modeler criteria. A constitutive equation approximates the response of a physical quantity to external stimuli using a law or principle. Darcy's law, heat, mass, and momentum rate of transfer laws, Arrhenius law, among others, are examples of constitutive equations. Contrary,

an assessment equation is a mathematical relation to assess a parameter numerical value, without any intention of linking in a descriptive way the calculated numerical value to the phenomena taken place in the process being modeled.

8. **Verification of freedom degrees:** the freedom degrees are the difference between the number of unknown quantities and the number of equations. This difference must be zero to obtain a solvable model.

9. **Construction of the computational model:** the solution of the mathematical model is carried out by a computational program able to solve the full set of algebraic-differential equations forming the model.

10. **Validation of the model:** the model validation is a combination of activities such as experimental verification of the assumptions and comparison of the model results with the behavior of the real process, with experimental data or by using information taken from other validated models.

2.4 Modeling of human physiological processes

In this section, the concept of the physiological system is presented aiming to show its similarity with industrial processes. Modeling and simulation have been hot topics of research from a while ago since it provides an alternative way to gather the knowledge, understand the human body functioning and study and test different conditions and diseases. In this sense, existing approaches in physiological models are reported in this section. Finally a new approach to physiological process modeling is presented. This approach uses the modeling methodology for PBSM summarized above.

2.4.1 What is a physiological system?

A system refers to a set of entities working together as parts of a mechanism or an interconnected network. From the modeling viewpoint, a system can be seen as a set of complex objects (or engineering entities) accomplishing a specific purpose and whose behavior needs to be understood, monitored, and even controlled [157]. Physiology can be regarded as a dynamic system where the organism's functions and activities, including all its physical and biochemical processes, take place [171]. The human body is organized in systems interacting and carrying out multiple processes to keep the entire organism alive. Cells in the body are inside tissues that form an organ. The organs are connected to other forming a unitary complex: the human body. Every organ carries out many vital functionswhich in turn needs to be synchronized to other organs or even human systems to keep us alive. The synchronization and combination of the functions of all parts of the body is known as physiological system. The sum of the physical and biochemical processes in the organism by which its material substance is produced, exchanged, maintained, and destroyed, and by which energy is made available is called metabolism. Material substances are taken from the environment into the organism in the form of nutrients and air, and they are then broken down into simpler substances. These substances are oxidized to provide the energy required for many life-sustaining processes within the body. Once broken down, the simpler substances also form the fundamental building blocks to synthesize more complex substances that are used to form structural tissues. The main

agent for the transport of chemicals substances within the body is the blood, which is circulating around the body through a system of blood vessels with the heart acting as a pump. Blood vessels carry the needed substances for nutrition and also serves for waste removal purposes [42; 130].

The physiological systems are subject to many external perturbations, but they are able to adapt to distinct forms of stress thanks to their regulatory mechanisms or homeostasis. These regulatory mechanisms are able to maintain the internal stability, due to the coordinated response of its component parts to any situation or stimulus tending to disturb the normal condition or function. Homeostatic mechanisms are originated to keep a regulated variable in the internal environment within a range of values compatible with life and, as has been more recently suggested, to reduce noise during information transfer in physiological systems [256]. Under this definition of a physiological system, reproducing one or more outputs in response to one or more stimuli is the basic idea of physiological system modeling [70]. This considering that the stimuli are input physiological signals generated from other organs or external environment, which produce responses following the physical laws, as occurs in many engineering processes.

2.4.2 Existing approaches in physiological modeling

Over the past six decades, there has been a considerable interest to understand complex mechanisms of physiological systems to find solutions to different health conditions [58]. As such, novel quantitative methods along with novel measurement processes have made possible the development of new methods for analysis and interpretation of the generated experimental data [56]. Additionally, mathematical models are increasingly gaining more attention to understand different physiological processes and their correlations with different pathological conditions [11]. In this regard, several mathematical models have emerged to represent the functions in the organism of isolated organs [52; 64; 100; 166; 225; 240]. Mathematical models are able to improve the physiological knowledge of the organs and the interpretation of the physiological data, allowing to perform *in silico* tests to carry out experiments without risking the life of a patient. They are also used to develop new medical technologies that replace functions of an organ of the body that has lost part of its normal functioning.

Physiological modeling involves the development of mathematical, electrical, chemical, or other analogues whose behavior closely approximates the behavior of a particular physiological system [70]. It is desirable that every aspect of the model corresponds to features of the physiological system under consideration. In this way, assumptions and hypothesis of the underlying physiological process must be considered regardless of the type of mathematical modeling process. In addition, assumptions and hypothesis will help to reduce the complexity of the model, since most physiological systems are complex and simple characterizations may not always be possible. The biggest current drawback in physiological modeling is that only few features are measurable and, therefore, several variables need to be mathematically estimated. Moreover, given the discrete nature of both computers and sensors, approximations of naturally-occurring continuous-time processes (as those occurring within the body) need also be taken into account [70].

The earliest models of physiological systems were devoted to physical analogies, which are useful in extending intuitive knowledge in one area to another. However, physiological models derived from physical analogies are limited by constraints of implementation

to rather simple systems. Most mathematical descriptions of physiological systems use differential equations that can be solved either analytically, physically (i.e., by building a physical analogue), or numerically (i.e., on a digital computer). However, the most common approach to model physiological processes has been the empirical, which in many cases either dismisses or reduces the complexity of the underlying phenomena [70]. This due to the nonlinear techniques not only have to be tailored specifically to each situation, but also they tend to be more complex and computationally tedious than linear techniques. Despite this, it is extremely important to understand under which conditions a physiological system can do submit to linear systems analysis. This approach is focused only on the measurable signals and determine the relationships between these signals. In such a case, the mathematical equations have little or no correspondence to the actual physiological system excepting in the input-output relations.

Computational models have been used to simulate physiological processes like the blood vessel hemodynamics and cardio-respiratory system [11]. Compartmental models have also emerged to describe physiological processes such as the endocrine system [44], renal system [150], and the pharmacokinetics in the body [211]. The method of compartment modeling considers a compartment-like representation of a homogeneous, uniform entity with variable inflow and outflow. This approach of modeling is also used to describe glucose dynamic in blood. A first compartmental model of glucose, known as minimal model [29], was proposed at the beginning of the 1980s by Bergman and coworkers where compartments of glucose, insulin, and remote insulin were considered as initial assumption. Later on, the minimal model became a great physiological model in which the role of the gastrointestinal tract, liver, and beta and alpha cells, among others, are considered [57]. From this contribution, many models related to the minimal model have been generated [58]. Additional physiological approaches to model glucose homeostasis were also proposed by Sorensen in 1985 [233], where human body was divided into a number of physiologic compartments that represent the capillary beds of various organs and tissues and was formulated by techniques similar to those originally developed for simulating drug distribution. In spite on being compartmental, it was an attempt to develop an explanatory physiologic model of glucose metabolism in the human body. The biggest drawback of the real application of these physiological models is their lack of parametric interpretability so that an individualized parameters identification has not been possible even nowadays.

The methodology to develop a PBSM may also be used in physiological modeling to obtain a set of mathematical equations that will mimic the physical behavior of the physiological system as detailed as possible. This means that particular chemical reactions, effects of structural arrangements, etc., will have corresponding mathematical formulations. These models are of great use in physiological research where the behavior of the model is used to validate experimental data, predict the response of the physiological system and study the behavior of the physiological system under conditions that are difficult to actually reproduce in clinical practice. Difficulties may come from actual physical complexities or due to ethical constraints.

According to the different approaches mentioned above, there are many strategies to model a physiological system. Any technique of process modeling in engineering can be applied in a physiological system. The methodology used depends on the modeler and on the intended use of the mathematical model. Obviously, some modeling techniques will give more information about the physiological behavior than others. The previously mentioned models classification is a guide to determine the kind of information expected from each class of possible mathematical model.

2.4.3 An approach for physiological modeling

The application of mathematical modeling and dynamic systems analysis methods are playing an increasingly important role in the study of physiological and metabolic processes, due to their high physical complexity and difficult experimental accessibility. Additionally, mathematical models are increasingly being leveraged as aids in diagnosis and treatment of different diseases [22; 44; 57; 84; 87; 193; 208; 227]. In this thesis, a novel approach for physiological process modeling is proposed, by applying the methodology for PBSMs by doing an analogy of the human body with a convenient and reasonable engineering process. In this approach, the organ-to-organ interaction of the system of interest is seen in a plant-wide viewpoint.

Human physiological processes can be modeled following the same procedure to build a PBSM. However, modeling physiological phenomena turns to be a complex task due to the high interaction among different systems including organs, tissues, and physiological systems. In addition, most phenomena taking place in the human body are described by means of nonlinear relationships with probably stochastic[2] and time-varying effects [57]. Complexity is exhibited at each level of the hierarchy and across levels within the physiological system. The physiological hierarchy includes the levels of molecule, cell, organ, and organism. Complex processes of regulation and control are evident at each level, but some of them are unknown. Likewise, the physiological organ systems exhibit explicit control mechanisms. As a result of this physiological complexity, it is not often possible to measure directly (*in vivo*) the quantities of interest. Only indirect measures may be feasible, implying the need for some model to be able to infer the value of the quantity of real interest [55; 68]. In this sense, models can also play a powerful role in experimental design. In this way, mathematical models help out to improve the understanding of the phenomena of interest.

Specific purposes for system modeling can be identified in the physiological context. These include understanding, testing of different hypotheses, inferring measures of interest, simulating, and evaluating a possible experimental design. Models are also being increasingly used as a medium of teaching and learning about processes, where by means of simulation, they can be tested into a richer range of physiological and pathophysiological situations than otherwise would not be possible in a conventional physiological laboratory setting [57].

Models of physiological systems, as well as other dynamical systems, are often composed of a set of ordinary differential and algebraic equations. These equations model how variables changes with time [212]. To achieve a detailed and consistent understanding of a physiological system in the human body, a hierarchical model with a multi-level structure can be built. Multilevel models include information provided by a combination of high level models, typically for organs such as liver, kidney, or muscles, communicating with models in a lower level of hierarchy, e.g., intracellular models [93]. The higher level is in charge of coordinate all the organs functions. On the other hand, complex models like physiological models, require both experimental data and knowledge of the system in order to be validated [190]. Otherwise, those models require additional assumptions which

[2]In living organisms, some effects are randomly determined and can be statistically analyzed, such as the activity of nervous fiber, the intrarenal system variation in glucose resorption for an increasing load of glycemia when the rate of glucosuria is studied, the sexual reproduction, the gene expression, the relationship between the molecules and its receptors or the nutrients and its absorption surface, just to mention a few.

may eventually introduce uncertainty. A successful outcome to the modeling process is critically dependent on both the quality of the model and the quality of experimental data, which in physiological models are obtained by means of clinical trials.

All the concepts presented in this chapter are the theoretical basis to demonstrate that any human physiological mechanism is a set of biochemical processes to which, despite its complexity, the existing mathematical modeling theory can be applied, leading to useful mathematical representations in the health field.

3

Glucose Homeostasis in Humans

The present chapter has one basic objective and it is to provide an introduction to the essential nature of the glucose homeostasis cycle in humans. The original intention is not to provide additional medical information, but just to furnish a comprehensive overview of this natural mechanism. It also intends to show the complexity of the regulatory system and exhibit the importance of some (often disregarded in current mathematical models) organs in such a homeostasis. A the end of the chapter, a brief section about glucose impairment (Diabetes Mellitus) is presented.

3.1 Importance of glucose in the human body

Glucose is the simplest of all carbohydrates, making it a monosaccharide. Most cells in the human body use glucose as their major source of energy. The human body creates energy mainly from glucose to stay alive, therefore, it is processed continuously. When we eat, our body immediately starts working to process glucose. Glucose mainly comes from foods rich in carbohydrates like bread, potatoes, and fruits. As we eat, nutrients travel throughout the esophagus to the intestine. Enzymes start the breakdown process in the mouth and going further to the small intestine by an additional intervention from the pancreas, who produces and releases hormones to regulate blood glucose levels. During that process, glucose is released and absorbed into the bloodstream. Once in blood, insulin hormone helps glucose to enter to the cells.

Glucose molecules are broken down inside the cells in order to produce, through glycolysis, adenosine triphosphate (ATP) molecules, energy-rich molecules that power numerous cellular processes. Glucose molecules are delivered to cells by the circulating blood and therefore, to ensure a constant supply of glucose to cells; it is essential that blood glucose levels be maintained at relatively constant levels. Level constancy is accomplished primarily through negative feedback systems [221], which ensure that blood glucose concentration is maintained within the normal range of 70 to 110 milligrams of glucose per deciliter (mg/dl) of blood [228]. Negative feedback systems are mechanisms that perceive changes in the human body and activate mechanisms that reverse the changes in order to restore conditions to their normal levels. Furthermore, negative feedback systems are critically important in glucose homeostasis in the maintenance of relatively constant internal conditions. Disruptions in glucose homeostasis lead to potentially life-threatening situations. For this reason, the maintenance of relatively constant blood glucose levels is essential for the health of cells and thus the health of the entire body. Later, diabetes mellitus, its complications and treatment are discussed in detail.

Along with glucose, the body also use amino acids (building blocks of proteins) and fats like source of energy. However, in spite of these alternative energy sources, it is of paramount importance to guaranteeing a minimum flux of glucose for the brain and nervous system. Glucose is the main source of fuel for the brain and nervous system. Nerve cells and chemical messengers need glucose to process information. Without it, the brain would not be able to work well. After the body has used the energy it needs, the leftover glucose is stored in little bundles called glycogen in the liver and muscles. The body can store enough fuel to work during a day. Glucose homeostasis and the role of every organ involved in this natural cycle is detailed in next section.

Major factors able to increase blood glucose levels include glucose absorption by the small intestine (after ingesting a meal) and the production of new glucose molecules by liver and renal cells. Sometimes, glucose levels in the blood can also go sky high under stressful conditions. Also, High Intensity Interval Training (HIIT) type of exercise is acknowledged to trigger (not completely understood) mechanisms able to rise the blood glucose levels. Major factors able to decrease blood glucose levels include the transport of glucose into cells (to be used as a source of energy or to be stored for future use) and the loss of glucose in urine (an abnormal event that occurs when glucose homeostasis is impaired). Some types of physical exercise are also able to decrease blood glucose levels. However, our body is designed to keep the level of glucose in the blood in healthy levels. People with Diabetes Mellitus are prone to an acute complication such as diabetic ketoacidosis and persistent high blood glucose leads to chronic complications such as retinopathy, diabetic nephropathy, neuropathy, and cardio-cerebrovascular disease. How does the body for regulating glucose levels in the blood? Next section introduces the regulation cycle in detail.

3.2 The glucose regulation cycle

Blood glucose regulation is the process in which the levels of blood glucose are maintained by the body within a narrow range. In this section, a general description of how this cycle works is introduced, along with nutrients affecting it and all organs involved in this essential physiological mechanism.

3.2.1 A general overview

Glucose homeostasis has the ability to regulate the blood glucose levels as a result of a complex interplay among a number of organs, hormones, metabolic sub-systems, and neuronal control mechanisms. As mentioned before, glucose allows cells to carry out vital actions such as breathing, tissue repair, cell multiplication, among others. Therefore, it is extremely important to guarantee the glucose plasma concentration near the range of $70mg/dl$ to $110mg/dl$. This natural mechanism is responsible for ensuring the stability of blood glucose levels by means of proper dosage of pancreatic hormones, mainly insulin and glucagon [228]. Figure 3.1 shows how the human body maintains glucose levels in a specific physiological range. When polysaccharides enter to the digestive tube from the ingestion of carbohydrates, the enzymatic action of disaccharidases in the small intestine are triggered for polysaccharide breakdown. In this process, smaller molecules called monosaccharides are produced and then absorbed to the blood stream through the intestinal wall, increasing blood glucose levels. Once food has been ingested, transformed,

and begins to be absorbed, incretin hormones GIP and GLP-1 stimulate beta cells from pancreas to produce insulin, a hormone responsible for increasing the amount of glucose transporters GLUT4 in the cell membrane of different tissues [228]. Insulin production is also stimulated by a constant blood glucose concentration and modulated by such incretin hormones. Glucose is transported through the cell membranes by specialized molecules called GLUT. GLUT transporters are responsible for glucose diffusion through the cell membrane, removing the excess blood glucose, represented in the figure with the plus sign, be transported within muscle cells, adipose cells, and hepatocytes, and then to be used as an energy source, thus reducing the blood glucose concentration. Once glucokinase enzyme from liver starts to sense high glucose concentration and hence stimulates the diffusion of glucose through the liver to produce glycogen which is a multi-branched polysaccharide of glucose that serves as a form of energy storage to be used in fasting periods [136].

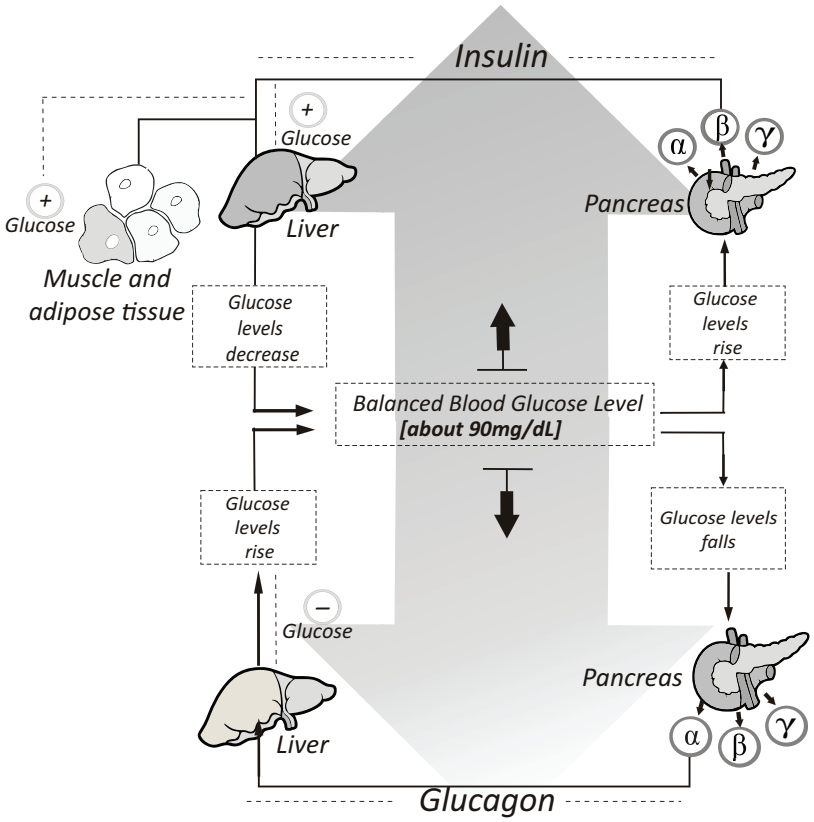

FIGURE 3.1. The glucose homeostasis in the human body.

When a person goes through a period of fasting, blood glucose levels decrease and, by action of the catecholamine hormones, insulin production is inhibited [136]. Also as a consequence of fasting, alpha cells of the pancreas are stimulated to produce glucagon, a hormone acting on different hepatocytes receptors triggering the action of the phosphorylase enzyme and hence stimulating the breakdown of glycogen through a process called glycogenolysis, which is the transformation of glycogen to glucose. When glycogenolysis occurs, the glucose produced in the liver is released into the bloodstream to recover the lack of glucose in the bloodstream, represented by the minus sign in Figure 3.1, and the plasma glucose concentration goes back to desired levels [136].

When the glucose homeostasis is broken, plasma glucose levels are no longer maintained at desired levels. This is mainly due to a deficit in the production of insulin from the pancreatic beta cells or from a resistance to the action of the produced insulin in a set of conditions known as *Diabetes Mellitus*.

3.2.2 Effects of nutrients in glucose homeostasis

Dietary composition could play a significant role in improving insulin sensitivity and reducing the risk of associated complications to diabetes mellitus. Several nutrients other than carbohydrates, such as dietary protein, amino acids, fat, vitamins, and minerals, can affect the way glucose enters into the bloodstream. A brief description of the effects of other macronutrients on glucose metabolism is presented.

3.2.2.1 Proteins

Proteins are large macromolecules. They consist of many amino acids linked to form highly complex long chains present in all living organisms. Proteins are of great nutritional value and are directly involved in most biochemical processes within the human being. Proteins perform many functions including catalysis in metabolic reactions, DNA replication, stimuli response, structural support for cells, and molecular transport, among others. Some recent studies have demonstrated that proteins are nutrients more satiating than either carbohydrate or fat [6; 13]. Also, the protein content of a food increases satiety and reduce both food intake and blood glucose response when consumed alone or with carbohydrate [5; 13; 97] while reducing postmeal insulin response due to insulinotropic [1] effects. The role of branched-chain amino acids seems to be insulin stimulation release and secretion [143; 174], mediated by an increase in glucagon-like peptide 1 (GLP-1) [26]. This last effect may also decrease gastric emptying [5; 97]. The effect of protein on blood glucose concentration depends very much on the kind of protein and its amino acids composition. Several studies have been carried out using food products with high protein content to compare the effects in the blood glucose concentration. It has been found that whey protein has a pronounced effect on lowering blood glucose levels [2; 36; 143; 195]. Proteins like casein or soy have shown a positive effect on insulin sensitivity [2].

Studies about insulinotropic effects of the protein are still being carried out but some cell experiments indicate that the increase of insulin secretion might be caused by an increased intracellular oxidation of amino acids, which raises the ATP content of the cell. An increase in intracellular ATP content leads to a closure of the ATP-sensitive potassium channels, and this channel closure leads to depolarization of the cell membrane and activation of the calcium channels. Activation of the calcium channels then causes an exocytosis of insulin from cells [37; 63]. In [78] it is shown that the depolarization of the plasma membrane could occur due to the co-transport of amino acids into the cells together with sodium, causing an exocytosis of insulin. Another feasibility is the decrease of insulin clearance by the liver, keeping the insulin levels in the serum increased [143]. Another studies have been carried out unveil the effects of proteins in insulin resistance and in [113] the authors have shown that high protein intake might positively affect glucose tolerance inducing a reduction in insulin sensitivity. All experimentations with proteins demonstrate that its ingestion may be an effective strategy for achieving blood glucose

[1] Insulinotropic refers to stimulating or affecting the production and activity of insulin.

control in healthy and insulin-resistant humans [5]. However, further long-lasting studies are needed before high protein intake might be recommended for subjects with diabetes.

3.2.2.2 Fats

The results in humans about the influence of dietaries fat in the glucose metabolism have been inconsistent and are likely confounded by differences in body weight. The link between dietary fat and glucose metabolism has not yet been fully elucidated. However, some experimental studies have shown a diet based on high-monounsaturated fatty acids appeared to reduce haemoglobin A1c (HbA1c) [226], improving glycaemic control and lipid profiles. Improvement of glycaemic control seems to be caused by an exchange of carbohydrates against fat, and also by a prolonged gastric emptying induced by high-fat intake independent of fatty acid composition. In addition to the fat content, the composition of dietary fat could play a role in improving insulin sensitivity and reducing risk of diabetes mellitus and its complications [168]. The fatty acid composition of cell membranes is thought to alter several cellular functions, including membrane fluidity, ion permeability, and insulin receptor binding or affinity, functions affected by translocation of glucose transporters interacting with second messengers [98]. Such alterations could, in turn, affect tissue and whole-body insulin sensitivity [215].

No long-term dietary intervention studies have been conducted to determine the relationship between the quality of dietary fat and the risk of diabetes mellitus. Although data from controlled feeding studies in metabolically healthy subjects and in patients with diabetes mellitus are very limited, there are studies suggesting beneficial effects on insulin sensitivity when saturated fatty acids are replaced with monounsaturated or polyunsaturated fatty acids [215]. Evidence from observational studies has suggested that *trans* fatty acids consumption may be associated with insulin resistance and T2DM [238], but other studies however [14] concluded that an increased *trans* fatty acids intake does not result in a potential benefit on glucose homeostasis. It has been shown, however, that increased unhealthy dietary fatty acids consumption is likely to increase the body weight and waist circumference which in turn may trigger insulin sensitivity changes and the onset of different metabolic syndromes. Despite the known benefits of fatty acids, the understanding of their role in glucose metabolism and insulin resistance in humans is still being object of scientific controversy.

3.2.2.3 Vitamins and minerals

Low vitamin D has been considered a risk factor for T2DM [139]. Moreover, supplements containing vitamin D have shown to increase insulin secretion in presence of pancreatic β-cells. Reported associations with insulin secretion, however, seem contradictory since the mechanisms mediating between such a vitamin deficiency and T2DM are not yet fully understood. Additionally, dietary vitamin D supplementation is probably associated with reduced risk of T1DM [126]. The multiple roles of vitamin D include the presence of specific vitamin D receptors on pancreatic β-cells [131], the expression of $1-\alpha$hydroxylase enzyme in pancreatic β-cells which catalyzes the conversion of vitamin D [34], and the presence of a vitamin D response element in the human insulin gene promoter [164]. Vitamin D deficiency may influence its effects on insulin secretion and sensitivity by directly influencing intracellular calcium [201].

Vitamin K might also play a role in glucose homeostasis. Vitamin K is a cofactor in several carboxylating GLA proteins such as bone and matrix GLA protein. The concentration of the bone-GLA protein osteocalcin, as well as the percentage of undercarboxylated osteocalcin, which reflects an insufficient vitamin K supply, seems to be associated with glucose metabolism and insulin secretion [112]. Moreover, serum osteocalcin concentrations were positively associated with insulin secretion and inversely correlated with glucose levels and adiposity [261]. Relation between insulin resistance and the percentage of undercarboxylated osteocalcin is still controversial [183]. Most of the studies showing a potential benefit of high calcium intake on glucose homeostasis are cross-sectional studies in which calcium has been dosed in combination with proteins, for instance, by increasing dairy or in combination with vitamin D supplementation [91; 200]. However, it has been difficult to derive whether the effect on blood glucose homeostasis is caused by high calcium intake or high protein intake, the quality of protein, the vitamin D supplementation, or its combinations. An additional mineral considered essential for being present in more than 300 metabolic reactions in the human body is the magnesium [246]. Research has indicated that a lower dietary intake of magnesium and lower serum magnesium concentrations may are associated with the metabolic syndrome and insulin resistance in people with T2DM [19]. There is little evidence of the benefit from magnesium in people with diabetes, but an analysis reported in [232] showed that magnesium supplementation has an effect on long-term glycaemic control.

3.2.3 Main organs involved in glucose homeostasis

In the human body, most tissues need glucose as the main source of energy. However, maintenance of glucose homeostasis involves several complementary physiological processes performed by the gastrointestinal tract (when the glucose absorption takes place), glycogenolysis and glucolysis in the liver, glucose reabsorption and excretion in the kidneys, and gluconeogenesis in the liver and kidneys. The role of the organs involved in glucose regulation cycle is described below.

3.2.3.1 Pancreas

The pancreas has both endocrine and exocrine functions. This study is primarily focused in the endocrine function given the primary role on glucose homeostasis. Endocrine cells in the pancreas are clustered, forming the so-called islets of Langerhans, which are small, island-like structures within the exocrine pancreatic tissue that account for only 1-2% of the entire organ [218]. Such a structure contains at least five different endocrine cell types responsible for the production of five different hormones: glucagon-producing α-cells, amylin-, C-peptide and insulin-producing β-cells [38], pancreatic polypeptide (PP)-producing γ-cells [133], somatostatin-producing δ-cells [38], and ghrelin-producing ε-cells [252]. Through its hormones, mainly for the action balanced between insulin and glucagon, the pancreas maintains blood glucose levels within a narrow range of 4-6mM (70 to 110 mg/dL) [218]. Glucagon and insulin are known as antagonistic hormones since insulin decreases blood glucose levels, whereas glucagon increases blood glucose levels [17]. However, both hormones are inhibited by somatostain [111]. Endocrine cells secrete their respective hormones in response to external signals, such as nutrient intake, fasting or stress. During sleep, in between meals, or in long fasting periods, for example, blood glucose decreases and glucagon is released from α-cells to promote glycogenolysis and gluconeogenesis. In

contrast, after a meal β-cells release insulin to decrease blood glucose levels via glycogenesis [137; 180; 237]. Despite insulin is released on demand, it is stored in large dense-core vesicles that are recruited to the proximity of the plasma membrane in the β-cells in the Langerhans islets, following stimulation such that insulin is readily available for next stimuli [108]. Insulin is released primarily in response to glucose, but other nutrients such as free fatty acids and amino acids can augment glucose-induced insulin secretion through the so-called incretin effect. This effect has its origin in the intestinal tract during food digestion.

Insulin gene encode in a 110-amino acid precursor known as preproinsulin. Then, the preproinsulin is processed to proinsulin. Later, proinsulin enters immature secretary vesicles and is cleaved to yield insulin and C-peptide [90]. Once insulin is released into the bloodstream, it enables the glucose uptake into the insulin-dependent tissues, removing glucose from the bloodstream [134; 140; 263]. Also, it promotes lipogenesis [173; 249], and the incorporation of amino acids into proteins [31]. Low insulin concentrations contribute to lipolysis in adipocytes, releasing free fatty acids to encourage utilization of lipid over glucose to meet resting energy needs [167]. Insulin release from beta-cells is tightly regulated meeting exactly the metabolic demand for calorigenic nutrients in the body [90; 167]. Regarding C-peptide, it has been important in order to follow some insulin states difficult to measure [146].

3.2.3.2 Liver

While it serves for a variety of functions, the liver plays a unique role in controlling carbohydrate metabolism by maintaining glucose concentrations in a normal range over both short and long periods of times. The key role of the liver in glucose homeostasis is storage (glycogenesis) and glucose dosing (glycogenolysis and gluconeogenesis) upon interaction with insulin and glucagon, respectively. Hepatocytes express dozens of enzymes that are alternatively turned on and off depending on whether blood glucose levels are either raising or falling out of the normal range [203]. In the postabsorptive state[2], hepatic glucose production ensures enough glucose supply to the central nervous system and at the same time it regulates fasting plasma glucose concentration. In the postprandial period, the liver is the first access to most ingested nutrients by virtue of their absorption into the hepatic portal vein. Thus, the liver takes up a portion of ingested carbohydrates to restore glycogen stores and to minimize the fluctuation of glycemia. The liver also contributes to the disposal of enteral glucose loads by increasing the rate of glycogen synthesis and suppressing hepatic glucose output. These result in a net switch from hepatic glucose output to hepatic glucose uptake [61]. The suppression of hepatic glucose output involves the suppression of hepatic glycogenolysis and gluconeogenesis [199]. Gluconeogenesis occurs when hepatic glycogen reserves become exhausted and additional groups of enzymes are activated to start synthesizing glucose out of such precursors as amino acids and non-hexose carbohydrates. The suppression of glycogenolysis and to a lesser extent gluconeogenesis and the activation of glycogen synthesis during the postprandial period is mainly driven by stimulation of insulin secretion and suppression of glucagon secretion.

[2]Postprandial state is the time frame after a meal or food intake. Postabsorptive state is the period following absorption of nutrients from the digestive tract, that is, is the time when enterocytes stop providing nutrients to the hepatic portal circulation. Fasting is the willing abstinence or reduction from some or all food, drink, or both, for a long period of time ($\sim$ 8 hours).

The liver is the major site of glucose utilization during the postprandial period. Simultaneously, the liver plays a major role in the metabolism of insulin, being the primary site of insulin clearance [77; 222]. Approximately 50% of portal insulin is removed during first-pass transit, but this percentage may widely vary under different conditions, e.g., when insulin clearance alteration by nutrient intake [116]. Removal of insulin from circulation does not imply the immediate destruction of the hormone [27]. A significant amount of receptor-bound insulin is released from the cell and reenters the circulation [76]. On the other hand, hepatic glucose uptake is maximally stimulated by conditions that mimic the postprandial state, such as portal venous hyperglycaemia and hyperinsulinaemia [194]. To be utilized, glucose enters the hepatocyte and is phosphorylated to glucose 6-phosphate. Glucose 6-phosphate may follow a number of metabolic pathways, including glycogen synthesis. Glucose in excess is used to synthesize fatty acids in the liver. In addition to glucose utilization, the human liver releases glucose to the systemic circulation either from previously stored glycogen (glycogenolysis) or by generating glucose from precursors such as glutamine, alanine, lactate and glycerol (gluconeogenesis) [3]. This unique ability of the human liver to store and release glucose is crucial to endure periods of fasting. During short-term periods of fasting, glycogenolysis is the predominant source of glucose released to the bloodstream. However, during prolonged periods of fasting, the glycogen reserve is gradually consumed and glycogenolysis decreases as glycogen store is depleted. Then, gluconeogenesis becomes the predominant source of glucose to the human body.

3.2.3.3 Kidneys

Kidneys are two bean-shaped organs mainly devoted to waste excretion. Its main function is cleaning the blood to send it back to the circulation, maintaining an overall fluid balance, creating hormones helping to produce red blood cells, promoting bone health, and regulate blood pressure [227]. However, recent studies have shown that kidneys also play a central role in glucose homeostasis through utilization of glucose, gluconeogenesis, and glucose filtration and reabsorption via sodium glucose co-transporters (SGLTs) and glucose transporters (GLUT-2). Moreover, the kidneys are the major site of insulin clearance from the systemic circulation, removing approximately 50% of peripheral insulin [106]. Kidneys have a microscopic structural and functional unit so specialized called nephron. Nephrons have the ability of distributing all the functions in all its parts. For instance, the glomerulus is the net of capillaries withing the Bowman's capsule. Blood is filtered across the glomerular capillaries into Bowman's space. These capillaries are multiple branches of the afferent arteriole but later they converge into efferent arteriole to leave from the glomerulus and surround the renal tubules: the proximal convoluted tubule, the proximal straight tubule, the loop of Henle, the distal convoluted tubule, and the collecting ducts. Within the tubules, urine is continually formed and is also where reabsorption, secretion, chemical reactions, and excretion occur [130].

According to glucose production and utilization, the kidneys may be considered as two separate organs since glucose release occurs predominantly in the renal cortex whereas glucose utilization is confined to the renal medulla [4; 103; 224; 242; 254]. Renal medulla has an appreciable glucose phosphorylating capacity and thus the ability to accumulate glycogen [103]. However, because of its low oxygen tension, and low levels of oxidative enzymes, the renal medulla consumes glucose anaerobically. Consequently, lactate is the main metabolic end product of glucose taken up at renal medulla, unlike carbon dioxide (CO_2) and water that are the end products of glucose uptake of aerobic energy require-

ments. In contrast, the renal cortex does not have appreciable glycogen stores [30] because has little glucose phosphorylation capacity but has a high level of oxidative enzymes like 6-phosphatase. Consequently, this part of the kidney does not take up and use much glucose, with oxidation of free fatty acids acting as the main source of energy [96]. It is thus likely that release of glucose by the normal kidney is due mainly to gluconeogenesis, that is, synthesis of glucose-6-phosphate from non-carbohydrate precursors as glutamine, lactate, alanine, glycerol, etc. [235], being glutamine the substrate with more specificity in the kidney but lactate the most abundant.

Additionally to their role in both glucose utilization and production, kidneys contribute to the blood glucose regulation by filtering and reabsorbing glucose. Glomeruli filter glucose once it reaches the kidneys, with other substances as precursors and insulin, toward proximal tubules, where all glucose is reabsorbed through glucose transporter proteins present in cell membranes within the proximal tubules [170], rendering the urine virtually glucose free. Before being reabsorbed, gluconeogenesis and glucose uptake occur. Glucose production is suppressed by insulin [235] or stimulated by non-carbohydrate precursors [7; 242]. An interesting fact is that GLUT-2 glucose transporters are insulin-independent and for that reason the kidneys can continue its physiological functions even in states of insulin deficiency [167].

Gluconeogenesis in the human body is mainly carried out by liver and kidneys. In the postabsorptive state, both liver and kidneys release glucose into the circulation in comparable amounts [234]. However, in the postprandial state, although overall endogenous glucose release decreases substantially, renal gluconeogenesis increases by approximately twice liver gluconeogenesis. In this sense, the hepatic and renal glucose release into the circulation in the postabsorptive state correspond to the 25-30% and 20-25% of total glucose, respectively, while in postprandial state, hepatic gluconeogenesis is reduced by $\sim$80% and the release of glucose molecules generated via this pathway decreases as these molecules are largely directed into the formation of hepatic glycogen. As a consequence of these changes, renal gluconeogenesis increases accounts for $\sim$60% of postprandial endogenous glucose release [178].

3.2.3.4 Gastrointestinal tract

The gastrointestinal (GI) tract is an organ system where humans take food, digest it to extract and absorb energy and nutrients, and expel the remaining waste as feces. The mouth, esophagus, stomach, and intestines are part of the gastrointestinal tract. However, glucose homeostasis models in the literature include the gastrointestinal tract as a whole organ disregarding physiological functions and glucose consumption of the stomach and small intestines as separated organs involved in glucose metabolism.

Meal is ingested through mouth and enters in the stomach to be mixed. The rate at which nutrients are passed from the stomach to the duodenum, known as gastric emptying rate, is a key determinant of postprandial glucose flux. In the fed state, glucose homeostasis becomes more complex as the gastrointestinal tract becomes a second source of (exogenous) glucose. Marked and rapid changes in glucose flux occur as a result of the considerable inflow of meal-derived glucose into the circulation [197]. The delivery of nutrients from the gastrointestinal tract occurs through an important ratelimiting mechanical step in the form of gastric emptying rate: the rate at which the pylorus allows small boluses of gastric content to pass into the duodenum for downstream absorption.

Importantly, neither insulin nor glucagon has direct effects on gastric emptying and exogenous glucose diffusion from the gastrointestinal tract [128]. However, the influx of glucose is accompanied by secretion of several other glucoregulatory hormones including amylin from β-cells in the pancreas and glucose-dependent inhibitory peptide (GIP), glucagon-like peptide-1 (GLP-1), and cholecystokinin (CCK) from endocrine cells in the small intestine. Endocrine cells in the small intestine collectively influence glucose homeostasis via several mechanisms of action including regulation of insulin and glucagon responses, as well as the modulation of nutrient passage from the gastrointestinal tract to appropriate tissue stores [120; 175; 220].

A key contribution of the GI tract over glucose homeostasis is the incretin effect. This physiological response came from the observation that an oral glucose load results in an augmented insulin response compared to the response observed when intravenous glucose administration replicates the same changes in plasma glucose [189; 198]. In other words, when glucose is ingested orally, an augmented β-cell response is observed as a result of a signal passed from the gut. The two hormones responsible for this effect are GIP and GLP-1. Both GIP, secreted from enteroendocrine K-cells in the proximal small bowel, and GLP-1, secreted from enteroendocrine L-cells in the distal ileum and colon, have a strong insulinotropic effect [75]. Additionally, GLP-1 inhibits postprandial glucagon secretion in a glucose-dependent way, slows gastric emptying, and reduces food intake, contributing to postprandial glucose regulation [121]. Regarding the role of the stomach in glucose metabolism, the stomach must consume glucose to generate the power necessary to carry out the digestion process. Although glucose consumption in the stomach is relatively low, it can affect the glucose concentration in the bloodstream.

3.2.3.5 Brain

The human brain depends on glucose as its main source of energy; neurons have the highest energy demand [122], requiring continuous delivery of glucose from blood. Glucose metabolism provides the fuel for physiological brain function through the generation of ATP, the foundation for neuronal and non-neuronal cellular maintenance, as well as the generation of neurotransmitters. Therefore, tight regulation of glucose metabolism is critical for brain physiology and disturbed glucose metabolism in the brain underlies several diseases affecting both the brain itself as well as the entire organism. Glucose in the brain is required to provide the precursors for neurotransmitter synthesis and the ATP to fuel their actions. Furthermore, glucose is important for the brain's energy demands not related to signaling. Cellular compartmentation of glucose transport and metabolism is intimately related to local regulation of blood flow, and glucose-sensing neurons govern the brain-body nutrient axis. Glucose metabolism is connected to cell death pathways by glucose-metabolizing enzymes [176]. Thus, disruption glucose delivery pathways and metabolism leads to debilitating brain diseases.

The brain uses about 120g of glucose daily: 60-70% of the total body glucose metabolism. The brain has little stored glucose, and no additional sources of stored energy. Brain function begins to become seriously affected when glucose levels fall below $40 mg/dL$. Levels of glucose significantly below this can lead to permanent damage and death. The brain cannot use fatty acids for energy (fatty acids do not cross the blood-brain barrier), but ketone bodies can enter the brain and can be used for energy under hypoglycemia conditions. In this sense, the brain can only use glucose, or, under conditions of starvation, ketone bodies (acetoacetate and hydroxybutyrate) for energy.

3.3 Diabetes mellitus (DM)

Diabetes mellitus is a chronic condition that occurs when the body is exposed to uncontrolled levels of glucose in the blood either because the body cannot produce insulin or it is not able to use efficiently the amount produced [67]. The lack of insulin or the inability of the cells to respond to insulin leads to high levels of blood glucose, or hyperglycaemia, which is the hallmark of diabetes. Hyperglycaemia, if left unchecked over a long term, can cause damage to various body organs, leading to the development of disabling and life-threatening health complications such as cardiovascular disease, neuropathy, nephropathy and eye disease, among others. On the other hand, when the level of glucose in the blood drops below normal, people are under hypoglycemia condition. Symptoms of hypoglycemia tend to come on quickly and can vary from person to person. Severe hypoglycemia is when the blood glucose level becomes so low that people are unable to treat themselves and need help from another person. Severe hypoglycemia is dangerous and needs to be treated right away. If appropriate management of diabetes is achieved, these serious complications can be delayed or prevented.

In spite of many known diabetes variants, there is a consensus among the three most widespread types: Type 1, Type 2, and gestational diabetes. There are also some less common types of diabetes which include monogenic diabetes and secondary diabetes. Monogenic diabetes is the result of a single genetic mutation in an autosomal dominant gene rather than the contributions of multiple genes and environmental factors as seen in type 1 and type 2 diabetes. Examples of monogenic diabetes include conditions like neonatal diabetes mellitus and maturity-onset diabetes of the young. Around 1-5% of all diabetes cases are due to monogenic diabetes [92; 187]. Secondary diabetes arises as a complication of other diseases such as hormone disturbances (e.g., Cushing's disease or acromegaly), diseases of the pancreas (e.g., pancreatitis) or as a result of drugs (e.g., corticosteroids) [82].

Type 1 diabetes is caused by an autoimmune reaction where the immune system attacks the insulin-producing beta cells at the islets of the pancreas gland. As a result, the body produces very little to none insulin. The causes of this destructive process are not fully understood but a combination of genetic susceptibility and environmental triggers such as viral infection, toxins or some dietary factors have been implicated [259]. People with type 1 diabetes need daily insulin injections in order to maintain glucose levels in the proper range [65]. Unfortunately, hypoglycemia condition is more common in people with type 1 diabetes due to the treatment insulin-dependent. People with type 1 diabetes, with proper daily insulin treatment, regular blood glucose monitoring, and maintenance of a healthy diet and lifestyle can live a healthy life and delay or avoid many of the complications associated with diabetes.

Type 2 diabetes is the most common type of diabetes, accounting for around 90% of all cases of diabetes [39]. In type 2 diabetes, hyperglycaemia is the result of an inadequate production of insulin and inability of the body to respond to insulin, which is known as insulin resistance. During a state of insulin resistance, insulin is ineffective and therefore initially prompts an increase in insulin production to reduce rising glucose levels but over time a state of inadequate insulin production can be developed. T2DM is more common in older adults, but it is increasingly seen in children, adolescents and younger adults due to rising levels of obesity, physical inactivity, and a poor diet. The causes of T2DM are not completely understood but there is a strong link with overweight and obesity and with

increasing age as well as with ethnicity and family history [119]. The cornerstone of T2DM treatment is healthy lifestyle which includes the adoption of a healthy diet, increased physical activity, smoking cessation plan, and a healthy body weight. If attempts to change lifestyle are not adequate to control blood glucose levels, oral medication is usually initiated for treatment of hyperglycaemia with metformin being it the most commonly used initial treatment.

4

Modeling Glucose Homeostasis

Glucose homeostasis has been modeled from the 1960s to look for controlling and describing blood glucose levels under health different situations. However, the corresponding models describe all involved processes in a highly reduced way, without considering many crucial aspects of this important regulatory mechanism in the human body. In this chapter, an alternative model of glucose homeostasis in humans is presented as the result of linking together five submodels: stomach, small intestine, liver, pancreas, and kidneys. The integration of the above five submodels with the glucose consumers like the brain, muscles, and adipose tissues is presented in a plantwide framework. The plantwide concept is first introduced to backup the proposed hypothesis to develop the whole model. The intention here is to demonstrate the nature of each organ as a system of biochemical reactions and transport and transfer processes and therefore, to show the similarities with usual engineering processes in terms of modeling, analysis, and identification.

4.1 Process analysis using plantwide view

Plantwide control is a holistic approach about integrating process design with process control at the whole plant level. The objective of this approach is to ensure a stable and flexible operation when the plant is affected by different disturbances, including major changes in the production rate and in the quality of raw materials. Also, plantwide control is useful in highly complex study cases. I use this approach the foundation to develop a PBSM of the glucose metabolism in the human body since this natural mechanism involves several organs, which are interconnected to each other through the circulatory system. In this section, plantwide view and its main characteristics are introduced. Then, the human body is analyzed like a chemical plant from a plantwide point of view.

4.1.1 What is plantwide view?

A process is a set of activities, actions, treatments or operations that interact among them to achieve a desired result. A chemical process consists of various interconnected units with material and energy recycle [132]. A process usually refers to the 'process itself' (without any control system) whereas a plant may be any system to be controlled (including a partially controlled process). In the chemical engineering community, the term plant has a somewhat different meaning, namely as the whole factory which consists of many process units [144]. The term plantwide is derived from this meaning of the word plant. Plantwide view considers all plant connections, all plant pieces of equipment, and

any information exchange among them. In this sense, plantwide approach determines a connectivity structure of the process and uses it as the basis for any plant description as a whole in spite of the plant complexity or inherent high number of pieces of equipment connected.

Two main process engineering tasks are associated to the concept of plantwide view: plantwide design and control, both useful to understand the concept of plantwide view used in this doctoral thesis. The plantwide design in chemical processes is a tool that suggests the use of energy recovery structures in order to minimize energetic losses to the environment, and the use of mass recycles in order to maximize the conversion and minimize the waste of raw materials [43]. On the other hand, plantwide process control involves the systems and strategies required to control an entire chemical plant consisting of many interconnected unit operations [163]. Plantwide control uses the knowledge of interconnections and interactions among process units in order to overcome the new challenges arising with the consideration of mass recycles and energy recover networks inside a highly interconnected chemical plant. In addition, the plantwide approach uses all available information about individual subsystems to form a complete map of signals about the current state of the plant as a whole.

Combining the previous concepts, the plantwide view is a way to analyze a real object considering the interactions among its declared parts. Plantwide view tries to minimize information losses coming from the real object partition. It must be noted that real object partition is a valid tool to reduce the complexity to build a PBSM. The plantwide view takes advantage of the phenomenological knowledge to make the appropriate connections among different units (seen as partitions from the overall plant) and follows the entire process sequence. In addition, plantwide view considers any connection different to mass and energy as service network transporting, together with energy or mass, information among partitions. In addition, plantwide view is not directly concerned with the behavior of each partition involved in the process plant individually, but the structure after object partition and the performance of the entire modeled object is considered.

4.1.2 Main characteristics of plantwide view

As mentioned before, plantwide process design and control involves the systems and strategies required to design and to control an entire chemical plant consisting of many interconnected unit operations [163]. The plantwide view is useful to determine how the best controlled, manipulated, and measured variables are chosen in the plant, and according to that select suitable multi-loop control structures. This is because plantwide control deals with the structural decisions of the control system, including what to control and how to pair the variables to form control loops [231]. Although there is not a unique way to design control systems for an entire plant, the literature has been inclined towards hierarchical control strategies [117]. Furthermore, a design procedure generally involves iteration of individual steps until a satisfactory design is achieved. In this way, the author in [231] has developed a design procedure based on the intrinsic hierarchical nature of plantwide control systems while incorporating the best aspects of top-down and bottom-up design approaches.

Missing from many control system design methodologies, even hierarchical ones, is the important role that decomposition and decentralization play in a plantwide design approach. Procedures that lead to decomposition of the overall design into smaller subprob-

lems can be advantageous. Even highly integrated plants do not require a multivariable approach linking all of the controlled variables with all of the manipulated variables [71]. The extent to which a plantwide control system can be decentralized into smaller control systems designed to work at the process unit level invariably determines how easily the control system can be designed, tuned, and understood by plant operators. Decentralized control system designs generally are more robust when operating conditions change and are more tolerant to failures of individual components [210]. The plantwide control design allows to divide the whole plant into smaller subsystems as individual sections, that is, to do a decomposition of the process to simplify control system and to make easier the multivariable control. This characteristic provides a direct analogy with homeostatic processes in the human body.

The identification of the disturbances that a control system must handle is one of the most important though least addressed issues even nowadays. Occasionally, it is important for the control system to track targets that move. Much more often, the control system is required to reject disturbances that affect the process. Plantwide control design is highly dependent on the disturbances that are assumed. The capability to identify the most difficult disturbances for the control system to manage would be a valuable step in the design process, due to actually this is a challenge of the plantwide control design [210]. For this reason, the importance of confidence that the plantwide control strategy will always take the plant to an acceptable, perhaps optimal, operating point after a persistent disturbance enters the plant cannot be overstated [191]. What characterizes plantwide design and control can be applied to the human body, the constructed PBSM that will be shown in next section exhibit common points with the plantwide concept. The control in the human body seems to be decentralized, each organ involved in the glucose homeostasis seems to exert a specific control function and can be modeled like a submodel. All submodels are coupled to a whole model linked by the blood. Also, this natural mechanism is highly complex and disturbed, and the system is too hard of controlling under several natural disturbances. Thus, the plantwide view is a good conceptual support to use in the construction of a PBSM representing the dynamic of the glucose in the bloodstream.

4.1.3 The human body like a chemical plant: an analogy

The human body can be considered a complex chemical plant where multiple biochemical reactions, physical, and physiological processes are occurring simultaneously. Each organ is a process unit belonging to the plant and has specific functions essential to the proper operation of the plant as a whole. At the same time, each organ is composed of smaller subunits, the cells, that inside carry out a manifold of biochemical reactions at the cellular level vitals to the good working of the entire plant. As such, the organs are communicated by the circulatory system transporting blood and the lymphatic system that carries a clear fluid derived from the interstitial fluid, directionally towards the heart. Blood transports all substances (glucose, oxygen, sodium, water, calcium, etc.) needed by the cells of the organs to perform their physiological functions. Also, blood transports the waste products of all cells of the body along with lymph, which contains lymphocytes and cellular debris together with bacteria and proteins. For glucose homeostasis, the blood and human circulatory system are assumed to be the media transporting all the species of interest among the organs as a field bus transporting specific information in an industrial control

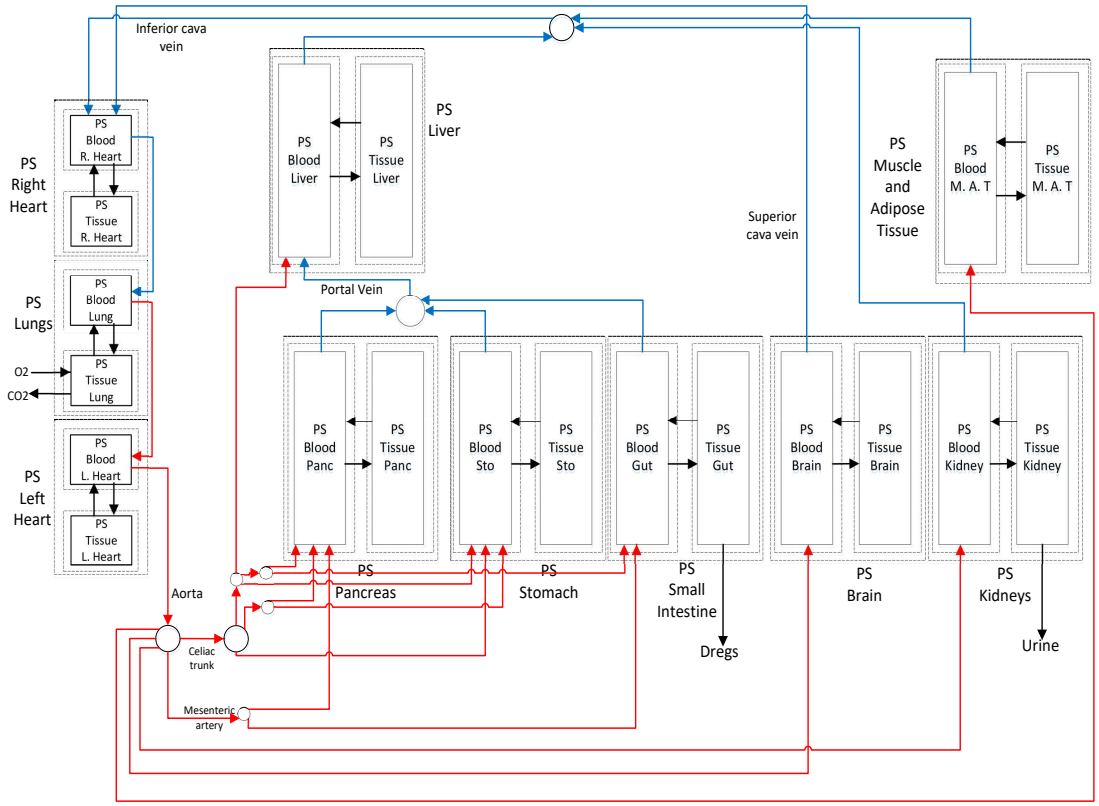

FIGURE 4.1. Representation of the human body in process systems. In red arterial blood and in blue venous blood.

environment. On the other hand, organ tissues act as a solid substratum where different hormones and other substances are produced and consumed.

A fieldbus is a useful way to connect instruments in a manufacturing plant [102]. The field bus works on a network structure which typically allows daisy-chain, star, ring, branch, and tree network topologies, similar to the blood that connects and communicates the organs and the systems in the human body. The circulatory system can then be seen as a field bus with only one communication point at the controller level and multiple (hundreds) analog and digital connection points.

Regarding the proposed model, the organs are considered as units belonging to an industrial plant (the human body) in a plantwide view. Each unit is then represented by multiple process systems to cover the needed organ functions related to glucose homeostasis. In a systematic way, every organ is partitioned in at least two process subsystems, one representing the blood acting as the transporting media (carrying out the produced and consumed nutrients in the organ), and the other representing the organ tissue, where the specialized cells are located. A schematic diagram of the human body's partitioning can be seen in Figure 4.1, showing the different Process Systems (PS) involved in the homeostatic mechanism of interest. A partition represents a detail level, which can be specified according to the different substances that enter and leave at any time. Although the glucose dynamics are mainly considered in the macro scale, sometimes is necessary to go back and forth from one size scale to another, e.g., cellular scale.

The effect of the smaller scales is modeled by some constitutive or assessment equations, always focusing on the outcome at the larger scale. Regarding the current work, I consider one level as the whole body, and at a lower level, the organs and their interactions with different components affecting glucose homeostasis. The top-level would then deal with the blood flows among the organs and the organ level would describe the details within the organs. Each constitutive or assessment equation is a submodel. Each formulated submodel provides knowledge of the smallest scales to its original subsystem, creating thus, a multiscale model. Moreover, the partition of the organs is possible because under real conditions, the organs are composed by tissues composed by cells. In turn, the cells belonging to a specific tissue produce and consume nutrients that are subsequently exchanged with the flow blood that irrigates the organ. For this reason, the application of the conservation principle is feasible, because there is not accumulation of mass in the organs (components are either released or consumed), and the proposed methodology for construction of PBSM then holds.

4.2 Modeling the organs involved in glucose homeostasis

Although glucose homeostasis is a unique mechanism in the human body, it involves several organs, and each one of them plays an important role to regulate the glucose levels in the bloodstream. In this sense, each organ is considered a submodel of a complete model representing the glucose homeostasis, which is introduced in next section. In the submodels, the reactions within the organ tissue and from the irrigating bloodstream are taken into account, without considering intracellular effects. Furthermore, the corporal temperature keeps constant, for this reason, balances of thermal energy are not developed. In a similar way, balances of mechanical energy are not considered since I assume the blood pressure constant. Only one mechanical energy balance was considered to calculate the glucose consumption by the stomach wall during the digestion process. The mathematical models are developed with as many interpretable parameters as the available phenomenological knowledge allows. The identification of the parameters was done manually, and no numerical method was applied to carry out the identification. Because of most parameters of the models are interpretable, the parameter identification of the models was not a difficult task. Most parameters were set at known numeric value (taken from literature as cited in every model), leaving only to identify the reaction kinetics k_0 and the activation energies Ea. These parameters were adjusted following an iterative proof of model response after changing the parameter value. To adjust reaction kinetics (k_0), the activation energies (Ea) were set at a mean value of the boundary range regarding the reported one for biochemical reactions [230]. Once the kinetics were adjusted, the activation energies were identified following the proof and change manual method. In the small intestine model, the mass transfer coefficients were additional parameters to identify. In this case, the mass transfer coefficients were blocked to first identify the reaction kinetics and activation energies, following the same manual form of identification of the other models. Once the reaction kinetics and activation energies were adjusted, the mass transfer coefficients were identified. Additionally, the mathematical models presented in this section are based on conservation principles and describe the role of each organ involved in the glucose homeostasis in humans. The methodology followed to construct the mathematical models is proposed in [123]. The benefits of the PBSM approach are established as a way to consolidate/accumulate knowledge which can be used further and connected with new findings. Note that the abstraction applied during the model construction does not aim

to offer an explanation about the real mechanism of the modeled process. Instead, the abstraction looks for facilitating the user a fast way to model the process without losing the rigor and formalism. In addition, a modular construction of a PBSM helped to model complex processes whether the process can be broken into smaller tractable parts and each one of those parts can be modeled by pre-stated phenomena. Below, the steps of the methodology to construct PBSMs are presented for each organ, with the exception of steps 4, 8, and 9. Step 4 is the development of the model basic structure, step 8 is the degrees of freedom analysis to solve the model as indicates in step 9. The models were programmed and solved using MatLab®.

4.2.1 Pancreatic model

The pancreas is an essential organ in the glucose regulation due to its hormonal secretions and endocrine functions. For this reason, a PBSM to describe the role of the pancreas in the glucose metabolism in humans is presented, although many physiological functions of this organ are still unknown from medical science. The model was constructed based on phenomena taken place. However, some parameters was defined by empirical correlations found them in the literature due to the natural mechanisms in the cells that produce and secrete hormones is matter of study.

4.2.1.1 Process description and model objective

As mentioned in subsection 3.2.3.1, this thesis is focused on the endocrine function of the pancreas due its key role in metabolism and energy homeostasis by releasing various pancreatic hormones. Pancreatic hormones regulate glucose homeostasis, but the principal level of control on glycaemia by the islet of Langerhans depends largely on the coordinated secretion of glucagon and insulin. Endocrine cells in the pancreas secrete specific hormones in response to external excitations, such as meal intake or stress, via humoral, neural or hormonal signaling pathways [89]. The pancreas is irrigated by the celiac artery as shown in Figure 4.2. Islets of Langerhans receive substances from blood to stimulate the hormonal secretions. Glucose goes through blood vessels irrigating the pancreas and enters the interstitial liquid to get inside $\beta-$cells and glycolysis takes place. Glycolysis in the $\beta-$cells produces ATP to stimulate insulin secretion [141] throughout potassium and calcium channels. Insulin secretion is also modeulated by gastrointestinal hormones, especially those released by the gut, such as gastric inhibitory peptide (GLP-1) and cholecystokinin. These hormones are released into the bloodstream after a meal. Glucose circulating in the bloodstream also gets inside α-cells to carry out the glucose phosphorylation. The phosphorylated glucose produces pyruvate to be used in the Krebs cycle and to generate ATP. Accumulation of ATP inside α-cells closes potassium channels and opens calcium channels to secret glucagon [130]. Waste substances of reactions and produced components in the pancreas are drained into superior mesenteric vein (see Figure 4.2) and later in the portal vein. The main objective of the model construction is to know how blood glucose concentration changes when insulin and glucagon are secreted into the bloodstream. Also, how glucose levels are affected by basal glucose consumption in the pancreas. It should be noted that the details of secretions previously described are not considered in this first approach to pancreas model, i.e., hormonal production occurring inside the specific cells are not modeled.

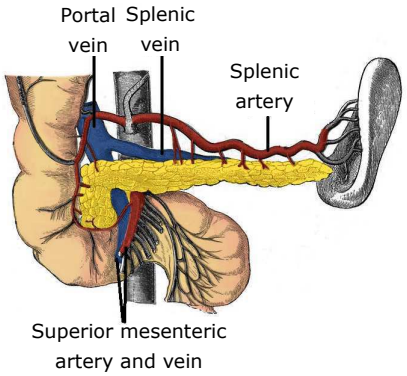

FIGURE 4.2. Blood irrigation in the pancreas.

4.2.1.2 Modeling hypothesis and level of detail

Although hormones secretion occurs at the cellular level, this model is considered to be macroscopic (lumped parameters). In this regard, hormone-producing biochemical pathways are not explicitly considered. The pancreas is modeled as two perfectly stirred tanks disposed of as shown in Figure 4.3. The tank representing the islets of Langerhans contains pancreatic cells and hormones produced ready for being secreted. This assumption is according to the real physiology since pancreatic cells produce and store hormones ready to be released in response to external stimuli. In this manner, modeling at the cellular level is circumvented to avoid excessive complexity. The other tank represents the blood feeding the pancreas, which receives the arterial blood via celiac artery. The substances of interest, such as oxygen and glucose, are transported to the islets from the circulatory system to be used by pancreatic cells as a requirement for their survival. Glucose and oxygen are consumed in demand by the pancreatic cells and that consumption is proportional to the number of cells contained in the islet. In addition, in this way, the pancreatic cells detect the concentration of glucose in the blood, through glucose transport function GLUT2 in β-cells and SLC2A1 in α-cells, to produce hormones. However, precursors needed for glucagon and insulin synthesis are not considered here. The products of cellular respiration reaction, mainly water and carbon dioxide return to the blood and leave the pancreas by venous blood.

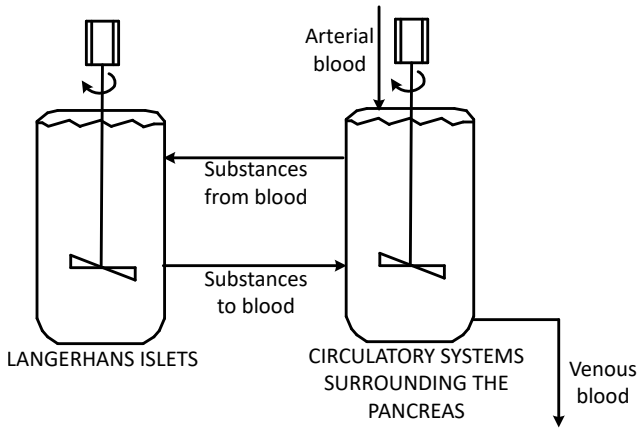

FIGURE 4.3. Proposed analogy for modeling the role of the pancreas in the glucose metabolism.

4.2.1.3 Process system definition

According to the presented hypothesis, the pancreas is divided in two process systems (PS): *PSI* is the blood irrigating the pancreas tissue, *PSII* represents the islets of Langerhans containing β-cells and α-cells, and produced insulin and glucagon available to be secreted. Arterial blood enters to the pancreas via celiac artery represented by stream 1. Stream 3 transports substances needed by α and β cells to secret glucagon and insulin, respectively. Products of the reactions taking place in the islets return to the bloodstream by means of flow 4, and continue in the blood circulation leaving the pancreas by venous blood represented by stream 2. In Figure 4.4, the block diagram representing the partition of the pancreas in the glucose metabolism can be observed.

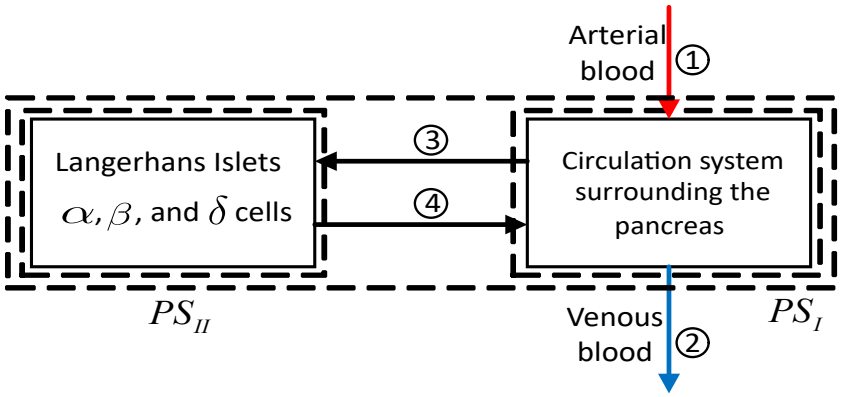

FIGURE 4.4. Block diagram of the considered process systems. Role of the pancreas in glucose metabolism.

4.2.1.4 The basic structure of the model

The mass balances were developed for both *PSs*: *PSI* and *PSII*, and the set of equations that give relevant information to the model are presented as the basic structure of the model as follow:

$$\dot{m}_2 = \dot{m}_1 \tag{4.1}$$

$$\frac{dw_{i,2}}{dt} = (w_{i,1}\dot{m}_1 - w_{i,2}\dot{m}_2 - \dot{m_{i,3}})\frac{1}{M_I} \tag{4.2}$$

$$\frac{dw_{j,2}}{dt} = (w_{j,1}\dot{m}_1 - w_{j,2}\dot{m}_2 + \dot{m_{j,4}})\frac{1}{M_I} \tag{4.3}$$

$$\dot{m}_4 = \dot{m}_3 \tag{4.4}$$

$$\frac{dw_{i,II}}{dt} = (\dot{m}_{i,3} - r_{cons,i})\frac{1}{M_{II}} \tag{4.5}$$

$$\frac{dw_{Ins,II}}{dt} = (-\dot{m}_{Ins,4} + r_{secr,Ins})\frac{1}{M_{II}} \tag{4.6}$$

$$\dot{m}_{Gn,4} = r_{sec,Gn} \tag{4.7}$$

$$\tag{4.8}$$

with i = glucose (G) and oxygen (O), and j = insulin (Ins) and glucagon (Gn). The meaning of the symbols that represents variables, parameters, and constants is reported in Table 4.1.

4.2.1.5 Variables, structural parameters, and structural constants

This step establishes the model variables, structural parameters, and constants of the model from its basic structure. The variables and the structural parameters are reported in Table 4.1. In this basic structure, there are no constants.

4.2.1.6 Constitutive and assessment equations for structural and functional parameters, and definition of constants

Constitutive and assessment equations to define both structural and functional parameters of the pancreatic model are reported in Table 4.2. If the parameter belongs to the model's basic structure then the parameter is classified as structural as shown in the column called "type" in the table. Contrary, if the parameter is described by means of a constitutive or assessment equation, then the parameter is classified as functional, according to the corresponding specification level. Symbols $C_{i,2}$, $C_{i,II}$, $C_{Ins,2}$, and $C_{Ins,II}$ are the variables $w_{i,2}$, $w_{i,II}$, $w_{Ins,2}$, and $w_{Ins,II}$, respectively, but in mass units. Likewise occurs with $C_{O,II}$. Additionally, the structural parameter $\dot{m}_3$ is not defined by an equation or numerical value because it is only used as verification of the variable $\dot{m}_4$.

$$r_{Ins,ph1} = r_{max,ins1} \frac{\frac{dC_{G,II}^{n_{ins1,gluc}}}{dt}}{\frac{d_C^{n_{ins1,gluc}}}{dt} + Ct_{Hf,ins1,gluc}^{n_{ins1,gluc}}} \sigma_{il,g}(C_{G,II}) \tag{4.9}$$

$$r_{Ins,ph2} = r_{max,ins2} \frac{C_{G,II}^{n_{ins2,gluc}}}{C_{G,II}^{n_{ins2,gluc}} + C_{Hf,ins2,gluc}^{n_{ins2,gluc}}} \tag{4.10}$$

In response to a stepwise increase of glucose, normal, functioning islets release insulin in a biphasic manner: a relatively quick first phase consisting of a transient spike of 5-10 min is followed by a sustained second phase that is slower and somewhat delayed. Both phases are represented by Equations 5.44 and 5.45. Total insulin release is obtained as the sum of first-and second-phase releases and an additional modulating function to account for the limiting effect of oxygen availability.

4.2.1.7 Results

In this section, dynamic blood of glucose, insulin, and glucagon concentration coming out of the pancreas through the superior mesenteric vein are reported in Figure 4.5. A comparison with a set of experimental data taken from the literature [40; 243] is also presented. A parametric adjustment was carried out with compensation factors corresponding to degradation of the insulin and glucagon hormones. The responses of the pancreas model for the three substances of interest follow the same trajectory of the curves of the data set found. Red lines represent the model of the pancreas, and black lines correspond to the data set taken from the literature. Glucose concentration (upper figure) reaches a

TABLE 4.1. Variables and structural parameters of the pancreas model.

Symbol	Physical meaning
Variables	
$\dot{m}_2$	Mass flow of blood coming out of the pancreas.
$w_{i,2}$	Mass fraction of glucose and oxygen coming out of the pancreas by superior mesenteric vein.
$w_{j,2}$	Mass fraction of insulin and glucagon coming out of the pancreas by superior mesenteric vein.
$w_{i,II}$	Mass fraction of glucose and oxygen being transferred to the islets of Langerhans to be consumed by the pancreatic cells.
$w_{Ins,II}$	Mass fraction of insulin being secreted from the islets of Langerhans to the circulation.
$\dot{m}_{j,4}$	Mass flow of insulin and glucagon being secreted to the circulation from islets of Langerhans.
$\dot{m}_{Gn,4}$	Mass flow of glucagon being secreted by $\alpha-$cells to the circulation.
Structural parameters	
$\dot{m}_1$	Mass flow rate of blood entering in the pancreas (stream 1).
$w_{i,1}$	Mass fraction of glucose and oxygen entering the pancreas.
$w_{j,1}$	Mass fraction of insulin and glucagon entering the pancreas.
$\dot{m}_{i,3}$	Mass flow of component i entering the islets of Langerhans.
$\dot{m}_{j,4}$	Mass flow of component j being secreted to the circulation.
M_I	Mass of blood irrigating the pancreas.
$\dot{m}_3$	Mass flow rate of basal glucose and oxygen required by α and β-cells (stream 3).
$r_{cons,i}$	Kinetic of consumption of component i in the islets of Langerhans.
$r_{secr,j}$	Kinetic of secretion of component j by the islets of Langerhans.
M_{II}	Mass of the islets of Langerhans.

i indicates glucose (G) and oxygen (O).
j indicates pancreatic hormones insulin (Ins) and glucagon (Gn).

TABLE 4.2. Constitutive and assessment equations to define structural and functional parameters of the pancreas model.

Symbol	Type	Description	Equation
$\dot{m}_1$	Struc.	Mass flow rate at current 1, blood entering in the pancreas.	$\dot{m}_1 = \dot{V}_1 \rho_b$
$\dot{V}_1$	Func.1	Volumetric flow in arterial blood.	$\dot{V}_1 = 3.833 * 10^{-6}\ m^3/s$
ρ_b	Func.1	Density of the blood.	$\rho = 1060 kg/m^3$
$w_{i,1}$	Struc.	Mass fraction of component i entering the pancreas.	$w_{i,1} = C_{i,1} * \frac{1}{\rho_b} * \mathfrak{M}_\mathfrak{i}$
$C_{i,1}$	Func.1	Concentration of component i at blood irrigating the pancreas (stream 1).	$C_{i,1} = Datum_i$
$\mathfrak{M}_\mathfrak{i}$	Func.1	Molecular mass of the component i.	$\mathfrak{M}_\mathfrak{i} = Datum_i$
$w_{j,1}$	Struc.	Mass fraction of component j entering the pancreas.	$w_{j,1} = C_{j,1} * \frac{1}{\rho_b} * \mathfrak{M}_\mathfrak{j}$
$C_{j,1}$	Func.1	Concentration of component j at blood irrigating the pancreas (stream 1).	$C_{j,1} = Datum_j$
$\mathfrak{M}_\mathfrak{j}$	Func.1	Molecular mass of the component j.	$\mathfrak{M}_\mathfrak{j} = Datum_j$
$\dot{m}_{i,3}$	Struc.	Mass flow of component i entering the islets of Langerhans.	$\dot{m}_{i,3} = A_s * D_{i-t} * \frac{(C_{i,2} - C_{i,II})}{L} * \mathfrak{M}_\mathfrak{i}$
A_s	Func.1	Mass transfer area of islets of Langerhans.	$A_s = 0.1132 m^2$
D_{i-t}	Func.1	Diffusion coefficient of the component i in the islet of Langerhans.	$D_{i-t} = Datum_i$
L	Func.1	Length of mass transfer.	$L = 150 \mu m$
$\dot{m}_{Ins,4}$	Struc.	Mass flow of insulin being secreted from islets of Langerhans.	$\dot{m}_{Ins,4} = A_s * D_{Ins-t} * \frac{(C_{Ins,2} - C_{Ins,II})}{L} * \mathfrak{M}_\mathfrak{j}$
D_{Ins-t}	Func.1	Diffusion coefficient of the insulin in the islet of Langerhans.	$D_{Ins-t} = 0.05 * 10^{-9} m^2/s$
M_I	Struc.	Mass of blood irrigating the pancreas.	$M_I = \rho_b * V_b$
V_b	Func.1	Blood volume irriganting the pancreas.	$V_b = 1.65 * 10^{-4} m^3$
M_{II}	Struc.	Mass of the islets of Langerhans.	$M_{II} = \rho_{Isl} * V_{Isl}$
ρ_{Isl}	Func.1	Density of islets of Langerhans.	$\rho_{Isl} = 1.109 * 10^{-3} kg/m^3$
V_{Isl}	Func.1	Volume of islets of Langerhans.	$V_{Isl} = 2.02 * 10^{-6} m^3$
$r_{cons,G}$	Struc.	Kinetic of consumption of glucose in the islets of Langerhans.	$r_{cons,G} = r_{max,G} \frac{C_{G,II}}{C_{G,II} + C_{Hf,G}}$
$r_{max,G}$	Func.1	Maximum reaction rate of glucose consumption.	$r_{max,G} = 0.028 mol/m^3 - s$
$C_{Hf,G}$	Func.1	Concentration corresponding to half-maximal response of glucose consumption.	$C_{Hf,G} = 10 * 10^{-3} mM$

i indicates glucose (G) and oxygen (O).
j indicates pancreatic hormones insulin (Ins) and glucagon (Gn).

Symbol	Type	Description	Equation
$r_{cons,O}$	Struc.	Kinetic of consumption of oxygen in the islets of Langerhans.	$r_{cons,O} = r_{max,O}\frac{C_{O,II}}{C_{O,II}+C_{Hf,O}}\varphi_{O,G}*(C_{G,II}) * \delta(C_{O,II} > C_{Cr,O})$
$r_{max,O}$	Func.1	Maximum rate of oxygen consumption.	$r_{max,O} = 0.034 mol/m^3 - s$
$C_{Hf,O}$	Func.1	Concentration corresponding to half-maximal response of oxygen consumption.	$C_{Hf,O} = 1 * 10^{-3} mM$
$\varphi_{O,G}$	Func.1	Oxygen consumption rate with blood glucose concentration variations.	$\varphi_{O,G}(C_{G,II}) = \varphi_{sc}(\varphi_{base} + \varphi_{metab}\frac{C_{G,II}^{n_{ins2,gluc}}}{C_{G,II}^{n_{ins2,gluc}}+C_{Hf,ins2,gluc}^{n_{ins2,gluc}}}$
δ	Func.1	Step-down function to account for necrosis and cut the oxygen consumption of those tissues where the oxygen concentration falls below a critical value ($C_{Cr,O}$).	$\delta = C_{O,II} - 1 * 10^{-4}$
$C_{Cr,O}$	Func.1	Critical value of oxygen concentration into the islets of Langerhans.	$C_{Cr,O} = 0.1 \mu M$
φ_{sc}	Func.2	Scaling factor to maintain the consumption rate at low (3 mM) glucose.	$\varphi_{sc} = 1.8$
φ_{base}	Func.2	Basal rate of oxygen consumption.	$\varphi_{base} = 0.5$
φ_{metab}	Func.2	Oxygen consumption as a function of metabolic demand.	$\varphi_{metab} = 0.5$
$n_{ins2,gluc}$	Func.2	Metabolic component. Hill slope characterizing the shape of the insulin response, second-phase.	$n_{ins2,gluc} = 2.5$
$C_{Hf,ins2,gluc}$	Func.2	Insulin concentration corresponding to half-maximal response of insulin secretion.	$C_{Hf,ins2,gluc} = 7mM$
$r_{secr,Ins}$	Struc.	Kinetic of secretion of insulin from the islets of Langerhans.	$r_{secr,Ins} = (r_{Ins,ph1} + r_{Ins,ph2})\varphi_{i,o}(C_{O,II})$
$r_{Ins,ph1}$	Func.1	Insulin secretion rate, first-phase. Relatively quick first phase consisting of a transient spike of 5-10 min.	See Equation 5.44
$r_{Ins,ph2}$	Func.1	Maximum (second phase) insulin secretion rate.	See Equation 5.45
$\varphi_{i,o}$	Func.1	Modulating function of the insulin secretion.	$\varphi_{i,o} = \frac{C_{O,II}^{n_{ins,O}}}{C_{O,II}^{n_{ins,O}}+C_{Hf,ins,O}^{n_{ins,O}}}$
$r_{max,ins1}$	Func.2	Maximum rate of insulin secretion, first-phase, from the islets of Langerhans.	$r_{max,ins1} = 21 * 10^{-5} mol/m^3 - s$
$r_{max,ins2}$	Func.2	Maximum rate of insulin secretion, second-phase, from the islets of Langerhans.	$r_{max,ins2} = 3 * 10^{-5} mol/m^3 - s$
$n_{ins1,gluc}$	Func.2	Hill slope characterizing the shape of the insulin response, first-phase.	$n_{ins1,gluc} = 2$
$Ct_{Hf,ins1,gluc}$	Func.2	Linear response for a range that likely covers normal physiologic conditions as well as dynamic perifusion conditions.	$Ct_{Hf,ins1,gluc} = 0.03 mM/s$

i indicates glucose (G) and oxygen (O).
j indicates pancreatic hormones insulin (Ins) and glucagon (Gn).

Symbol	Type	Description	Equation
$n_{ins,O}$	Func.2	Hill slope characterizing the shape of the oxygen consumption.	$n_{ins,O} = 3$
$C_{Hf,ins,O}$	Func.2	Oxygen concentration corresponding to half-maximal response of oxygen consumption.	$C_{Hf,ins,O} = 3\mu M$
$\sigma_{il,g}$	Func.2	Modulating function to reduce the glucose gradient-dependent response for islets that are already operating at an elevated second phase secretion rate and to maximize it around $C_{G,II}$ values where islets are likely to be most sensitive.	$\sigma_{i,l,g} = \frac{4C_{G,II}^4 C_m}{(C_{G,II}^4 + C_m^4)^2}$
C_m	Func.3	Glucose concentration where islets are likely to be most sensitive.	$C_m = 5mM$
$r_{secr,Gn}$	Struc.	Kinetic of secretion of glucagon from the islets of Langerhans.	$r_{secr,Gn} = c_0 + \frac{c_1}{c_2 + C_{Ins,2}e}(C_{GE} - C_{G,2})u(C_{GE} - C_{G,2})$
c_0	Func.1	Glucagon basal secretion.	$c_0 = 0.656ng/dL - min$
c_1	Func.1	Glucose action on glucagon.	$c_1 = 2.5441\frac{ng_{Gn}/dL-min}{ng_{Ins}/dL-min}$
c_2	Func.1	Insulin action on glucagon.	$c_2 = -5.2523ng_{Ins}/dL-min$
e	Func.1	Insulin effectiveness.	$e = 1$
C_{GE}	Func.1	Glucose threshold value.	$C_{GE} = 5mM$

i indicates glucose (G) and oxygen (O).
j indicates pancreatic hormones insulin (Ins) and glucagon (Gn).

maximum in 133 mg/dl, the insulin response (medium figure) is directly proportional to glucose variations, while glucagon responses (lower figure) are inverse to glucose variations. The increase in glucose concentration within the islets of Langerhans due to mass transfer from bloodstream causes a decrease of a concentration gradient in the inner of the islets membrane, resulting in a loss of glucose concentration coming out by mesenteric vein, after approximately 100 minutes, as can be seen in Figure 4.5. This result agrees with the physiology.

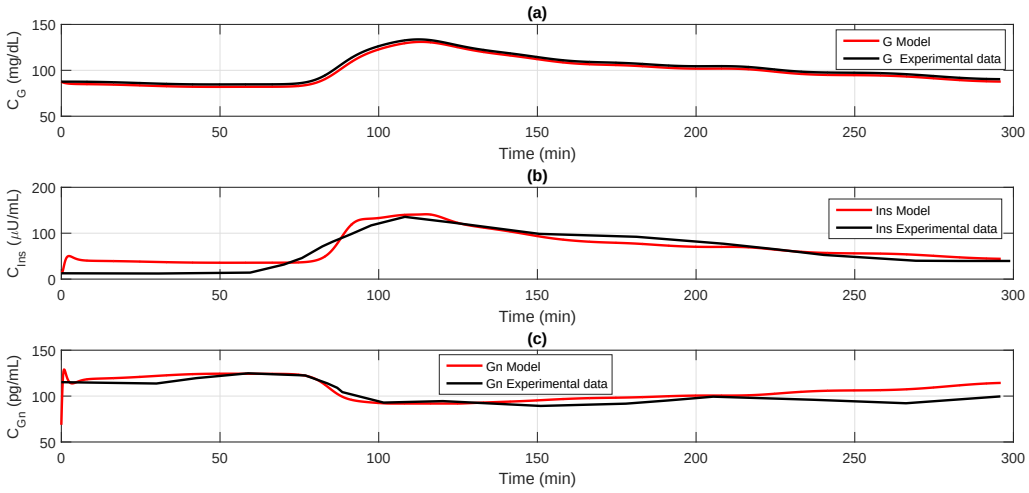

FIGURE 4.5. Concentration of glucose, insulin, and glucagon in the mesenteric vein through which drains the blood that supplies the pancreas. Comparison of the model obtained with a set of experimental data taken from the literature [40; 243].

4.2.2 Hepatic model

A PBSM to describe the role of the liver in glucose homeostasis is proposed. As in the pancreas, a model analogy is used to build the mathematical model. In addition, the liver is considered a whole system, generating a lumped parameters model. A detail of the model development is reported in [182]. The obtained results show the liver is able to regulate the blood glucose levels under hyperglycemia or hypoglycemia conditions.

4.2.2.1 Process description and model objective

The liver is a fundamental organ for glucose regulation in the human body since plays a central role in controlling the rate of uptake and release of glucose. As a curious fact, this is the only organ being irrigated by venous and arterial blood simultaneously. The portal vein carries blood with nutrients and digested substances absorbed from the small intestine together with the hormonal discharge from the pancreas. The portal vein provides 75% of the blood supply to the liver, while the remaining 25% comes through the hepatic artery, which carries blood rich in oxygen from the aorta [83]. The terminal branches of the hepatic artery and the portal vein of the portal triad empty its blood content into small channels called sinusoids. Those sinusoids are low-pressure vascular tunnels that carry blood from the portal triads toward the central vein. The lobule contains millions

of sinusoids that are lined in parallel to groups of highly fenestrated endothelial cells and are surrounded circumferentially by plates of parenchymal cells-hepatocytes allowing the exchange of nutrients and oxygen between the blood and the hepatocytes [49]. Once the hepatocytes carry on all metabolic functions, the resulting substances return to the bloodstream via the hepatic vein.

The liver affects substantially glucose homeostasis by means of three metabolic processes: gluconeogenesis, glycogenesis, and glycogenolysis. During the absorptive phase, the liver removes excess blood glucose by transforming it into glycogen via the glycogenesis pathway, and then by transforming glycogen into triglycerides through glycolysis and liponeogenesis. During the postabsorptive phase, the liver initially restores the normal blood glucose level by breaking down the glycogen stored in the liver via glycogenolysis. When stored glycogen is exhausted the hepatocytes respond by activating an alternate metabolic pathway-gluconeogenesis [49; 241]. Gluconeogenesis is mainly concerned with synthesizing glucose from non-hexose precursors such as lactate, amino acids, and glycerol. The hepatocytes achieve these different metabolic functions by switching through a network with regulation by hormones, like insulin and glucagon, and other effectors [241]. Glycolysis is a metabolic process consisting on a sequence of ten enzyme-catalyzed reactions to produce energy for the cell. In this model this process is only considered as glucose consumption by the liver. In addition, the liver also plays a major role in bile secretion (necessary in lipid digestion in the intestine), and clearance of insulin and toxins such as ammonia and drugs. However, bile production does not affect glucose regulation in the body, therefore it is not included in the model development. Figure 4.6 shows the role of the liver in glucose homeostasis in a schematic way.

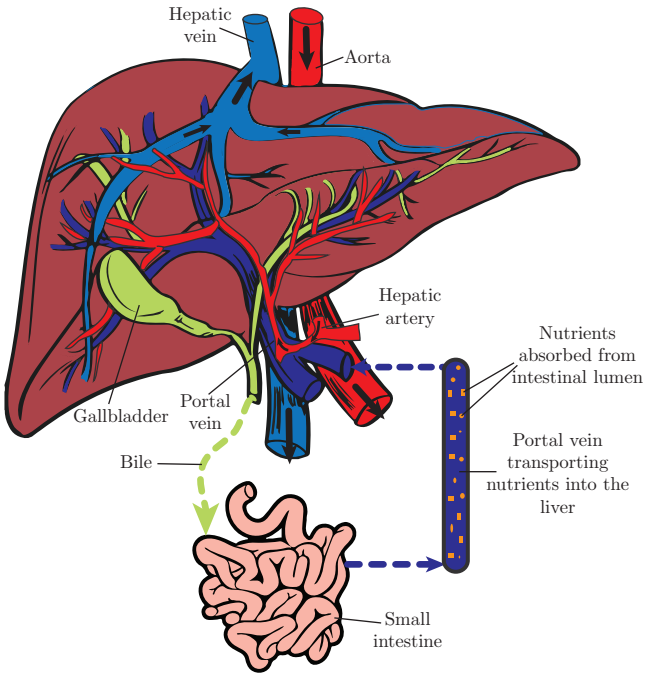

FIGURE 4.6. Representation of the hepatic metabolism in glucose regulation.

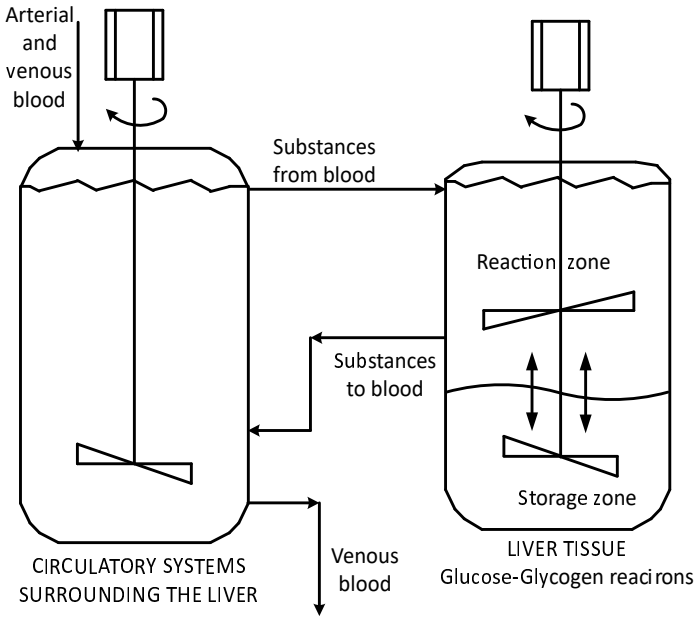

FIGURE 4.7. Analogy used for modeling the role of the liver in glucose metabolism.

4.2.2.2 Modeling hypothesis and level of detail

The model of the liver is developed at macroscopic scale. The hepatic metabolism is analyzed in the hepatocytes as a whole, but metabolic processes at the cellular level are not analyzed. In this regard, the liver is considered as a tank with two immiscible phases. The upper phase behaves like a continuous stirred-tank reactor (CSTR) where all chemical reactions are carried out. The lower phase, on the other hand, is denser (compared to the upper phase), has a perfect agitation, and acts as the glycogen reservoir. This lower phase is never emptied because in the liver there is always a minimal quantity of glycogen that is not synthesized by the liver, remaining as basal glycogen. The reactor's total volume is considered constant to balance the water inlet and outlet from interstice. As it is a CSTR, the concentrations and the temperature are the same in all positions in each phase of the reactor but no in the output, because this stream is not a bulk flow.

The two phases are separated by an interface where the glycogen interchange is carried on: glycogen produced in the upper phase goes down to the lower phase, and glycogen needed to be dephosphorylated to glucose goes to the upper phase. For this reason, glycogen is not considered a substance entering to and leaving from the reactor because its production and consumption depends on glucose concentrations. Although having a CSTR, the two phases are not mixed due to be immiscible and the agitations is not as strong to be a emulsification phase. Therefore, the assumption of CSTR holds for every phase and not for the whole tank. Figure 4.7 shows the model hypothesis to model the role of the liver in glucose homeostasis. As it can be observed, a perfectly stirred tank is considered to represent the blood irrigating the liver. Substances of interest: glucose, hormones, nutrients, precursors, circulating in the bloodstream enter in the tank representing the blood surrounding the liver. These substances go to the tank representing the liver tissue to perform the corresponding biochemical reactions. The products of all reactions return into the blood and leave from liver by the venous bloodstream.

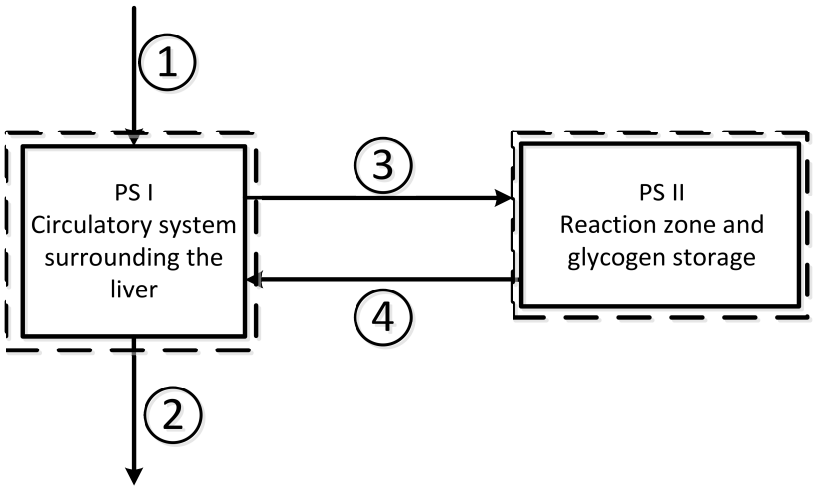

FIGURE 4.8. Block diagram representing the partition in PS assumed for the liver.

4.2.2.3 Process system definition

In this model, two PS are considered as shown in Figure 4.8. *PSI* refer to the sinusoids transporting the blood with all nutrients, hormones, glucose, and products of reactions. This PS contains the blood surrounding the liver. *PSII* is the reaction zone and the glycogen storage place in the hepatocytes. In this *PSII*, all biochemical reactions occur and also glycogen is stored. Stream 1 represents both the arterial and venous blood entering the liver. This stream transports absorbed nutrients in the small intestine, hormones released in the pancreas, precursors, and oxygen. In spite of the liver has two inflows (hepatic artery and portal vein), in this model only one inflow is considered due to both of them are perfectly mixed just before entering in the sinusoids. Stream 2 is the venous blood leaving the liver by hepatic vein. Stream 3 represents the mass transfer of all substances of interest from sinusoids to the liver tissue. Biochemical reactions occurring in the liver tissue generate products that returns in the bloodstream by stream 4, yielding a dynamic equilibrium.

4.2.2.4 The basic structure of the model

After applying the conservation law in the mentioned PSs and with all assumptions stated before, the follow model's basic structure is gotten.

$$\dot{m}_2 = \dot{m}_1 + \dot{m}_4 - \dot{m}_3 \tag{4.11}$$

$$\frac{dw_{n,2}}{dt} = (w_{n,1}\dot{m}_1 + w_{n,4}\dot{m}_4 - w_{n,2}\dot{m}_2 - w_{n,3}\dot{m}_3)\frac{1}{M_I} \tag{4.12}$$

with n the components of interest in stream 2: glucose (G), insulin (Ins), glucagon (Gl), lactate (L), glutamine (Glut), glycerol (Gly), alanine (A).

$$\frac{dw_{k,2}}{dt} = (w_{k,4}\dot{m}_4 - w_{k,2}\dot{m}_2)\frac{1}{M_I} \tag{4.13}$$

with k the inactive form of insulin and glucagon, represented by In* and Gl*, respectively, and Gly the glycogen. The produced moles of every component are expressed in the following equations in molar units.

$$\frac{dN_{In,II}}{dt} = \dot{n}_{In,3} - \dot{n}_{In,4} + \sigma_{In,4} r_4 \tag{4.14}$$

$$\frac{dN_{In*,II}}{dt} = \sigma_{In*,4} r_4 - \dot{n}_{In*,4} \tag{4.15}$$

$$\frac{dN_{Gl,II}}{dt} = \sigma_{Gl,3} - \dot{n}_{Gl,4} + \sigma_{Gl,5} r_5 \tag{4.16}$$

$$\frac{dN_{Gl*,II}}{dt} = \sigma_{Gl*,5} r_5 - \dot{n}_{Gl*,4} \tag{4.17}$$

$$\frac{dN_{Glyc,II}}{dt} = \sigma_{Glyc,1} r_1 + \sigma_{Glyc,2} r_2 \tag{4.18}$$

$$\tag{4.19}$$

Finally, the mole conservation equations by components are formulated as:

$$\frac{dN_{j,II}}{dt} = \dot{n}_{j,3} - \dot{n}_{j,4} + \sigma_{j,3i} r_{3i} \tag{4.20}$$

with j the non-glucidic precursor and i: reactions 1 for glycogenesis, 2 for glycogenolysis, 3a for gluconeogenesis via lactate, 3b for gluconeogenesis via glutamine, 3c for gluconeogenesis via glycerol, and 3d for gluconeogenesis via alanine.

4.2.2.5 Variables, structural parameters, and structural constants

Variables, structural parameters, and structural constants of the hepatic model are reported in Table 4.3.

4.2.2.6 Constitutive and assessment equations for structural and functional parameters, and definition of constants

Constitutive and assessment equations to define both structural and functional parameters of the hepatic model are reported in Table 4.4. As in the pancreas model, parameters of the hepatic model are classified in structural and functional according to the location and the classification.

4.2.2.7 Results

The dynamic behavior of the hepatic model was compared to real values of glucose reported in the literature. Values of blood glucose concentration reported in [15] were adjusted by the same two polynomial expressions used in the pancreas model, and are represented here by red curve in the Figure 4.9. A constant basal glucose concentration of $90\,mg/dL$ was considered as the desired value (set point) in the bloodstream. Under the postprandial state, glucose levels in portal vein increase, then the liver begins biochemical reactions to convert glucose into glycogen, therefore restoring the blood glucose levels to normal levels.

TABLE 4.3. Variables, structural parameters, and structural constants of the hepatic model.

Symbol	Physical meaning
Variables	
$\dot{m}_2$	Mass flow at stream 2.
$w_{n,2}$	Mass fraction of component n at stream 2.
$N_{n,II}$	Total moles of component n in the process system II.
$N_{Gly,II}$	Total moles of glycogen in the process system II.
Structural parameters	
$\dot{m}_1$	Mass flow at stream 1.
$\dot{m}_3$	Mass flow at stream 3.
$\dot{m}_4$	Mass flow at stream 4.
$\dot{n}_{n,3}$	Molar flow of component n at stream 3.
$\dot{n}_{n,4}$	Molar flow of component n at stream 4.
r_j	Reaction rate of reaction j.
$w_{n,1}$	Mass fraction of component n at stream 1.
$w_{n,3}$	Mass fraction of component n at stream 3.
$w_{n,4}$	Mass fraction of component n at stream 4.
M_I	Total mass of process system I.
Structural constants	
$\mathfrak{M}_n$	Molecular mass of component n.
R	Universal ideal gas constant.
$\sigma_{G,j}$	Stoichiometric coefficient of glucose in reaction j.
$\sigma_{Glyc,1}$	Stoichiometric coefficient of glycogen in glycogenesis reaction (reaction 1).
$\sigma_{Glyc,2}$	Stoichiometric coefficient of glycogen in glycogenolysis reaction (reaction 2).
$\sigma_{L,3a}$	Stoichiometric coefficient of lactate in reaction 3a (gluconeogenesis via lactate).
$\sigma_{Glut,3b}$	Stoichiometric coefficient of glutamine in reaction 3b (gluconeogenesis via glutamine).
$\sigma_{A,3c}$	Stoichiometric coefficient of alanine in reaction 3c (gluconeogenesis via alanine).
$\sigma_{Gly,3d}$	Stoichiometric coefficient of glycerol in reaction 3d (gluconeogenesis via glycerol).

n indicates the component of interest G, In, In*, Gl, Gl*, Glyc, L, Glut, A, Gly.
j indicates the reaction: 1 or glycogenesis, 2 or glycogenolysis, 3a or gluconeogenesis via lactate, 3b or gluconeogenesis via glutamine, 3c or gluconeogenesis via glycerol, 3d or gluconeogenesis via alanine.

TABLE 4.4. Constitutive and assessment equations of the parameters in the hepatic model.

Symbol	Type	Description	Equation
$\dot{m}_1$	Struc.	Mass flow at stream 1.	$\dot{m}_1 = \rho_b \dot{V}_b$
ρ_b	Func.1	Density of the blood.	$\rho_b = 1060 kg/m^3$
$\dot{V}_b$	Func.1	Volumetric flow in arterial blood entering in the liver.	$\dot{V}_b = \dot{V}_{Vein} + \dot{V}_{Artery}$
$\dot{V}_{Vein}$	Func.2	Volumetric flow in portal vein entering in the liver.	$\dot{V}_{Vein} = 1L/min$
$\dot{V}_{Artery}$	Func.2	Total volumetric flow in hepatic artery entering in the liver.	$\dot{V}_{Artery} = 0.8L/min$
$\dot{m}_3$	Struc.	Mass flow at stream 3.	$\dot{m}_3 = \dot{n}_{n,3}\mathfrak{M}_n$
$\dot{m}_4$	Struc.	Mass flow at stream 3.	$\dot{m}_4 = \dot{n}_4 \mathfrak{M}_{Prom}$
$\mathfrak{M}_{Prom}$	Func.1	Average molecular mass of the components.	$\mathfrak{M}_{Prom} = x_{n,4}\mathfrak{M}_n$
$x_{n,4}$	Func.2	Mass fraction of component n at stream 4.	$x_{n,4} = N_n/N_{Total}$
N_{Total}	Func.3	Total moles in the liver.	$N_{Total} = \sum N_n$
$\dot{n}_4$	Func.1	Molar flow at stream 4.	$\dot{n}_4 = \dot{V}_4 \overline{\rho}_4$
$\overline{\rho}_4$	Func.2	Molar density of the components n at stream 4.	$\overline{\rho}_4 = 1/\sum \frac{x_{n,4}}{\overline{\rho}_n}$
$\overline{\rho}_G$	Func.3	Molar density of glucose.	$\overline{\rho}_G = 4\overline{\rho}_0$
$\overline{\rho}_L$	Func.3	Molar density of lactate.	$\overline{\rho}_G = 1.5\overline{\rho}_0$
$\overline{\rho}_{Glut}$	Func.3	Molar density of glutamine.	$\overline{\rho}_{Glut} = 3\overline{\rho}_0$
$\overline{\rho}_A$	Func.3	Molar density of alanine.	$\overline{\rho}_A = 1.75\overline{\rho}_0$
$\overline{\rho}_{Gly}$	Func.3	Molar density of glycerol.	$\overline{\rho}_{Gli} = 2\overline{\rho}_0$
$\overline{\rho}_0$	Func.3	Molar density of oxygen.	$\overline{\rho}_0 = 55.5e9$
$\dot{V}_4$	Func.2	Volumetric flow at stream 4.	$\dot{V}_4 = \dot{V}_3 + \dot{V}_{r1} + \dot{V}_{r2}$
$\dot{V}_3$	Func.3	Volumetric flow at stream 3.	$\dot{V}_3 = \dot{n}_3(\frac{1}{\overline{\rho}_3})$
$\dot{n}_3$	Func.4	Molar flow at stream 3.	$\dot{n}_3 = \sum \dot{n}_{n,3}$
$\overline{\rho}_3$	Func.4	Molar density of the components n at stream 3.	$\overline{\rho}_3 = 1/\sum \frac{x_{n,3}}{\overline{\rho}_n}$
$x_{n,3}$	Func.5	Molar fraction of component n at stream 3.	$x_{n,3} = \dot{n}_{n,3}/\dot{n}_3$
$\dot{V}_{r1}$	Func.3	Volumetric flow of reaction 1 (glycogenesis).	$\dot{V}_{r1} = \sigma_{G,1} r_1 \frac{1}{\overline{\rho}_G}$
$\dot{V}_{r2}$	Func.3	Volumetric flow of reaction 2 (glycogenolysis).	$\dot{V}_{r2} = \sigma_{G,2} r_2 \frac{1}{\overline{\rho}_G}$
$\dot{n}_{G,3}$	Struc.	Molar flow of glucose at stream 3.	$\dot{n}_{G,3} = \lvert Diff_{G,3}\rvert \dot{V}_{Total}$
$\lvert Diff_{G,3}\rvert$	Func.2	Difference between current and normal blood glucose value.	$\lvert Diff_{G,3}\rvert = \lvert C_{G,Normal} - C_{G,1}\rvert$
$C_{G,Normal}$	Func.3	Normal blood glucose concentration.	$C_{G,Normal} = 90 mg/dl$
$C_{G,1}$	Func.3	Current blood glucose concentration.	$C_{G,1} = Datum$
$\dot{n}_{n,3}$	Struc.	Molar flow of component n at stream 3.	$\dot{n}_{n,3} = C_{n,basal}\dot{V}_{Total} PC_n$
$C_{n,basal}$	Func.1	Basal concentration of component n.	$C_{n,basal} = Datum_n$
PC_n	Func.1	Catchment percentage of non-glucidic precursor.	$PC_n = Datum_n$

n indicates the component of interest G, L, Glut, A, Gly.

j indicates the reaction: 1 or glycogenesis, 2 or glycogenolysis, 3a or gluconeogenesis via lactate, 3b or gluconeogenesis via glutamine, 3c or gluconeogenesis via glycerol, 3d or gluconeogenesis via alanine.

Symbol	Type	Description	Equation
M_I	Struc.	Total mass of process system I.	$M_I = \rho_b V_I$
V_I	Func.1	Volumetric flow of process system I.	$V_I = 0.6 V_{hep,total}$
$w_{G,1}$	Struc.	Mass fraction of glucose at stream 2.	$w_{G,1} = C_{G,1}/\rho_b$
$w_{n,1}$	Struc.	Mass fraction of component n at stream 1.	$w_{n,1} = C_{n,basal}/\rho_b$
$w_{n,3}$	Struc.	Mass fraction of component n at stream 3.	$w_{n,3} = \dot{n}_{n,3}\mathfrak{M}_n/\dot{m}_3$
$w_{n,4}$	Struc.	Mass fraction of component n at stream 4.	$w_{n,4} = N_n\mathfrak{M}_n/M_{Total}$
M_{Total}	Func.1	Total mass of all components.	$M_{Total} = \sum N_n\mathfrak{M}_n$
$\dot{m}_2$	Struc.	Mass flow at stream 2.	$\dot{m}_2 = \dot{m}_1$
$\dot{n}_{n,4}$	Struc.	Molar flow of component n at stream 4.	$\dot{n}_{n,4} = x_{n,4}\dot{n}_4$
r_j	Struc.	Reactions carried out in the hepatocytes.	$r_j = k_{0,j} e^{\frac{-Ea_j}{RT}} \frac{N_n}{V_{hep_t otal}}$
$k_{0,j}$	Func.1	Rate constant due to the frequency of molecular collisions in the correct orientation for reaction j.	$k_{0,j} = Datum_j$
Ea_j	Func.1	Activation energy for j reaction.	$Ea_j = Datum_j$
T	Func.1	Body temperature.	$T = 37°C$
$V_{hep,total}$	Func.1	Total volume of hepatocytes.	$V_{hep,total} = 0.00149 m^3$

n indicates the component of interest G, L, Glut, A, Gly.
j indicates the reaction: 1 or glycogenesis, 2 or glycogenolysis, 3a or gluconeogenesis via lactate, 3b or gluconeogenesis via glutamine, 3c or gluconeogenesis via glycerol, 3d or gluconeogenesis via alanine.

Blood glucose concentrations in the hepatic vein, represented with blue curve in Figure 4.9, follow the same behavior of the blood entering in the liver, but always the liver trying to regulate those levels in the bloodstream to desired set point ($90\,mg/dL$), as it does after 4.45 hours.

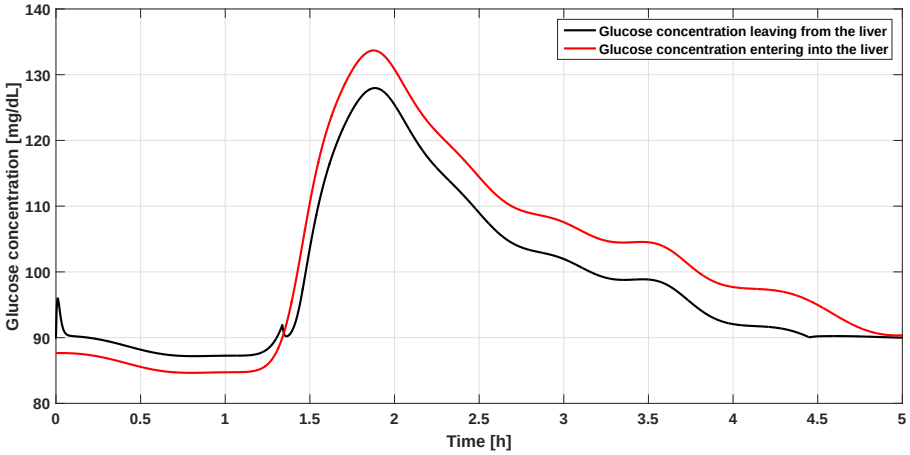

FIGURE 4.9. Blood glucose concentration at the hepatic vein.

4.2.3 Renal Model

In this section, a mathematical model to describe the role of the kidneys in glucose homeostasis in humans is presented. Particularly, this model does not represent the kidney as a whole, but rather a mathematical model for describing the functional unit of the kidney, the nephron. This is because each component part of the nephron on average has a specific function inside the renal physiology. Therefore, the results obtained will be multiplied by the 2 millions of nephrons that form both human kidneys.

4.2.3.1 Process description and model objective

The kidneys play an important role in the glucose homeostasis. Together with the liver, the kidneys are able to perform gluconeogenesis from non-carbohydrate carbon substrates by means of three main mechanisms: 1) glucose utilization for doing its metabolic processes, 2) endogenous glucose production from non-carbohydrate precursors, and 3) glomerular filtration and glucose reabsorption. The glucose circulating in the blood reaches the renal artery and enters the kidney through the hilum. The hilum then becomes the afferent arterioles which lead to the glomerular capillaries. The glomerular capillaries are covered by epithelial cells, and the total of glomerulus is encased in the Bowman's capsule [42]. There, all glucose circulating is filtered while is crossing the Bowman's capsule towards the proximal tubules which lie in the kidney's cortex. The proximal tubules are the only part of the nephrons with appropriate enzymes for gluconeogenesis [172]. Endogenous glucose production in the kidneys is stimulated mainly by for substrates ($\sim$ 90% of the gluconeogenesis): lactate, glutamine, glycerol, and alanine [94; 172]. All of these precursors are fully filtered by the glomerulus and almost completely reabsorbed in the proximal tubules [24; 251], following the same pathway of the glucose. Some studies suggest that insulin is normally filtered at the glomerulus and then almost completely reabsorbed or destroyed in the proximal tubule [50]. In contrast, glucagon has little or no effect on renal gluconeogenesis [47; 48; 177]. Depending on the concentrations of glucose, insulin, and precursors in the blood, a certain amount of glucose is produced in the proximal tubule. This glucose production occurs by biochemical reactions of different substrates. Simultaneously, cells in the renal medulla consume glucose both in the postabsorptive and the postprandial state. Glucose utilization is proportional to glucose production, leading to a net glucose balance at equilibrium. All the end products of reactions are separated, one part of them are reabsorbed to the blood by means of cotransporters (SGLTs) in the proximal convoluted tubules, and what is not reabsorbed continues flowing by the loop of Henle, until it reaches the collecting duct to be finally excreted in the urine. The glucose reabsorbed from the proximal tubules by SGLTs is then released into the circulation through the action of facilitative glucose transporters (GLUTs) at the basolateral membrane of the epithelial cells lining the proximal tubules [96]. The distal ends of the capillaries of each glomerulus coalesce to form the efferent arteriole, which leads to a second capillary network, the peritubular capillaries, that surrounds the renal tubules. There, the glucose reabsorption to the blood occurs. Virtually all glucose filtered is subsequently reabsorbed in the proximal convoluted tubule thanks to sodium-dependent glucose cotransporter (SGLT) proteins [172]. The peritubular capillaries progressively turn into larger venules and veins, and then exits the kidneys via the renal vein, containing all the reabsorbed substances. Figure 4.10 aims to a graphical representation of a nephron and its role in glucose homeostasis.

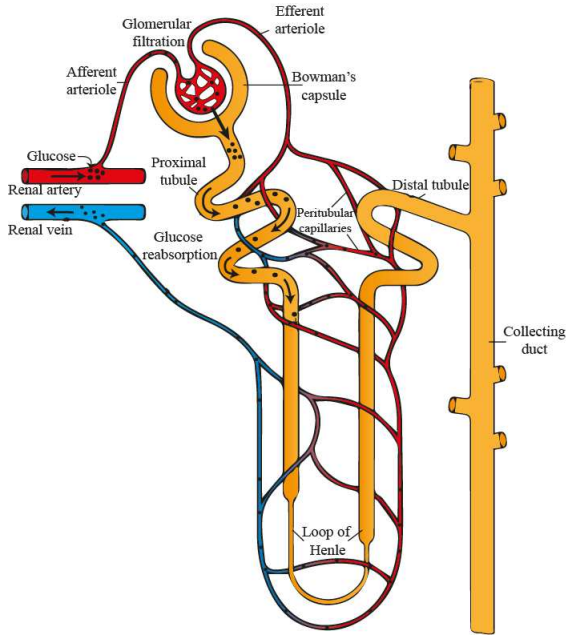

FIGURE 4.10. Glucose handling by the nephrons.

4.2.3.2 Modeling hypothesis and level of detail

The nephrons are specialized multi-cellular structures composed of different parts. Each specific part carries out a specific function affecting blood glucose concentrations. Therefore, an equivalent nephron is modeled like a representation of all nephrons forming the renal tissue, developing a macroscopic model of the role of the kidneys in glucose homeostasis. The glomerulus and the extension of the proximal tubule, where re-absorption of substances occurs, are represented as two filters. The proximal tubule, where renal gluconeogenesis occurs, is hypothesized like a continuous stirred-tank reactor (CSTR) even if it is a long circular duct. The glucose consumption by kidneys is evaluated like dissipated energy $\frac{dQ}{dt}$, assumed by simplicity, as totally consumed over proximal tubule. Blood contained in all vessels surrounding each nephron, i.e., the renal artery, renal vein, efferent and afferent arterioles, and peritubular capillaries, are represented as perfectly stirred-tanks. The analogy proposed for representing an equivalent nephron to model the role of the kidneys in the glucose homeostasis is shown in the Figure 4.11. The question which the model will answer is how does renal physiology affect blood glucose concentrations in the human body?

Glucose-related biochemical reactions occurring in the kidneys are considered in this model. An important thing is that renal tissue is separated from blood both by endothelium of capillaries and by the proximal tubule wall. Main variable is the glucose, but insulin, water, and non-carbohydrate precursors are also considered because are involved in the glucose production and consumption in the kidneys.

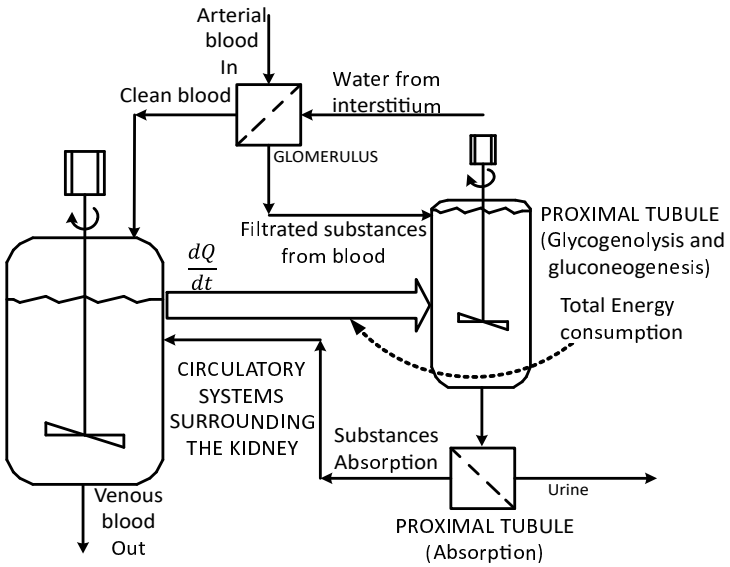

FIGURE 4.11. Proposed analogy of a nephron and its role in glucose homeostasis.

4.2.3.3 Process system definition

In the kidneys, four PS are defined, as shown in Figure 4.12. PS I represents the glomerulus where blood and relevant substances go through Bowan's capsule to reach the proximal tubule. Blood entering into the glomerulus by renal artery is represented by stream 1. The filtered substances travel for stream 3 and enter into the proximal tubule where gluconeogenesis takes place. This part of proximal tubule is represented by a CSTR (PS II in Figure 4.12). In this way, blood continues in the capillaries (stream 2) until leaving from kidneys by the renal vein (stream 7). The blood surrounding the kidneys is represented as a reactor with perfect agitation, PS IV in the block diagram. Every biochemical reaction occurs in the first portion of proximal tubule where glucose is produced before being transported to the second filter by stream 4, that is the third process system, PS III, and then be reabsorbed into the blood by stream 5. Non-reabsorbed substances reach the collector duct to be later eliminated by the urine (stream 6). Finally, the water coming from the interstice to the internal part of the tubules is represented by stream 8.

4.2.3.4 The basic structure of the model

After applying the conservation law in the previously stated PSs and after considering all assumptions mentioned before, the following basic structure of the model is obtained:

$$\dot{m}_2 = \dot{m}_1 - \dot{m}_3 + \dot{m}_8 \tag{4.21}$$

$$w_{j,3} = \frac{w_{j,1}\dot{m}_1}{\dot{m}_3} \tag{4.22}$$

$$w_{W,3} = \frac{w_{W,8}\dot{m}_8}{\dot{m}_3} \tag{4.23}$$

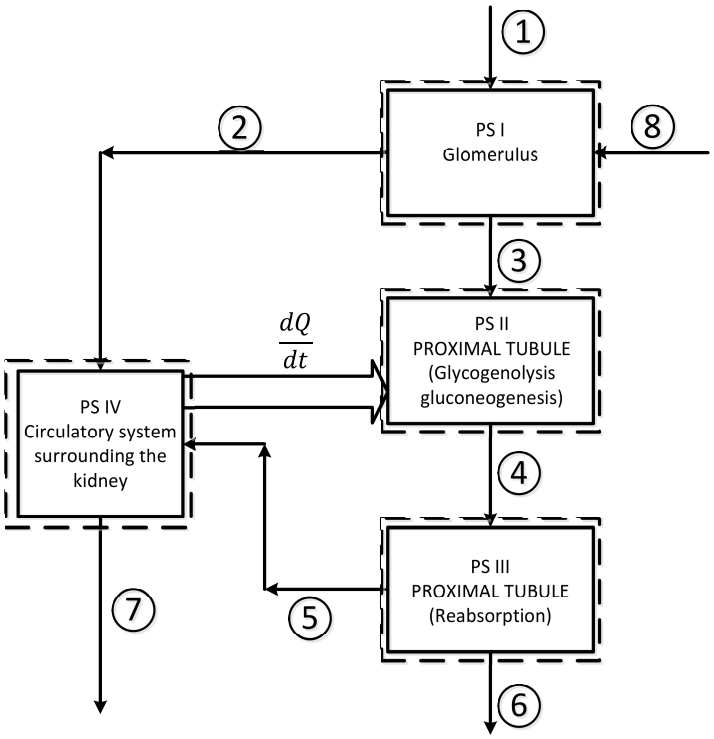

FIGURE 4.12. Block diagram of process systems taken for modelling the kidneys

with j = glucose (G), insulin (Ins), glutamine (Glut), lactate (Lac), alanine (Ala), glycerol (Gly), and W represents water. Total moles in PS II are calculated as:

$$\frac{dN_{II}}{dt} = \dot{n}_3 - \dot{n}_4 + \sum_i \sum_j (\sigma_{j,i}\ r_{EGP_i}) \tag{4.24}$$

with j indicates the same substances of Equation 4.22 and i the reactions of gluconeogenesis taking place in the kidneys:

- Reaction 1 - Endogenous glucose production via glutamine. Renal glutamine to produce glucose approximates the following balanced stoichiometric equation:

$$Glutamine + 2NAD^+ + 2NAD^+ + ATP + 5H_2O \rightarrow$$
$$2NH_3 + 2CO_2 + 2NADH^+ + 2H^+ + FADH_2 + ADP + Pi + 0.5Glucose$$

- Reaction 2 - Endogenous glucose production via lactate. Renal lactate to produce glucose approximates the following balanced stoichiometric equation:

$$L - Lactate + 2ATP + GDP + 3H_2O \rightarrow 0.5Glucose + 2ADP + GDP + 3Pi \tag{4.25}$$

- Reaction 3 - Endogenous glucose production via alanine. Alanine follows a metabolic pathway similar to lactate, but alanine produces ammonia that is eliminated with urine:

$$Alanine + 2ATP + GTP + 4H_2O \rightarrow 0.5Glucose + NH_3 + 2ADP + GDP + 3Pi \quad (4.26)$$

- Reaction 4 - Endogenous glucose production via glycerol. Glycerol has a metabolic pathway shorter than other precursors. The balanced stoichiometric equation is:

$$Glycerol + ATP + NAD^+ + H_2O \rightarrow 0.5Glucose + ADP + 0.5Pi + NADH^+ + H^+ \quad (4.27)$$

$$\frac{dx_{j,4}}{dt} = \left(x_{j,3}\dot{n}_3 - x_{j,4}\dot{n}_4 + \sum_i \sum_j (\sigma_{j,i}\ r_{EGP_i}) - r_{cons,j} - x_{j,4}\frac{dN_{II}}{dt} \right) \frac{1}{N_{II}} \quad (4.28)$$

$$\dot{m}_5 = \dot{m}_4 - \dot{m}_6 \quad (4.29)$$

$$w_{p,5} = \frac{w_{p,4}\ \dot{m}_4}{\dot{m}_5} \quad (4.30)$$

$$w_{G,5} = \frac{w_{G,4}\ \dot{m}_4 - w_{G,6}\ \dot{m}_6}{\dot{m}_5} \quad (4.31)$$

$$w_{k,6} = \frac{w_{k,4}\ \dot{m}_4}{\dot{m}_6} \quad (4.32)$$

$$\dot{m}_7 = \dot{m}_2 + \dot{m}_5 \quad (4.33)$$

$$\frac{dw_{j,7}}{dt} = (w_{j,5}\ \dot{m}_5 - w_{j,7}\ \dot{m}_7)\frac{1}{M_{IV}} \quad (4.34)$$

In the case of Equation 4.28, j = glucose (G), insulin (Ins), glutamine (Glut), lactate (Lac), alanine (Ala), glycerol (Gly), water (W), ammonia (NH_3), and carbon dioxide (CO_2). Sub-index p in Equation 4.30 is indicated for insulin and for non carbohydrate precursors. Equation 4.31 represents the mass fraction of glucose being reabsorbed in the bloodstream. In healthy people glucose is reabsorbed completely into the bloodstream and is not eliminated by urine ($w_{G,6} = 0$). However, in case of having a diabetic person, the term $w_{G,6}$ is the renal glucose excretion. Sub-index k in Equation 4.32 is indicated for ammonia, carbon dioxide, and water. It should be noted that Equation 4.34 does not exist for water, ammonia or carbon dioxide because all of them are completely eliminated by urine and do not return to the bloodstream.

4.2.3.5 Variables, structural parameters, and structural constants

Variables, structural parameters, and structural constants of the model describing the role of the kidneys in glucose metabolism are reported in Table 4.5. Parameters as $w_{p,4}$, $w_{G,4}$, and $w_{k,4}$ are considered variables, because $x_{j,4}$ is a variable to be solved by the model and $w_{p,4}$, $w_{G,4}$, and $w_{k,4}$ are the conversion from mass fraction to molar fraction. For this reason, symbol $w_{p,4}$, $w_{G,4}$, and $w_{k,4}$ do not explicitly appear in the Table 4.5. Likewise

occurs with symbol $x_{j,3}$, which is considered a variable to solved by the model through $w_{j,3}$.

4.2.3.6 Constitutive and assessment equations for structural and functional parameters, and definition of constants

Constitutive and assessment equations for defining both structural and functional parameters of the complete model are reported in Table 4.6. Symbols $w_{j,4}$ and $x_{j,3}$ are considered the same variables $x_{j,4}$ and $w_{j,3}$, respectively. The molecular mass of the water $\mathfrak{M}_W$ is included in the functional parameter $\mathfrak{M}_j$. For the reasons before mentioned, these symbols are not explicitly reported in Table 4.6.

4.2.3.7 Results

A quantitative validation of this model was realized taking several bibliographic sources and calculating an average of all the reported values of both production and consumption of glucose in the kidneys. In Table 4.7 some experimental data found in the literature are reported to validate the renal model. In the postprandial state, renal glucose production is around 60% of the total glucose production in the human body. In the postabsorptive state, renal gluconeogenesis is lower and contributes 20 to 25% to whole-body glucose production. A comparison between renal gluconeogenesis of the model developed and renal gluconeogenesis of experimental data is shown in Figure 4.13. Dotted lines are validation data extracted from the literature. The blue cyan line represents the production of renal glucose in the post-prandial state and the red line is the production of renal glucose in a post-absorptive state.

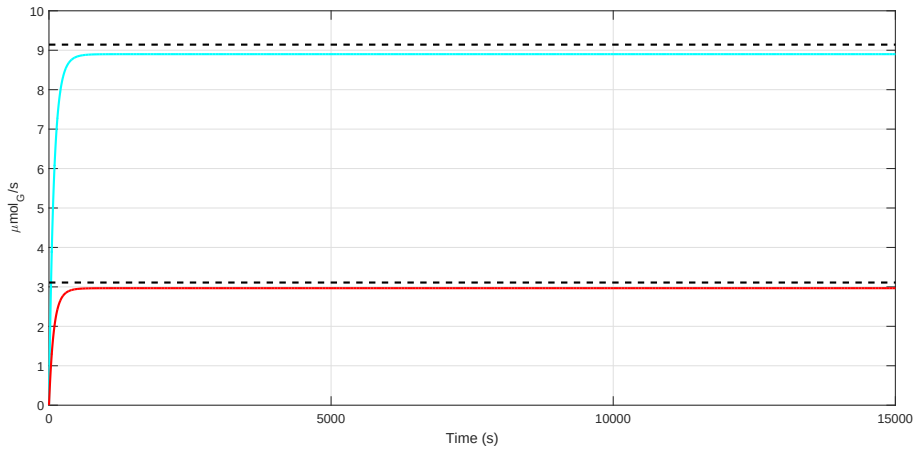

FIGURE 4.13. Renal gluconeogenesis in postprandial and postabsorptive state.

The results also were validated with renal glucose production regarding every non-carbohydrate precursor. Glutamine, for example, is the most abundant amino acid in the human body and is involved in glucose metabolism in the kidneys. Rate of glucose production via glutamine can be seen in Figure 4.14 where red and continuous line represents

TABLE 4.5. Variables, structural parameters and structural constants of the renal model.

	Symbol	Physical meaning
Variables		
	$\dot{m}_2$	Mass flow of blood filtered in the glomerulus.
	$w_{j,3}$	Mass fraction of j component being filtered in the glomerulus.
	$w_{W,3}$	Mass fraction of water being filtered in the glomerulus from the interstitium.
	N_{II}	Total moles in the part of proximal tubule where glycogenolysis and gluconeogenesis take place.
	$x_{j,4}$	Molar fraction of j component that continues through proximal tubule after reactions.
	$\dot{m}_5$	Mass flow of substances reabsorbed into the bloodstream.
	$w_{p,5}$	Mass fraction of insulin and non carbohydrate precursors reabsorbed into the bloodstream from proximal tubule (p component).
	$w_{G,5}$	Mass fraction of glucose reabsorbed into the bloodstream from proximal tubule.
	$w_{k,6}$	Mass fraction of k component (water, ammonia, and carbon dioxide) that continues to the collecting duct.
	$\dot{m}_7$	Mass flow of blood leaving from kidneys by renal vein.
	$w_{j,7}$	Mass fraction of j component leaving from kidneys by renal vein.
Structural parameters		
	$\dot{m}_1$	Mass flow rate of blood entering in the kidneys (stream 1).
	$\dot{m}_3$	Mass flow rate of components of interest filtered in the glomerulus (stream 3).
	$\dot{m}_8$	Mass flow rate of components entering in the glomerulus from the interstitium (stream 8).
	$w_{j,1}$	Mass fraction of j component entering in the kidneys by renal artery.
	$w_{W,8}$	Mass fraction of water entering in the glomerulus from the interstitium.
	$\dot{n}_3$	Molar flow of substances of interest being filtered in the glomerulus.
	$\dot{n}_4$	Molar flow of reaction products in the proximal tubule.
	r_{EGP_i}	Reactions of endogenous glucose production via non-glucidic precursors.
	r_{cons_j}	Reaction of consumption of j component.
	$\dot{m}_6$	Mass flow of reaction products going to the collecting duct.
	$w_{G,6}$	Mass fraction of glucose in the urine.
	M_{IV}	Total mass of blood irrigating the kidneys.
Structural constants		
	$\sigma j, i$	Stoichiometric coefficient of j component in the endogenous glucose production through the reactions i.

TABLE 4.6. Constitutive and assessment equations of the parameters of the renal model.

Symbol	Type	Description	Equation
$\dot{m}_1$	Struc.	Mass flow rate of blood entering in the kidneys (stream 1).	$\dot{m}_1 = \rho_b \dot{V}_b$
ρ_b	Func.1	Density of the blood.	$\rho_b = 1060\ kg/m^3$
$\dot{V}_b$	Func.1	Volumetric flow of blood irrigating the kidneys.	$\dot{V}_b = 1.2\ L/min$
$\dot{m}_3$	Struc.	Mass flow rate of components of interest filtered in the glomerulus (stream 3).	$\dot{m}_3 = \dot{m}_1\ \sum_j w_{j,1} + \dot{m}_8\ w_{W,8}$
$\dot{m}_8$	Struc.	Mass flow rate of components entering the glomerulus from the interstitium (stream 8).	$\dot{m}_8 = w_{W,6}\ \dot{m}_6 + \dot{n}_W\ \mathfrak{M}_W$
$\dot{n}_W$	Func.1	Number of moles of water consumed during the reactions in the proximal tubule per second.	$\dot{n}_W = 13 mol/s$
$w_{j,1}$	Struc.	Mass fraction of component j entering in the kidneys by renal artery.	$w_{j,1} = C_{j,1}\ \frac{1}{\rho_b}\ \mathfrak{M}_j$
$C_{j,1}$	Func.1	Molar-volumetric concentration of component j at stream 1.	$C_{j,1} = Datum_j$
$\mathfrak{M}_j$	Func.1	Molar mass of component j.	$\mathfrak{M}_j = Datum_j$
$w_{W,8}$	Struc.	Mass fraction of water entering the glomerulus from the interstitium.	$w_{W,8} = 1$
$\dot{n}_3$	Struc.	Total molar flow of mix being filtered in the glomerulus.	$\dot{n}_3 = \sum_j \dot{n}_{j,3}$
$\dot{n}_{j,3}$	Func.1	Molar flow of substances of interest being filtered in the glomerulus.	$\dot{n}_{j,3} = \dot{n}_{j,1}$
$\dot{n}_{j,1}$	Func.2	Molar flow of substances of interest entering the kidneys by renal artery.	$\dot{n}_{j,1} = \frac{\dot{m}_1 \dot{w}_{j,1}}{\mathfrak{M}_j}$
$\dot{n}_4$	Struc.	Molar flow of reaction products in the proximal tubule.	$\dot{n}_4 = \frac{\dot{V}_4\ \rho_{mix}}{\mathfrak{M}_{mix}}$
$\dot{V}_4$	Func.1	Volumetric flow of products or reactions taking place in proximal tubule.	$\dot{V}_4 = \dot{V}_3$
ρ_{mix}	Func.1	Density of mix in the reactor representing the first part of proximal tubule.	$\rho_{mix} = \frac{1}{\sum \frac{w_{j,4}}{\rho_j}}$
$\mathfrak{M}_{mix}$	Func.1	Molar mass of mix in the reactor representing the first part of proximal tubule.	$\mathfrak{M}_{mix} = \sum x_{j,4} \mathfrak{M}_j$
$\dot{V}_3$	Func.2	Volumetric flow of substances entering in the proximal tubule.	$\dot{V}_3 = \sum \dot{V}_{j,3}$
ρ_j	Func.2	Density of component j.	$\rho_j = Datum_j$
$\dot{V}_{j,3}$	Func.3	Volumetric flow of component j filtered in the glomerulus.	$\dot{V}_{j,3} = \dot{n}_{j,3}\ \mathfrak{M}_j \frac{1}{\rho_j}$
r_{EGP_i}	Struc.	Reaction velocity of endogenous glucose production via non-glucidic precursors.	$r_{EGP_i} = k_{0,EGP_i}\ C_{j,4}\ e^{\frac{Ea_{EGP_i}}{RT}}$
k_{0,EGP_i}	Fun.1	Rate constant due to the frequency of molecular collisions of substances in the proximal tubule in the reaction i.	$k_{0,EGP_i} = Datum_i$

j indicates the component of interest: glucose (G), insulin (Ins), glutamine (Glut), lactate (Lac), alanine (Ala), glycerol (Gly), ammonia (NH_3), water (W), and CO_2.
i indicates the reactions of gluconeogenesis taking place in the kidneys: 1 is the endogenous glucose production via glutamine, 2 is the endogenous glucose production via lactate, 3 is the endogenous glucose production via alanine, and 4 is the glucose production via glycerol.

Symbol	Type	Description	Equation
$C_{j,4}$	Func.1	Molar-volumetric concentration of component j, after every gluconeogenesis reaction i (in stream 4).	$C_{j,4} = \frac{x_{j,4}\rho_{mix}}{\mathfrak{M}_{mix}}$
Ea_{EGP_i}	Func.1	Activation energy for gluconeogenesis reaction i.	$Ea_{EGP_i} = Datum_i$
R	Func.1	Universal ideal gas constant.	$R = 8.314\ J/molK$
T	Func.1	Corporal temperature.	$T = 37\ ^\circ C$
r_{cons_j}	Struc.	Reaction of consumption of j component.	$r_{cons_j} = Datum_j$
$\dot{m}_6$	Struc.	Mass flow of reaction products going to the collecting duct.	$\dot{m}_6 = \dot{V}_u\ \rho_u$
$\dot{V}_u$	Func.1	Volumetric flow leaving from collecting duct to form urine.	$\dot{V}_u = 1.5L/dia$
ρ_u	Func.1	Density of urine.	$\rho_u = 1017.5g/L$
$w_{G,6}$	Struc.	Mass fraction of glucose in the urine.	$w_{G,6} = \frac{\dot{m}_{G,6}}{\dot{m}_6}$
$\dot{m}_{G,6}$	Func.1	Mass flow of glucose in the urine. It is zero in healthy people.	$\dot{m}_{G,6} = \dot{m}_1(w_{G,1} - w_{G,Lim})$
$w_{G,Lim}$	Func.2	Mass fraction limit of glucose absorbed by the kidneys.	$w_{G,Lim} = C_{G,Lim}\frac{\mathfrak{M}_G}{\rho_b}$
$C_{G,Lim}$	Func.3	Concentration limit of glucose absorbed by the kidneys.	$C_{G,Lim} = 180mg/dl$
M_{IV}	Struc.	Total mass of blood irrigating the kidneys.	$M_{IV} = \rho_b\ V_b$
V_b	Func.1	Blood volume irrigating the kidneys.	$V_b = 37m^3$

j indicates the component of interest: glucose (G), insulin (Ins), glutamine (Glut), lactate (Lac), alanine (Ala), glycerol (Gly), ammonia (NH_3), water (W), and CO_2.
i indicates the reactions of gluconeogenesis taking place in the kidneys: 1 is the endogenous glucose production via glutamine, 2 is the endogenous glucose production via lactate, 3 is the endogenous glucose production via alanine, and 4 is the glucose production via glycerol.

TABLE 4.7. Renal glucose production in postprandial and postabsortive state.

State	Renal glucose production	Percentage	Reference
Postprandial	9.142 $\mu mol_G/s$	60	[7; 96; 253]
Postabsortive	3.114 $\mu mol_G/s$	20-25	[94; 95; 96]

the response of the model achieving the rate of glucose production found in the literature as $0.623 \mu mol_G/s$, which is represented as black and dotted lines.

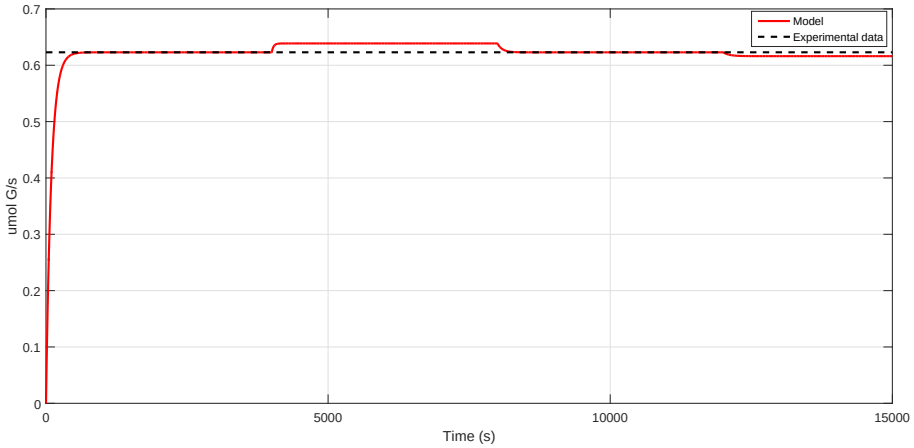

FIGURE 4.14. Renal glucose production in the kidneys via glutamine.

As can be seen in the figure, there is a higher glucose production between 4000 and 8000 seconds and a lower glucose production between 12000 and 15000 seconds. This is caused by two disturbances, the first one is a hyperglycaemia, that is, the glucose level rises to $250 mg/dl$, and the second one is a hypoglycaemia state, where blood glucose levels entering the kidneys decreases to $70 mg/dl$. This result agrees with the physiology, renal glucose production is proportional to blood glucose levels.

4.2.4 Model of the stomach

In this section, a PBSM of the role of the stomach in glucose homeostasis is developed. The steps followed are stated in the procedure to obtain the PSBM. A complete development of the model construction has been published published in [147].

4.2.4.1 Process Description and Model Objective

The stomach is a muscular organ that receives food from the esophagus. As food reaches the stomach, its role is to churn the meal and make a partial digestion of proteins and lipids before these are fed into the small intestine. This partial digestion and meal churning is performed by periodic contractions of the stomach muscles and by secreted acid and enzymes. As a result, a homogeneous mixture reaches the small intestine. The flow of the meal entering to the stomach is regulated by a cardiac sphincter located between esophagus and stomach. Meanwhile, the outflow of the gastric mass into the duodenum is controlled by the pyloric sphincter, located at the end of the pyloric canal, connecting the stomach to the duodenum. Figure 4.15 shows a time sequence of digestion in the stomach. Digestion in the stomach is classified into 4 stages: the first one is the entering of the food through the cardiac sphincter. Once all food is in the stomach, the cardiac sphincter is closed and the mechanical work begins. Food is mixed to achieve adequate rheological properties to pass through the pyloric valve. Then, the pylorus is opened to

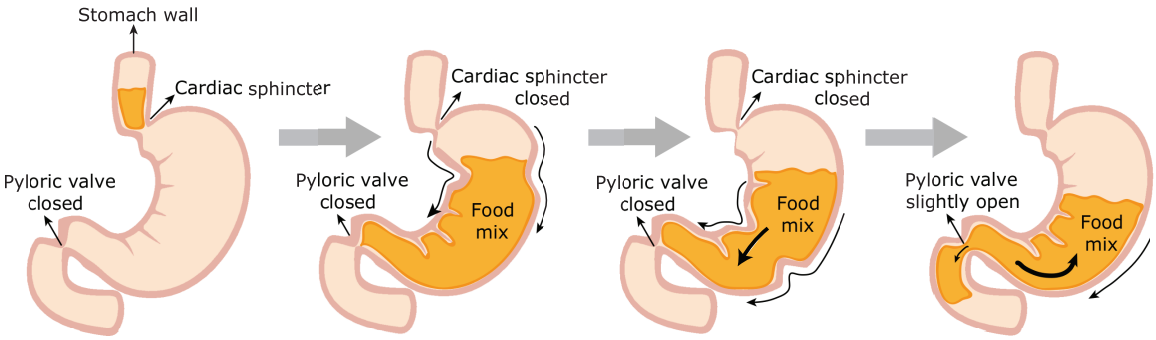

FIGURE 4.15. Time sequence illustrating the digestion in the stomach.

allow the transit of the food toward small intestine. The mechanical work performed by the stomach is the result of peristaltic movements of stomach muscular cells, which require glucose consumption for carrying out such a task.

The entire digestive process starts in the mouth, where the meal is chewed and mixed with enzymes from saliva to obtain smaller and moisturized pieces of food. Protein and fat digestion begins in the stomach when gastric juices, mainly hydrochloric acid (HCl) and pepsin enzyme are released. The acidity of the stomach facilitates protein unfolding, but only around 5% of proteins find active protease in the stomach allowing their unfolding into smaller aminoacids. Regarding the remaining proteins, digestion is finished in the small intestine [262]. On the other hand, the digestion of dietary fat also starts in the stomach, where lingual lipase hydrolyzes about 10 - 30 % of digested triglycerides to free fatty acids and partial glycerides at pH 3-6 [1; 151]. The hydrolysis of fat in the stomach is essential for normal fat absorption. The secretionary and motor responses of the stomach are significantly affected by the characteristics of the individual, digestion time and amount, meal composition, and the physicochemistry of the ingested meal [60; 196]. Regarding carbohydrates, only physical modifications occur in the stomach. No matter how mixed and broken down the food is, once in the intestine, carbohydrates (CHO) are digested together with the remaining long-chain proteins and lipids which were not digested in the stomach. Small compounds such as glucose, fatty acids, and amino acids are then diffused through the intestinal wall.

Bearing the above in mind, the question to be solved by the model (model objective) is: how does glucose consumption in the stomach change during the digestion process? Once this question is answered, this consumption may be included into a glucose homeostasis model of the human body.

4.2.4.2 Modeling Hypothesis and Level of Detail

The model is considered to be macroscopic, i.e., the stomach will be considered as a whole, executing its mixing function to churn the ingested meal until it becomes a homogeneous fluid. Food digestion is considered here as a semi-batch process, without considering the time needed for stomach charge (ingestion), but considering a continuous gastric emptying. This fact is supported by the difference in the needed times for both stomach charge and digestion which are on average 15-20 min and over 3 hours, respectively. Moreover, it is considered a standard consumption of a mixed meal in which the ingestion does not have a considerable effect over digestion. Therefore, considering the stomach digestion as a batch

process is not unrealistic. At the initial time of digestion, ingested food, enzymes, and water are assumed to be into the stomach. The cardiac sphincter is closed while digestion is taking place in the stomach, but the pylorus is partially opened to let the mix flow into the small intestine. Therefore, the cardiac sphincter is considered as an on-off valve (two positions), contrary to pylorus, which is considered a continuous (infinite positions) valve.

The walls of the stomach consist of an outer mucosa, inner submucosa, muscularis externa, and serosa [262]. All these cells need glucose for survival (basal glucose consumption). The specialized muscularis externa requires additional energy to mix the food. To evaluate this mixing energy, an analogy of energy loss by friction is used when a mixture of liquid and solid particles flowing through a circular pipe. In the same way, the movements of gastric mass into the stomach produce energy losses due to friction between fluid and the internal stomach surface, and between different layers of the flowing gastric mass.

With the previous statements in mind, the modelling hypothesis proposed for the stomach model is an analogy between the movements of gastric mass into the stomach and the movement of a mixture of liquid and solid particles flowing through a pipe and fittings closed circuit. The length and size of each hypothetical pipeline section and the type of fitting are obtained by dividing the stomach through a longitudinal axis in accordance to the flow patterns reported in [84]. In Figure 4.16, a sequence showing the genesis of the abstraction used is presented (from left to right).

The minimum energy requirement for the fluid to make a complete lap is obtained from the mechanical energy balance taken between departure and arrival points, as shown in Figure 4.16. The energy is provided by a driver machine like a pump, taken in this thesis as the musculature of the stomach as a whole. Following the findings of several researchers [85; 86; 105], the high energy jet is formed at the stomach pyloric antrum. Thus, this point is selected to gather all the energy from stomach peristalsis and musculature contractions. This energy is indicated as a thick arrow coming from the external musculature of the stomach, as shown in the right hand side of Figure 4.16. As an additional assumption, the pipe circuit is considered completely full with the meal, although in a real scenario, both air and meal would be present and gastric emptying would be considered. To compensate for the last assumption, the friction factor is corrected and the velocity of the mixture is gradually slowed down. The above helps to hold the full pipe condition and to account for gastric emptying. Additionally, the viscosity of the meal in the stomach changes with the power applied by the stomach, affecting the energy consumption calculation. Finally, the mechanical efficiency of the stomach is considered as 50%. This implies a stomach glucose consumption equal to a half of the power supplied by the driving machine $\dot{W}$, which is thus required to maintain the gastric mass in continuous movement against the friction. The remaining 50% of this energy is used in all metabolic process within the stomach cell.

Additional considerations for the modeling hypothesis: *i*) gastric emptying and gastric dilution rate are known polynomial functions of the digestion time, *ii*) the tissue forming the stomach wall does not retain or lose mass, *iii*) the stomach wall properties are not affected by the internal wall concentration of substances, and *iv*) complex carbohydrates are considered as equivalent glucose (G), since no chemical changes occur for carbohydrates. It is clear that food rheology has a strong effect on the overall stomach operation. In this regard, the presented polynomial functions for gastric emptying and gastric dilution are valid for a given food composition. In addition, dilution affects the food rheology which make the phenomena analysis even more complex. Given the poor understanding of these interactions from the dynamic viewpoint, it is clear that more appropriate submodels for

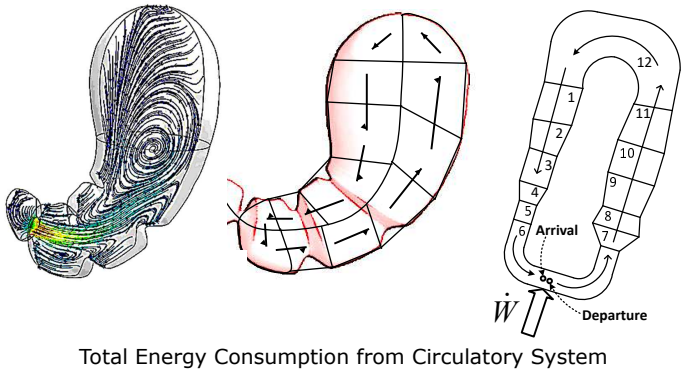

FIGURE 4.16. Figure adaptated from [84]. Stomach geometry and proposed analogy for flow of fluids inside.

both gastric dilution and emptying are needed, considering different meal compositions. Since the current model is a first approximation, those submodels are presented as polynomial functions, a simple way to represent these characteristics for a specific food. Further developments in this direction will be carried out in the future.

4.2.4.3 Process System Definition

Three main PSs are defined in the stomach, as shown in Figure 4.17. PS_I represents the gastric mass in the stomach formed by carbohydrates, fats, proteins, fiber, water, gastric juices, and enzymes. The ingested food arriving to the stomach from the esophagus is the stream 8 (thin arrow), while the stream 5 is the output of the meal to the small intestine. PS_{II} corresponds to the stomach wall, involving both muscular and stomach tissue. It receives by stream 4 (from interstitial tissue and other organs) the reactant needed to produce gastric juices and delivers by stream 3 the produced gastric juice to PS_I. This stream is the only mass interaction between PS_I and PS_{II}, since no absorption of substances from gastric mass to the stomach wall takes place. The stomach wall consumes glucose to produce mechanical energy to maintain the gastric mass circulating into the assumed pipe circuit. This energy, which compensates the frictional energy losses of gastric mass, is represented in Figure 4.17 by a thick arrow of mechanical work flow $\dot{W}$. Finally, PS_{III} represents the blood contained in the capillaries irrigating the stomach. This blood is considered circulating through a major circuit like a "field bus", transporting substances of interest to the stomach wall and receiving the waste substances from the stomach tissue through streams 1 and 2, respectively. Stream 1 represents the reactant for the glucose combustion reaction (oxygen and glucose), while stream 2 takes the products of this reaction away (water and carbon dioxide). Streams 6 and 7 represent the arterial blood from the celiac trunk and vein blood leaving the stomach irrigation system, respectively. PS_{II} acts like an energetic connection between the stomach contents (PS_I) and bloodstream (PS_{III}).

4.2.4.4 The Basic Structure of the Model

The equations with valuable information for the model are as follows, bearing in mind that (4.36) leads to 12 equations, one for every component: glucose (G), natural fats (NtF), bioavailable fats (BaF), natural proteins (NtP), bioavailable proteins (BaP), active lipase

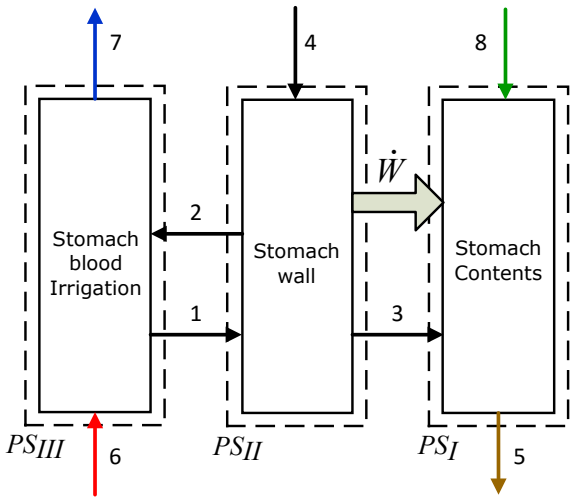

FIGURE 4.17. Block diagram of process systems considered for modeling the stomach.

(ActL), inactive lipase (InaL), active protease (ActP), inactive protease (InaP), water (W), gastric juices (GJ), and fiber (Fib).

$$\frac{dN_I}{dt} = \dot{n}_3 - \dot{n}_5 + \sum_i \sum_j (\sigma_{j,i}\, r_i) \tag{4.35}$$

$$\frac{dx_{j,5}}{dt} = \frac{1}{N_I}\left(x_{j,3}\,\dot{n}_3 - x_{j,5}\,\dot{n}_5 + \sum_i \sum_j (\sigma_{j,i}\, r_i) - x_{j,5}\frac{dN_I}{dt} \right) \tag{4.36}$$

$$\dot{W} = \frac{1}{\eta}\left(\dot{m}_{pc}\, h_{f_{d\to a}} \right) \tag{4.37}$$

$$\dot{n}_2 = \dot{n}_1 + \sum_l (\sigma_{l,gc}\, r_{gc}) \tag{4.38}$$

$$\dot{n}_1 = \frac{1}{x_{G,1}}\, \sigma_{G,gc}\, r_{gc} \tag{4.39}$$

$$r_{gc} = -\frac{1}{\Delta \bar{H}_{r_{gc}}}\, \dot{W} \tag{4.40}$$

$$\frac{dM_{III}}{dt} = 0 \Rightarrow M_{III} = C_1 \tag{4.41}$$

$$\frac{dw_{G,7}}{dt} = \frac{1}{M_{III}}\left(w_{G,6}\,\dot{m}_6 - w_{G,1}\,\dot{m}_1 - w_{G,7}\,\dot{m}_7 \right) \tag{4.42}$$

4.2.4.5 Variables, structural parameters, and structural constants

A summary with the model variables and both structural parameters and constants for every PS is provided in Table 4.8.

TABLE 4.8. Variables and structural parameters of the stomach model.

Symbol	Physical meaning
Variables	
N_I	Total moles in PS_I.
$x_{j,5}$	Molar fraction of component j at stream 5, with j = G, NtF, BaF, NtP, BaP, ActL, InaL, ActP, InaP, W, GJ, Fib.
$\dot{W}$	Mechanical flow of work from the stomach wall.
$\dot{n}_1$	Molar flow at stream 1.
$\dot{n}_2$	Molar flow at stream 2.
r_{gc}	Reaction velocity of the glucose consumption reaction.
M_{III}	Total mass of blood contained in the system irrigating the stomach.
$w_{G,7}$	Mass fraction of glucose into stream 7.
Structural parameters	
$\dot{n}_3$	Molar flow rate of gastric juices.
$\dot{n}_5$	Molar flow rate due to gastric emptying.
r_{Fat}	Reaction velocity of fat reaction.
r_{Pro}	Reaction velocity of protein reaction.
$\frac{dN_I}{dt}(t)$	Total mass change in molar units.
$\dot{m}_{pc}$	Flow of gastric mass through the pipe circuit.
$h_{f_{d\to a}}$	Friction losses in the pipe circuit.
$x_{G,1}$	Glucose molar fraction at current 1.
$\dot{m}_1$	Mass flow rate at current 1.
$w_{G,6}$	Mass fraction of glucose at current 1.
$\dot{m}_6$	Mass flow rate at current 6.
$\dot{m}_2$	Mass flow rates at currents 1 and 2.
$\dot{m}_7$	Mass flow rates at currents 6 and 7.
x_j	Molar fraction for component j.
Structural constants	
$\sigma_{G,gc}$	Stoichiometric coefficient of glucose in glucose combustion reaction.
$\sigma_{O_2,gc}$	Stoichiometric coefficient of oxygen in glucose combustion reaction.
$\sigma_{CO_2,gc}$	Stoichiometric coefficient of carbon dioxide in glucose combustion reaction.
$\sigma_{H_2O,gc}$	Stoichiometric coefficient of water in glucose combustion reaction.

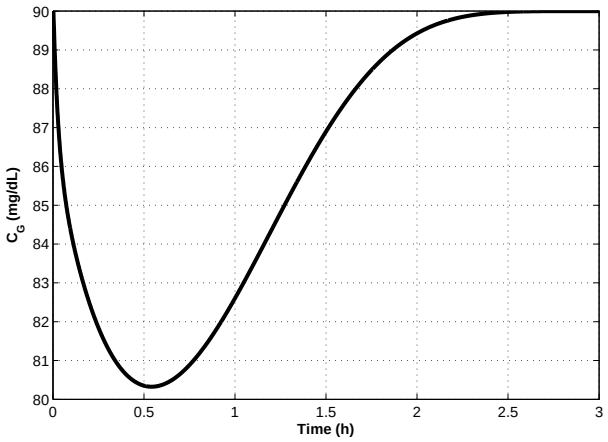

FIGURE 4.18. Blood glucose concentration C_G at the stomach venous drainage.

4.2.4.6 Constitutive and assessment equations for structural and functional parameters, and definition of constants.

A summary of all constitutive and assessment equations for the structural parameters of the stomach model is given in Table 4.9, where the classification of all parameters of the model is introduced in the column called "type". Parameters $k_{0,Fat}$, $k_{0,Pro}$, $E_{a,Fat}$, $E_{a,Pro}$ are identified from data reported in the literature, considering that stomach digests approximately 5% and 20% of proteins and fats, respectively. Although food rheology has a high impact on the fluid flow behavior in the stomach, in this study the flow within the pipe sections is assumed to be laminar due to the characteristics of the considered food.

4.2.4.7 Results

Changes in blood glucose concentration during digestion in the stomach are shown in Figure 4.18. A basal glucose concentration of $90\,mg/dL$ in the arterial blood entering to stomach blood irrigation system is assumed as a constant value during all the digestion process. Since the stomach consumes glucose to carry out the digestion, that concentration of glucose in venous blood leaving the stomach irrigation system decreases to $80.31\,mg/dL$ as minimum value. This result shows a drop in blood glucose concentration of almost $10\,mg/dL$ while digestion is taking place in the stomach, assuming constant glucose concentration in the arterial blood.

4.2.5 Model of small intestine

In this section, a mathematical model to describe how nutrients are digested and absorbed in the small intestine is developed.

TABLE 4.9. Constitutive and assessment equations for structural and functional parameters of the stomach model.

Symbol	Type	Description	Equation
$\dot{n}_3$	Struc.	Molar flow rate of gastric juices.	$\dot{n}_3 = \frac{1}{\mathfrak{M}_{GJ}} \rho_{GJ} \left[\left(\frac{1}{Dil} V_{gm,t_0} \right) - V_{gm,t_0} \right]$
$\mathfrak{M}_{GJ}$	Func.1	Molecular mass of gastric juices.	$\mathfrak{M}_{GJ} = 36.46\ g/mol$
ρ_{GJ}	Func.1	Density of gastric juices.	$\rho_{GJ} = 1.19\ g/cm^3$
Dil	Func.1	Dilution factor.	$Dil = -6.0070249 \times 10^{-8}\ {t_m}^3 + 7.0181077 \times 10^{-6}\ {t_m}^2 - 0.002301354\ t_m + 0.9912266$
t_m	Func.2	Elapsed time after digestion start.	$t_m = min$
V_{gm,t_0}	Func.1	Volume of gastric mass at t_0.	$V_{gm,t_0} = \frac{M_{gm,t_0}}{\rho_{gm,t_0}}$
M_{gm,t_0}	Func.2	Gastric mass at t_0 (Ingested meal).	$M_{gm,t_0} = 97$
ρ_{gm,t_0}	Func.2	Density of gastric mass at t_0.	$\rho_{gm,t_0} = Datum$
$\dot{n}_5$	Struc.	Molar flow rate due to gastric emptying.	$\dot{n}_5 = \frac{1}{\mathfrak{M}_{gm}} \rho_{gm} \left[\frac{V_{gm,t_0}}{Dil} - \frac{V_{gm,t_0}}{Dil} * Emp \right]$
$\mathfrak{M}_{gm}$	Func.1	Molecular mass of the gastric mass (stomach content).	$\mathfrak{M}_{gm} = \sum_j x_{j,5} \mathfrak{M}_j$
$\mathfrak{M}_j$	Func.2	Molecular mass of compound j.	$\mathfrak{M}_j = Datum_j$
ρ_{gm}	Func.1	Density of gastric mass.	$\rho_{gm} = VF_{FGJ}\rho_{gm,t_0} + (1 - VF_{FGJ})\rho_{GJ}$
VF_{FGJ}	Func.2	Volumetric fraction of ingested food with respect to gastric juices.	$VF_{FGJ} = \frac{V_{gm,t_0}}{V_{gm}}$
V_{gm}	Func.3	Volume of gastric mass.	$V_{gm} = \frac{V_{gm,t_0}}{Dil}$
Emp	Func.1	Emptying factor.	$Emp = 2.65 \times 10^{-9} t_m^4 - 5.4098 \times 10^{-7} t_m^3 - 1.3812 \times 10^{-5} t_m^2 - 8.3192 \times 10^{-4} t_m + 0.9969$
$x_{j,3}$	Struc.	Molar fraction of compound j at stream 3.	$x_{GJ,3} = 1$
r_{Fat}	Struc.	Velocity of fat reaction.	$r_{Fat} = k_{0,Fat}\, C_{NtF}\, C_{ActL}\, e^{\frac{-E_{a,Fat}}{RT}}$
$k_{0,Fat}$	Func.1	Rate constant due to the frequency of molecular collisions in the correct orientation for fats.	$k_{0,Fat} = 6.15 \times 10^{-2}$
C_j	Func.1	Molar-volumetric concentration of component j.	$C_j = \frac{x_j N_I}{V_{gm}}$
$E_{a,Fat}$	Func.1	Activation energy for fat reaction.	$E_{a,Fat} = 1.35 \times 10^7$
R	Func.1	Universal ideal gas constant.	$R = 8.314\ J/mol\dot{K}$
T	Func.1	Corporal temperature.	$T = 37\ ^\circ C$
r_{Pro}	Struc.	Velocity of protein reaction.	$r_{Pro} = k_{0,Pro}\, C_{NtP}\, C_{ActP}\, e^{\frac{-E_{a,Pro}}{RT}}$
$k_{0,Pro}$	Func.1	Rate constant due to the frequency of molecular collisions in the correct orientation for proteins.	$k_{0,Pro} = 0.95 \times 10^{-2}$
$E_{a,Pro}$	Func.1	Activation energy for protein reaction.	$E_{a,Pro} = 1.3 \times 10^7$
$\frac{dN_I}{dt}(t)$	Struc.	Total mass change in molar units.	$\frac{dN_I}{dt}(t) = \frac{N_I(t+\Delta t) - N_I(t)}{\Delta t}$
Δt	Func.1	Sample time to approximate dN_I/dt.	$\Delta t = 5\ s$
η	Struc.	Stomach efficiency as a driver machine.	$\eta = 1$

Indexes: j = G, NtF, BaF, NtP, BaP, ActL, InaL, ActP, InaP, W, GJ, Fib.

Symbol	Type	Description	Equation
$\dot{m}_{pc}$	Struc.	Flow of gastric mass through the pipe circuit.	$\dot{m}_{pc} = \rho_{gm}\, v_{gm,distal}\, A_s$
$v_{gm,distal}$	Func.1	velocity of gastric mass measured at the pyloric antrum (distal extreme).	$v_{gm,distal} = 10.5\ cm/s$
A_s	Func.1	Cross sectional area of the fitting at the distal extreme.	$A_s = \pi \frac{D_s^2}{4}$
D_s	Func.2	Internal diameter of section s.	$D_s = Datum$
$h_{f_{d\to a}}$	Struc.	Friction losses in the pipe and fittings circuit.	$h_{f_{d\to a}} = \sum_s \left(K_s \frac{v_s^2}{2} \right)$
K_s	Func.1	Friction factor for section s.	$K_s =$ $\begin{cases} K_{straight} = f_{Darcy} \frac{L_{straight}}{D_s} \\ K_{expan} = \left[1 - \left(\frac{SD}{HD} \right)^2 \right]^2 \\ K_{cont} = 0.5 \left[1 - \left(\frac{SD}{HD} \right)^2 \right]^2 \\ K_{180^\circ Elbow} = \frac{1000}{Re_s} + 0.6 \left(1 + \frac{1}{ID} \right) \end{cases}$
f_{darcy}	Func.2	Darcy factor.	$f_{darcy} = 64/Re_s$
Re_s	Func.3	Reynolds number.	$Re_s = \frac{\rho_{gm} v_s D_s}{\mu_{gm}}$
μ_{gm}	Func.4	Viscosity of the gastric mass.	$\mu_{gm} = -4.34648\, MDF^4 + 5.85569\, MDF^3 - 1.7678\, MDF^2 + 0.29556\, MDF - 0.02$
MDF	Func.5	Modified dilution factor.	$MDF = Dil^{2.97}$
$L_{straight}$	Func.2	Length of the straight section. s	$L_{straight} = Datum$
SD	Func.2	Smaller diameter in contraction/expansion.	$SD = Datum$
HD	Func.2	Higher diameter in contraction/expansion.	$HD = Datum$
ID	Func.2	Diameter in fittings.	$ID = Datum$
v_s	Func.1	Velocity of the gastric mass at section s.	$v_s = \frac{1}{A_s} \frac{\dot{m}_{pc}}{\rho_{gm}}$
$x_{G,1}$	Struc.	Glucose concentration at current 1.	$x_{G,1} = \frac{1 kmol\, C_6H_{12}O_6}{7 kmol\, Total\, Stream} = \frac{1}{7}$
$\Delta \bar{H}_{r_{gc}}$	Struc.	Specific molar heat of reaction of glucose combustion.	$\Delta \bar{H}_{r_{gc}} = 2.813\ kJ/kmol$
$\dot{m}_1$	Struc.	Mass flow rate at current 1.	$\dot{m}_1 = \frac{1}{w_{G,1}} \mathfrak{M}_G\, \sigma_{G,gc}\, r_{gc}$
$w_{G,1}$	Func.1	Mass fraction of glucose at stream 1.	$w_{G,1} = 0.484$
$\mathfrak{M}_G$	Func.1	Molecular mass of glucose.	$\mathfrak{M}_G = 180\ kg/kmol$
$w_{G,6}$	Struc.	Mass fraction of glucose at current 1.	$w_{G,6} = \frac{1}{1000} \frac{pgm}{\rho_{blood}}$
pgm	Func.1	Plasma glucose measurement.	$pgm = 90\ mg/dl$
ρ_{blood}	Func.1	Blood density.	$\rho_{blood} = 1060\ kg/m^3$
$\dot{m}_6$	Struc.	Mass flow rate at current 6.	$\dot{m}_6 = C_2$
$\dot{m}_2$	Struc.	Mass flow rates at currents 1 and 2.	$\dot{m}_2 = \dot{m}_1$
$\dot{m}_7$	Struc.	Mass flow rates at currents 6 and 7.	$\dot{m}_7 = \dot{m}_6$
x_j	Struc.	Molar fraction of component j.	$x_j = 1 - \sum_{i \neq j} x_i$

Indexes: j = G, NtF, BaF, NtP, BaP, ActL, InaL, ActP, InaP, W, GJ, Fib.

4.2.5.1 Verbal description and process flow diagram

Most digestion and absorption of nutrients occurs in the small intestine. The intestinal epithelium is a critical interface between the organism and its environment. While digestion continues in the small intestine, it also becomes a major site for nutrients absorption. The small intestine absorbs water, salts, micronutrients such as vitamins and minerals, and macronutrients such as carbohydrates, fats, and proteins. Macronutrients generally cannot be absorbed in their natural forms through the gastrointestinal mucosa. For this reason, they must be digested to simpler components in the gastrointestinal tract before absorption and assimilation can occur [127]. Digestion in the small intestine, unlike the stomach, is more chemical than mechanical. The chemistry of digestion is based on hydrolysis of the three macronutrients, in which several types of digestive enzymes are involved in order to promote the hydrolysis reactions for each type of food [42]. Trypsin and chymotrypsin facilitate digestion of proteins, lipases facilitate fat digestion, and amylase facilitates polysaccharides digestion. Physical processing and mixing of food in stomach lead to the formation of a semi-solid paste which is gradually released, when sufficiently fluid, into the small intestine through pylorus to continue its digestion. During the initial phase of food intake, the gallbladder contractions are stimulated. Once the food reaches the duodenum, cholecystokinin is released by cells in the small bowel mucosa causing a strong contraction of the gallbladder and allowing the flow of bile into the duodenum. Cholecystokinin also inhibits gastric emptying, causes a sensation of satiety, and stimulates the secretion of pancreatic juices. Cells of the exocrine pancreas function produce an alkaline fluid rich of bicarbonate and digestive enzymes known like pancreatic juice. This alkaline fluid neutralizes the gastric acid that enters the duodenum. Most enzymes are secreted as inactive proenzymes and are later converted into active enzymes [35]. Digestion of the liquefied food begins in the duodenum and continues during the journey through the jejunum, which is also the major site of nutrient absorption. Epithelial cells of the villi (enterocytes) absorb the end products of digestion and express membrane-bound enzymes in their microvilli (brush-border enzymes) that contribute to the final digestive process. Moreover, final absorption of nutrients and solutes from the gut lumen is not a simple diffusive process. More than 350 solute-specific channels and transporters have been identified, subdivided into 46 families of solute carriers [127].

Carbohydrates digestion is initiated in the mouth by salivary amylase secreted from the parotid and submandibular glands, which begins to break down starches and glycogens into simpler disaccharides and trisaccharides. Due to the salivary amylase is inactivate in the acidic pH of the stomach, the not digested polysaccharides in the mouth are hydrolyzed by pancreatic $\alpha-$amylase upon entry into the duodenum, yielding disaccharides and trisaccharides [127]. The final oligosaccharide products of intraluminal starch digestion and the disaccharides lactose and sucrose are hydrolyzed by specific enzymes that are integral to the brush border membrane and have their active hydrolytic sites available at the intestinal surface, where these saccaridases perform a crucial role in the final digestion of dietary carbohydrates [101]. Once polysaccharides are digested to glucose molecules, they are absorbed to the bloodstream via the enterocytes. The classical pathway of glucose absorption is across the intestinal brush-border membrane, which was predominantly mediated by SGLT1, a membrane protein that couples two molecules of Na^+ together with one molecule of glucose [51]. The passive move out of the basolateral surface of enterocytes contains a facilitated-diffusion glucose transporter GLUT2, which allows glucose

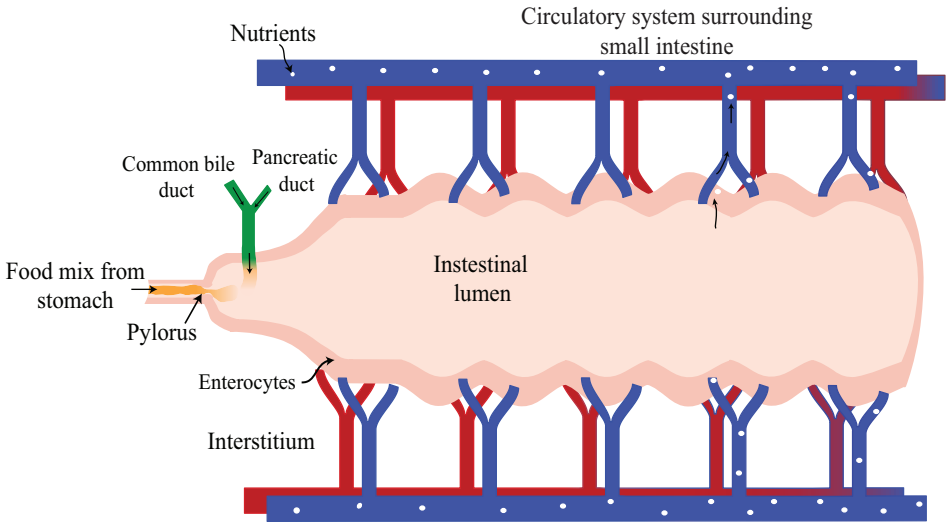

FIGURE 4.19. Representation of the nutrients digestion and absorption in the small intestine.

to move from the intestinal epithelial cells into the extracellular medium near the blood capillaries [217].

Proteins and fats digestion occur partially in the stomach. Stomach empties the chyme containing the broken down proteins and fats pieces into the small intestine. Trypsin, chymotrypsin, elastase, and carboxypeptidases represent the fundamental activated enzymes in proteolysis. The cells that line the small intestine release additional enzymes that finally break apart the smaller protein fragments into individual amino acids. The muscle contractions of the small intestine mix and propel the digested proteins to the absorption sites. In the lower parts of the small intestine, the amino acids are transported from the intestinal lumen through the intestinal cells to the blood. This movement of individual amino acids requires special transport proteins and adenosine triphosphate (ATP). Once the amino acids are in the bloodstream, they are transported to the liver.

Under normal circumstances, a substantial amount of dietary carbohydrates escapes absorption in the small intestine, finishing in the colon where they suffer bacterial fermentation [255]. The colon can absorb glucose, but this capability is probably rarely exploited because fermentation proceeds rapidly. An outcome of fermentation is the production of volatile fatty acids (acetate, propionate, and butyrate), which are important metabolic products for colonic metabolism, but these fatty acids are also absorbed and may be used for combustion and hepatic gluconeogenesis (particularly propionate) [207].

4.2.5.2 Modeling hypothesis and level of detail

The scope of this model is to asses how glucose metabolism is affected by the intestinal absorption of nutrients. Small intestine is modeled as a plug flow reactor (PFR) to describe chemical reactions of the nutrients in continuous time. This hypothesis is used due to the small intestine is a flowing system of cylindrical geometry, where digestion and absorption of nutrients take place. Small intestine is mediated by the digestion products of carbohydrates, fats, and proteins and is regulated by both the length and the region of small intestinal exposure to nutrients [154]. The model is developed at macroscopic scale, being the glucose concentration and absorption the variables of interest. The aim

of the model is to know how is glucose appearing in the portal vein and what is the role of the small intestine in glucose metabolism. Figure 4.20 shows a tubular reactor representing the digestion and absorption processes in the small intestine. Figure 4.21 shows the representation of each slice i of the model. The small intestine is modeled as a distributed parameters model to account for the progressive nutrients appearance into the bloodstream and due to the differences in absorption capacity of duodenum, jejunum, and ileum. Gastric mass going through the small intestine is modeled as flowing through the reactor as a series of infinitely thin coherent plugs, each with a uniform composition. The plugs are assumed to travel into the axial direction of the reactor leading to a composition gradient as it travels. For simulation purposes, each part of the small intestine is divided into a number of equidistant slices depending on the length of the part: 20, 72, and 144 slices for the duodenum, jejunum, and ileum, respectively. The key assumption here is that as a plug flows through a PFR, the gastric mass is perfectly mixed in both every slice and radial direction but not in the axial direction (either forwards or backwards). Each plug of differential volume is considered as a separate entity, an infinitesimally small continuous stirred tank reactor, tending to zero volume. As it flows down the tubular PFR, the residence time of the plug is a function of its position in the reactor.

The tubular reactor in Figure 4.20 is a jacketed reactor to represent both the exchanges with blood irrigating the small intestine and the exchanges of water with interstitial tissue. Stomach flow with nutrients and pancreatic and bile fluids are mixed just when entering to the duodenum and continue through the intestinal lumen until achieving the large intestine.

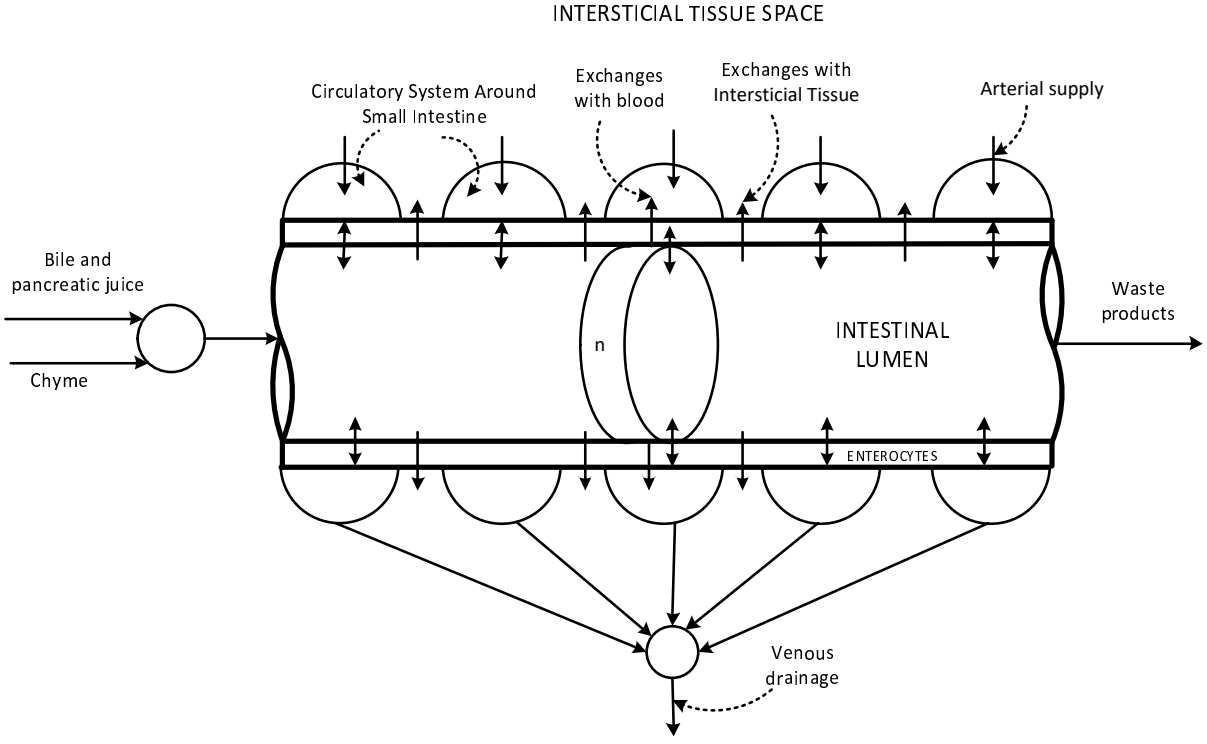

FIGURE 4.20. Hypothesis assumed to model the small intestine.

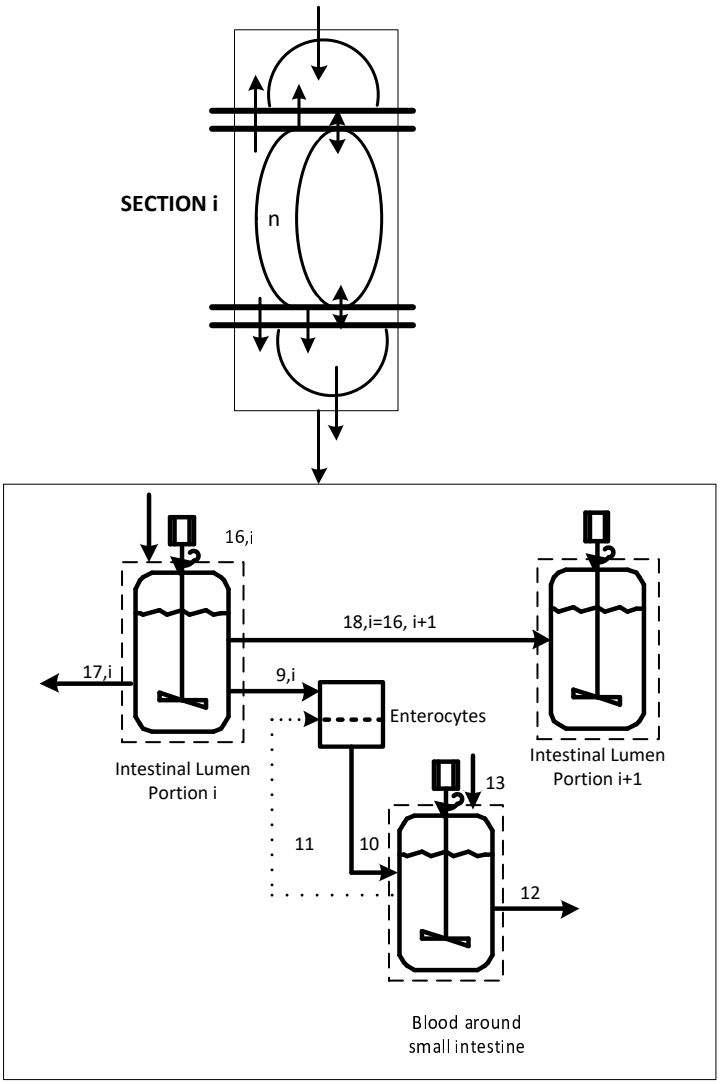

FIGURE 4.21. Modeling hypothesis assumed for each section i of the small intestine. Upper scheme shows one slice or complete section i, and lower scheme reports every part forming section i

4.2.5.3 Process System Definition

The small intestine is divided into three process systems. *PSI* represents the blood irrigating the small intestine, *PSII* are the enterocytes, which are the intestinal absorptive cells and nutrients absorption takes place, and *PSIII* is the intestinal lumen where digestion of nutrients occurs. The pancreatic duct merges with the common bile duct just before the beginning of the duodenum. In that sense, both ducts are joined in the same inflow, represented by stream 15 in Figure 4.22. Stomach gastric flow is the stream 14. Both flows (14 and 15) are mixed to enter intestinal lumen (stream 16). Water exchanges with the interstitial tissue are represented by stream 17. Nutrients uptake from intestinal lumen by the enterocytes is represented here by stream 9, which reaches the portal vein by stream 10, and continues to the circulation through stream 12. Arterial blood surrounding the small intestine is represented by stream 13. Finally, the remaining mass gastric that passes to large intestine is represented by stream 18.

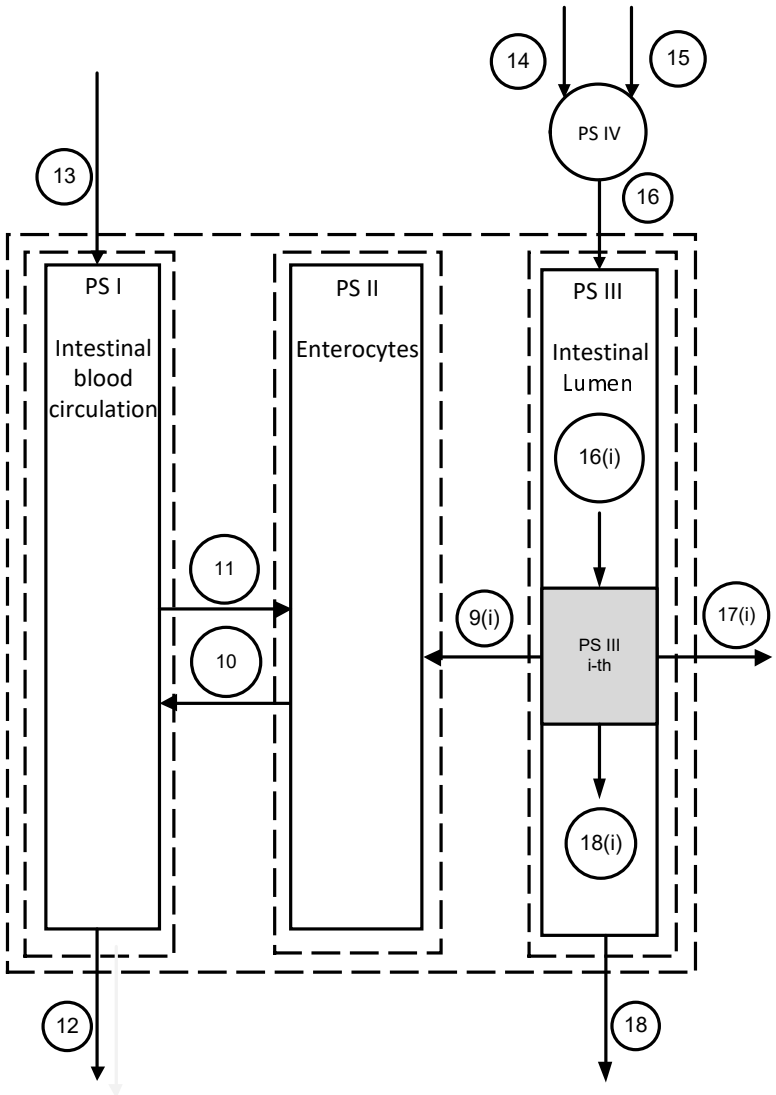

FIGURE 4.22. Block diagram of the small intestine partition in process systems.

4.2.5.4 The Basic Structure of the Model

The set of equations that forms the structure of the small intestine model are:

$$\dot{n}_{12} = \dot{n}_{10} + \dot{n}_{13} - \dot{n}_{11} \tag{4.43}$$

$$\frac{dx_{G,12}}{dt} = (x_{G,10}\dot{n}_{10} + x_{G,13}\dot{n}_{13} - x_{G,11}\dot{n}_{11} - x_{G,12}\dot{n}_{12})\frac{1}{N_I} \tag{4.44}$$

$$\dot{n}_{10} = \dot{n}_{11} + \dot{n}_{9} \tag{4.45}$$

$$\frac{dx_{G,10}}{dt} = (x_{G,9}\dot{n}_{9} + x_{G,11}\dot{n}_{11} - x_{G,10}\dot{n}_{10} - r_{G_{II}})\frac{1}{N_{II}} \tag{4.46}$$

$$\dot{n}_{18,i} = \dot{n}_{16,i} - \dot{n}_{9,i} - \dot{n}_{17,i} \tag{4.47}$$

$$\frac{dx_{n,18,i}}{dt} = (x_{n,16,i}\dot{n}_{16,i} - x_{n,9,i}\dot{n}_{9,i} - x_{n,18,i}\dot{n}_{18,i} + r_{n,i})\frac{1}{N_{III,i}} \tag{4.48}$$

$$\frac{dx_{n,18,i}}{dt} = (x_{n,16,i}\dot{n}_{16,i} - x_{n,18,i}\dot{n}_{18,i} - r_{n,i})\frac{1}{N_{III,i}} \tag{4.49}$$

$$x_{f,18,i} = \frac{x_{f,16,i}\dot{n}_{16,i}}{\dot{n}_{18,i}} \tag{4.50}$$

$$\frac{dx_{w,18,i}}{dt} = (x_{w,16,i}\dot{n}_{16,i} - x_{w,18,i}\dot{n}_{18,i} - \dot{n}_{17,i})\frac{1}{N_{III,i}} \tag{4.51}$$

$$\frac{dM_{EzTot,18,i}}{dt} = w_{EzTot,16,i}\,\dot{m}_{16,i} - w_{EzTot,18,i}\,\dot{m}_{18,i} \tag{4.52}$$

$$w_{EzTot,18,i} = \frac{M_{EzTot,18,i}}{M_{III,i}} \tag{4.53}$$

$$\frac{dM_{EzAct,18,i}}{dt} = w_{EzTot,16,i}\,\dot{m}_{16,i}\,w_{EzAct,16,i} - w_{EzTot,18,i}\,\dot{m}_{18,i}\,w_{EzAct,18,i} + r_{EzAct,i} \tag{4.54}$$

$$w_{EzAct,18,i} = \frac{M_{EzAct,18,i}}{M_{III,i}} \tag{4.55}$$

$$ActEz_{18,i} = \frac{M_{EzAct,18,i}}{\epsilon} \tag{4.56}$$

$$\dot{n}_{16} = \dot{n}_{14} + \dot{n}_{15} \tag{4.57}$$

$$\frac{dN}{dt}|_{PS_V} = \frac{dN_V}{dt} = \dot{n}_{16} + \dot{n}_{13} - \dot{n}_{12} - \dot{n}_{17} - \dot{n}_{18} \tag{4.58}$$

$$\tag{4.59}$$

with n = Glucose, Amino acids, Fatty acids, CC, Proteins, Lipids. Equation 4.52 is for each pancreatic enzyme released by pancreas (summarize them here).

4.2.5.5 Variables, structural parameters, and structural constants of the model

Table 4.10 reports the variables and structural parameters of the small intestine model. In this model there are no constants.

4.2.5.6 Constitutive and assessment equations for structural and functional parameters, and definition of constants

Constitutive and assessment equations to define both structural and functional parameters of the small intestine model are reported in Table 4.11. As in previous models, column

TABLE 4.10. Variables and structural parameters of the small intestine model.

Symbol	Physical meaning
Variables	
$\dot{n}_{12}$	Blood molar flow draining to the portal vein.
$x_{G,12}$	Glucose molar fraction in the oulet flow from the circulatory system.
$\dot{n}_{10}$	Molar flow of the absorbed nutrients that come from the intestinal lumen and go to the circulation system.
$x_{G,10}$	Glucose molar fraction in the enterocytes.
$n_{18,i}$	Total moles leaving each slice i towards the next one.
$x_{n,18,i}$	Molar fraction of component n in the flow 18 that pass to the next portion of the lumen.
$M_{EzTot,18,i}$	Mass of total enzyme in the flow 18 that passes to the next portion of the lumen.
$w_{EzTot,18,i}$	Mass fraction of total enzyme in the flow 18 that passes to the next portion of the lumen.
$M_{EzAct,18,i}$	Mass of active enzyme in the flow 18 that pass to the next portion of the lumen.
$w_{EzAct,18,i}$	Mass fraction of total active enzyme in the flow 18 that passes to the next portion of the lumen.
$ActEz, 18, i$	Enzyme activity of each pancreatic enzyme in the flow 18 that passes to the next portion of the lumen.
$\dot{n}_{16}$	Molar flow of substances that enter to the intestinal lumen (nutrients, pancreatic juice and bilis).
N_V	Total moles in process system V.
Structural parameters	
$\dot{n}_{13}$	The blood flow irrigating the small intestine.
$\dot{n}_{11}$	Molar flow that passes to the blood from the enterocytes.
$x_{G,13}$	Glucose molar fraction in the flow $\dot{n}_{13}$.
$x_{G,11}$	Glucose molar fraction in the flow $\dot{n}_{11}$.
N_I	Total moles in process system I.
$\dot{n}_9$	Total molar flow of the absorbed nutrients from the intestinal lumen.
$x_{G,9}$	Glucose molar fraction in the flow $\dot{n}_9$.
$r_{G,II}$	Velocity of glucose degradation in the enterocytes.
N_{II}	Total moles in process system II.
$\dot{n}_{16,i}$	Molar flow of nutrients entering to slice i.
$\dot{n}_{9,i}\, x_{n,9,i}$	Molar flux of absorbed nutrients in slice i that passes to the enterocytes.
$\dot{n}_{17,i}$	Molar flow of absorbed water, which passes to the intestinal interstitium.
$x_{n,16,i}$	Molar fraction of the component n entering to the slice i in the stream $16, i$.
$r_{n,i}$	Velocity of degradation or generation of the component n in the slice i.
$N_{III,i}$	Total moles in the slice i of the process system III.

Symbol	Physical meaning
Structural parameters	
$w_{EzTot,16,i}$	Mass fraction of total enzyme entering to the slice i in stream $16,i$.
$\dot{m}_{16,i}$	Mass flow entering to the slice i in stream $16,i$.
$\dot{m}_{18,i}$	Mass flow leaving the slice i in stream $18,i$.
$M_{III,i}$	Total mass in the slice i of the process system III.
$w_{EzAct,16,i}$	Mass fraction of total active enzyme entering to the slice i in stream $16,i$.
$r_{EzAct,n,i}$	Velocity of enzyme deactivation of the pancreatic enzyme n in the slice i.
$\dot{n}_{14}$	Molar flow of pancreatic juice and bilis.
$\dot{n}_{15}$	Molar flow of chyme that comes from the stomach.
$\dot{n}_{17}$	Molar flow of absorbed water, which passes to the intestinal interstitium.
$\dot{n}_{18}$	Molar flow of nutrients leaving the intestinal lumen.
Structural constants	
ϵ	Ratio of enzyme mass necessary to obtain one enzymatic activity unit.

"type" reports the classification of all parameters of the model as structural and functional, according to the definitions presented in Chapter 2.

4.2.5.7 Results

Figure 4.23 shows the filling of glucose in each slice. Initially, the intestine is considered full of water, but as glucose enters the intestinal lumen, the water is emptied to lead to glucose. In addition, the figure shows the glucose absorption and its residence time in the small intestine. The faster kinetics occur in the duodenum for glucose, in which a 25 % of glucose is absorbed. However, the major glucose absorption takes place in the jejunum with a 50%, being the kinetics slower than in the duodenum. Finally, a 10% of glucose is absorbed in the ileum, in which the reactions are carried out slower. The remaining glucose in the lumen, i.e., the glucose that is not absorbed in the small intestine, passes to colon to be fermented. Table 4.13 reports some data taken from the literature about the percentages of absorption of the macronutrients in every section of the small intestine. These experimental data were used to validate the model. This model also allows calculating the molar flow of glucose in the portal vein, i.e., the rate of glucose appearance in the bloodstream is $2.6482e^{-08}$ $kmol/s$. The water emptying occurs because the model assumes the small intestine filled with water at the beginning of digestion. Table 4.12 shows the most important characteristics for each section of the small intestine, as well as its absorption, digestion and the percentages of enzymatic deactivation. Data available in the literature was used to adjust the parameters of the model.

TABLE 4.11. Constitutive and assessment equations to define structural and functional parameters of the small intestine model.

Symbol	Type	Description	Equation
$\dot{n}_9$	Struc.	Mass flow of absorbed nutrients from the intestinal lumen.	$\dot{n}_9 = Datum$
$\dot{n}_{11}$	Struc.	Molar flow of nutrients that passes from the blood to the enterocytes.	$\dot{n}_{11} = Datum$
$\dot{n}_{13}$	Struc.	The blood flow that irrigates the small intestine .	$\dot{n}_{13} = Datum$
$\dot{n}_{14}$	Struc.	Molar flow of chyme that comes from the stomach.	$\dot{n}_{14} = 2.41 \times 10^{-8} kmol/s$
$\dot{n}_{15}$	Struc.	Molar flow of pancreatic juice and bilis.	$\dot{n}_{15} = Datum$
$\dot{n}_{17}$	Struc.	Molar flow of absorbed water, which passes to the intestinal interstitium.	$\dot{n}_{17} = 9.292 \times 10^{-6} mol_w/s$
$\dot{n}_{18}$	Struc.	Molar flow of nutrients that passes to the colon.	$\dot{n}_{18} = 1.597 \times 10^{-6} mol/s$
$x_{G,11}$	Struc.	Glucose molar fraction in the flow $\dot{n}_{11}$.	$x_{G,11} = 6.966 \times 10^{-5} mol_G/s$
$x_{G,13}$	Struc.	Glucose molar fraction in the flow $\dot{n}_{13}$.	$x_{G,13} = Datum$
N_I	Struc.	Moles total in PSI.	$N_I = 1.28 \times 10^{-4} mol$
N_{II}	Struc.	Moles total in PSII.	$N_{II} = Datum$
$x_{G,9}$	Struc.	Glucose molar fraction in the flow $\dot{n}_9$.	$x_{G,9} = Datum$
$r_{G,II}$	Struc.	Velocity of glucose degradation in the enterocytes.	$r_{G,II} = Datum$
$\dot{n}_{16,i}$	Struc.	Molar flow of nutrients entering to slice i.	Data inherited from the solution of the differential equation for $\dot{n}_{18,i}$
$\dot{n}_{17,i}$	Struc.	Molar flow of absorbed water, which passes to the intestinal interstitium.	$\dot{n}_{17,i} = Datum$
$x_{n,16,i}$	Struc.	Molar fraction of the component n entering to the slice i in the stream $16, i$.	Data inherited from the solution of the differential equation for $x_{n,18,i}$ with n=Glucose, amino acids, fatty acids, water, carbohydrates, proteins, lipids, fiber.
$x_{n,9,i}\, \dot{n}_{9,i}$	Struc.	Molar flux of absorbed nutrients in slice i that passes to the enterocytes.	$x_{n,9,i}\ n_{9,i} = A_{TM,i} * N_{TM,n,i}$ with n=Glucose, amino acids, fatty acids
$A_{TM,i}$	Func.1	Mass transfer area.	$A_{TM,i} = 0.023 m^2$
$N_{TM,n,i}$	Func.1	Mass transfer flux.	$N_{TM,n,i} = K_{TM,n} * (C_{n,18,i} - CAst_n)$
$K_{TM,n}$	Func.2	Mass transfer coefficient.	$K_{TM,n} = Datum_n$
$C_{n,18,i}$	Func.2	Concentration of component n.	$C_{n,18,i} = \frac{x_{n,18,i} * \rho_{mix,i}}{MW_{mix,i}}$
$\rho_{mix,i}$	Func.3	Mix density.	$\rho_{mix,i} = \frac{1}{\sum_i (w_i * \rho_i)}$
$\mathfrak{M}_{mix,i}$	Func.3	Mix molecular weight.	$MW_{mix,i} = \sum_i (x_i * \mathfrak{M}_{mix,i})$
$CAst_n$	Func.2	Equilibrium concentration of component n.	$CAst_n = Datum_n$

Symbol	Type	Description	Equation
$r_{CC,i}$	Struc.	Velocity of complex carbohydrates degradation in the slice i.	$r_{CC,i} = K_{0CC} * Act_{PA,i} * Vslice_i * C_{CC,i}$
$K0_{CC}$	Func.1	Arhenious constant.	$K0_{CC} = Datum_{duo,ye,il}$
$Vslice_i$	Func.1	Slice volume.	$Vslice_i = Datum_i$
$C_{CC,i}$	Func.1	Carbohydrates concentration in the slice i.	$C_{CC,i} = \frac{x_{CC,18,i} * \rho_{mix,i}}{\mathfrak{M}_{mix,i}}$
$r_{G,i}$	Struc.	Velocity of glucose generation in the intestinal lumen.	$r_{G,i} = \theta_G * r_{CC,i}$
θ_G	Func.1	Coefficient for glucose degradation.	$\theta_G = \frac{\mathfrak{M}_G}{\mathfrak{M}_{CC}}$
$\mathfrak{M}_G$	Func.2	Glucose molecular weight.	$\mathfrak{M}_G = 180 kg/mol$
$\mathfrak{M}_{CC}$	Func.2	Carbohydrates molecular weight.	$\mathfrak{M}_{CC} = 180 \times 10^3 kg/kmol$
$r_{L,i}$	Struc.	Velocity of lipids degradation in the intestinal lumen.	$r_{L,i} = K_{0L} * Act_{PL,i} * Vslice, i * C_{L,i}$
$K0_L$	Func.1	Arhenious constant.	$K0_L = Datum_{duo,ye,il}$
$C_{L,i}$	Func.1	Lipids concentration in the slice.	$C_{L,i} = \frac{x_{L,18,i} * \rho_{mix,i}}{MW_{mix,i}}$
$r_{FA,i}$	Struc.	Velocity of fatty acids generation in the intestinal lumen.	$r_{FA,i} = \theta_{FA} * r_{L,i}$
θ_{FA}	Func.1	Coefficient for fatty acids.	$\theta_{FA} \frac{\mathfrak{M}_{FA}}{\mathfrak{M}_L}$
$\mathfrak{M}_{FA}$	Func.2	Fatty acids molecular weight.	$\mathfrak{M}_{FA} = 47.07 kg/kmol$
$\mathfrak{M}_L$	Func.2	Lipids molecular weight.	$\mathfrak{M}_L = 282.47 kg/mol$
$r_{P,i}$	Struc.	Velocity of proteins degradation in the intestinal lumen.	$r_{P,i} = K_{0P} * Act_{PP,i} * Vslice, i * C_{P,i}$
$K0_P$	Func.1	Arhenious constant.	$K0_P = Datum_{duo,ye,il}$
$C_{P,i}$	Func.1	Proteins concentration in the slice i.	$C_{P,i} = \frac{x_{P,18,i} * \rho_{mix,i}}{MW_{mix,i}}$
$r_{aa,i}$	Struc.	Velocity of amino acids generation in the intestinal lumen.	$r_{aa,i} = \theta_{aa} * r_{P,i}$
θ_{aa}	Func.1	Coefficient for amino acids.	$\theta_{aa} \frac{\mathfrak{M}_{aa}}{\mathfrak{M}_P}$
$\mathfrak{M}_{aa}$	Func.2	Amino acids molecular weight.	$\mathfrak{M}_{aa} = 137 kg/kmol$
$\mathfrak{M}_P$	Func.2	Proteins molecular weight.	$\mathfrak{M}_P = 20961 kg/kmol$
$N_{III,i}$	Struc.	Total mass in molar units of enterocytes.	$N_{III,i} = \frac{V_{flow,i} * \rho_{mix,i}}{MW_{mix,i}}$
$V_{flow,i}$	Func.1	This volume is only for flows calculations. *	$V_{flow,i} = Vslice * \beta$
β	Func.2	This correction factor considers the changes of volume that suffer the intestinal lumen due to the different muscular movements.	$\beta = Datum$
$w_{EzTot,16,i}$	Struc.	Mass fraction of total enzyme entering to the slice i in stream 16, i.	Data inherited from the solution of the equation for $w_{EzTot,18,i}$
$w_{EzAct,16,i}$	Struc.	Mass fraction of total active enzyme entering to the slice i in stream 16, i.	Data inherited from the solution of the equation for $w_{EzAct,18,i}$
$\dot{m}_{16,i}$	Struc.	Mass flow entering to the slice i in stream 16, i.	$\dot{m}_{16,i} = \dot{n}_{16,i} * \mathfrak{M}_{mix,i}$
$\dot{m}_{18,i}$	Struc.	Mass flow leaving the slice i in stream 18, i.	$\dot{m}_{18,i} = \dot{n}_{18,i} * \mathfrak{M}_{mix,i}$
$M_{III,i}$	Struc.	Total mass in the slice i of the process system III.	$M_{III,i} = N_{III,i} * \mathfrak{M}_{mix,i}$

Symbol	Type	Description	Equation
$r_{EzAct,PA,i}$	Struc.	Velocity of enzyme deactivation of the active pancreatic amylase enzyme in the slice i.	$r_{EzAct,PA,i} = -Act_{PA,i} * K2 - Act_{PP,i} * K2_{deg,i} * 0.06$ with 0.06 a units conversion factor
$K2$	Func.1	Degradation factor by time of the enzyme *n*.	$K2 = Datum$
$K2_{deg,i}$	Func.1	Degradation factor by proteases, has different value in each intestine section.	$K2_{deg,i} = Datum$
$r_{EzAct,PL,i}$	Struc.	Velocity of enzyme deactivation of the active pancreatic lipase enzyme in the slice i.	$r_{EzAct,PL,i} = -Act_{PL,i} * K6 - Act_{PP,i} * K6_{deg,i} * 0.06$ with 0.06 a units conversion factor
$K6$	Func.1	Degradation factor by time of the enzyme *n*.	$K6 = Datum$
$K6_{deg,i}$	Func.1	Degradation factor by proteases, has different value in each intestine section.	$K6_{deg,i} = Datum$
$r_{EzAct,PP,i}$	Struc.	Velocity of enzyme deactivation of the active pancreatic protease enzyme in the slice i.	$r_{EzAct,PP,i} = -Act_{PP,i} * K4 * 0.06$ with 0.06 a units conversion factor
$K4$	Func.1	Degradation factor by proteases, has different value in each intestine section.	$K4 = Datum$

* This volume considers a reduction of the total volume of the small intestine in each section (duodenum,jejunum and ileum) due to the muscular movements; therefore, this has a direct effect on the residence time as well as on the flow of the food.

TABLE 4.12. Reported data used to perform the parameters adjustment of the model

Data	Duodenum	Jejunum	Ileum	Bibliography
Lenght [m]	0.25	0.90	1.80	[115]
Residence time of chyme [s]	1220	4393	8786	—
Number of slices	320	72	144	—
Glucose absorption [%]	25	50	10	[129; 142]
Fatty acids absorption [%]	30	55	15	[129; 142]
Amino acids absorption [%]	30	50	10	[129; 142]
Water absorption [%]	14	30	39	[129; 142]
Carbohydrates digestion [%]	53	35	0	[118; 127]
Lipids digestion [%]	47	31	0	[118; 127]
Proteins digestion [%]	56	37	0	[118; 127]
Pancreatic amylase deactivation [%]	15	10	0	[145]
Pancreatic lipase deactivation [%]	92	6	0	[145]
Pancreatic protease deactivation [%]	35	45	0	[145]

TABLE 4.13. Percentages of nutrients absorption in every section of the small intestine.

Nutrient	**Duodenum**	**Jejunum**	**Ileum**	**Total**	**References**
Glucose	25	50	10	85	[127; 142]
Fats	30	55	15	95-100	
Proteins	30	50	10	66-95	
Water	14	30	39	83-84	

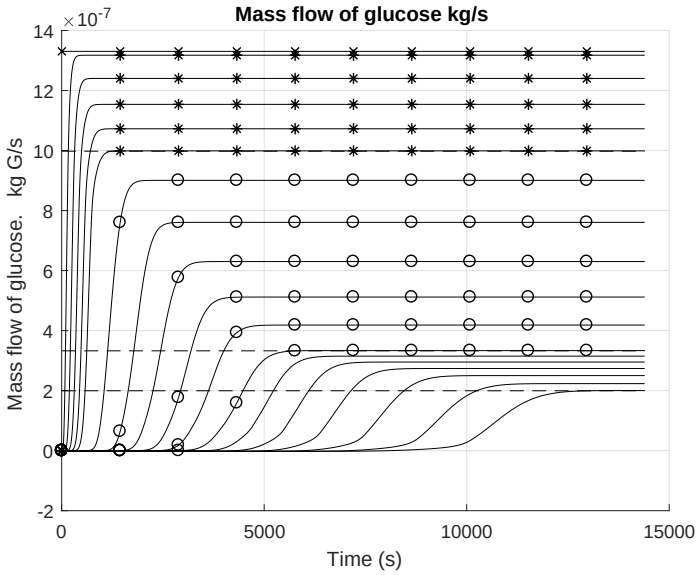

FIGURE 4.23. Glucose concentration in the lumen of the small intestine during digestion and absorption process. Lines with ∗ represent the process in the duodenum, lines with circle are the jejunum, and simple lines are the ileum. Discontinue lines represent the theoretical values that the absorption in each section of the small intestine should reach according to the data reported in the literature.

4.3 Results of model integration

A complete model of glucose homeostasis in the human body is developed as phenomenological as possible. The whole model is composed of five sub-models representing the role of the organs involved in glucose metabolism. The sub-models are linked sequentially following the natural connection of the human body via the circulatory system. As it was mentioned, the inspiration or analogy is the plantwide view to get all the pieces together. In Figure 4.25, the analogy of a plantwide view is applied on the human body. The organs involved in glucose homeostasis, modeled in this thesis, are presented in the figure. The natural sequence of the circulatory system is followed resulting in two internal loops. Also, an approximation of the blood flows in every organ is included, according to data reported in the literature. Mix point 1 represents the link between hepatic vein and venous drainage of the brain. The junction between the portal vein and the hepatic artery is represented with the mix point 2. Mix point 3 is the portal vein where blood from the abdominal organs drains to reach the liver. Mix points 4 and 5 represent the

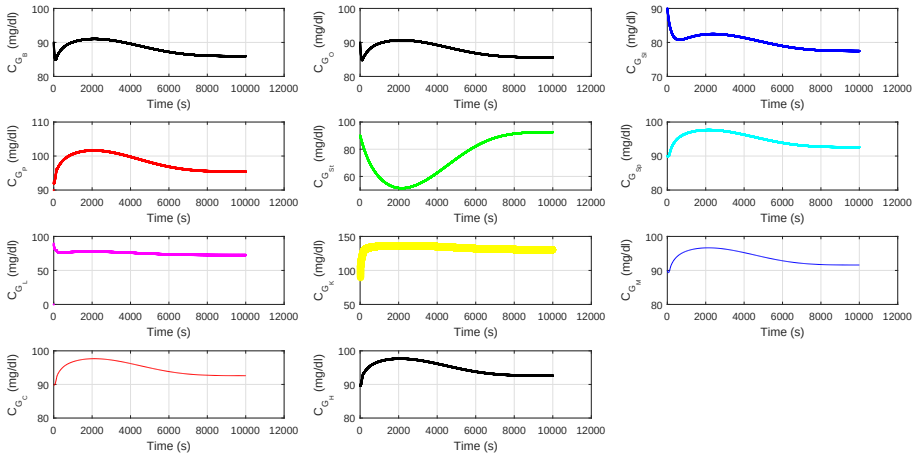

FIGURE 4.24. A representation of the glucose regulation in each organ of the human body. Model coupled.

venous drainage of the kidneys and muscle and adipose tissues, respectively. Finally, the junction between superior and inferior cava veins to enter in the heart is mix point 6. The brain, muscular tissue, large intestine, and others, are included as algebraic equations representing their respective glucose consumption. A detailed mathematical model is not necessary for these parts due to their constant glucose consumption. The models of the stomach, small intestine, liver, kidneys, and pancreas are as reported before.

In Figure 4.24 can be observed a preliminary result of the model coupled where the blood glucose regulation is shown. A little glucose consumption occur in every modeled organ according to the physiology. Glucose concentration leaving from liver is a constant as can be seen in Figure 4.24, pink line (C_{G_L}). The liver plays an important role in glucose regulation through hormones released by the pancreas. This organ is responsible for maintaining blood glucose levels regulated through biochemical processes. In a similar way the kidneys act as can be noted in the figure, yellow line (C_{G_K}), where endogenous glucose production also takes place. Black line (C_{G_H}) representing the glucose concentration in the bloodstream shows a regulation of the glucose levels, keeping this concentration around $90 mg/dL$. The results of a coupled model demonstrated that it is possible to obtain a phenomenological-based semiphysical model with parameters interpretability.

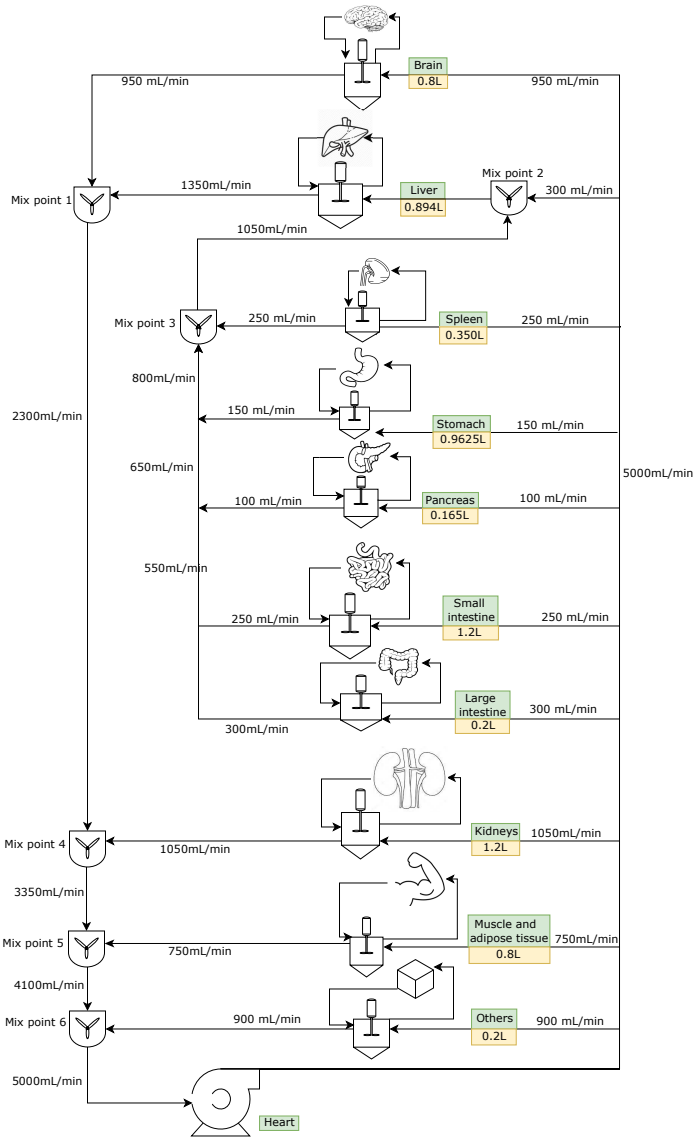

FIGURE 4.25. Human body analogy using the plantwide view approach.

5

A proposal for defining parameters interpretability

A major goal of the modelers is to know the mechanisms that are happening within the system under study, regardless of whether the model is empirically or phenomenologically based. Knowing the internal mechanisms implies the understanding of the phenomena. However, this understanding of the phenomena is just the interpretation of the process by the modeler. Through the interpretation of the phenomena, for example, empirical models seek to imitate the human behavior when those models support human tasking. While process modeling of phenomenological-based models looks for providing knowledge of the phenomena of the process. In this way, concepts about interpretability and identifiability are discussed together due to it was found that both have common interesting things complement each other. The core of this thesis is presented in this chapter. The main contribution is to propose a definition of parametric interpretability on phenomenological based semi-physical models, to cover the lack of conceptual formalism existing in the literature, and to develop a methodology to endow interpretability to the parameters of a PBSM. Hence, a theoretical formalism of interpretability in mathematical modeling is proposed. A link between interpretability and identifiability is also presented aiming at the improvement of the parameter identification.

5.1 Could be identifiability an inspiration for parameters interpretability?

Identifiability is an existing concept in the literature, useful here to propose interpretability concept leveraged in this work to obtain an accurate definition of interpretability. While identifiability allows to know whether the existing model structure and available data are well suited for a unique (numerical) assignment of parameters, interpretability will play a central role in getting insight into the internal structure of a system from the physical meaning of the parameters. Here, a short report of identifiability is introduced as a theoretical-based for proposing later a conceptual framework for parameters interpretability.

5.1.1 A brief recall on parameter identifiability

Identifiability is a structural property of the model that refers to the ability to find a unique best set of values of the model parameters from available measurements [53; 206].

Under the assumption that the model perfectly represents the system, model identifiability is tested in the hypothetical scenario set by continuous noise-free data and experimental conditions providing sufficient excitation of the process inputs reaching a full information data set. The theoretical ability to recover the best model parameters uniquely is called structural identifiability of parameters [23]. Structural identifiability does not depend on experimental data. Identifiability is a necessary condition for the parameter identification problem to be mathematically well posed. Identifiability testing is of great relevance for models where the parameters are biologically meaningful (as is the case for PBSMs applied to human body organs) due to it may be desirable to identify them uniquely [186].

Structural identifiability is categorized in global and local identifiability [206]. It is said that a single parameter p_i is *structurally globally identifiable* if there exist a unique solution for p_i on an interval $[t_0, T]$. That is, if all parameters $\hat{p}$ of the model are equal to those parameters p^* of the process, considering that both structures $M(p^*)$ and $M(\hat{p})$ are identical:

$$M(\hat{p}) = M(p^*) \Rightarrow \hat{p}_i = {p_i}^*$$

Otherwise, if the parameter p_i has a finite number of solutions (greater than zero), the parameter is structurally locally identifiable. A parameter p_i is *structurally locally identifiable* if for almost any parameter of the process p^*, there exists a region $V(p^*)$ such that

$$\hat{p} \in V(p^*) \qquad \text{and} \qquad M(\hat{p}) = M(p^*) \Rightarrow \hat{p}_i = {p_i}^*$$

If for p_i there exist an infinite number of solutions in the interval $[t_0, T]$, the parameter is said to be unidentifiable. Local identifiability is therefore a necessary condition for global identifiability. The model structure is structurally globally/locally identifiable if all parameters p_i are globally/locally identifiable. Contrarily, if at least one parameter p_i is structurally unidentifiable, then the model structure is unidentifiable [44; 206].

The property of structural identifiability is set in an ideal context of perfect measurements. However, in practice the uncertainty on the model structure and noise in the measurements are present, affecting the identifiability of the parameters of the model [25] and an accurate identification of the model parameters is not guaranteed. In this way, it is valuable to formulate a dynamic model describing the internal structure of a system based on phenomenological laws and not totally from experimental data. Identifiability may also help on experimental design by providing guidelines on the selection of inputs and outputs physical location into the process to guarantee the model identifiability [219], which is useful to models of physiological systems, where measurements and the number and physical location of possible inputs and outputs are often limited.

5.1.2 Identifiability analysis

Identifiability testing can be helpful to provide guidelines to deal with non-identifiability, either by providing hints on how to simplify the model structure or by indicating when more information (measured data) is needed from an specific experimental setting [25] to gain identifiability. Different methods have been proposed to test identifiability of linear and nonlinear models. The interested reader is reffered to dedicated literature:

[202] for Taylor series method, [248] for generating series method, [244] for the similarity of transformation approach, for the differential algebra based method [25; 156], for the direct test [69; 247], a method based on the implicit function theorem [258], and the recently developed test for reaction networks [62; 66]. To facilitate identifiability testing, software tools such as DAISY (Differential Algebra for Identifiability of SYstems) [25] and GenSSI (Generating Series for testing Structural Identifiability) have been developed [54]. Both of them are freely available and used in this thesis.

In 2007, DAISY was developed as a software tool implementing a differential algebra algorithm to perform structural identifiability analysis for linear and nonlinear models. DAISY is a completely automatized software that requires minimum prior knowledge of mathematical modeling and no in-depth understanding of the underlying mathematical tools. This software is used in biological modeling studies, specially in physiology and clinical medicine [25]. The algorithm can assume that the initial conditions of a dynamical model are known. In addition, to check global identifiability, first, it is necessary to check if the corresponding states are algebraically observable to proceed with the identifiability test. The model structure must be only made up by differential equations, that means, all algebraic equations should be replaced into differential equations to run the software. Furthermore, it is limited in the size and the functional form of the non-linearities that can be handled in the model (only polynomial or rational). DAISY is implemented in the symbolic language REDUCE.

On the other hand, GenSSI is a software tool to check structural identifiability for arbitrary non-linear dynamic models. GenSSI enables non-expert users to carry out such analysis. This software was implemented as a free toolbox for the MatLab® computing language [54]. GenSSI is easy to use and does not require user knowledge of higher mathematics, a programming language or computer algebra system (other than being familiar with MatLab®). To run GenSSI, the user needs to specify the model equations, input variables [1] (controls), output variables (observables), initial conditions and parameters for model calibration. After a series of automatic symbolic computations, the toolbox produces rich text and graphical output with information about the identifiability of such a model.

5.1.3 An example of identifiability analysis

As it was mentioned in Section 2.4.2, around 1980s Bergman and coworkers proposed the so-called minimal model [29] which later on was to become in a standard model for diabetes technology. From this contribution, many studies directly related to the Bergman's minimal model arose [58]. This section focuses on the structural identifiability analysis of one of the derived forms of Bergman's minimal model, that is the subcutaneous oral glucose minimal model (SOGMM) presented in [138]. This model is a compartmental model and was originally intended to describe a specific procedure like the intravenous glucose tolerance test (IVGTT). According to [44], a compartment is an idealized store of a substance present in a biological system in many forms and locations. It should be noted that the compartmental approach, from the partition used to state the model, presents difficulties for interpretability due to the unreal application of the compartments. Thus, a mathematical model was built to describe the chemical

[1] In general in the literature, the inputs of the model are commonly called variables, but really they are input parameters of the process model, characterized because are parameters that change, that is, they are not fixed values, but they are not solved by the model as it happens with the variables.

reaction and material transfer processes in glucose system. The structure of this extended version of the *minimal model* is as follows. The model parameters are reported in Table 5.1.

TABLE 5.1. Parameters of the SOGMM.

Symbol	**Meaning**	**Units**
S_g	Fractional glucose effectiveness measuring glucose ability to promote glucose disposal and inhibit glucose production.	$1/min$
G_b	"Basal" glucose concentration associated with the patient's basal rate of insulin delivery.	mg/dl
$Ra(t)$	Glucose rate of appearance in blood.	$mg/kg/min$
${}^*V_g$	**Distribution volume of glucose**.	kg/dl
p_2	Rate constant of the remote insulin compartment from which insulin action is emanated.	$1/min$
S_I	Insulin sensitivity. Ability of insulin to control glucose production and utilization.	$1/min$ per mU/L
$I(t)$	Plasma insulin concentration.	mU/L
I_b	Reference value for $I(t)$ associated with the fasting plasma glucose concentration of the patient.	mU/L
k_{sc}	Time constant that encompasses both the physiological lag and the sensor lag.	$[1/min]$
k_τ	Rate constant associated with oral glucose absorption.	$1/min$
k_{abs}	Rate constant associated with oral glucose absorption.	$1/min$
k_d	Rate constants of subcutaneous insulin transport.	$1/min$
k_{cl}	Rate constants of subcutaneous insulin transport.	$1/min$
${}^*f$	**Fraction of intestinal absorption which actually appears in the plasma**.	$dimensionless$
BW	Body weight of the subject.	kg
V_I	Distribution volume of insulin.	L/kg

- A two-state compartmental model

$$\dot{G}(t) = -(S_g + X(t))\ G(t) + S_g\ G_b + (R_a(t)/V_g)$$
$$\dot{X}(t) = -p_2\ X(t) + p_2\ S_I(I(t) - I_b)$$

  where $G(t)[mg/dl]$ represents the plasma glucose concentration and $X(t)[1/min]$ is the proportion of insulin in the remote compartment.

- Subcutaneous Glucose Measurement Submodel

$$\dot{G}_{cgm}(t) = -k_{sc}(G_{cgm} - G(t))$$

where $\dot{G}_{cgm}(t)$ represents the interstitial glucose concentration generally measured in the adipose tissue with the continuous glucose monitoring, and modeled as a first order delay from the plasma glucose concentration $G(t)$.

- Gastrointestinal submodel

$$\dot{Q}_1(t) = -k_\tau \; Q_1(t) + \omega(t)$$
$$\dot{Q}_2(t) = -k_{abs} \; Q_2(t) + k_\tau \; Q_1(t)$$

where $Q1(t)[mg]$ and $Q2(t)[mg]$ are the two compartments representing the oral glucose transport. Input $\omega(t)[mg/min]$ is the rate of mixed-meal carbohydrate absorption at time t.

- Subcutaneous Insulin Kinetic Submodel

$$\dot{I}_{sc1}(t) = -k_d \; I_{sc1}(t) + J_{ctrl}(t)$$
$$\dot{I}_{sc2}(t) = -k_d \; I_{sc2}(t) + k_d \; I_{sc1}(t)$$
$$\dot{I}_p(t) = -k_{cl} \; I_p(t) + k_d \; I_{sc2}(t)$$

where $I_{sc1}(t)[mU]$ and $I_{sc2}(t)[mU]$ represent compartments related to the interstitial insulin transport, $I_p(t)[mU]$ represents the plasma insulin, and $J_{ctrl}(t)[mU/min]$ represents the insulin input signal.

The next two constitutive equations of this model are used to calculate the parameters $Ra[t]$ and $I[t]$:

$$R_a(t) = (Q_2(t) \; k_{abs}) \; f/BW$$
$$I(t) = (I_p(t))/(V_I \; BW)$$

As stated in previous section, there are several methods for testing structural identifiability and facilitate the identifiability analysis. To carry out an identifiability analysis in the SOGMM in this thesis, DAISY is used. The analysis demonstrated that, under ideal conditions of noise-free observations, error-free model structure, and all the state variables observable, the model is non identifiable. However, if some parameters are set as known, the subset of unknown parameters are structurally globally identifiable and the model is globally identifiable. Conversely, if all the parameters must be estimated and ideally all states are observable, the model is not identifiable. In Table 5.1, parameters with the asterisk and in bold must be estimated to make the model globally identifiable, with G_b, BW, and I_b known. Later, an interpretability analysis of the SOGMM parameters is done and common interesting points between both analysis identifiability and interpretability are found and reported.

5.2 Setting a conceptual framework for interpretability

In this section, existent attempts to use/define interpretability are brought up. Then, a formal definition of parameter interpretability is made and further applied to a case study. Using a simple model, the parts of a PBSM as they were previously presented in Chapter 2 are declared. Additional definitions to build both a parameter interpretability definition and a methodology to endow a PBSM's parameter with interpretability are introduced. Moreover, the classification of model parameters, including interpretability property, and other developments of the doctoral contribution concepts are elaborated.

5.2.1 Interpretability in models

Interpretability is still a fuzzy concept in the literature. Many studies propose interpretability as a means to engender trust in the models and to reach features as close as possible to humans [45; 74; 135; 181; 214]. Machine learning models, for example, are increasingly used in the field of medicine and healthcare but there is still an inability by humans to understand how those models work. In this way, Caruana et al. [45] evaluated a method rule-based learning [12] and applied generalized additive models (GAMs) [110; 160; 161] to real healthcare problems to get *intelligible* and accuracy models, in order to predict risk prior to hospitalizations, to have a more informed decision about hospitalization, and to reduce healthcare costs by reducing hospital admissions [45]. In this context, Lou et al. [160; 161] call *intelligible* models those models that can be easily interpreted by users. Been Kim in his thesis [135] developed a framework for human-in-the-loop machine learning that enables people to interact effectively with machine learning models to make better decisions, without requiring in-depth knowledge about machine learning techniques. Been Kim states that machine learning techniques are a good computational tool at the lowest level of granularity, and humans are capable of abstracting knowledge from their experiences, and transferring the knowledge across different domains. In consequence, both machine learning techniques and people have skills that complement each other. Granularity term is referred in [165] as the model property that describes the level of detail in the description of various aspects of the target system. [214] proposed an interpretable Naïve Bayes classifier with competitive discrimination ability and transparent reasoning to improve the classification performance in many problem domains, such as credit approval and medical diagnosis. Equally, for Ribeiro, et al [213] judgement the role of the humans using machine learning classifiers as tools. Therefore, they developed an algorithm that can explain the predictions of any classifier or regressor in a faithful way, by approximating it locally with an interpretable model. Authors like Swartout [236] have worked in the building of expert systems. Expert systems involve a knowledge engineer eliciting procedures, strategies, and rules of thumb from a domain expert and transferring this heuristic knowledge into a computer program [250]. Since then, several authors have incorporated domain knowledge into data mining [79; 80; 229] and they have been interested into combine knowledge engineering and machine learning in order to construct decision support systems. Other authors think that a particular decision is reached when we are able to understand how the model works [125], i.e., model representation, not model operation as mathematical structure. The validation by an analyst or domain expert may be improved if a trade-off is often done between the predictive accuracy of black box models such as neural networks or support vector machines and interpretability of other types of representations.

Doshi-Velez defines interpretability as the ability to explain or to represent in understandable terms to a human [73], that is, looking for doing systems that make decisions like a human being make them. Biran and Cotton [32] define interpretability as the degree to which an observer can understand the cause of a decision, i.e., the ability of a system to be understood by humans either through introspection or a produced explanation. Miller [179] adopts Lipton's assertion [153] that explanation is post-hoc interpretability and used it in artificial intelligence models. For Miller, explanation is one mode in which an observer may obtain understanding, thus he equates interpretability with *explainability*. Biran and Cotton [32] argue that an alternative to methods for interpreting or justifying black-box models is to produce models that are inherently interpretable. However and as it has been mentioned throughout this thesis, inherent interpretability is a property only of the basic structure of the phenomenological-based models, because they include the phenomena occurring under the system in study. Contrarily, empirical models are derived from model predictions, experiments and observations, and, therefore, they use equation fitting or existing mathematical structures [107], to find the best relationship between the model and the data set, in which the parameters have little or no physical meaning.

After a thorough literature review, it can be said that interpretability is a qualitative property rather than a quantitative one. Indeed, interpretability is a latent property of mathematical models, that can be influenced by different factors such as the number of features, complexity of the model, level of detail, level of specification, and basic structure of the model [204]. Due to the lack of formalism about interpretability as a mathematical property of the models, and despite the increase of activity and innovation in mathematical modeling, there is still no consensus about how to define, quantify or measure the parameter interpretability. In this thesis, a conceptual formalism of parameters interpretability in PBSMs is provided. Finally, interpretability concept has been used in empirical-based models to seek interpretations that might explain predictions without elucidating the mechanisms by which models work [153], or to infer properties or generating hypotheses about the natural world. Then next two sections introduce the interpretability concept on phenomenological-based semi-physical models.

5.2.2 Proposed definitions related to parameter interpretability

As previously mentioned, some authors define interpretability as a trust [2] issue and a matter of transparency, focused on empirical models and not on phenomenological based models. However, parameter interpretability as a structural property of PBSMs allowing to obtain knowledge about the modeled process and facilitating the parameter identification, has not been yet studied. In this sense, it is worth asking how reliable is our model? Our evolved brain can easily be tricked into understanding a model which in fact is completely wrong, hence the importance of building a phenomenological-based model with interpretable parameters. A model with interpretable parameters is a mathematical expression based on the known phenomena, which seeks to provide additional knowledge to the process being modeled through the description of the process mechanisms. In this thesis, interpretability is associated with the knowledge contained in the parameters of the model. Here, the knowledge within a parameter is about the process, and not about the interpretation of the model responses as proposed in the literature. That is, in the literature, the concept of interpretability refers to the understanding of the performance

[2]Trust in a model consists of having the certainty that the results given by the model correspond to those of the process of the real object being modeled.

of the model, its results, and to the confidence in its predictions. However, a model with interpretable parameters could predict more precisely the different operation modes of the process. An interpretable parameter allows the modeler to define a numerical value interval to get a better parameter identification, according to its knowledge of the process. Giving a numerical value interval facilitates the practical parameter identification, but not the theoretical identification, due to the practical identification assigns a numerical value to the parameter, while structural identification only indicates if the parameter is identifiable. A model with interpretable parameters has a story, can be explained by other authors easily, and uses interpretable transformations. Also, it helps the user to understand what is really going on, and gives more intuition about the subject matter. This type of models are better for persuading and has fewer chances for human error.

The following definitions are proposed attempting to close the gap existing in the literature about parameter interpretability. Using the definition of the word *interpret* [205] as "*a way to explain, give or provide the meaning of something*", a formal definition of parameter interpretability for PBSMs is proposed as follows.

Definition 5.1. ***Parameter interpretability.*** *Given a model structure for a system, a parameter p_i is said to be interpretable if it has physical meaning into the real object. This means that in a specific context, the symbol of a given interpretable parameter provides additional information or knowledge about the phenomena under consideration when compared to a single numerical value (instead of the symbol). The interpretability of a parameter as a property depends on the model structure. Also, the parameter location into the model structure helps to provide interpretability to that parameter being defined.*

An interpretable parameter in a specific context could provide additional information to the phenomena occurring in the processes. The detailed approximations and idealizations that go into forming models of phenomena make them context-specific, in contrast to the generality of templates that gives them their flexibility and degree of independence from the subject matter [124]. In this sense, the knowledge contained in a parameter is always within a scientific domain, and there the physical meaning of the symbol representing a parameter to be endowed interpretability is placed. In engineering, the scientific contexts where an interpretable parameter can be placed are chemistry, physics, and biology [124]. Engineering, placed within these three scientific contexts, includes processes like chemical, mechanical, and biological processes. Different types of reactors give place to an inner scientific context of chemical processes as well as cellular reactions belong to biological processes. A parameter can be interpretable in any of the named contexts, depending on the knowledge domain, and process phenomena being modeled. Figure 5.1 shows as an example two scientific domains of engineering where different processes are placed. The context of biomedical engineering has an additional context, the biological processes, in which two different biological processes are contained here as examples: Krebs cycle at cellular level and pancreas physiology at organ level. On the other hand, the context of chemical engineering has an additional context, the reactors, in which two different types of reactors are illustrated: continuous stirred-tank reactor (CSTR) and plug flow reactor (PFR). Each context may have specific interpretable parameters, but there also may be the case where the context of a given parameter is general (in a high hierarchy level) encompassing many types of processes. The viscosity of a fluid μ for example, is an interpretable parameter general in any engineering context and valid for all processes: in Krebs cycle μ can be the viscosity of the cellular fluid, in the pancreas μ can be the viscosity of blood irrigating the pancreas, in both reactors μ is the viscosity of the interest

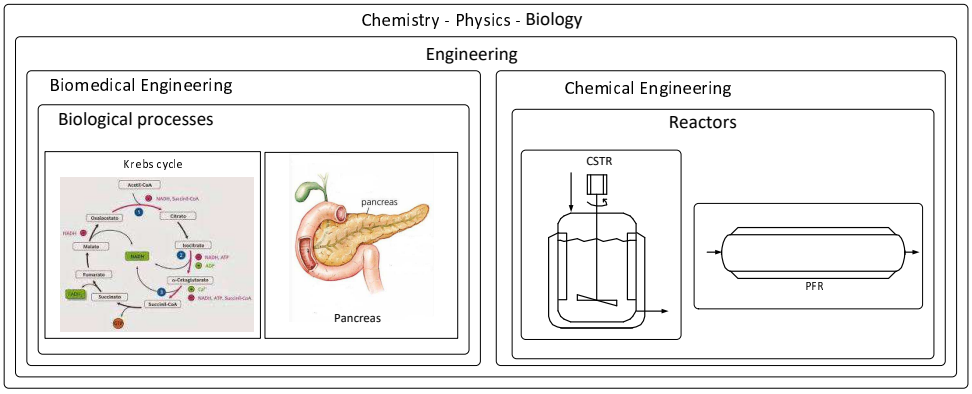

FIGURE 5.1. Two scientific domains where the knowledge associated to any specific physical meaning of a parameter can be placed.

fluid inside each reactor, etc. On the other hand, the rate constant due to the frequency of molecular collisions k_0 is an interpretable parameter inside both reactors CSTR and PFR belonging to the chemical engineering context, but inside biological processes, this parameter has no direct interpretation. However, if an analogy from the context where reactors belong is used to model the unknown phenomena of a biological process, then a biochemical reaction within a biomedical engineering context can be represented by the Arrhenius' equation in which the interpretable parameter k_0 is used.

As it was previously discussed, parameter interpretability can be significantly affected by the type of model. Phenomenological models are derived from the knowledge of the phenomena taking place within the system being studied. When a process is modeled from first principles, all the parameters belongin to the model's basic structure have inherent interpretability. Each distinct phenomenon has a unique mathematical representation [124]. This fact avoids the use of an analogy and makes the model basic structure unique and universal. As consequence, structural parameters of a phenomenological based model are interpretable because they come from physical laws governing the real object and for this reason, an analysis or evaluation of its interpretability is not necessary. However, in empirical and semi-physical models, the interpretability is not guaranteed and therefore, there is a need for interpretability that appears from an incompleteness in the problem formalization [73], creating a fundamental barrier to model the real object as real as possible and thus making hard its optimization and evaluation.

As mentioned earlier, the basic structure of a PBSM is generated by the conservation law applied as balances of matter, mass, energy, and momentum [3]. This type of models are based on the phenomena occurring in the real object. When a real object is modeled using the PSBM approach, a first step implies the definition of the study object. This study object can be described either from theories and concepts from the object's domain or from an analogy a different other domain. One of the most preferred domains to take analogies are the chemical processes. In this way, two situations are possible: *i*) The first principles of physics, chemistry, biology, etc. are directly applied to the real or **primitive object** and *ii*) the first principles are not directly applied to the **object to be modeled**, but they can be applicable using a **process analogy**. In the first case, it is possible to say that

[3]These three balances are the most commonly used in chemical and biological processes. However, other balances may also be found in other scientific fields, all using the conservation law as phenomena explanation.

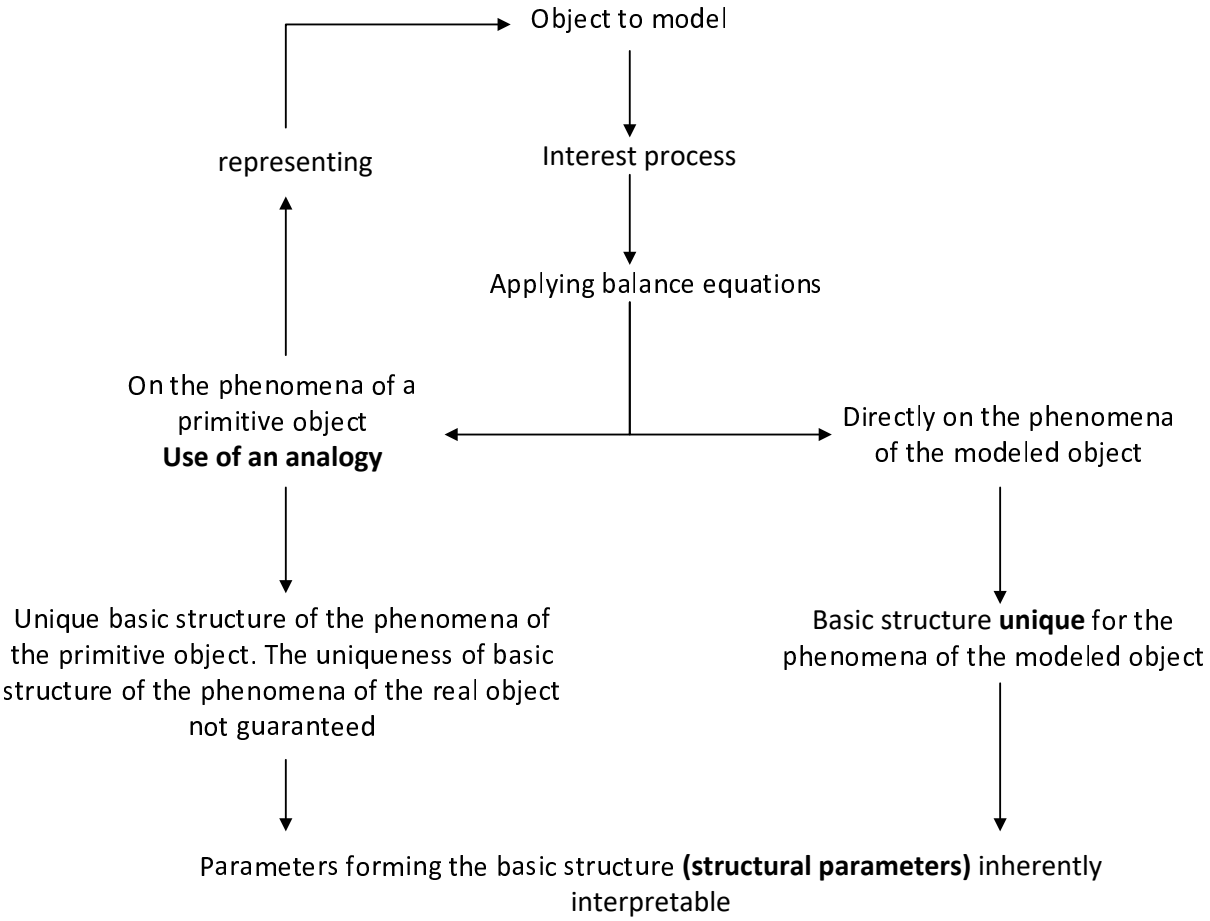

FIGURE 5.2. Options to model the process in an interest object.

obtained basic structure of the model is unique for the kind of process to which the real object belongs. In the second case, the model's basic structure is not unique for the object to be modeled, since a new model may possibly be derived with a new analogy. However, in any case, the interpretability of the parameters in the basic structure is guaranteed and hence, structural parameters enjoy inherent interpretability. Instead, interpretability of functional parameters cannot always be guaranteed. Functional parameters may have either direct or non-direct interpretability, or they may be non-interpretable according to the type of the model use [9]. Figure 5.2 shows two options to model a process of an object of interest. For example, if our interest is to model biochemical processes carried on the liver with respect to glucose metabolism, the object to be modeled would be the liver, as shown in Figure 5.3. However, the phenomena governing the liver are unknown, then balance equations can not be applied directly in the liver. In this case, a primitive or real object with known phenomena is required. The primitive object used to apply balance equations is sought to have an analogue process to the process of interest in the liver. Thus, a stirred tank with two immiscible phases is used like primitive object to model the processes of interest in the liver, instead to model directly the biochemical processes in the organ. In this sense, the basic structure of the model is unique for the stirred tank, but not for the liver.

Functional parameters are those found in constitutive and assessment equations and can be associated with a function (constitutive or assessment) or directly with a numer-

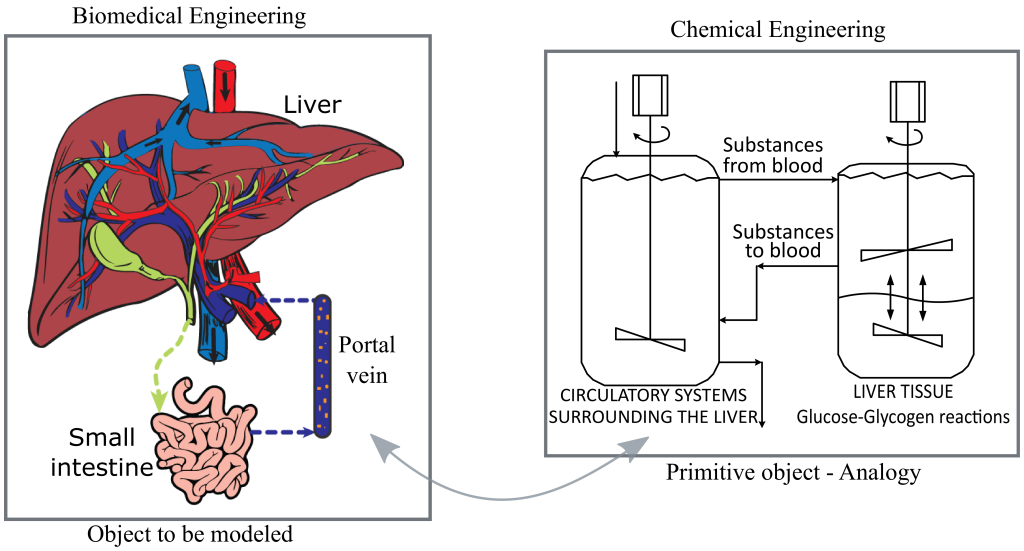

FIGURE 5.3. An example of an analogy. Primitive object or analogy from chemical engineering is used to model the role of the liver in glucose homeostasis in humans.

ical value. Functional parameters extend the mathematical model and they can change from one model to another because it is up to the modeler to decide the constitutive or assessment equations to be used. For this reason, the complete structure of a PBSM may not be unique, even if its basic structure is. Due to structural parameters are inherent to the phenomenology and therefore interpretable, interpretability is evaluated only for functional parameters in a PBSM. A functional parameter may not have general interpretability but interpretability within a specific process, or may not be interpretable. For example, when parameters are originated from data through parametric identification techniques, they only could be interpreted knowing the laws or principles that govern the real object. According to this, interpretability of functional parameters can be classified into three degrees as defined as follows.

Definition 5.2. ***General interpretability.*** *Inherent physical meaning of the parameter within a model in a specific scientific domain, i.e., its interpretation is independent on assumptions used to deduce the basic model structure.*

Definition 5.3. ***Contextualized interpretability.*** *Physical meaning of a parameter is valid only into a specific mathematical model. The meaning is dependent on the considerations and hypothesis used to deduce the mathematical model within a given context.*

Definition 5.4. ***Non-interpretability.*** *The parameter has not physical meaning within the model.*

Furthermore, functional parameters can be associated to an equation including a model variables or not. If a constitutive or assessment equation includes state variable and is used to define a functional parameter, then this functional parameter is called coupled parameter. If this is not the case, it may be a non coupled parameter or a scalar parameter. Definitions of different types of functional parameters are also proposed in this thesis as follows.

Definition 5.5. ***Coupled parameter.*** *Parameter that depends on at least one variable of the model. These parameters result from the extended structure, once the mathematical equations of the structural parameters are specified.*

Definition 5.6. ***Non-coupled parameter.*** *Parameter associated to a mathematical function that does not dependent on any variable of the model.*

Definition 5.7. ***Scalar parameter.*** *Parameter with numerical value (datum) independent on the time. This type of parameter can be known a priori or be determined by parameter identification.*

Definitions previously presented are useful to build the methodology to endow interpretability a parameter of a PBSM as introduced in Section 5.3. The interpretability concept is faced from different points of views in empirical and phenomenological based models. In empirical models, the basic structure of the model is not universal but changeable according with the data and the available pre-stated mathematical formulations chosen to build the model equations, while basic structure of PBSMs are based on laws or principles of the phenomena. When an empirical model is constructed, a parametric identification is done by using a prediction error as fitting criterion. Once the values of the parameters are obtained, it is hoped to discover the set of possible laws or principles governing the phenomena, but this is not possible in all cases. In this way, the parameter interpretability is implemented in an empirical model. That is, empirical models use parametric interpretability after identifying the parameters to know the possible laws governing the operative data. Hence, parameters interpretability is questionable and is not guaranteed. On the other hand, parametric interpretability is applied on PBSMs to obtain additional knowledge about the phenomena of the process being modeled. A detailed description about the use of parametric interpretability concept of both empirical and phenomenological based semi-physical models can be seen in Figure 5.4.

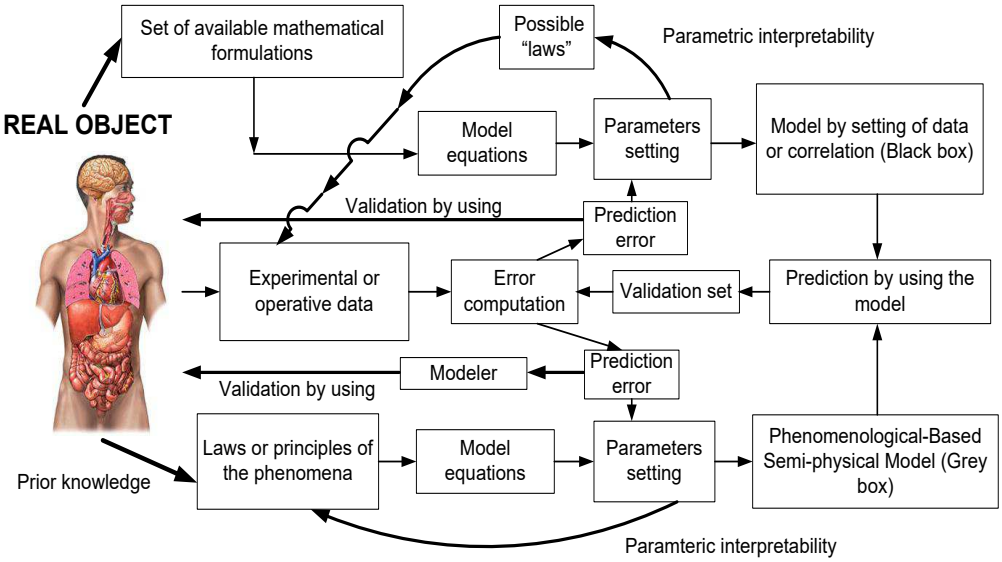

FIGURE 5.4. Parametric interpretability explanation in empirical models and PBSMs [159].

In PBSMs, each functional parameter formulated in a second scale has the possibility of gaining interpretability. The interpretability of new parameters in this submodel of the functional parameters can be obtained by partitioning the system and increasing the specification levels. Thanks to the hierarchy of systems specification levels, which provides a stratification for constructing models, an orderly way of presenting and working with such relationships is available. A hierarchy among levels of specification would allow to

associate the next lower level specification with any given one [260], at deeper levels of system specification it can be described more about the internal behavior of the system, increasing the information thereby the physical laws that govern the real object, without to change the detail level of the model. Functional parameters can be organized in terms of their variability and/or dynamics, i.e., in terms of their standard deviations (variation) and time constants (dynamics).

Typically, the practical or empirical object is a mathematical model with at least two levels: one for the basic model structure, and one for parameter calculations. In what follows they will be referred as superior and inferior levels, respectively. Under the inferior level can be one or more subordinated lower levels. In this way, a multi-level mathematical model will be well suited for most engineering endeavours. Classify the parameters of a model like structural and functional parameters is an initial way to organize them hierarchically, thus a first level appears. Structural parameters are in a superior level because they are directly related to the basic structure of the model, while functional parameters will appear as soon as a new structural parameter is replaced by a new constitutive/assessment equation, which in turn will create new levels of specification. New functional parameters could generate new submodels in lower levels, and so on. Parameters can be organized hierarchically according to its influence on the dynamic responses of the process [159]. This organization is found to be useful for identification, fitting, identifiability analysis, and understanding of the process phenomena [18]. Parameter hierarchy can be related to parameter interpretability. Those not interpretable parameters are normally located at the lowest level and parameters with direct interpretability, like structural, are located at the highest level of the model. If a PBSM is built considering multiple levels with the aim to increase the degree of specification of functional parameters without direct interpretability, it is possible both to gain knowledge in smaller scales and to obtain more information.

An interpretability analysis, only following the conceptual definitions but not the methodology that will be proposed later, was carried on the Subcutaneous Oral Glucose Minimal Model (SOGMM) presented in [138]. The proposed methodology in this thesis will be later applied in SOGMM in spite of the structure of the model is originated from compartments and empirical relations derived from a set of experiments with the adult *in silico* population given by the FDA-accepted UVa/Padova Type 1 Simulator [64], from University of Virginia and University of Padova. To perform the interpretability analysis, five expert people in this subject were asked to classify the parameters of the SOGMM in general interpretability, contextualized interpretability, or non-interpretability, after knowing the respective definitions. As can be noted in Table 5.2, the parameters that must be estimated to guarantee the identifiability of the model (V_G and f) do not have general interpretability. Results presented demonstrated that a theoretical analysis of interpretability is not advisable because, although to be carried out by experts, the result is subjective, not consistent, and make difficult to propose a theoretical formalism from only the knowledge of the modeler. For this reason, it was necessary to propose a methodology to analyze and to endow interperetability the parameters of a PBSM and thus to make this result objective and consistent.

5.2.3 Parameter interpretability in PBSMs

In this section, the conceptual framework for parameter interpretability analysis is presented. For the sake of clarity, concepts defined in both previous section and in Chatper

TABLE 5.2. Theoretical interpretability of the parameters of the SOGMM.

Symbol	Meaning	Interpretability by Experts				
		E1	E2	E3	E4	E5
S_g	Fractional glucose effectiveness measuring glucose ability to promote glucose disposal and inhibit glucose production.	NI	CI	CI	CI	CI
G_b	"Basal" glucose concentration associated with the patient's basal rate of insulin delivery.	GI	CI	GI	CI	GI
$Ra(t)$	Glucose rate of appearance.	CI	GI	CI	CI	CI
V_g	Distribution volume of glucose.	CI	NI	CI	CI	CI
p_2	Rate constant of the remote insulin compartment from which insulin action is emanated.	NI	CI	CI	NI	CI
S_I	Insulin sensitivity. Ability of insulin to control glucose production and utilization.	CI	GI	CI	CI	CI
$I(t)$	Plasma insulin concentration.	GI	GI	GI	GI	GI
I_b	Reference value for $I(t)$ associated with the fasting plasma glucose concentration of the patient.	CI	CI	NI	CI	CI
k_τ	Rate constant associated with oral glucose absorption.	CI	CI	CI	CI	CI
k_{abs}	Rate constant associated with oral glucose absorption.	CI	CI	CI	CI	CI
k_d	Rate constants of subcutaneous insulin transport.	NI	CI	CI	CI	CI
k_{cl}	Rate constants of subcutaneous insulin transport.	NI	CI	CI	CI	CI
f	Fraction of intestinal absorption which actually appears in the plasma.	NI	CI	CI	CI	CI
BW	Body weight of the subject.	GI	GI	GI	GI	GI
V_I	Distribution volume of insulin.	CI	NI	GI	CI	CI

Abbreviations: NI: No Interpretable, CI: Contextualized Interpretability, GI: General Interpretability. E1 to E5: five experts.

2 are applied into a simple mathematical model that describes the dynamics of enzymatic hydrolysis of β-casein in a batch system [185]. The **basic structure** of the model is obtained by applying a mass balance, which results in the following unique differential equation:

$$\frac{dx}{dt} = -r(\cdot) \tag{5.1}$$

where x [μM] is the concentration of the substrate and the $r(\cdot)$ [μM/min] is the reaction rate, using the symbol $(\cdot)$ to indicate the dependency of this parameter with respect to time and any other variable or parameter of the model. According to definitions reported in Chapter 2, x is the **variable** whose dynamic trajectory is obtained by solving the model and $r(\cdot)$ is the unique **structural parameter**. Note that at this level of detail, the mathematical equation that represents $r(\cdot)$ is not yet defined. This fact suggests that for this example, Equation (5.1) is a unique representation of the phenomena of interest

(*i.e*, the hydrolysis of β-casein), which is inside a bigger family, the reactive processes.

The mathematical definition of the structural parameter $r(\cdot)$ is the key element for the construction of the complete **model structure**, that is, for the set of equations defining the model in its basic and extended form. Multiple mathematical functions exist to define $r(\cdot)$ and then describe the hydrolysis rate of the intact β-casein. In the study analyzed here [185], the authors evaluate four kinetic candidate functions to determine the best function for $r(\cdot)$ in terms of the goodness of fit:

- First-order kinetics:
$$r(\cdot) = k_1 E x \tag{5.2}$$
- *nth*-order kinetics:
$$r(\cdot) = k_n E x^n \tag{5.3}$$
- Michaelis-Menten kinetics:
$$r(\cdot) = k_c E \frac{x}{K_m + x} \tag{5.4}$$
- Competitive inhibition kinetics:
$$r(\cdot) = k_c E \frac{x}{K_m(1 + \frac{I}{K_i}) + x} \tag{5.5}$$
with $I = x_0 - x$. This expression can be further manipulated to reduce the number of its parameters to:
$$r(\cdot) = b_1 E \frac{x}{b_2 - x} \tag{5.6}$$
with
$$b_1 = \frac{k_c K_i}{K_m - K_i} \tag{5.7}$$
$$b_2 = \frac{K_m(K_i + x_0)}{K_m - K_i} \tag{5.8}$$

where E is the enzyme concentration, measured in optical density units [OD_{600}]. The parameter k_1 [$1/OD_{600}$ min] is the hydrolysis rate constant for the first-order kinetics, and k_n [$1/\mu M^{n-1} OD_{600}$min] is the rate constant for the kinetics of order n. For the Michaelis-Menten equation, k_c [$\mu M/OD_{600}$min] denotes the catalytic rate constant and K_m [μM] the substrate affinity constant. For the inhibition kinetics, K_i [μM] is the inhibition constant. The concentration of the inhibitor I [μM] is considered to be equal to the concentration of β-casein that has been hydrolyzed ($x_0 - x$), with x_0 the initial protein concentration.

It is up to the modeler to decide which kinetic function to use to represent the hydrolysis rate of β-casein. Once the kinetic function is defined by a new equation in addition to the basic structure, the **extended structure** of the model is obtained.

The selected kinetic function is a **constitutive equation** of the model that allows the determination of $r(\cdot)$. For example, if the first-order kinetic function ((5.2)) is selected, it is said that $r(\cdot)$ is a **structural coupled parameter** that depends on the **variable** x and two **functional parameters**: k_1 and E. In this case, both functional parameters have physical meaning and are thus considered to be **interpretable**. While the enzyme concentration E is a known numerical value imposed by the experimental protocol, k_1 is a rate constant that needs to be determined using parameter estimation.

Consider now $r(\cdot)$ specified as the first-order kinetic rate (Equation (5.2)). The following analysis also applies to other candidate kinetic functions, bearing in mind that the Michaelis-Menten equation is derived from a biological hypothesis on the enzyme action and thus its parameters have a stronger level of interpretability than those of the kinetic of order n. By analyzing different experimental conditions, it was found that the hydrolysis rate of β-casein was dependent on the initial protein concentration x_0 [185], i.e., the kinetic rate was slower at higher initial protein concentrations. To account for the dependency of the kinetic rate on the initial β-casein concentration, the authors performed a regression analysis with the estimated parameter values obtained for each experimental condition. After that regression, the parameter k_1 was further expressed as a power function of the initial β-casein concentration

$$k_1 = \frac{c_1}{{x_0}^{m_1}} \tag{5.9}$$

Equation (5.9) is referred to as an **assessment equation**, defined by two new **functional parameters**: c_1 and m_1. These **scalar parameters** are numerical values identified by regression analysis. Table 5.3 shows a classification of the components of the β-casein model according to the conceptual framework presented above and considering that $r(\cdot)$ is defined by the first-order kinetic rate in Equation (5.2). It is important to note that for the remaining kinetics options (Equations (5.3) - (5.5)) this classification also holds. In this regard, the basic structure or zero specification level is preserved, but the extended structure changes according to the chosen kinetic equation. The extended structure begins with the first specification level while the basic structure is the zero specification level and is the only one with inherent interpretability under the proposed framework.

Regarding to the **parameter interpretability** of this simple model, it can be said that the **structural parameter** $r(\cdot)$ has **general interpretability** because in the specific scientific domain of chemical and process engineering, the symbol $r(\cdot)$ denotes a reaction rate. The reaction rate is the speed at which reactants are converted into products, *i.e.,* it is the number of moles of substance reacting per time unit within the reaction. The **functional parameter** k_1 has **contextualized interpretability** and refers to the kinetic rate constant derived from the assumption that the hydrolysis rate follows a first-order kinetics. The **functional parameter** E has also **contextualized interpretability** representing the enzyme concentration. Contextualized means that these symbols, k_1 and E, in other contexts can be used for representing other physical properties of the process.

TABLE 5.3. Classification of the β-casein model components when using the first-order kinetic rate to represent β-casein hydrolysis.

Symbol	Type	Equation	Interpretability	Total
Basic structure and basic specification or zero specification level				
x	Variable.	$\frac{dx}{dt} = -r(\cdot)$	Non required. [a]	1
r	Structural parameter.	$r(\cdot) = k_1 E x$	General.	1
1st specification level				
k_1	Non-coupled functional parameter.	$k_1 = \frac{c_1}{x_0^{m_1}}$	Contextualized.	2
E	Scalar functional parameter.	$E = known$	Contextualized.	
2nd specification level				
c_1	Scalar functional parameter.	$c_1 = known$	Non-interpretable.	3
m_1	Scalar functional parameter.	$m_1 = known$	Non-interpretable.	
x_0	Scalar functional parameter.	$x_0 = known$	General.	

[a] Any model variable has inherent interpretability.

When k_1 is further defined by the constitutive equation (5.9) with the scalar functional parameters c_1 and m_1, the model looses in the overall parameter interpretability since c_1 and m_1 are empirical parameters without physical meaning and thus they are **not interpretable**. However, the parameter k_1 is still interpretable in spite of being expressed as a function of non-interpretable parameters. This fact yields an interesting property: the interpretability of a parameter does not depend on which equation is used to deep down into a further specification level. In this case, the parameter k_1 continues being interpretable in spite of being defined by an expression with no interpretable parameters.

The above example was useful to show the concept of basic structure and how modeler-dependent may a further specification of the extended structure be. One basic structure can lead to multiple extended structures. This extended structure results from the mathematical specification of the structural parameters. Additionally, this example highlights how the parameter interpretability of the model can be affected when new specification levels appear, that is when the structural and functional parameters must be expressed with further parametrization to be defined mathematically. A graphical explanation of the concepts applied in the example is shown in Figure 5.5.

5.3 A proposal to analyze and endow interpretability to a parameter of a PBSM

This section proposes a methodology to address the interpretability property of the parameters of a PBSM and endow them interpretability in case of having a non-interpretable parameter. The methodology is based on the conceptual framework presented before.

Do you want to understand the model or the prediction? There is a notable difference. Understanding a model may bring additional insights about the underlying process of interest, in the best case, you may even identify causes for certain effects. But this is

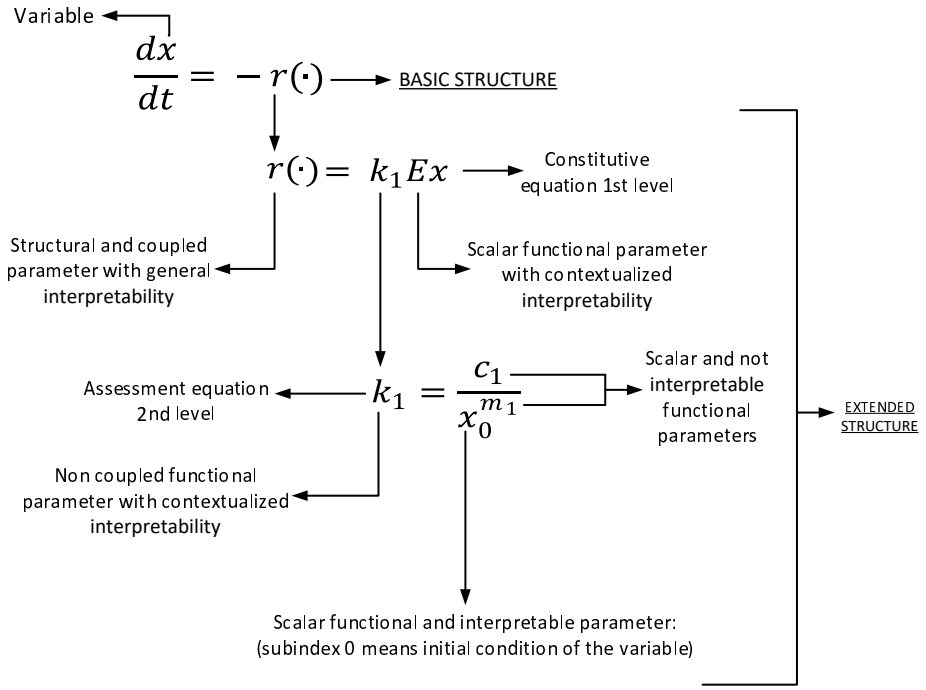

FIGURE 5.5. Concepts applied in a simple model of β-casein hydrolysis.

different from having to explain a specific prediction in which you only evaluate the response of your modeled system under certain scenarios. The idea is neither to understand the model nor to understand its predictions. This thesis aims at constructing a model with parameters interpretability in order to guarantee both model and predictions understanding. Such a model should be built on *a priori* knowledge of the phenomena [4] taking place in the underlying process under study. Conversely, when a process is described by an empirical model (disregarding which model template was used) there are two main concerns: i) the equations lack phenomena description and ii) any link of any parameter to the underlying phenomena becomes practically impossible. Moreover, the parameters are only fit to the available data (lack of generalization) which makes the model useful only for the data it was trained for. The key attributes of a useful model to describe a real physiological process of interest are those biologically or physiologically interpretable and also those that provide a simplest sufficient description of the real object (parsimony principle). These attributes are important when it comes to subsequently get responses in different scenarios. That means, a model physiologically interpretable leads to do an evaluation of the process or an analysis of the results directly by the knowledge of the object under study. Additionally, the obtained results can give further insight about the phenomena occurring into the real object. The development of models to incorporate, in a logical and general manner, effects such as dynamics of a substance of interest or the response to certain stimuli depends on a clear association between the underlying biological phenomena and its parameters in a given model. A model is interpretable because its

[4] An analogy is a knowledge-based guesswork, i.e., to use the imagination to describe what is unknown. Obviously, the imagination is based on what is known, which means that imagination has not a totally free flight. In this way, the unknown part described by using the imagination gains similarity with a known object, although there is uncertainty about the credibility of such similarities. That credibility begins to be certified by the results of the analogy when the measured behavior of the unknown part can be predicted using what the imagination build as the phenomena taking place.

parameters are interpretable. That is, the parameters have a physical meaning within the process, and such physical meaning represent something of the phenomena: an inflow, an outflow, an accumulation, a reaction, etc. Thus, the parameters of the model are associated to the process and can be interpreted. The choice of which parametrization to use is dependent on how well the parameter interpretations relate to the purpose for which the model is to be used.

To find out the type of interpretability for a specific functional parameter, we must analyze either the symbol that represents it or the relation between the equation used to calculate it with the assumptions made to deduce the mathematical model. Analyzing the symbol representing the parameter under evaluation is important since, depending on the knowledge domain in which it is located and defined, it will have an associated physical meaning. For example, in process engineering domain, the symbol μ usually means viscosity, but the same symbol μ may be the average population in statistics. In addition, its mathematical definition depends on the context where it has interpretability.

After performing the interpretability analysis over the functional parameters of a PBSM, it is possible to endow of interpretability those non-interpretable parameters. The above basically depends on whether the model is already constructed or is in construction. In both cases, the format of the model's basic structure must be written as a balance equation in terms of fluxes and coefficients, and originated from the application of the conservation law, i.e., the structure of these equations must be clearly expressed as:

$$\frac{dX}{dt} = inputs - outputs + generation - consumption$$

where X is the element being balanced and $\frac{dX}{dt}$ indicates its change in a given volume (process system). This standard format is achieved when the structural parameters are not replaced by their constitutive and assessment equations. However, most phenomenological-based models found in the literature does not preserve its basic structure. In this case, the methodology proposed is applied from step 2, as indicated in Table 5.4, considering the structure reported as basic, and classifying all the parameters as functional, due to structural parameters are "hidden" in the equations. In case of having a constructed PBSM, note that the basic structure of the model, reported in the standard format, must be distinguished from extended structure, i.e., none parameter must be explicitly replaced in the equations containing it. Each parameter must be calculated by a constitutive or assessment equation explicitly indicated like part from model extended structure. Thus, all specification levels remain explicit and the basic structure is not yet altered. Once both basic and extended structures are obtained, every specification level can be distinguished. Identify all constitutive or assessment equations without a phenomenological origin and try to find out an alternative phenomenological constitutive or assessment equation when possible. In this way, non-interpretable parameters belonging to replaced equations disappear and remaining non-interpretable parameters are endowed interpretability. In all cases, if a given non-interpretable parameter cannot be defined by a mathematical expression associated with a process phenomenon or with interpretable parameters, then interpretability analysis finishes there and it is declared that non-interpretable parameters cannot be endowed with interpretability. In case of having a PBSM under construction, it is suggested to follow the steps of the methodology here proposed.

TABLE 5.4. Application of the methodology here proposed to endow with interpretability the parameters of a PBSM depending on the standard format of the model basic structure.

Step of methodology	Standard format	No standard format
1	✓	x
2	✓	✓
3	✓	✓
4	✓	✓
5	✓	✓
6	✓	✓

1. **Identify of the model's basic structure.** Identify the set of balance equations generated from the application of the conservation law. This origin equations are called **basic structure, basic specification level** or **zero specification level**. Parameters of the balance equations are called structural parameters. Identify all the structural parameters and describe its physical meaning. Remember that the basic structure is a unique mathematical representation of the phenomena under study if an analogy is not being used, and its interpretability is inherent, that is, all structural parameters are interpretable.

2. **Obtain the first specification level.** Once the basic structure of the mathematical model is obtained, it is important to find the mathematical expressions to define each unknown structural parameter. To do that, propose new phenomenological-based constitutive or assessment equations describing the structural parameters when possible [5]. When the structural parameters have an equation that defines them, do not replace them in the basic structure equations. In this way, the basic structure of the model does not loss interpretability. The new set of mathematical equations are constitutive and assessment equations of **first level of specification** and the new parameters generated are **functional parameters** of first level. Once the first specification level is gotten, describe the physical meaning of every functional parameter of the first specification level.

3. **Obtain the extended model structure.** Complete the extended model structure by defining each of the generated functional parameters. After getting the first level of specification, the specification levels under that will be gotten when a functional parameter needs to be defined by a constitutive or assessment equation. If a functional parameter of the first level is unknown, find out a constitutive or assessment equation to define it. The set of constitutive and assessment equations that defines the parameters of the first specification level corresponds to the second specification level and so on. The process is repeated with every new level of specification until the resulting parameters are either easily defined by a scalar or described as a function of some variables and/or parameters from upper levels of specification. To

[5] Based on the phenomena occurring in the process to model, that is, on the existing and known facts causing the behavior of the interest system. Equation with the greatest possible knowledge of the process.

guarantee parameters interpretability, choose constitutive and assessment equations as phenomenological as possible. In addition, remember that the constitutive or assessment equations cannot be replaced in the upper specification level because the interpretability of previous expression can be affected.

4. **Classify the functional parameters.** Classify all functional parameters of all specification levels according to their defining constitutive or assessment equation. Check whether the functional parameter is defined by a simple numerical value (trivial equality equation) or by a mathematical function. The above yields the following three possibilities: i) if the parameter is defined by a simple numerical value, it is a **scalar** functional parameter; ii) if the parameter is defined by a mathematical function depending on at least one variable of the model, it is called **coupled** functional parameter; iii) if the mathematical function does not depend on any model variable and it is not a simple numerical value, the parameter is a **non-coupled** parameter.

5. **Evaluate the interpretability of functional parameters.** Evaluate every functional parameter according to their capability to describe the phenomena occurring in the process under study as follows:

   - **General interpretability.** If the parameter has an inherent physical meaning within a model in a specific scientific domain, i.e., its interpretation is independent of the assumptions used to deduce the model's basic structure. The parameter with general interpretability can be coupled, non-coupled, or scalar. Just it is necessary that the symbol of the parameter be universal [6], i.e., the symbol must have a conceptual definition into a specific knowledge context and must be potentially calculated by a mathematical function coincident with its conceptual definition, e.g., density is the relation of mass to volume, and mathematically $\rho = \frac{M}{V}$. Obviously, the density can be identified from data or be directly obtained by a lab test.
   - **Contextualized interpretability.** If the parameter is classified as coupled parameter and defined by a functional structure [7] with phenomenological inspiration, the parameter is said to have contextualized interpretability (since a coupled parameter is likely to depend on at least one process variable). If the parameter is classified as a non-coupled parameter, and moreover has a conceptual definition in the context of the modeled process and is described by a mathematical function associated to some known phenomena, then this non-coupled parameter is said to have contextualized interpretability. An example is the body mass index BMI, which is a non-coupled parameter defined by two interpretable parameters, *body mass,* BM and *body height,* BH. In this case, BMI is interpretable in some contexts (e.g. medicine and sport-related disciplines, among others.), independently of its conceptual definition: "*attempt to quantify the amount of tissue mass in an individual*" is not coincident with the

[6] Physical meaning of the symbol can be applied in any knowledge context, e.g., molecular mass of a chemical element.

[7] Functional structure is referred to mathematical equation structure used to know that functional parameter.

mathematical definition: $BMI = \frac{BM}{BH^2}$. In the case that the parameter is classified as scalar, but the symbol is associated with the knowledge of the process, then this scalar parameter is said to have contextualized interpretability, e.g., heart rate is associated to the speed of the heartbeat measured by the number of contractions (beats) of the heart per minute. The physical meaning of a parameter with contextualized interpretability is dependent on the considerations and hypothesis used to deduce the mathematical model within a given context.

- **No interpretable.** If a parameter is represented by a mathematical expression without any physical meaning (except for parameters stated before as interpretable), then that parameter is said to be non-interpretable. That is, if a parameter is associated with a phenomenon and has a physical meaning in the knowledge domain in which the model is being constructed, but the parameter is represented by a mathematical expression without any physical meaning, that parameter continues to be interpretable.

6. **Endow the model of parametric interpretability.** As it has been pointed out, only functional parameters of the extended structure are endowed of interpretability, because as it was said, the structural parameters of a PBSM has inherent interpretability. A parameter p_i is not interpretable when it has not physical meaning in the context where the model is being constructed. In this case, these parameters cannot have physical meaning because they arose as part of correlations or analogies that does not describe the phenomena. However, even when an interpretable parameter p_i is defined by a mathematical expression not associated with a phenomenon or originated from experimental data, p_i continues being interpretable and its interpretability is not affected. For example, the temperature expressed by the following empirical relation $T = a_0 + a_1\,V + a_2\,V^2 + a_3\,V^3 ... + a_i\,V^i$, keeps its physical meaning and, therefore continues being an interpretable parameter, despite being defined by a polynomial expression. To endow interpretability a parameter, first of all, assign a conceptual definition to the symbol representing it. Then, look for a mathematical expression based on the phenomena, with interpretable parameters to define that parameter p_i non-interpretable, or use the conceptual definition to find out a good estimation or guess. If that expression non-interpretable can be not replaced by another one inherently interpretable or based on the phenomena of the process, the interepretability analysis finishes for that parameter and from this point, every functional parameter generated in lower specification levels can not be endowed of interpretability. To give interpretability to a non-interpretable parameter, define it with a mathematical expression with interpretable parameters from the beginning, that is, look for equations that describe the underlying phenomena to define the non-interpretable parameters.

5.4 Relationship between identifiability and interpretability

The parameter identification problem is a problem whose solution is not unique. This characteristic is the result of different aspects related to the model's basic structure, experimental data, and numerical algorithms [206; 245]. The parameter identification problem could be reduced if the model structure is unique and universal. As it is known, a unique

and universal model basic structure can be only obtained if the model is derived from physical laws governing the phenomena. That unique and universal model basic structure has structural parametric interpretability which eases the parameters identification. A model with parametric interpretability would give useful hints on the experimental design and therefore to obtain a better suited dataset. When a parameter has physical meaning, the definition of the variation interval becomes straightforward.

Perhaps, the main role of parameter interpretability is to narrow the search space of the cost function where the identification procedure operates, constraining the feasible parameters values to match with the existing body of knowledge. On the other hand, structural identifiability is considered a theorerical property. In practice, however, model structure misspecification and noisy data can affect the identifiability of the parameters of the model [25] and therefore an accurate identification of the model parameters is not guaranteed. Practical identifiability is then subjected to the quality of available data. Interpretability can be of help in parameter identification [59] by adding previous knowledge that can be used to constrain parameter estimation. For instance, if a parameter is interpretable, it is possible to know the numerical interval at which it should be placed. Also, that numerical interval could be restricted to improve practical identification. A parameter can be non-identifiable, but if it is interpretable, then previous information can be used to facilitate its practical identifiability.

In any successful engineering work the practical object must provide enough interpretability for its variables and parameters. However, any abstraction from the real object to the practical object may hide the meaning of one and/or more variables or parameters. In this sense, the use of conceptual and theoretical tools with low abstraction effects [8] is a good practice. Additionally, chosen modeling tool must reduce its abstraction to zero in order to non-introduce lost of meaningful in variables and parameters. Regarding with final effect of loss of meaningful, when it occurs to a variable can be said it is catastrophic. When the meaning loss is on a parameter, the effect over the model prediction is less aggressive but strongly restricts the use of previous knowledge on parameter identification. In addition, if a parameter or variable have an unclear physical meaning, experimental design may become a challenging task.

Identifiability and interpretability are relevant properties of PBSMs constructed to gain mechanistic insight of the system under study. A PBSM has a basic structure that is universal and interpretable, that is, all its structural parameters are interpretable. However, it is often necessary to specify the structural parameters in the extended structure, though maintaining the interpretability of a model become more challenging.

An additional characteristic is that identifiability analysis applies only to scalar parameters. In the β-casein model, the structural parameter $r(\cdot)$ is a time variant quantity and thus identifiability testing is not relevant. Although the quantity $r(\cdot)$ is interpretable yet there exist the question on whether it is possible to estimate it from the available measurements (x). The reconstruction of $r(\cdot)$ from process measurements and inputs belongs to another subject namely observability, which is not here detailed.

To provide a link between identifiability and interpretability, a structural identifiability analysis is performed for the β-casein model by using both the DAISY software tool [25] and GenSSI-MatLab [54], to evaluate how the identifiability properties of the model

[8] An abstraction is a conceptual process where general rules and concepts are derived from the usage and classification of specific examples, literal ("real" or "concrete") meanings, first principles, or other methods.

change with respect to the level of granularity and the candidate constitutive or assessment equations. Table 5.5 summarizes the identifiability and intepretability analysis in β-casein model. It can be noted that the basic structure of the model is interpretable but its identifiability cannot be tested because $r(\cdot)$ is not scalar parameter. However, its identifiability is later applied and is affected when the structural parameter r is defined by different kinetics. When r is replaced by the first-order kinetic, the model is still identifiable. But, when k_1 is further defined by a mathematical expression dependent on the initial concentration of the protein (located in the second specification level), its identifiability is modified. In the same way, regarding the competitive inhibition kinetics, where functional parameters b_1 and b_2 are not replaced, the model is globally identifiable, but once b_1 and b_2 are defined and replaced at the next level of specification, the identifiability of the model is affected. Parameters k_1, k_n, k_c, K_m, and K_i are interpretable from the Michaelis-Menten kinetics, but parameters b_1 and b_2 are not interpretable. When the mathematical expression of Michaelis-Menten is changed by the expression with parameters b_1 and b_2 to make its identification easier, interpretability is affected. It was deduced that a PBSM may have an extended structure to identify its parameters and an extended structure to interpret the model. In the case of the $\beta-$casein model, two extended structures of the model can be considered depending on the goal: if the goal is to perform parameter identification, the mathematical expression containing parameters b_1 and b_2 is more convenient. On the other hand, if the goal is to exploit the descriptive ability of the model, the mathematical expression with interpretable parameters is then selected. Note that to perform an identifiability analysis of the whole model, all parameters must be replaced by the mathematical expression defining them, whilst interpretability analysis does not require replacing the constitutive or assessment equations in the upper specification levels.

As aforementioned, identifiability and interpretability are structural properties of a mathematical model which can be leveraged to gain valuable process insight. If a mathematical model is globally identifiable, it means that the unknown parameters of the postulated model can be uniquely (and exactly) recovered from the knowledge of the input-output variables of the designed input-output experiment [25]. If the interest system is represented with a phenomenological based semi-physical model, the model basic structure is universal and interpretable. Moreover, if the basic structure was enough to explain the observations of the system, it would not be necessary to deep down in those structural parameters with constitutive or assessment equations. Thus, global interpretability of the model is guaranteed, and its identifiability analysis it turns out to be irrelevant. If it is found that a parameter is identifiable, then it is likely interpretable. Otherwise, if it is found that a functional parameter is interpretable, it does not necessarily imply that is identifiable. However, if that parameter is interpretable and all its states are measurable then the parameter likely be identifiable.

There is a particular matter on interpretability and identifiability concepts and that is the lack of mathematical formalism to analyze the interpretability in a parameter. Parameter interpretability still cannot be explained by mathematics due to mathematical formalism can affect the interpretability of a parameter. An example is shown in Equation 5.10, where the interpretability is clear for the first equation but is not for the second. Although both representing the same process, the first one is a differential equation came from balances, whereas the second one arises from data and seems to be solved. Furthermore, mathematical formalism cannot exist without a theoretical formalism, which is proposed in this thesis. This does not occur with identifiability, due to identifiability

TABLE 5.5. A comparison between identifiability and interpretability analysis in β-casein model.

Mathematical expression	**Unknown parameters**	**Identifiability**	**Interpretability**
Basic structure and basic specification or zero specification level			
$\frac{dx}{dt} = -r$	r	Identifiability does not apply at this level.	General.
Extended structure - 1st specification level			
$r = k_1 E x$	k_1	Globally identifiable.[a]	Contextualized.
$r = k_n E x^n$	k_n,n	Locally identifiable.[b]	Contextualized.
$r = k_c E \frac{x}{K_m + x}$	k_c,K_m	Globally identifiable.	Contextualized.
$r = k_c E \frac{x}{K_m(1+\frac{I}{K_i})+x}$	k_c,K_m,K_i	Non identifiable.	Contextualized.
$r = b_1 E \frac{x}{b_2 - x}$	b_1,b_2	Globally identifiable.	No interpretable.
2nd specification level			
$k_1 = \frac{c_1}{x_0^{m_1}}$	c_1,m_1	Locally identifiable.	No interpretable.

[a] Global analysis is performed by using DAISY.
[b] Local analysis is performed by using GenSSI.

is a property more developed in the literature and therefore has already a mathematical formalism defined. Nevertheless and only regarding to the out of the model, functional parameters can be mathematically treated in order to be evaluated by observability. In this sense, making an interpretability analysis is more difficult than an identifiability analysis because the interpretability of a parameter cannot be tested numerically, while the identifiability of the parameters can.

$$\begin{aligned} \frac{dx}{dt} &= -kx \\ x_1 &= x_0 * e^{-kx} \end{aligned} \tag{5.10}$$

An interpretation of the model predictions might explain the behavior of the process without providing a deep insight into the causal associations in the underlying data, as with empirical models when pretends to know the process. A parameter can be interpreted but its interpretation does not agree with the phenomenon. In this way, it is important to keep the model's basic structure interpretable, because a mathematical model with parameters interpretability can give deep insight on the causal associations between the excitations and the data. In addition, a mathematical model identifiable and interpretable can help to understand better the dynamic of the process. A simple mathematical symbol allows an analysis of identifiability and interpretability, but if that symbol is replacing by a numerical value, both parameter properties could be lost.

5.5 Application cases

In this section, the proposed methodology is applied in several illustrative case studies in order to assess the benefits of the interpretability analysis in PBSMs and as support for constructing other models with parametric interpretability. This is because the interpretability property is proposed from a qualitative point of view and its quantification in a model is not yet guaranteed. Parameter interpretability of four PBSMs is evaluated following the proposed methodology in this thesis. In the first case study, the SOGMM is revisited, where the expert opinion provided in Section 5.5 is compared with the proposed methodology of interpretability. The second case study is devoted to the interpretability analysis of the pancreas model (role in glucose homeostasis). In this case, the model's basic structure is reported in the standard format and the extended structure has some non-interpretable parameters useful to apply the methodology. The third case study is related to the model of energy consumption in the acute inflammatory response. This model is more challenging if compared with the two previous models since it has more differential equations and, as well as the SOGMM, it does not have the basic structure in standard form. Finally, a more difficult and maximal PBSM with the model basic structure reported in the standard format is analyzed to show that it is possible to obtain a complex model with most of its parameters being interpretable. These four cases studies demonstrate the importance of having a model basic structure in the standard format and all parameters explicit when the goal is to have a physical interpretation both the parameters and the model responses.

5.5.1 Subcutaneous Oral Glucose Minimal Model

The extended version of the minimal model proposed by Bergman, is known as the subcutaneous oral glucose minimal model (SOGMM). SOGMM includes compartments for oral glucose consumption of carbohydrates and subcutaneous measurement of glucose concentration. The structural identifiability of this model has already been addressed Section 5.5 and a theoretical analysis of interpretability has also been provided in Section 5.2.2. Here, the proposed methodology is followed to analyze and to try to endow with interpretability the parameters of the SOGMM in order to compare the results previously obtained with the theoretical analysis with the results that will be obtained applying the methodology. The abstraction of this model is made with compartments, that is, the authors considered the body parts of interest as compartments to develop the balance equations. Some parameters were estimated from experimental data and the numerical values were replaced in the model basic structure. So, the zero specification level of this model is hidden and, therefore, the model basic structure is not reported in the proposed standard format necessary to apply the methodology from step 1.

1. **Identify the model's basic structure**: the model's basic structure is not reported in the standard format required to apply the proposed methodology. Then, this step is skipped because the balance equations do not preserve the flow terms and coefficients explicitly. Furthermore, the structural parameters cannot be distinguished because constitutive and assessment equations were replaced in the model's basic structure.

2. **Obtain the first specification level**: the set of equations 5.11-5.18 reported as the model is considered the first specification level of the model. The original

mathematical notation of the model was respected, that is, the superior dot indicates a derivative term, e.i., the dynamics of the elements to be solved by the model.

$$\dot{G}(t) = -(S_g + X(t))\ G(t) + S_g\ G_b + (R_a(t)/V_g) \tag{5.11}$$
$$\dot{X}(t) = -p_2\ X(t) + p_2\ S_I(I(t) - I_b) \tag{5.12}$$
$$\dot{G}_{cgm}(t) = -k_{sc}(G_{cgm} - G(t)) \tag{5.13}$$
$$\dot{Q}_1(t) = -k_\tau\ Q_1(t) + \omega(t) \tag{5.14}$$
$$\dot{Q}_2(t) = -k_{abs}\ Q_2(t) + k_\tau\ Q_1(t) \tag{5.15}$$
$$\dot{I}_{sc1}(t) = -k_d\ I_{sc1}(t) + J_{ctrl}(t) \tag{5.16}$$
$$\dot{I}_{sc2}(t) = -k_d\ I_{sc2}(t) + k_d\ I_{sc1}(t) \tag{5.17}$$
$$\dot{I}_p(t) = -k_{cl}\ I_p(t) + k_d\ I_{sc2}(t) \tag{5.18}$$

As can be seen, the equations are originated from balances between compartments declared by the authors. However, structural parameters were replaced by constitutive and assessment equations and therefore the basic structure of the model cannot be distinguished.

The symbols $w(t)$ and J_{ctrl} are parameters declared as inputs of the model and represent the rate of mixed-meal carbohydrate absorption at time t and the insulin input signal, respectively. In addition, G, X, G_{cgm}, Q_1, Q_2, I_{sc1}, I_{sc2}, and I_p are variables of the model. Variables are not reported in Table 5.6 because this table only reports the parameters of the first specification level, which are the subject of interpretability analysis.

3. **Obtain the whole extended model structure**: there are few parameters in this model that are rewritten in terms of further parameters (second specification level). The three generated parameters make up the second specification level of the model formed by the next set of equations:

$$Ra(t) = \frac{(Q_2(t)k_{abs}f)}{BW} \tag{5.19}$$
$$S_I = e^{(-6.4417 - 0.063546\ TDI_{whole} + 0.057944\ TDI_{basal})} \tag{5.20}$$
$$I(t) = \frac{I_p(t)}{V_I BW} \tag{5.21}$$

As can be observed in Table 5.7, where parameters of the second specification level are reported, five new parameters are generated in this level and all of them can be fixed with a datum or simple numerical value. Parameter k_{abs} appeared before as parameter of first specification level and for this reason, is marked in blue and does not report in Table 5.7. The set of equations assigning a numerical value to those parameters of second specification level forms the third specification level. However, no new parameter is generated and hence, there are no more specification levels in this model.

4. **Classify the functional parameters**: functional parameters are classified in coupled, non-coupled, and scalar as it was presented before. As can be seen in Table

TABLE 5.6. Parameters of the first specification level of the SOGMM.

#	Symbol	Physical meaning	Defined by	Location
1	S_g	Fractional glucose effectiveness measuring glucose ability to promote glucose disposal and inhibit glucose production.	datum	5.11
2	G_b	"Basal" glucose concentration associated with the patient's basal rate of insulin delivery.	datum	5.11
3	$Ra(t)$	Glucose rate of appearance in blood.	5.19	5.11
4	V_g	Distribution volume of glucose.	datum	5.11
5	p_2	Rate constant of the remote insulin compartment from which insulin action is emanated.	datum	5.12
6	S_I	Insulin sensitivity. Ability of insulin to control glucose production and utilization.	5.20	5.12
7	$I(t)$	Plasma insulin concentration.	5.21	5.12
8	I_b	Reference value for $I(t)$ associated with the fasting plasma glucose concentration of the patient.	datum	5.12
9	k_{sc}	Time constant that encompasses both the physiological lag and the sensor lag.	datum	5.13
10	$\omega(t)$	Rate of mixed-meal carbohydrate absorption at time t.	input	5.14
11	k_τ	Rate constant associated with oral glucose absorption.	datum	5.14
12	k_{abs}	Rate constant associated with oral glucose absorption.	datum	5.15
13	k_d	Rate constants of subcutaneous insulin transport.	datum	5.16
14	k_{cl}	Rate constants of subcutaneous insulin transport.	datum	5.18
15	$J_{ctrl}(t)$	Insulin input signal.	input	5.16

TABLE 5.7. Parameters of the second specification level of the SOGMM.

#	Symbol	Physical meaning	Defined by	Location
1	f	Fraction of intestinal absorption which actually appears in the plasma.	datum	5.19
2	BW	Body weight of the subject.	datum	5.19 5.21
3	V_I	Distribution volume of insulin.	datum	5.21
4	TDI_{whole}	Total daily insulin.	datum	5.20
5	TDI_{basal}	Total daily basal insulin.	datum	5.20

TABLE 5.8. Classification of the functional parameters of SOGMM.

Type	Parameter
Coupled	$Ra(t)$, $I(t)$
Non-coupled	S_I
Scalar	S_g, G_b, V_g, p_2, I_b, k_{sc}, k_τ, k_{abs}, k_d, k_{cl}, f, BW, TDI_{whole}, TDI_{basal}, V_I

TABLE 5.9. Interpretability analysis of functional parameters of SOGMM.

Interpretability	Parameters
General	BW
Contextualized	G_b, Ra, V_g, S_I, I, I_b, k_{sc}, k_τ, k_{abs}, k_d, k_{cl}, f, V_I, TDI_{whole}, TDI_{basal}
Non-interpretable	S_g, p_2

5.8, parameters $Ra(t)$ and $I(t)$ depend on the variables $Q_2(t)$ and $I_p(t)$, respectively (coupled parameters). Parameter S_I is a non-coupled parameter because it is computed according to the regression formula 5.20 using i) the patient's average total daily insulin TDI_{whole} computed from the overall insulin utilization over a one week of open-loop data collection and ii) the patient's average total daily basal insulin TDI_{basal}. The remaining parameters are scalar parameters because are defined by a simple numerical value.

5. **Evaluate the interpretability of functional parameters**: interpretability of functional parameters is evaluated according to the proposed methodology. The evaluation is reported in Table 5.9.

   According to the interpretability evaluation, body weight BW has general interpretability because the conceptual definition is in the physiological context and refers to a mass or weight (both interpretable in the physic domain) of the human body. Parameters classified as contextualized interpretable have a physical meaning associated with a physiological phenomenon of the process, therefore, out of this context they have not interpretability. Finally, only two parameters S_g and p_2 are non-interpretable because its physical meaning is no associated with any conceptual definition in some scientific domain.

6. **Endow the model of parameter interpretability**: to endow with interpretability the parameters of the SOGMM it is necessary to have the basic structure of the model explicit, that is, in the standard format, to decide new equations to define parameters S_g and p_2. That does not happen in this case. The other option is to provide an assessment equation for each one of this parameters, but guaranteeing those equations has phenomenological inspiration or they are mathematical definitions for the parameters. However, this second option is not possible because the parameters have a noninterpretable physical meaning, then providing an assessment equation phenomenological inspired is not possible.

5.5.2 Role of the human pancreas in glucose metabolism

Among the organs involved in the glucose homeostasis, the pancreas is perhaps one of the most relevant, given its role to regulate blood glucose levels by producing important hormones like insulin, glucagon, and somatostatin, among others. Blood glucose concentration is directly affected by the pancreatic secretion of these hormones into the bloodstream. Therefore, the construction of a pancreatic model that represents the role of the α, β, and δ cells in the human glucose homeostasis based on the phenomena associated to the known pancreas physiology is relevant to the scientific community. The developed model of the pancreas that is reported in Chapter 4, is analyzed here and endowed of parameter interpretability following the proposed methodology. The aim of the interpretability analysis of this model is to show the application of the methodology in a simple model with the basic structure reported in the standard format and with some parameters defined by empirical relations but with only one non-interpretable parameter.

1. **Identify the model's basic structure**: the model's basic structure presented below comes directly from mass balance equations representing the mass flow and the concentration of glucose, oxygen, insulin, and glucagon, in the blood leaving the pancreas. This version of the pancreas model does not include the somatostatin effect.

$$\dot{m_2} = \dot{m_1} \tag{5.22}$$

$$\frac{dw_{i,2}}{dt} = (w_{i,1}\dot{m_1} - w_{i,2}\dot{m_2} - \dot{m_{i,3}})\frac{1}{M_I} \tag{5.23}$$

$$\frac{dw_{j,2}}{dt} = (w_{j,1}\dot{m_1} - w_{j,2}\dot{m_2} + \dot{m_{j,4}})\frac{1}{M_I} \tag{5.24}$$

$$\dot{m_4} = \dot{m_3} \tag{5.25}$$

$$\frac{dw_{i,II}}{dt} = (\dot{m}_{i,3} - r_{cons,i})\frac{1}{M_{II}} \tag{5.26}$$

$$\frac{dw_{Ins,II}}{dt} = (-\dot{m}_{Ins,4} + r_{secr,Ins})\frac{1}{M_{II}} \tag{5.27}$$

$$\dot{m}_{Gn,4} = r_{sec,Gn} \tag{5.28}$$

$$\tag{5.29}$$

with i = glucose (G) and oxygen (O), and j = insulin (Ins) and glucagon (Gn). The meaning of the symbols that represents variables, parameters, and constants is reported in Table 4.1.

Table 5.10 reports the structural parameters in the model's basic structure, a.k.a. zero specification level. Symbols $\dot{m_2}$, $w_{i,2}$, $w_{j,2}$, $\dot{m_4}$, $w_{i,II}$, $w_{Ins,II}$ and $\dot{m}_{Gn,4}$ are the variables of the model, therefore these variables are not reported in Table 5.10. As can be observed, the basic structure of the model is reported in the standard format, that is, constitutive and assessment equations do not replace any parameter and the flows and coefficients terms are explicitly in the balance equations. Thus, all steps of the methodology to analyze and endow with interpretability the functional parameters can be applied.

TABLE 5.10. Structural parameters of the pancreas model.

#	Symbol	Physical meaning	Defined by	Location
1	$\dot{m}_1$	Mass flow rate of blood entering in the pancreas (stream 1).	5.82	5.22-5.24
2	$w_{i,1}$	Mass fraction of glucose and oxygen entering the pancreas.	5.31	5.23
3	$w_{j,1}$	Mass fraction of insulin and glucagon entering the pancreas.	5.32	5.24
4	$\dot{m}_{i,3}$	Mass flow of component i entering the islets of Langerhans.	5.33	5.23 5.26
5	$\dot{m}_{j,4}$	Mass flow of component j being secreted to the circulation.	5.34	5.24 5.27
6	M_I	Mass of blood irrigating the pancreas.	5.35	5.23 5.24
7	$\dot{m}_3$	Mass flow rate of basal glucose and oxygen required by α and β-cells (stream 3).		5.25
8	$r_{cons,i}$	Kinetic of consumption of component i in the islets of Langerhans.	5.37 5.38	5.26
9	$r_{secr,j}$	Kinetic of secretion of component j by the islets of Langerhans.	5.39 5.40	5.27
10	M_{II}	Mass of the islets of Langerhans.	5.36	5.26 5.27

i indicates glucose (G) and oxygen (O).
j indicates pancreatic hormones insulin (Ins) and glucagon (Gn).

2. **Obtain the first specification level**: the following constitutive and assessment equations define the structural parameters and yield the first specification level of the model.

$$\dot{m}_1 = \dot{V}_1 \rho_b \tag{5.30}$$

$$w_{i,1} = C_{i,1} * \frac{1}{\rho_b} * \mathfrak{M}_{\mathfrak{i}} \tag{5.31}$$

$$w_{j,1} = C_{j,1} * \frac{1}{\rho_b} * \mathfrak{M}_{\mathfrak{j}} \tag{5.32}$$

$$\dot{m}_{i,3} = A_s * D_{i-t} * \frac{(C_{i,2} - C_{i,II})}{L} * \mathfrak{M}_{\mathfrak{i}} \tag{5.33}$$

$$\dot{m}_{Ins,4} = A_s * D_{Ins-t} * \frac{(C_{Ins,2} - C_{Ins,II})}{L} * \mathfrak{M}_{\mathfrak{j}} \tag{5.34}$$

$$M_I = \rho_b * V_b \tag{5.35}$$

$$M_{II} = \rho_{Isl} * V_{Isl} \tag{5.36}$$

$$r_{cons,G} = r_{max,G} \frac{C_{G,II}}{C_{G,II} + C_{Hf,G}} \tag{5.37}$$

$$r_{cons,O} = r_{max,O} \frac{C_{O,II}}{C_{O,II} + C_{Hf,O}} \varphi_{O,G} * (C_{G,II}) * \delta(C_{O,II} > C_{Cr,O}) \tag{5.38}$$

$$r_{secr,Ins} = (r_{Ins,ph1} + r_{Ins,ph2}) \varphi_{i,o}(C_{O,II}) \tag{5.39}$$

$$r_{secr,Gn} = c_0 + \frac{c_1}{c_2 + C_{Ins,2} e} (C_{GE} - C_{G,2}) u(C_{GE} - C_{G,2}) \tag{5.40}$$

$$\tag{5.41}$$

Note that each structural parameter is defined by a constitutive equation that generates new parameters that belong to the second level of specification of the model. The second specification level is reported in the next step to get the whole extended model structure. Functional parameters of the first specification level are reported in Table 5.11.

3. **Obtain the whole extended model structure**: computation of the new parameters generated in the first specification level produces the second specification level. The equation forming the second specification level is as follows:

$$\varphi_{O,G}(C_{G,II}) = \varphi_{sc}(\varphi_{base} + \varphi_{metab}\frac{C_{G,II}^{n_{ins2,gluc}}}{C_{G,II}^{n_{ins2,gluc}} + C_{Hf,ins2,gluc}^{n_{ins2,gluc}}} \tag{5.42}$$

$$\delta(C_{O,II} > C_{Cr,O}) = C_{O,II} - 1 * 10^{-4} \tag{5.43}$$

$$r_{Ins,ph1} = r_{max,ins1}\frac{\frac{dC_{G,II}^{n_{ins1,gluc}}}{dt}}{\frac{d_C^{n_{ins1,gluc}}}{dt} + Ct_{Hf,ins1,gluc}^{n_{ins1,gluc}}}\sigma_{i,l,g}(C_{G,II}) \tag{5.44}$$

$$r_{Ins,ph2} = r_{max,ins2}\frac{C_{G,II}^{n_{ins2,gluc}}}{C_{G,II}^{n_{ins2,gluc}} + C_{Hf,ins2,gluc}^{n_{ins2,gluc}}} \tag{5.45}$$

$$\varphi_{i,o} = \frac{C_{O,II}^{n_{ins,O}}}{C_{O,II}^{n_{ins,O}} + C_{Hf,ins,O}^{n_{ins,O}}} \tag{5.46}$$

$$\tag{5.47}$$

As can be seen, five equations belong to the second level of specification because the rest of the parameters of the first specification level are data or fixed numerical values, as introduced in Table 5.11. Functional parameters of the second specification level are reported in Table 5.12.

As shown in the Table 5.12, only the parameter $\sigma_{i,l,g}$ is defined by a constitutive equation. The rest of the functional parameters of the second specification level are defined by assessment equations, whose value was reported in chapter 4 when the development of the pancreas model is presented. Therefore, the equation that defines the parameter $\sigma_{i,l,g}$ is the only constitutive equation that forms the third level of specification, as follows.

$$\sigma_{il,g} = \frac{4C_{G,II}^4 C_m}{(C_{G,II}^4 + C_m^4)^2} \tag{5.48}$$

The only functional parameter generated in the third level of specification is reported in the Table 5.13.

When C_m is defined by a datum, the equation $C_m = datum$ is the fourth specification level and at this point, no new parameter is generated and, therefore, there are no more specification levels.

4. **Classify the functional parameters**: in this step, all functional parameters of the model are classified in coupled, non-coupled, or scalar according to the con-

TABLE 5.11. Functional parameters of first specification level.

#	Symbol	Physical meaning	Defined by	Location
1	$\dot{V}_1$	Volumetric flow in arterial blood.	datum	5.82 5.82
2	ρ_b	Density of the blood.	datum	5.31 5.32
3	$C_{i,1}$	Concentration of component i at blood irrigating the pancreas (stream 1).	datum	5.31
4	$C_{j,1}$	Concentration of component j at blood irrigating the pancreas (stream 1).	datum	5.32
5	$\mathfrak{M}_\mathfrak{i}$	Molecular mass of the component i.	datum	5.31 5.33
6	$\mathfrak{M}_\mathfrak{j}$	Molecular mass of the component j.	datum	5.32 5.34
7	A_s	Mass transfer area of islets of Langerhans.	datum	5.33 5.34
8	D_{i-t}	Diffusion coefficient of the component i in the islet of Langerhans.	datum	5.33
9	D_{Ins-t}	Diffusion coefficient of the insulin in the islet of Langerhans.	datum	5.34
10	L	Length of mass transfer.	datum	5.33 5.34
11	V_b	Blood volume irriganting the pancreas.	datum	5.35
12	ρ_{Isl}	Density of islets of Langerhans.	datum	5.36
13	V_{Isl}	Volume of islets of Langerhans.	datum	5.36
14	$r_{max,G}$	Maximum reaction rate of glucose consumption.	datum	5.37
15	$C_{Hf,G}$	Concentration corresponding to half-maximal response of glucose consumption.	datum	5.37
16	$r_{max,O}$	Maximum rate of oxygen consumption.	datum	5.38
17	$C_{Hf,O}$	Concentration corresponding to half-maximal response of oxygen consumption.	datum	5.38
18	$\varphi_{O,G}$	Oxygen consumption rate with blood glucose concentration variations.	5.42	5.38
19	δ	Step-down function to account for necrosis and cut the oxygen consumption of those tissues where the oxygen concentration falls below a critical value ($C_{Cr,O}$).	5.43	5.38
20	$C_{Cr,O}$	Critical value of oxygen concentration into the islets of Langerhans.	datum	5.38
21	$r_{Ins,ph1}$	Insulin secretion rate, first-phase. Relatively quick first phase consisting of a transient spike of 5-10 min.	5.44	5.39
22	$r_{Ins,ph2}$	Maximum (second phase) insulin secretion rate.	5.45	5.39
23	$\varphi_{i,o}$	Modulating function of the insulin secretion.	5.46	5.39

#	Symbol	Physical meaning	Defined by	Location
24	c_0	Glucagon basal secretion.	datum	5.40
25	c_1	Glucose action on glucagon.	datum	5.40
26	c_2	Insulin action on glucagon.	datum	5.40
27	e	Insulin effectiveness.	datum	5.40
28	C_{GE}	Glucose threshold value.	datum	5.40

TABLE 5.12. Functional parameters of second specification level.

#	Symbol	Physical meaning	Defined by	Location
1	φ_{sc}	Scaling factor to maintain the consumption rate at low (3 mM) glucose.	datum	5.42
2	φ_{base}	Basal rate of oxygen consumption.	datum	5.42
3	φ_{metab}	Oxygen consumption as a function of metabolic demand.	datum	5.42
4	$n_{ins2,gluc}$	Metabolic component. Hill slope characterizing the shape of the insulin response, second-phase.	datum	5.42 5.45
5	$C_{Hf,ins2,gluc}$	Insulin concentration corresponding to half-maximal response of insulin secretion.	datum	5.42 5.45
6	$r_{max,ins1}$	Maximum rate of insulin secretion, first-phase, from the islets of Langerhans.	datum	5.44
7	$r_{max,ins2}$	Maximum rate of insulin secretion, second-phase, from the islets of Langerhans.	datum	5.45
8	$n_{ins1,gluc}$	Hill slope characterizing the shape of the insulin response, first-phase.	datum	5.44
9	$Ct_{Hf,ins1,gluc}$	Linear response for a range that likely covers normal physiologic conditions as well as dynamic perifusion conditions.	datum	5.44
10	$n_{ins,O}$	Hill slope characterizing the shape of the oxygen consumption.	datum	5.46
11	$C_{Hf,ins,O}$	Oxygen concentration corresponding to half-maximal response of oxygen consumption.	datum	5.46
12	$\sigma_{il,g}$	Modulating function to reduce the glucose gradient-dependent response for islets that are already operating at an elevated second phase secretion rate and to maximize it around $C_{G,II}$ values where islets are likely to be most sensitive.	5.48	5.44

TABLE 5.13. Functional parameters of third specification level.

#	Symbol	Physical meaning	Defined by	Location
1	C_m	Glucose concentration where islets are likely to be most sensitive.	datum	5.48

TABLE 5.14. Classification of the functional parameters of 2^{nd}, 3^{rd}, and 4^{th} specification levels.

Type	Parameter
Coupled	$\varphi_{O,G}(C_{G,II})$, $\delta(C_{O,II} > C_{Cr,O})$, $r_{Ins,ph1}$, $r_{Ins,ph2}$, $\varphi_{i,o}$, $\sigma_{il,g}$
Non-coupled	N.A.
Scalar	$\dot{V}_1$, ρ_b, $C_{i,1}$, $C_{j,1}$, $\mathfrak{M}_\mathrm{i}$, $\mathfrak{M}_\mathrm{j}$, A_s, D_{i-t}, D_{Ins-t}, L, V_b, ρ_{Isl}, V_{Isl}, $r_{max,G}$, $C_{Hf,G}$, $r_{max,O}$, $C_{Hf,O}$, $C_{Cr,O}$, c_0, c_1, c_2, e, C_{GE}, φ_{sc}, φ_{base}, φ_{metab}, $n_{ins2,gluc}$, $C_{Hf,ins2,gluc}$, $r_{max,ins1}$, $r_{max,ins2}$, $n_{ins1,gluc}$, $Ct_{Hf,ins1,gluc}$, $n_{ins,O}$, $C_{Hf,ins,O}$, C_m

cepts introduced previously. Table 5.14 reports the classification of the functional parameters of second, third, and fourth specification levels, taking into account that fourth level has only parameter C_m. Equations of the first specification level define structural parameters and it is worth remembering that this classification is only for functional parameters.

From Table 5.14, there is no non-coupled functional parameters. Six parameters are coupled parameters, the remaining ones are scalar parameters.

5. **Evaluate the interpretability of functional parameters**: interpretability analysis is carried on the functional parameters of the model and reported in Table 5.15.

   Eighteen parameters have general interpretability (remember that parameters $C_{i,1}$, $C_{j,1}$, $\mathfrak{M}_\mathrm{i}$, $\mathfrak{M}_\mathrm{j}$, and D_{i-t} generate two functional parameters, for glucose and for oxygen) because the symbols used to represent it have a universal meaning. Most of the functional parameters of the model have contextualized interpretability because they only have a physical meaning within the physiology of the pancreas that is modeled, outside of this context they lose their meaning. On the other hand, from the table can be noted that there are no non-interpretable parameters, i.e., all functional

TABLE 5.15. Interpretability analysis of functional parameters.

Interpretability	Parameters
General	$\dot{V}_1$, ρ_b, $C_{i,1}$, $C_{j,1}$, $\mathfrak{M}_\mathrm{i}$, $\mathfrak{M}_\mathrm{j}$, A_s, D_{i-t}, D_{Ins-t}, L, V_b, ρ_{Isl}, V_{Isl}
Contextualized	$r_{max,G}$, $C_{Hf,G}$, $r_{max,O}$, $C_{Hf,O}$, $\varphi_{O,G}(C_{G,II})$, $\delta(C_{O,II} > C_{Cr,O})$, $C_{Cr,O}$, $r_{Ins,ph1}$, $r_{Ins,ph2}$, $\varphi_{i,o}$, c_0, c_1, c_2, e, C_{GE}, φ_{sc}, φ_{base}, φ_{metab}, $n_{ins2,gluc}$, $C_{Hf,ins2,gluc}$, $r_{max,ins1}$, $r_{max,ins2}$, $n_{ins1,gluc}$, $Ct_{Hf,ins1,gluc}$, $n_{ins,O}$, $C_{Hf,ins,O}$, $\sigma_{il,g}$, C_m
Non-interpretable	N.A.

parameters of the model have a physical meaning within the pancreas physiology context and they are associated with some phenomenon of this underlying process.

6. **Endow the model of parameter interpretability**: from the previous step, it is known that there are no non-interpretable parameters. Therefore, there are no parameters to endow with interpretability in this model.

5.5.3 Mathematical modeling of energy consumption in the acute inflammatory response

A computational model to study the dynamics of acute inflammation that incorporates a reduced representation of relevant metabolic pathways and energy resources and demands is presented in [209]. The model is also used to investigate the role of energetics during infection and explore the relation in the overproduction of nitric oxide, altered ATP levels, and sepsis. This model consists of eight nonlinear ordinary differential equations that describe the interactions between the immune response to a pathogen and the associated energy production and demand. The analysis and endowment of interpretability in the parameters of this model is performed here to show a more complex example of a phenomenological based model without knowing a priori the model's basic structure reported in standard format. Thus, the significance of having explicit both structural and functional parameters in the model structure is beef-up.

1. **Identify the model's basic structure**: the set of eight nonlinear ordinary differential equations are:

$$\frac{dP}{dt} = k_{pg}P\left(1-\frac{P}{P_\infty}\right) - (1+k_{ns}g(A_b))\frac{k_{pm}P}{\mu_m + k_{mp}P} - \frac{k_{pn}g(A_n)f\left(\frac{C_A}{C^*}\right)NP}{1+k_{ps}P} \tag{5.49}$$

$$\frac{dN}{dt} = \frac{s_{nr}g(A_n)f\left(\frac{C_A}{C^*}\right)(k_{nnN+k_{np}P}+k_{nd}D)}{\mu_{nr}+f\left(\frac{C_A}{C^*}\right)(k_{nn}N+k_{np}P+k_{nd}D)} - \mu_n\left(1+\frac{k_{de}g(A_n)f\left(\frac{C_A}{C^*}\right)P}{1+k_{ps}P}\right)N \tag{5.50}$$

$$\frac{dD}{dt} = k_{dn}h(X+P) - g(A_b)\mu_d D \tag{5.51}$$

$$\frac{dC_A}{dt} = s_c + k_{cn}\left(\frac{g(A_n)f\left(\frac{C_A}{C^*}\right)N}{\mu_{cq}+f\left(\frac{C_A}{C^*}\right)N} + \frac{g(A_b)f\left(\frac{C_A}{C^*}\right)k_{cnd}D}{\mu_{cq}+f\left(\frac{C_A}{C^*}\right)k_{cnd}D}\right) - \mu_c C_A \tag{5.52}$$

$$\frac{dA_b}{dt} = c(A_b)\left(f\left(\frac{X}{X^*}\right)\left(1-\lambda_{gn}\right)+\lambda_{gn}\right) - g(A_b)\sum_{i\epsilon(1,4,6)}\phi_i - \mu_A A_b \tag{5.53}$$

$$\frac{dA_n}{dt} = c(A_n)\left(f\left(\frac{X}{X^*}\right)\left(1-\lambda_{gn}\right)+\lambda_{gn}\right) - g(A_n)\sum_{i\epsilon(2,3,5)}\phi_i - \mu_A A_n \tag{5.54}$$

$$\frac{dX}{dt} = f\left(\frac{C_A}{C^*}\right)(k_{non}N+k_{nod}D) - \mu_{no}X \tag{5.55}$$

$$\frac{dL}{dt} = \lambda_L\left(1-f\left(\frac{X}{X^*}\right)\right)\left((1-\lambda_{gb})c(A_b)+(1-\lambda_{gn})c(A_n)\right) - \mu_L L \tag{5.56}$$

where symbols P, N, D, C_A, A_b, A_n, X, and L indicate the variables of the model. As it can be seen, it is not straightforward to distinguish the basic structure of the

model. Coefficients and flows in the balance equations were replaced by constitutive and assessment equations and for this reason, the structural parameters are somehow "hidden" and cannot be identified directly from the reported structure. Therefore, the step one of the methodology is skipped as mentioned before.

2. **Obtain the first specification level**: the set of reported differential equations is considered the first specification level of the model and the goal from now is getting the extended model structure. Table 5.16 reports functional parameters of the first specification level with the corresponding physical meaning, the numerical value or corresponding constitutive or assessment equation, and the equation(s) where the parameter is located. Parameters g, f, and h are defined by the Equations 5.57, 5.58, and 5.59, respectively. The physical meaning of the structural parameters is into the knowledge context of human physiology, and processes engineering from its analogy.

3. **Obtain the whole extended model structure**: the set of equations to define some functional parameters of the first specification level is 5.57-5.66. This set of equations makes up the second specification level. Parameters marked in blue are parameters of first specification level as they are reported in Table 5.16. These parameters were classified before as parameters of first specification level and for this reason, they are not considered parameters of the second specification level in spite of appearing in this level too.

TABLE 5.16. Functional parameters of the first specification level of model of the energy consumption in the acute inflammatory response.

#	Symbol	Physical meaning	Defined by	Location
1	k_{pg}	Pathogen growth rate.	datum	5.49
2	P_∞	Carrying capacity for pathogen.	datum	5.49
3	k_{ns}	Weighting of the energy-dependent component of non-specific pathogen elimination.	datum	5.49
4	g	Saturating function modulating energy-intensive terms based on availability of relevant ATP supplies.	5.57	5.49-5.54
5	k_{pm}	Rate parameter for the elimination of pathogens by the non-specific local response.	datum	5.49
6	μ_m	Half-activation parameter for the non-specific local response.	datum	5.49
7	k_{mp}	Saturation rate parameter for the non-specific local response.	datum	5.49
8	k_{pn}	Phagocytosis rate.	datum	5.49
9	f	Hill function representing inhibitory effects.	5.58	5.49 5.50 5.52-5.56
10	C^*	Saturation parameter for effects of anti-inflammatory mediators.	datum	5.49 5.50 5.52 5.535.55
11	k_{ps}	Phagocytosis saturation constant.	datum	5.49 5.50
12	s_{nr}	Production rate for activated phagocytes (based on resting phagocyte level).	datum	5.50
13	k_{nn}	Weighting of contribution to activation of resting phagocytes by previously activated phagocytes and their cytokines.	datum	5.50
14	k_{np}	Weight of contribution to activation of resting phagocytes by pathogen.	datum	5.50
15	k_{nd}	Weight of contribution to activation of resting phagocytes by tissue damage.	datum	5.50
16	μ_{nr}	Decay rate of resting phagocytes.	datum	5.50
17	μ_n	Decay rate of activated phagocytes.	datum	5.50
18	k_{de}	Pathogen degradation enhancement constant.	datum	5.50
19	k_{dn}	Maximum rate of damage produced by activated phagocytes.	datum	5.51
20	h	Hill function that controls the production of tissue damage D. Saturation function.	5.59	5.51
21	μ_d	Decay rate of damage.	datum	5.51
22	S_c	Source of anti-inflammatory mediators.	datum	5.52
23	k_{cn}	Maximum production rate of anti-inflammatory mediators.	datum	5.52
24	μ_{cq}	Determines the levels of activated phagocytes and damage that are needed to bring rate of anti-inflammatory mediator production to half its maximum.	datum	5.52
25	k_{cnd}	Effectiveness of damaged tissue relative to activated phagocytes in inducing production of anti-inflammatory mediators.	datum	5.52

#	Symbol	Physical meaning	Defined by	Location
26	μ_c	Decay rate of anti-infammatory mediators.	datum	5.52
27	c	Decreasing sigmoidal function representing a ramping up of energy production when supplies diminish.	5.60	5.535.545.56
28	X^*	Half saturation level of nitric oxide.	datum	5.53 5.54 5.56
29	λ_{gb}	Fraction of A_b produced via the anaerobic pathway in the absence of nitric oxide.	datum	5.535.56
30	ϕ_i	Energy flux terms of all processes in the model that consume energy, with $i = 1-6$.	5.61-5.66	5.535.54
31	μ_A	Baseline depletion rate of both ATP supplies.	datum	5.53 5.54
32	λ_{gn}	Fraction of An produced via the anaerobic pathway in the absence of nitric oxide.	datum	5.545.56
33	k_{non}	Rate of nitric oxide release due to presence of pro-inflammatory cytokines.	datum	5.55
34	k_{nod}	Rate of nitric oxide release due to tissue damage.	datum	5.55
35	μ_{no}	Natural depletion rate of nitric oxide.	datum	5.55
36	λ_L	Production rate of lactate.	datum	5.56
37	μ_L	Decay rate of lactate.	datum	5.56

$$g(A_x) = \frac{A_x^2}{c_g + A_x^2} \tag{5.57}$$

$$f(V) = \frac{1}{1+V^2} \tag{5.58}$$

$$h(V) = \frac{V^6}{x_{dn}^6 + V^6} \tag{5.59}$$

$$c(A_x) = \frac{\mu_A(1+k_2)}{k_2 + e^{k_1(A_x-1)}} \tag{5.60}$$

$$\phi_1 = c_1 \frac{k_{pm} s_m k_{ns} P}{\mu_m + k_{mp} P} \tag{5.61}$$

$$\phi_2 = c_2 \frac{k_{pn} f\left(\frac{C_A}{C^*}\right) NP}{1 + k_{ps} P} \tag{5.62}$$

$$\phi_3 = c_3 \frac{s_{nr} f\left(\frac{C_A}{C^*}\right)(k_{nn}N + k_{np}P + k_{nd}D)}{\mu_{nr} + f\left(\frac{C_A}{C^*}\right)(k_{nn}N + k_{np}P + k_{nd}D)} \tag{5.63}$$

$$\phi_4 = c_4 \mu_d D \tag{5.64}$$

$$\phi_5 = c_5 \frac{k_{cn} f\left(\frac{C_A}{C^*}\right) N}{\mu_{cq} + f\left(\frac{C_A}{C^*}\right) N} \tag{5.65}$$

$$\phi_6 = c_6 \frac{k_{cn} f\left(\frac{C_A}{C^*}\right) k_{cnd} D}{\left(C_a\right.} \tag{5.66}$$

TABLE 5.17. Functional parameters of the model of the energy consumption in the acute inflammatory response.

#	Symbol	Physical meaning	Defined by	Location
1	C_g	Half-saturation energy level for the driving of various processes	datum	5.57
2	x_{dn}	Determines levels of pathogens and nitric oxide needed to bring damage production up to half its maximum	datum	5.59
3	μ_A	Baseline depletion rate of both ATP supplies.	datum	5.60
4	k_1	Phenomenological energy production parameter.	datum	5.60
5	k_2	Phenomenological energy production parameter.	datum	5.60
6	C_1	Energy consumption rate of ϕ_1.	datum	5.61
7	C_2	Energy consumption rate of ϕ_2.	datum	5.62
8	C_2	Energy consumption rate of ϕ_3.	datum	5.63
9	C_4	Energy consumption rate of ϕ_4.	datum	5.64
10	C_5	Energy consumption rate of ϕ_5.	datum	5.65
11	C_6	Energy consumption rate of ϕ_6.	datum	5.66
12	s_m	Source of non-specific local response.	datum	5.61

TABLE 5.18. Classification of the functional parameters of all specification levels of the model of the energy consumption in the acute inflammatory response.

Type	Parameter
Coupled	ϕ_i
Non-coupled	g, f, h, c
Scalar	k_{pg}, P_∞, k_{ns}, k_{pm}, μ_m, k_{mp}, k_{pn}, C^*, k_{ps}, s_{nr}, k_{nn}, k_{np}, k_{nd}, μ_{nr}, μ_n, k_{de}, k_{dn}, μ_d, S_c, k_{cn}, μ_{cq}, k_{cnd}, μ_c, X^*, λgb, μ_A, λ_{gn}, k_{non}, k_{nod}, μ_{no}, λ_L, μ_L, C_g, x_{dn}, μ_A, k_1, k_2, C_1, C_2, C_3, C_4, C_5, C_6, s_m

Table 5.17 reports the parameters of the second specification level. Parameter A_x from equation 5.57 is refereed to parameters A_b and A_n previously defined in Table 5.16. As noted in Table 5.17, parameters of the second specification level are associated with a numerical value and not with an equation. Then, in this level of specification, there are not new parameters to generate a third specification level.

4. **Classify the functional parameters**: in this step, all functional parameters reported in Tables 5.16 and 5.17 are classified as coupled, non-coupled, or scalar according to the concepts introduced previously. Table 5.18 reports this classification for all functional parameters.

5. **Evaluate the interpretability of functional parameters**: interpretability analysis is carried only on functional parameters since the basic structure of the model is not available in standard format. The goal is to show the importance of having the model's basic structure reported in the standard format and the lost of parameter interpretability in a PBSM when the structural parameters are replaced by the

TABLE 5.19. Interpretability analysis of functional parameters of the model of the energy consumption in the acute inflammatory response.

Interpretability	Parameters
General	No functional parameter has general interpretability
Contextualized	P_∞, k_{pg}, k_{ns}, g, k_{pm}, μ_m, k_{mp}, k_{pn}, f, C^*, k_{ps}, s_{nr}, k_{nn}, k_{np}, k_{nd}, μ_{nr}, μ_n, k_{de}, k_{dn}, h, μ_d, S_c, k_{cn}, μ_{cq}, k_{cnd}, μ_c, c, X^*, λgb, ϕ_i, μ_A, λ_{gn}, k_{non}, k_{nod}, μ_{no}, λ_L, μ_L, C_g, x_{dn}, μ_A, C_1, C_2, C_3, C_4, C_5, C_6
Non-interpretable	k_1, k_2, s_m

constitutive and assessment equations and the specification levels cannot be clearly distinguished. Table 5.19 reports the interpretability evaluation of the model's functional parameters.

6. **Endow the model of parameter interpreteability**: as shown in Table 5.19, non-interpretable parameters are g, f, h, μ_d, ϕ_i, k_1, k_2, C_1, C_2, C_3, C_4, C_5, C_6, and s_m. To endow them with interpretability the conceptual definition that every symbol has should be checked. Symbols k_1 and k_2 are defined as *phenomenological energy production parameter*. This meaning is non-interpretable because it is not associated with a given phenomenon of the real process: it cannot be clearly known where is the energy produced nor the origin of these parameters, despite being named as phenomenological. Therefore, to give a conceptual definition to these non-interpretable parameters and to define them mathematically with a phenomenological expression is not possible. It also happens with symbol s_m, defined as *source of non-specific local response*, but note that the meaning is non-interpretable, cannot be defined by a concept because the description is not associated with some phenomena of the real process.

5.5.4 Role of the human stomach in glucose metabolism

The organs in the human body with an important role in glucose metabolism were modeled in Chapter 4. The methodology previously proposed is now applied to the human stomach model given the availability of the basic structure reported in the standard format, almost all of its parameters are interpretable, is a model bigger than analyzed models previously with five specification levels, each specification level is explicitly reported in the complete model structure, i.e., no functional parameter was replaced by the equation defining it, and currently it is a model published in the literature [147]. An interpretability analysis is carried over this stomach model. In addition, non-interpretable parameters were endowed with interpretability according to step six of the methodology.

1. **Identify of the model's basic structure**: the set of balance equations giving significant information and thus representing the basic structure or the zero specification level of the human stomach model is given as follows:

$$\frac{dN_I}{dt} = \dot{n}_3 - \dot{n}_5 + \sum_i \sum_j (\sigma_{j,i} r_i) \tag{5.67}$$

$$\frac{dx_{j,5}}{dt} = \frac{1}{N_I}\left(x_{j,3}\dot{n}_3 - x_{j,5}\dot{n}_5 + \sum_i \sum_j (\sigma_{j,i} r_i) - x_{j,5}\frac{dN_I}{dt} \right) \tag{5.68}$$

$$\frac{dw_{G,7}}{dt} = \frac{1}{M_{III}}\left(w_{G,6}\dot{m}_6 - w_{G,1}\dot{m}_1 - w_{G,7}\dot{m}_7 \right) \tag{5.69}$$

$$\dot{W} = \frac{1}{\eta}\left(\dot{m}_{pc}\, h_{f_{d\to a}} \right) \tag{5.70}$$

$$\dot{n}_1 = \frac{1}{x_{G,1}}\, \sigma_{G,gc}\, r_{gc} \tag{5.71}$$

$$\dot{n}_2 = \dot{n}_1 + \sum_l (\sigma_{l,gc}\, r_{gc}) \tag{5.72}$$

$$r_{gc} = -\frac{1}{\Delta \bar{H}_{r_{gc}}} \dot{W} \tag{5.73}$$

$$M_{III} = C_1 \tag{5.74}$$

Table 5.20 reports all the structural parameters with the corresponding physical meaning, disregarding if they are associated to a numerical value or a constitutive or assessment equation. In this table, it is also indicated in which equation every structural parameter is located and if it is defined by a datum or an equation. Some structural parameters lay down under the chemical engineering context while some others under human physiology. Symbols $\sigma_{j,i}$ and C_1 are constants of the model, and N_I, $x_{j,5}$, $w_{G,7}$, W, $\dot{n}_1$, $\dot{n}_2$, r_{gc}, and M_{III} are the variables of the model. Therefore, constants and variables are not reported in the Table 5.20. Henceforth, one table for each specification level is introduced with the respective parameters. If a parameter appears in more than one specification level, the parameter belongs to the first level where it appeared. This will be clarified as the specification levels appear during the interpretability analysis.

2. **Obtain the first specification level**: the following set of constitutive and assessment equations is proposed to define the structural parameters that are previously defined with a numerical value:

TABLE 5.20. Structural parameters of the stomach model.

#	Symbol	Physical meaning	Defined by	Location
1	$\dot{n}_3$	Molar flow rate of gastric juices.	5.75	5.67 5.68
2	$\dot{n}_5$	Molar flow rate due to gastric emptying.	5.76	5.67 5.68
3	r_{fat}	Rate of fat reaction.	5.77	5.67 5.68
4	r_{pro}	Rate of protein reaction.	5.78	5.67 5.68
5	$\frac{dN_I}{dt}$	Total mass change in molar units.	5.79	5.68
6	$x_{j,3}$	Molar fraction of compound j at stream 3, with $j = GJ$.[a]	datum	5.68
7	η	Stomach efficiency as a driver machine.	datum	5.70
8	$\dot{m}_{pc}$	Flow of gastric mass through the pipe circuit.	5.80	5.70
9	$h_{f_{d\to a}}$	Friction losses in the pipe circuit.	5.81	5.70
10	$x_{G,1}$	Glucose concentration at current 1.	datum	5.71
11	$\Delta\bar{H}_{r_{gc}}$	Specific molar heat of reaction of glucose combustion.	datum	5.73
12	$\dot{m}_1$	Mass flow rate at current 1.	5.82	5.69
13	$w_{G,1}$	Mass fraction of glucose at stream 1.	datum	5.69
14	$w_{G,6}$	Mass fraction of glucose at current 6.	5.83	5.69
15	$\dot{m}_6$	Mass flow rate at current 6.	5.84	5.69
16	$\dot{m}_7$	Mass flow rate at current 7.	5.85	5.69

[a] The others compounds j are zero at stream 3.

$$\dot{n}_3 = \frac{1}{\mathfrak{m}_{GJ}} \rho_{GJ} \left[\left(\frac{1}{Dil} V_{gm,t_0} \right) - V_{gm,t_0} \right] \tag{5.75}$$

$$\dot{n}_5 = \frac{1}{\mathfrak{m}_{gm}} \rho_{gm} \left[\frac{V_{gm,t_0}}{Dil} - \frac{V_{gm,t_0}}{Dil} * Emp \right] \tag{5.76}$$

$$r_{Fat} = k_{0,Fat} C_{NtF} C_{ActL} e^{\frac{-E_{a,Fat}}{RT}} \tag{5.77}$$

$$r_{Pro} = k_{0,Pro} C_{NtP} C_{ActP} e^{\frac{-E_{a,Pro}}{RT}} \tag{5.78}$$

$$\frac{dN_I}{dt}(t) = \frac{N_I(t + \Delta t) - N_I(t)}{\Delta t} \tag{5.79}$$

$$\dot{m}_{pc} = \rho_{gm} v_{gm,distal} A_s \tag{5.80}$$

$$h_{f_{d \to a}} = \sum_s \left(K_s \frac{v_s^2}{2} \right) \tag{5.81}$$

$$\dot{m}_1 = \frac{1}{w_{G,1}} \mathfrak{m}_G \sigma_{G,gc} r_{gc} \tag{5.82}$$

$$w_{G,6} = \frac{1}{1000} \frac{pgm}{\rho_{blood}} \tag{5.83}$$

$$\dot{m}_6 = C_2 \tag{5.84}$$

$$\dot{m}_7 = \dot{m}_6 \tag{5.85}$$

Table 5.21 reports the functional parameters belonging to the first specification level. Note that parameter $w_{G,1}$ appears first time in the basic structure of the model, i.e., it is a structural parameter of the model, then it is not considered as a parameter of the first specification level. Symbols R, $\sigma_{G,gc}$, pgm, ρ_{blood}, C_2 are constants of the model, and N_I, r_{gc} are variables of the model. Therefore, they are not reported in Table 5.21 as parameters of first level of specification.

3. **Obtain the whole extended model structure**: the final extended model is obtained as soon as we stop digging into the functional parameters. In this case, we needed five specification levels to define a reliable set of interpretable parameters. The set of constitutive and assessment equations to obtain the second specification level becomes:

TABLE 5.21. Functional parameters of first specification level of the stomach model.

#	Symbol	Physical meaning	Defined by	Location
1	$\mathfrak{m}_{GJ}$	Molecular mass of gastric juices.	datum	5.75
2	ρ_{GJ}	Density of gastric juices.	datum	5.75
3	Dil	Dilution factor.	5.86	5.75 5.76
4	V_{gm,t_0}	Volume of gastric mass at t_0.	5.87	5.75 5.76
5	$\mathfrak{m}_{gm}$	Molecular mass of the stomach content.	5.88	5.76
6	ρ_{gm}	Density of gastric mass.	5.89 5.76 5.80	
7	Emp	Emptying factor.	5.90	5.76
8	$k_{0,Fat}$	Rate constant due to the frequency of molecular collisions in the correct orientation for fats.	datum	5.77
9	$k_{0,Pro}$	Rate constant due to the frequency of molecular collisions in the correct orientation for proteins.	datum	5.78
10	$E_{a,Fat}$	Activation energy for fat reaction.	datum	5.77
11	$E_{a,Pro}$	Activation energy for protein reaction.	datum	5.78
12	C_j	Molar-volumetric concentrations.	5.91	5.77 5.78
13	T	Corporal temperature.	datum	5.77 5.78
14	$v_{gm,distal}$	velocity of gastric mass measured at the pyloric antrum (distal extreme).	datum	5.80
15	A_s	Cross sectional area of the fitting at the distal extreme.	5.93	5.80
16	K_s	Friction factor for section s.	5.94	5.81
17	v_s	Velocity of the gastric mass at section s.	5.95	5.81
18	$\mathfrak{m}_G$	Molecular mass of glucose	datum.	5.82

$$Dil = -6.0070249 \times 10^{-8}\, {t_m}^3 + 7.0181077 \times 10^{-6}\, {t_m}^2 - 0.002301354\, t_m + 0.9912266$$

(5.86)

$$V_{gm,t_0} = \frac{M_{gm,t_0}}{\rho_{gm,t_0}} \tag{5.87}$$

$$\mathfrak{m}_{gm} = \sum_j x_{j,5}\mathfrak{m}_j \tag{5.88}$$

$$\rho_{gm} = VF_{FGJ}\rho_{gm,t_0} + (1 - VF_{FGJ})\rho_{GJ} \tag{5.89}$$

$$Emp = 2.65 \times 10^{-9} t_m^4 - 5.4098 \times 10^{-7} t_m^3 - 1.3812 \times 10^{-5} t_m^2 - 8.3192 \times 10^{-4} t_m + 0.9969 \tag{5.90}$$

$$C_j = \frac{x_j N_I}{V_{gm}} \tag{5.91}$$

$$v_{gm,distal} = 10.5 cm/s \tag{5.92}$$

$$A_s = \pi \frac{D_s^2}{4} \tag{5.93}$$

$$K_s = \begin{cases} K_{straight} = f_{Darcy} \frac{L_{straight}}{Ds} \\ K_{expan} = \left[1 - \left(\frac{SD}{HD}\right)^2\right]^2 \\ K_{cont} = 0.5 \left[1 - \left(\frac{SD}{HD}\right)^2\right]^2 \\ K_{180° Elbow} = \frac{1000}{Re_s} + 0.6 \left(1 + \frac{1}{ID}\right) \end{cases} \tag{5.94}$$

$$v_s = \frac{1}{A_s} \frac{\dot{m}_{pc}}{\rho_{gm}} \tag{5.95}$$

(5.96)

Table 5.22 reports functional parameters of second specification level. It can be noted that parameters ρ_{gm} and ρ_{GJ} are in blue since they were already accounted for at the first level. Likewise occurs with parameters A_s and $\dot{m}_{pc}$, used to define v_s but both of them are classified as parameters of first specification level and structural, respectively. The following constitutive and assessment selected equations produce the third specification level :

TABLE 5.22. Functional parameters of second specification level of the stomach model.

#	Symbol	Physical meaning	Defined by	Location
1	t_m	Elapsed time after digestion start.	datum	5.86 5.90
2	M_{gm,t_0}	Gastric mass at t_0 (Ingested meal).	datum	5.87
3	ρ_{gm,t_0}	Density of gastric mass at t_0.	datum	5.87 5.89
4	$\mathfrak{m}_j$	Molecular mass of compound j.	datum	5.88
5	VF_{FGJ}	Volumetric fraction of ingested food with respect to gastric juices.	5.97	5.89
6	V_{gm}	Volume of gastric mass.	5.98	5.91
7	D_s	Internal diameter of section s.	datum	5.93
8	f_{darcy}	Darcy factor.	5.99	5.94
9	$L_{straight}$	Length of the straight section s.	datum	5.94
10	SD	Smaller diameter in contraction/expansion.	datum	5.94
11	HD	Higher diameter in contraction/expansion.	datum	5.94
12	ID	Internal diameter in elbows.	datum	5.94
13	Re_s	Reynolds number.	5.100	5.94

TABLE 5.23. Functional parameters of third specification level of the stomach model.

#	Symbol	Physical meaning	Defined by	Location
1	μ_{gm}	Viscosity of the gastric mass.	5.101	5.100

$$VF_{FGJ} = \frac{V_{gm,t_0}}{V_{gm}} \tag{5.97}$$

$$V_{gm} = \frac{V_{gm,t_0}}{Dil} \tag{5.98}$$

$$f_{darcy} = \frac{64}{Re_s} \tag{5.99}$$

$$Re_s = \frac{\rho_{gm} v_s D_s}{\mu_{gm}} \tag{5.100}$$

Table 5.23 reports the only one functional parameter of third level of specification. Note that symbols in blue V_{gm,t_0}, Dil, ρ_{gm}, v_s are parameters of first specification level, and symbols V_{gm}, D_s, and Re_s are parameters of the second specification level. Only one parameter, μ_{gm}, appears in the third specification level. The following equation is used to define μ_{gm} further:

$$\mu_{gm} = -4.34648\, MDF^4 + 5.85569\, MDF^3 - 1.7678\, MDF^2 + 0.29556\, MDF - 0.02 \tag{5.101}$$

Table 5.24 report the functional parameter of fourth specification level. It can be observed that a new parameter is generated in fourth specification level. Then, it is necessary to declare a new specification level to define it. MDF can be defined further as:

TABLE 5.24. Functional parameters of fourth specification level.

#	Symbol	Physical meaning	Defined by	Location
1	MDF	Modified dilution factor	5.102	5.101

TABLE 5.25. Classification of the functional parameters of all specification levels.

Type	Parameter
Coupled	$\mathfrak{m}_{gm}$, C_j
Non-coupled	Dil, V_{gm,t_0}, ρ_{gm}, Emp, A_s, K_s, v_s, VF_{FGJ}, V_{gm}, f_{darcy}, Re_s, μ_{gm}, MDF
Scalar	$\mathfrak{m}_{GJ}$, ρ_{GJ}, $k_{0,Fat}$, $k_{0,Pro}$, $E_{a,Fat}$, $E_{a,Pro}$, T, $v_{gm,distal}$, $\mathfrak{m}_G$, t_m, M_{gm,t_0}, ρ_{gm,t_0}, $\mathfrak{m}_j$, D_s, $L_{straight}$, SD, HD, ID

$$MDF = Dil^{2.97} \tag{5.102}$$

This fifth specification level does not generate new functional parameters. The only functional parameter of the fifth specification level, MDF, is a function of the functional parameter Dil, marked in blue and previously defined in the first specification level. In this case, five specification levels are generated to obtain the extended model structure. The zero specification level as the basic structure of the model plus five specification levels in the extended model structure made up the whole model structure.

4. **Classify the functional parameters**: Table 5.25 reports the classification of the functional parameters of all specification levels. Structural parameters are not classified because this classification seeks to help to endow of interpretability those non interpretable parameters, and structural parameters are inherently interpretable.

5. **Evaluate the interpretability of functional parameters**: functional parameters are taken to evaluate and analyze its interpretability. As shown in Table 5.26, non-interpretable parameters are adjusted by empirical relations, are defined by a polynomial regression, or appear in the model as parameters within an empirical equation. For example, the dilution factor, Dil, is a non-interpretable parameter because is defined by a polynomial equations and this mathematical expression has not based on the knowledge of the phenomena of the process. Similarly occurs with emptying factor, Emp. Parameter MDF has a decimal exponent making loss complete interpretability of this functional parameter. MDF is an adjustment parameter to fix the model results and for that reason it is a non-interpretable parameter. Parameters $k_{0,Fat}$, $k_{0,Pro}$, $E_{a,Fat}$, $E_{a,Pro}$ are contextualized to the chemical kinetics of fats and proteins in the stomach. Parameter K_s has contextualized interpretability with the flow of the gastric mass throughout the section s.

6. **Endow the model of parametric interpretability**: according to the interpretability analysis of functional parameters of the model, only three of them are not interpretable. To endow interpretability these non-interpretable parameters, it is important to give them a conceptual definition before replacing the mathematical

TABLE 5.26. Interpretability analysis of functional parameters.

Interpretability	Parameters
General	$\mathfrak{m}_{gm}$, C_j, V_{gm,t_0}, ρ_{gm}, v_s, A_s, VF_{FGJ}, V_{gm}, f_{darcy}, Re_s, μ_{gm}, $\mathfrak{m}_{GJ}$, ρ_{GJ}, T, $v_{gm,distal}$, $\mathfrak{m}_G$, t_m, M_{gm,t_0}, ρ_{gm,t_0}, $\mathfrak{m}_j$, D_s, $L_{straight}$, SD, HD, ID
Contextualized	K_s, $k_{0,Fat}$, $k_{0,Pro}$, $E_{a,Fat}$, $E_{a,Pro}$
Non interpretable	Dil, Emp, MDF

equation used to define them. Thus, a conceptual definition is given to parameters dilution factor Dil and emptying factor Emp.

- **Dilution factor**: this is the relation of the initial volume of the solution to dilute and the current volume at any moment after diluting. In the case of the human stomach model, the dilution factor is the relation of the volume of the ingested food entering to the stomach and the volume of the stomach content at any moment of digestion. Thus, the polynomial expression used to calculate this parameter could be replaced for the following expression $Dil = \frac{V_c(i)}{V_i}$, with $V_c(i)$ the current volume at any time i and V_i the initial volume. This mathematical definition is based on the *dilution* concept, associated with the known phenomenon from chemistry and biology. Initial volume V_i is a constant value that can be obtained easily by knowing the amount of ingested food, but $V_c(i)$ is a parameter that must be calculated with the following equation: $V_c(i) = V_i + V_{GJ}(i)$, where $V_{GJ}(i)$ is the volume of gastric juices at any time. This parameter is calculated by knowing the phenomena occurring in the pancreas. However, since the role of the pancreas in the stomach digestion has not be fully understood (at least in quantitative terms), a phenomenological-based expression to describe such a volume is not yet available. Note that the conceptual definition could be used to define mathematically the parameter Dil. However, under conditions before mentioned, parameter Dil can be endowed interpretability from its conceptual definition, due to the mathematical representation of its conceptual definition cannot be implemented. In this way, Dil could cease to be non-interpretable and becomes a parameter with contextualized interpretability. Additionally, parameter Dil can be defined like *gastric dilution factor* instead dilution factor, to better agree with the physical meaning in the physiological context.

- **Emptying factor**: is the rate in which the fluid is emptied from the stomach, after stomach digestion, to escape into the duodenum. Parameter Emp only can be endowed interpretability after providing a phenomenological-based conceptual definition, because the calculation depends on the knowledge of the phenomena governing the digestion. But these phenomena are unknown and a phenomenological based mathematical expression does not exist yet. Parameter Emp can be defined like *gastric emptying factor* instead only emptying factor to better agree with physiological context of the model.

Finally, parameter MDF is a modification of the dilution factor Dil taken from the literature to calculate the viscosity of gastric mass μ. Furthermore, parameter MDF was used to adjust the model results and thus to get the computational solution. Therefore, a conceptual definition can not be provided to this parameter and the parameter cannot be endowed interpretability.

6

Conclusions and future work

A model is a tool used to answer questions about a process of interest, without the need to experiment on it, because experiments can be very expensive, destructive, dangerous or simply because the system does not exist yet. If a model of the system is posse, it can be used to calculate or predict how the system would have reacted, solving mathematically the equations that describe the system and studying the answers. This type of experimentation is called simulation. However, the value of the results of such experimentation depends entirely on the quality of the available model.

The difficulty in constructing models is to make them good and reliable. For a model to be useful, one must have confidence in the results and predictions that can be inferred from it. This reliability can be obtained by means of the parameters interpretability, and also verifying or validating the model, generally comparing the behavior of the model with the behavior of the system and evaluating the difference. Uncertainty is an important factor to take into account when talking about model reliability. Sometimes the mathematical structure of the system is not completely known (or it is known but simplified), it can also happen that the system parameters can not be completely known, or are only known in a limited range of operation. It can be spoken about a model with uncertainty, when there is uncertainty in the knowledge of the structure of the system, parameters and effects of disturbances. One of the reasons for uncertainty in the parameters is to use simplified or reduced order models to model complex systems. Another reason is the lack of interpretability of the parameters of the model.

Physiological processes in the human body are complex and highly non-linear systems. Therefore, to model a physiological process is a hard task, also because many of those processes are unknown today. In this thesis, a PSBM to describe the glucose homeostasis in humans was developed by coupling five submodels. Every submodel represents an organ involved in glucose metabolism and was constructed following the methodology to construct PBSMs. The submodels are based on the physiological knowledge available in the literature. The validation of every organ model was carried out with data reported in the literature. The most relevant characteristic of the models developed is the interpretability of its parameters. In this sense, a conceptual framework to define parameters interpretability in PBSMs was also proposed, along with a methodology to analyze and endow the parameters of a PBSM with interpretability. The conceptual framework and methodology were proposed from a qualitative point of view and based on the identifiability concept. However, it is hoped that a quantitative formalism of parameters interpretability can later rise and that the submodels presented in this thesis with parameters

defined by empirical mathematical relations can be replaced by mathematical expressions phenomenological inspired in accordance with the advances in medical discoveries.

As mentioned throughout the thesis, the term of interpretability has not a formal definition in the literature and several authors refer to model interpretability instead parameters interpretability. Nevertheless, the meaning of that term is not direct because the model as a whole is a complex piece of knowledge. Therefore, model interpretability is not an on-off property; rather, its evaluation requires grading a model on a scale of interpretability. Obviously, that scale requires a metric to generate the value of interpretability for a given model. This metric is the major problem of establishing an interpretability scale. As an example to evince the difficult to propose a formalism of parameters interpretability from a quantitative point of view is to consider two models of 30 and 3 parameters, respectively. If each model has only one noninterpretable parameter, an on-off approach would indicate that both models are not interpretable. But if an interpretability index (II) is stated as: $II = 1 - \frac{NP_{NoI}}{N_{TotP}}$, with NP_{NoI} the number of noninterpretable parameters and N_{TotP} the total number of parameters, the II for the first model will be $1 - \frac{1}{30} = 0.9666$ and for the second one will be $1 - \frac{1}{3} = 0.6666$. Does this proposed II give useful information about model size or complexity? Due to this unsolved item, in this thesis, interpretability was only evaluated in terms of individual parameters. The proposed conceptual framework can provide useful information to develop in the future further a mathematical formalism to characterize parameter interpretability.

Given that the validation of the model was carried out organ by organ and using data reported in the literature, in the future a complete validation of the coupled model, maybe using real data taken from real patients, could be realized. In this sense, a clinical study is hoped to face in the future to become more realistic the model and to help to that validation. Also, modifications in the model structure could carry out to adjust the model to patients with pathologies as diabetes mellitus.

Bibliography

[1] C. K. Abrams, M. Hamosh, V. S. Hubbard, S. K. Dutta, and P. Hamosh, *Lingual Lipase in Cystic Fibrosis*, The American Society for Clinical Investigation **73** (1984), 374–382.

[2] K. J. Acheson, A. Blondel-Lubrano, S. Oguey-Araymon, M. Beaumont, S. Emady-Azar, C. Ammon-Zufferey, I. Monnard, S. Pinaud, C. Nielsen-Moennoz, and L. Bovetto, *Protein choices targeting thermogenesis and metabolism*, The American Journal of Clinical Nutrition **93** (2011), no. 3, 525–534.

[3] M. M. Adeva-Andany, N. Perez-Felpete, C. Fernandez-Fernandez, C. Donapetry-Garcia, and C. Pazos-Garcia, *Liver glucose metabolism in humans*, Bioscience Reports **36** (2016), no. 6, e00416–e00416.

[4] Horacio J. Adrogué, *Glucose homeostasis and the kidney*, Kidney International **42** (1992), no. 5, 1266–1282.

[5] T. Akhavan, B. L. Luhovyy, P. H. Brown, C. E. Cho, and G. H. Anderson, *Effect of premeal consumption of whey protein and its hydrolysate on food intake and post-meal glycemia and insulin responses in young adults*, American Journal of Clinical Nutrition **91** (2010), no. 4, 966–975.

[6] T. Akhavan, S. Panahi, G.H. Anderson, and B.L. Luhovyy, *Application of dairy-derived ingredients in food intake and metabolic regulation*, Dairy-Derived Ingredients (Milena Corredig, ed.), Woodhead Publishing Series in Food Science, Technology and Nutrition, Woodhead Publishing, 2009, pp. 212 – 237.

[7] M. Alsahli and John E. Gerich, *Renal glucose metabolism in normal physiological conditions and in diabetes*, Diabetes Research and Clinical Practice **33** (2017), 1–9.

[8] H. Alvarez, *Efectos dinámicos en operaciones unitarias. Modelado de procesos para su análisis y control*, Universidad Nacional de Colombia, 2017.

[9] H. Alvarez, P. Vega, S. Revollar, and R. Lamanna, *Metodología para la Obtención de Modelos Semifísicos de Base Fenomenológica Aplicada a una Sulfitadora de Jugo de Caña de Azúcar*, Revista Iberoamericana de Automática e Informática Industrial RIAI **6** (2009), no. 3, 10–20.

[10] H. Alvarez Z., *Diseño simultáneo de procesos y control. uso de efectos dinámicos en ingeniería de procesos*, Universidad Nacional de Colombia, 2010.

[11] D. Ambrosi, A. Quarteroni, and G. Rozza, *Modeling of Physiological Flows*, 1 ed., vol. 5, Springer-Verlag Mailand, 2012.

[12] R. Ambrosino, B. G. Buchanan, G. F. Cooper, and M. J. Fine, *The use of misclassification costs to learn rule-based decision support models for cost-effective hospital admission strategies.*, Proceedings of the Annual Symposium on Computer Application in Medical Care (1995), 304–8.

[13] G. H. Anderson and S. E. Moore, *Dietary proteins in the regulation of food intake and body weight in humans*, The Journal of Nutrition **134** (2004), no. 4, 974S–979S.

[14] K. N. Aronis, S. M. Khan, and C. S. Mantzoros, *Effects of trans fatty acids on glucose homeostasis: A meta-analysis of randomized, placebo-controlled clinical trials*, American Journal of Clinical Nutrition **96** (2012), no. 5, 1093–1099.

[15] S. L. Aronoff, K. Berkowitz, B. Shreiner, and L. Want, *Glucose metabolism and regulation: Beyond insulin and glucagon*, Diabetes Spectrum **17** (2004), no. 3, 183–190.

[16] Craig A. Aumann, *A methodology for developing simulation models of complex systems*, Ecological Modelling **202** (2007), no. 3, 385 – 396.

[17] Göke B, *Islet cell function: alpha and beta cells–partners towards normoglycaemia*, Int J Clin Pract Suppl. (2008), no. 159, 2–7.

[18] E. Balsa-Canto, A. A. Alonso, and J. R. Banga, *An iterative identification procedure for dynamic modeling of biochemical networks.*, BMC systems biology **4** (2010), no. 11.

[19] M. Barbagallo and L. J. Dominguez, *Magnesium metabolism in type 2 diabetes mellitus, metabolic syndrome and insulin resistance*, Archives of Biochemistry and Biophysics **458** (2007), no. 1, 40 – 47, Highlight Issue on Cellular Regulation of Magnesium.

[20] D. Basmadjian and R. Farnood, *The art of modeling in science and engineering with mathematica*, 2nd ed., 2006.

[21] G. Bastin and D. Dochain (eds.), *Copyright*, Process Measurement and Control, Elsevier, Amsterdam, 1990.

[22] C. L. Beck, *Modeling and control of pharmacodynamics*, European Journal of Control **24** (2015), 33–49.

[23] R. Bellman and K.J. Åström, *On structural identifiability*, Mathematical Biosciences **7** (1970), no. 3, 329 – 339.

[24] Rinaldo Bellomo, *Bench-to-bedside review: Lactate and the kidney*, Critical Care **6**, 322–326.

[25] G. Bellu, M. P. Saccomani, S. Audoly, and L. D'Angiò, *DAISY: A new software tool to test global identifiability of biological and physiological systems*, Computer Methods and Programs in Biomedicine **88** (2007), no. 1, 52–61.

[26] L. Q. Bendtsen, J. K. Lorenzen, N. T. Bendsen, C. Rasmussen, and A. Astrup, *Effect of dairy proteins on appetite, energy expenditure, body weight, and composition: a review of the evidence from controlled clinical trials*, Advances in Nutrition **4** (2013), no. 4, 418–438.

[27] L. Benzi, P. Cecchetti, A. Ciccarone, A. Pilo, G. Di Cianni, and R. Navalesi, *Insulin degradation in vitro and in vivo: A comparative study in men: Evidence that immunoprecipitable, partially rebindable degradation products are released from cells and circulate in blood*, Diabetes **43** (1994), no. 2, 297–304.

[28] B W. Bequette, *Process Control. Modeling, Design, and Simulation*, Prentice Hall PTR, New Jersey, 2003.

[29] R. N. Bergman, L. S. Phillips, and C. Cobelli, *Physiologic evaluation of factors controlling glucose tolerance in man: measurement of insulin sensitivity and beta-cell glucose sensitivity from the response to intravenous glucose.*, The Journal of clinical investigation **68** (1981), no. 6, 1456–67.

[30] C. Biava, A. Grossman, and M. West, *Ultrastructural observations on renal glycogen in normal and pathologic human kidneys*, Lab Invest. **15** (1966), 330–356.

[31] G. Biolo, D. R.Y. Fleming, and R. R. Wolfe, *Physiologic hyperinsulinemia stimulates protein synthesis and enhances transport of selected amino acids in human skeletal muscle*, J Clin Invest **95** (1995), 811–819.

[32] O. Biran and C. Cotton, *Explanation and Justification in Machine Learning : A Survey*, International Joint Conference on Artificial Intelligence Workshop on Explainable Artificial Intelligence (IJCAI-XAI) (2017), 8–13.

[33] J. B. Bird and W. J. Palm, *Modeling, analysis, and control of dynamic systems*, 2 ed., Wiley Publishers of Canada, 1972.

[34] R. Bland, D. Markovic, C. E. Hills, S. V. Hughes, S. L. F. Chan, P. E. Squires, and M. Hewison, *Expression of* $25{-}hydroxyvitamin\ d_3 - 1\alpha$*-hydroxylase in pancreatic islets*, The Journal of Steroid Biochemistry and Molecular Biology **89-90** (2004), 121 – 125, Proceedings of the 12th Workshop on Vitamin D.

[35] Albert J Bredenoord, André Smout, and Jan Tack, *A Guide to Gastrointestinal Motility Disorders*, Springer Science+Business Media, Inc., 2010.

[36] L. Breen, A. Philp, C. S. Shaw, A. E. Jeukendrup, K. Baar, and K. D. Tipton, *Beneficial effects of resistance exercise on glycemic control are not further improved by protein ingestion*, PLoS One **6** (2011), no. 6.

[37] L. Brennan, A. Shine, C. Hewage, J. P. G. Malthouse, K. M. Brindle, N. McClenaghan, P. R. Flatt, and P. Newsholme, *A nuclear magnetic resonance-based demonstration of substantial oxidative l-alanine metabolism and l-alanine-enhanced glucose metabolism in a clonal pancreatic* β*-cell line*, Diabetes **51** (2002), no. 6, 1714–1721.

[38] M. Brissova, MJ. Fowler, WE. Nicholson, A. Chu, B. Hirshberg, DM. Harlan, and AC. Powers, *Assessment of human pancreatic islet architecture and composition by laser scanning confocal microscopy*, J Histochem Cytochem. **53** (2016), no. 9, 1087–1097.

[39] G. Bruno, C. Runzo, P. Cavallo-Perin, F. Merletti, M. Rivetti, S. Pinach, G. Novelli, M. Trovati, F. Cerutti, and G. Pagano, *Incidence of type 1 and type 2 diabetes in adults aged 30–49 years*, Diabetes Care **28** (2005), no. 11, 2613–2619.

[40] Peter Buchwald, *A local glucose-and oxygen concentration-based insulin secretion model for pancreatic islets*, Theoretical Biology and Medical Modelling **8** (2011), no. 1, 20.

[41] Mario Bunge, *Method, Model and Matter*, Media, Springer Science & Business, 2012.

[42] A. C. Guyton and Jonh E. Hall, *Textbook of medical physiology*, 7th ed., Philadelphia, Pennsylvania, 2006.

[43] Juan Camilo Calderón O., *Una aproximación al diseño y control total de planta usando controlabilidad de estado*, 2012.

[44] E. R. Carson, C. Cobelli, and L. Finkelstein, *The mathematical modeling of metabolic and endocrine systems: Model formulation, identification and validation*, Biomedical Engineering and Health Systems Series, Books on Demand, 1983.

[45] R. Caruana, Y. Lou, J. Gehrke, P. Kock, M. Sturm, and N. Elhadad, *Accurate intelligible models with pairwise interactions*, Proceedings of the 19th ACM SIGKDD international conference on Knowledge discovery and data mining - KDD '13 (2015).

[46] J. Casillas, O. Cordón, F. Herrera Triguero, and L. Magdalena, *Interpretability Issues in Fuzzy Modeling*, Springer-Verlag Berlin Heidelberg, 2013.

[47] E. Cersosimo, P. Garlick, and J. Ferretti, *Renal substrate metabolism and gluconeogenesis during hypoglycemia in humans*, Diabetes **49** (2000), 1186–1193.

[48] E. Cersosimo, P. Garlick, and Ferretti J., *Renal glucose production during insulin-induced hypoglycemia in humans*, Diabetes **48** (1999), 261–266.

[49] E. Chalhoub, *an in Silico Liver : Model of Gluconeogensis*, PhD thesis (2013), no. March.

[50] M.J. Chamberlain and L. Stimmler, *The renal handling of insulin*, Journal of Clinical Investigation **46** (1967).

[51] L. Chen, B. Tuo, and H. Dong, *Regulation of intestinal glucose absorption by ion channels and transporters*, nutrients **8** (2016).

[52] Y. Chen, B. C. Fry, and A. T. Layton, *Modeling glucose metabolism and lactate production in the kidney*, Mathematical Biosciences **289** (2017), 116–129.

[53] S. V. Chin and M. J. Chappell, *Structural identifiability and indistinguishability analyses of the Minimal Model and a Euglycemic Hyperinsulinemic Clamp model for glucose-insulin dynamics*, Computer Methods and Programs in Biomedicine **104** (2011), no. 2, 120–134.

[54] O. Chis, J. R. Banga, and E. Balsa-Canto, *GenSSI: A software toolbox for structural identifiability analysis of biological models*, Bioinformatics **27** (2011), no. 18, 2610–2611.

[55] S.P. Choukem and J.F. Gautier, *How to measure hepatic insulin resistance?*, Diabetes & Metabolism **34** (2008), no. 6, Part 2, 664 – 673, Liver and diabetes.

[56] C. Cobelli and E. Carson, *Introduction to modeling in physiology and medicine*, Biomedical Engineering, Academic Press, Burlington, 2008.

[57] ———, *An Introduction to Modelling Methodology*, second edi ed., Elsevier Inc., 2014.

[58] Claudio Cobelli, C. Dalla Man, G. Sparacino, L. Magni, G. Nicolao, and B. P. Kovatchev, *Diabetes : Models , Signals , and Control*, IEEE Trans Biomed Eng **2** (2009), 54–96.

[59] J. Contreras Montes, R. Misa Llorca, and L. Uruera Vivanco, *Algoritmos para identificación de modelos difusos interpretables*, IEEE Latin America Transactions **5** (2007), no. 5, 346–351.

[60] A. J. Coupe, S. S. Davis, and I. R. Wilding, *Variation in gastrointestinal transit of pharmaceutical dosage forms in healthy subjects*, Pharm Res **8** (1991), no. 3, 604–4.

[61] M. Courtney Moore, K. C. Coate, J. J. Winnick, Z. An, and A. D. Cherrington, *Regulation of hepatic glucose uptake and storage in vivo.*, Advances in Nutrition **3** (2012), no. 3, 286–294.

[62] G. Craciun and C. Pantea, *Identifiability of chemical reaction networks*, Journal of Mathematical Chemistry **44** (2008), 244–259.

[63] G. A. Cunningham, N. H. Mcclenaghan, P. R. Flatt, and P. Newsholme, *L-alanine induces changes in metabolic and signal transduction gene expression in a clonal rat pancreatic β-cell line and protects from pro-inflammatory cytokine-induced apoptosis*, Clinical Science **109** (2005), no. 5, 447–455.

[64] C. Dalla Man, F. Micheletto, D. Lv, M. Breton, B. Kovatchev, and C. Cobelli, *The UVA/PADOVA Type 1 Diabetes Simulator: New Features.*, Journal of diabetes science and technology **8** (2014), 26–34.

[65] Denis Daneman, *Type 1 diabetes*, The Lancet **367** (2006), no. 9513, 847 – 858.

[66] F. P. Davidescu and S. B. Jørgensen, *Structural parameter identifiability analysis for dynamic reaction networks*, Chemical Engineering Science **63** (2008), no. 19, 4754 – 4762, Model-Based Experimental Analysis.

[67] R. A. DeFronzo, E. Ferrannini, and P. Zimmet, *International textbook of diabetes mellitus*, fourth ed., 2015.

[68] R. A. DeFronzo, J. D. Tobin, and R. Andres, *Glucose clamp technique: a method for quantifying insulin secretion and resistance.*, American Journal of Physiology-Endocrinology and Metabolism **237** (1979), no. 3, E214, PMID: 382871.

[69] L. Denis-Vidal, G. Joly-Blanchard, and C. Noiret, *Some effective approaches to check the identifiability of uncontrolled nonlinear systems*, Mathematics and Computers in Simulation **57** (2001), no. 1, 35 – 44.

[70] S. R. Devasahayam, *Signals and systems in biomedical engineering: Signal processing and physiological systems modeling*, 1 ed., Springer US, 2000.

[71] A. C. Dimian, C. S. Bildea, and A. A. Kiss, *Chapter 15 - plantwide control*, Integrated Design and Simulation of Chemical Processes (Alexandre C. Dimian, Costin S. Bildea, and Anton A. Kiss, eds.), Computer Aided Chemical Engineering, vol. 35, Elsevier, 2014, pp. 599 – 647.

[72] T. G. Dobre and J. G. Sanchez Marcano, *Chemical engineering: Modelling, simulation and similitude*, Alemania, 2007.

[73] F. Doshi-Velez and B. Kim, *Towards A Rigorous Science of Interpretable Machine Learning*, (2017), no. Ml, 1–13.

[74] A. D. Dragan, K. C.T. Lee, and S. S. Srinivasa, *Legibility and predictability of robot motion*, 8th ACM/IEEE International Conference on Human-Robot Interaction (HRI) (2013).

[75] D.J. Drucker and M.A. Nauck, *The incretin system: glucagon-like peptide-1 receptor agonists and dipeptidyl peptidase-4 inhibitors in type 2 diabetes*, Lancet **368** (2006), 1696–1705.

[76] W. C. Duckworth, R. G. Bennett, and F. G. Hamel, *Insulin degradation: Progress and potential*, Endocrine Reviews **19** (1998), no. 5, 608–624.

[77] W. C. Duckworth, F. G. Hamel, and D. E. Peavy, *Hepatic metabolism of insulin*, The American Journal of Medicine **85** (1988), no. 5, Supplement 1, 71 – 76, New Horizons in Diabetes: A Veterans Administration Medical Research Service Symposium.

[78] M.J. Dunne, D.I. Yule, D.V. Gallacher, and O.H. Petersen, *Effects of alanine on insulin-secreting cells: Patch-clamp and single cell intracellular ca2+ measurements*, Biochimica et Biophysica Acta (BBA) - Molecular Cell Research **1055** (1990), no. 2, 157 – 164.

[79] R. Dybowski, K. B. Laskey, J. W. Myers, and S. Parsons, *Introduction to the special issue on the fusion of domain knowledge with data for decision support*, Journal of Machine Learning Research **4** (2003).

[80] Philip E.Johnson, *What kind of expert should a system be?*, Journal of Medicine and Philosophy **8** (1983), 77–97.

[81] Pieter Eykhoff, *System identification: Parameter and state estimation*, first ed., 1974.

[82] International Diabetes Federation, *Idf diabetes atlas*, eighth edition ed., 2017.

[83] J. A. Fernandez-Tresguerres, C. Ariznavarreta Ruiz, V. Cachofeiro, D. P. Cardinali, E. Escrich Escriche, P. E. Gil-Loyzaga, V. Lahera Juliá, F. Mora Teruel, M. Romano Pardo, and J. Tamargo Menéndez, *Fisiología humana*, 3 ed., 2005.

[84] M. J. Ferrua and R. P. Singh, *Modeling the Fluid Dynamics in a Human Stomach to Gain Insight of Food Digestion*, **75** (2010), no. 7, 151–162.

[85] M. J. Ferrua, Z. Xue, and R. P. Singh, *On the kinematics and efficiency of advective mixing during gastric digestion - a numerical analysis*, Journal of Biomechanics **47** (2014), no. 15, 3664–3673.

[86] M.J. Ferrua, Z. Xue, and R. P. Singh, *Chapter 12 - dynamics of gastric contents during digestion - computational and rheological considerations*, Food Structures, Digestion and Health (Mike Boland, Matt Golding, and Harjinder Singh, eds.), Academic Press, San Diego, 2014, pp. 319 – 360.

[87] W.F. Fincham and F.T. Tehrani, *A mathematical model of the human respiratory system*, Journal of Biomedical Engineering **5** (1983), no. 2, 125 – 133.

[88] Jay W. Forrester, *Lessons from system dynamics modeling*, Systems Dynamic Review **3** (1987), no. 2, 136–149.

[89] L. Freychet, S.W. Rizkalla, N. Desplanque, A. Basdevant, P. Zirinis, G. Tchobroutsky, and G. Slama, *Effect of intranasal glucagon on blood glucose levels in healthy subjects and hypoglycaemic patients with insulin-dependent diabetes.*, The Lancet **331** (1988), 1364–1366.

[90] Z. Fu, E. R. Gilbert, and D. Liu, *Regulation of Insulin Synthesis and Secretion and Pancreatic Beta-Cell Dysfunction in Diabetes*, Current Diabetes Reviews **9** (2013), no. 1, 25–53.

[91] F. Fumeron, A. Lamri, C. Abi Khalil, R. Jaziri, I. Porchay-Baldérelli, O. Lantieri, S. Vol, B. Balkau, and M. Marre, *Dairy consumption and the incidence of hyperglycemia and the metabolic syndrome*, Diabetes Care **34** (2011), no. 4, 813–817.

[92] R. G. Gandica, W. K. Chung, L. Deng, R. Goland, and M. P. Gallagher, *Identifying monogenic diabetes in a pediatric cohort with presumed type 1 diabetes*, Pediatric Diabetes **16** (2015), no. 3, 227–233.

[93] W. Garcia-Gabin and E. W. Jacobsen, *Multilevel model of type 1 diabetes mellitus patients for model-based glucose controllers*, J Diabetes Sci Technol **7** (2013), no. 1, 193–205.

[94] J. E. Gerich, C. Meyer, H. J. Woerle, and M. Stumvoll, *Renal gluconeogenesis its importance in human glucose homeostasis*, Diabetes Care **24** (2001), 382–391.

[95] John E Gerich, *Physiology of glucose homeostasis*, Diabetes, Obesity and metabolism **2** (2000), no. 6, 345–350.

[96] John E. Gerich, *Role of the kidney in normal glucose homeostasis and in the hyperglycaemia of diabetes mellitus: therapeutic implications*, Diabetic Medicine **27** (2010), 136–142.

[97] Anderson GH., Luhovyy B., Akhavan T., and Panahi S., *Milk proteins in the regulation of body weight, satiety, food intake and glycemia*, Nestle Nutr Workshop Ser Pediatr Program **67** (2011), 147–159.

[98] B. H. Ginsberg, T. J. Brown, I. Simon, and A. A. Spector, *Effect of the membrane lipid environment on the properties of insulin receptors*, Diabetes **30** (1981), no. 9, 773–780.

[99] L. Gómez, A. Amicarelli, H. Alvarez, and F. Di Sciascio, *El Rol De Los Modelos En El Diseño De Equipos De Procesos Y Sistemas De Control*, VI Congreso Nacional de la Asociación Colombiana de Automática (2004), 521–526.

[100] V. González-Vélez, G. Dupont, A. Gil, A. González, and I. Quesada, *Model for glucagon secretion by pancreatic α-cells*, PLoS ONE **7** (2012), no. 3, 1–11.

[101] G. M. Gray, *The role of the gastrointestinal tract in nutrient delivery*, Academic Press, Inc, 1984.

[102] FieldComm Group, *Fieldcomm group. connecting the world of process automation*, 2015.

[103] W. G. Guder and B. D. Ross, *Enzyme distribution along the nephron*, Kidney International **26** (1984), no. 2, 101–111.

[104] J. W. Haefner, *Modeling Biological Systems. Principles and Applications*, second ed., Springer Science+Business Media, Inc., New York, 2005.

[105] K. D. Hall, *Predicting metabolic adaptation , body weight change , and energy intake in humans*, Am J Physiol Endocrinol Metab **298** (2010), E449–E466.

[106] F. G. Hamel, W. C. Duckworth, and R. G. Bennett, *Insulin Degradation : Progress and Potential*, Endocrine Reviews **19** (1998), no. 5, 608–624.

[107] K. Hangos and I. T. Cameron, *Process Modelling and Model Analysis*, vol. 4, Academic Press, 2001.

[108] M. Hao, X. Li, M. A. Rizzo, J. V. Rocheleau, B. M. Dawant, and D. W. Piston, *Regulation of two insulin granule populations within the reserve pool by distinct calcium sources*, Journal of Cell Science **118** (2005), 5873–5884.

[109] J. R. Harrison, Z. Lin, G. R. Carroll, and K. M. Carley, *Simulation modeling in organizational and management research*, Academy of Management Review **32** (2017), no. 4, 1229–1245.

[110] T. Hastie and R. Tibshirani, *Generalized additive models: Some applications*, Journal of the American Statistical Association **82** (1987), no. 398, 371–386.

[111] A. C. Hauge-Evans, A. J. King, D. Carmignac, C. C. Richardson, I. Robinson, M. J. Low, M. R. Christie, S. J. Persaud, and P. M. Jones, *Somatostatin secreted by islet delta-cells fulfills multiple roles as a paracrine regulator of islet function.*, Diabetes **58** (2009), no. 2, 403–11.

[112] M. Heer and S. Egert, *Nutrients other than carbohydrates: their effects on glucose homeostasis in humans*, Diabetes/Metabolism Research and Reviews **31** (2015), no. 1, 14–35.

[113] M. Heer, S. M. Smith, P. Frings-Meuthen, S. R. Zwart, and N. Baecker, *High protein intake improves insulin sensitivity but exacerbates bone resorption in immobility (wise study)*, Faseb **26** (2012), no. 1.

[114] E. Heinzle, A. P. Biwer, and C. L. Cooney, *Development of sustainable bioprocesses: Modeling and assessment*, Inglaterra, 2006.

[115] Herbert F. Helander and Lars Fändriks, *Surface area of the digestive tract-revisited*, Scandinavian Journal of Gastroenterology **49** (2014), no. 6, 681–689.

[116] M. M.I. Hennes, A. Dua, and A. H. Kissebah, *Effects of free fatty acids and glucose on splanchnic insulin dynamics*, Diabetes **46** (1997), no. 1, 57–62.

[117] H. Hernandez, *Multiscale simulation of heterophase polymerization Application to the synthesis of multicomponent colloidal polymer particles*, 2008.

[118] A. Hinsberger and B. K. Sandhu, *Digestion and absorption*, Current Paediatrics **14** (2004), no. 7, 605–611.

[119] N. Holman, B. Young, and R. Gadsby, *Current prevalence of type 1 and type 2 diabetes in adults and children in the uk*, Diabetic Medicine **32** (2015), no. 9, 1119–1120.

[120] J. J. Holst, *Glucagon-like peptide 1 (glp-1): An intestinal hormone, signalling nutritional abundance, with an unusual therapeutic potential*, Trends in Endocrinology and Metabolism **10** (1999), no. 6, 229 – 235.

[121] J. J. Holst and J. Gromada, *Role of incretin hormones in the regulation of insulin secretion in diabetic and nondiabetic humans*, American Journal of Physiology-Endocrinology and Metabolism **287** (2004), no. 2, E199–E206.

[122] C. Howarth, P. Gleeson, and D. Attwell, *Updated energy budgets for neural computation in the neocortex and cerebellum*, Journal of Cerebral Blood Flow & Metabolism. **32** (2012), no. 7, 1222–1232.

[123] E. Hoyos, D. López, and H. Alvarez, *A phenomenologically based material flow model for friction stir welding*, Materials and Design **111** (2016), 321–330.

[124] P. Humphreys, *Extending Ourselves: Computational Science, Empiricism, and Scientific Method*, Oxford University Press, Oxford, 2004.

[125] J. Huysmans, K. Dejaeger, C. Mues, J. Vanthienen, and B. Baesens, *An empirical evaluation of the comprehensibility of decision table, tree and rule based predictive models*, Decision Support Systems **51** (2011), no. 1, 141–154.

[126] E. Hypponen, E. Laara, A. Reunanen, and M.R. Jarvelin, *Intake of vitamin d and risk of type 1 diabetes: a birth-cohort study*, The Lancet **358** (2001), 1500–1503.

[127] A. D. Jackson and J. McLaughlin, *Digestion and absorption*, Surgery (Oxford) **27** (2009), no. 6, 231–236.

[128] G. Jiang and B. B. Zhang, *Glucagon and regulation of glucose metabolism*, American Journal of Physiology-Endocrinology and Metabolism **284** (2003), no. 4, E671–E678.

[129] C. Johansson, *Studies of gastrointestinal interactions. VII. Characteristics of the absorption pattern of sugar, fat and protein from composite meals in man. A quantitative study.*, Scandinavian journal of gastroenterology **10** (1975), no. 1, 33–42.

[130] John E. Hall, *Textbook of Medical Physiology*, 13 ed., Guyton Physiology, 2015.

[131] J.A. Johnson, J.P. Grande, P.C. Roche, and R. Kumar, *Immunohistochemical localization of the 1,25(oh)2d3 receptor and calbindin d28k in human and rat pancreas.*, American Journal of Physiology-Endocrinology and Metabolism **267** (1994), 356–360.

[132] N. Kaistha, *Plantwide Control of Integrated Chemical Processes*, National Program on Technology Enhanced Learning (NPTEL) (2013), 9.

[133] G. Katsuura, A. Asakawa, and A. Inui, *Roles of pancreatic polypeptide in regulation of food intake*, Peptides. **23** (2002), no. 2, 223–229.

[134] A. Khan and J. Pessin, *Insulin regulation of glucose uptake: a complex interplay of intracellular signalling pathways*, Diabetologia **45** (2002), no. 11, 1475–1483.

[135] Been Kim, *Interactive and Interpretable Machine Learning Models for Human Machine Collaboration*, 2015.

[136] E. Barrett Kim, M. Barman Susan, Scott Boitano, and Heddwen Brooks, *Ganong medical physiology*, 24th ed., Mc Graw Hill, 2012.

[137] S. Y. Kim, H. Il Kim, T. H. Kim, S. S. Im, S. K. Park, I. K. Lee, K. S. Kim, and Y. H. Ahn, *SREBP-1c mediates the insulin-dependent hepatic glucokinase expression*, Journal of Biological Chemistry **279** (2004), no. 29, 30823–30829.

[138] H. Kirchsteiger, J. Bagterp, J. Eric, and R. Luigi del Re, *Prediction methods for blood glucose concentration*, Springer International Publishing, 2016.

[139] P. Knekt, M. Laaksonen, C. Mattila, T. Härkänen, J. Marniemi, H. Heliövaara, M. Rissanen, J. Montonen, and A. Reunanen, *Serum vitamin d and subsequent occurrence of type 2 diabetes.*, Epidemiology **19** (2008), 666–671.

[140] A. D. Kohn, S. A. Summers, M. J. Birnbaum, and R. A. Roth, *Expression of a constitutively active akt ser/thr kinase in 3t3-l1 adipocytes stimulates glucose uptake and glucose transporter 4 translocation.*, J Biol Chem. **271** (1996), no. 49, 31372–8.

[141] M. Komatsu, M. Takei, H. Ishii, and Y. Sato, *Glucose-stimulated insulin secretion: A newer perspective*, Journal of Diabetes Investigation **4** (2013), no. 6, 511–516.

[142] Rosa Krajmalnik-Brown, Zehra Esra Ilhan, Dae Wook Kang, and John K. DiBaise, *Effects of gut microbes on nutrient absorption and energy regulation*, Nutrition in Clinical Practice **27** (2012), no. 2, 201–214.

[143] X. Lan-Pidhainy and T. Wolever, *The hypoglycemic effect of fat and protein is not attenuated by insulin resistance*, The American Journal of Clinical Nutrition **91** (2010), no. 1, 98–105.

[144] T. Larsson and S. Skogestad, *Plantwide control - A review and a new design procedure*, Modeling, identification and control (MIC) **21** (2000), no. 4, 209–240.

[145] Peter Layer and G Gröger, *Fate of Pancreatic Enzymes in the Human Intestinal Lumen in Health and Pancreatic Insufficiency*, Digestion (1993), 10–14.

[146] E. Leighton, C. A. Sainsbury, and G. C. Jones, *A practical review of c-peptide testing in diabetes*, Diabetes therapy **8** (2017), 475–487.

[147] L. Lema-Perez, J. Garcia-Tirado, C. Builes-Montaño, and H. Alvarez, *Phenomenological-Based model of human stomach and its role in glucose metabolism*, Journal of Theoretical Biology **460** (2019), 88–100.

[148] O. Levenspiel, *Modeling in chemical engineering*, Chemical Engineering Science **57** (2002), no. 22-23, 4691–4696.

[149] Alexander H. Levis, *Simple versus realistic modeling*, Computational and Mathematical Organization Theory **15** (2009), 5–7.

[150] John K. Leypoldt, *The artificial kidney: Physiological modeling and tissue engineering*, ilustrada ed., vol. 3, 1999.

[151] T. H. Liao, P. Hamosh, and M. Hamosh, *Fat digestion by lingual lipase: mechanism of lipolysis in the stomach and upper small intestine.*, Pediatric research **18** (1984), no. 5, 402–409.

[152] Siegwart Lindenberg, *Rational choice theory - advocacy and critique*, vol. 1, SAGE, International Educational and Professional Publisher, 1992.

[153] Z. C. Lipton, *The mythos of model interpretability*, CoRR **abs/1606.03490** (2016).

[154] T. J. Little, S. Doran, J. H. Meyer, A. J. P. Smout, D. G. O. Donovan, K. Wu, K. L. Jones, J. Wishart, C. K. Rayner, M. Horowitz, C. Feinle-bisset, J. Tanya, S. Doran, J. H. Meyer, J. P M Andre, D. G. O. Donovan, K. Wu, K. L. Jones, J. Wishart, C. K. Rayner, and M. Horowitz, *The release of GLP-1 and ghrelin , but not GIP and CCK , by glucose is dependent upon the length of small intestine exposed*, (2006), 647–655.

[155] L. Ljung and T. Glad, *Modeling of Dynamic Systems*, PTR Prentice Hall, 1994.

[156] ———, *On global identifiability for arbitrary model parametrizations*, Automatica **30** (1994), no. 2, 265 – 276.

[157] L. Ljung and T. Söderström, *Theory and practice of recursive identification*, vol. 4, 1985.

[158] Lennart Ljung, *System Identification: Theory for the User*, 2 ed., Education, Pearson, 1998.

[159] S. López Restrepo, *Metodología Para la Jerarquización de Parámetros en un MSBF Metodología Para la Jerarquización de Parámetros en un MSBF*, 2017.

[160] Y. Lou, R. Caruana, and J. Gehrke, *Intelligible models for classification and regression*, KDD '12: Proceedings of the 18th ACM SIGKDD international conference on Knowledge discovery and data mining (2012), 150–158.

[161] Y. Lou, R. Caruana, J. Gehrke, and G. Hooker, *Accurate intelligible models with pairwise interactions*, Proceedings of the 19th ACM SIGKDD international conference on Knowledge discovery and data mining - KDD '13 (2013), 623–631.

[162] W. L. Luyben, *Process modeling, simulation, and control for chemical engineers*, 2 ed., McGraw-Hill, 1990.

[163] W. L. Luyben, B. D. Tyréus, and M. Luyben, *Plantwide Process Control*, McGraw-Hill, 1998.

[164] B. Maestro, N. Dávila, M.C. Carranza, and C. Calle, *Identification of a vitamin d response element in the human insulin receptor gene promoter*, The Journal of Steroid Biochemistry and Molecular Biology **84** (2003), no. 2, 223 – 230, Proceedings of the 15th International Symposium of the Journal of Steroid Biochemistry and Molecular Biology - Poster Presentations.

[165] J. F. Maier, C. M. Eckert, and P. J. Clarkson, *Model granularity and related concepts*, Proceedings of International Design Conference, DESIGN **DS 84** (2016), 1327–1336.

[166] I. Mainville, Y. Arcand, and E. R. Farnworth, *A dynamic model that simulates the human upper gastrointestinal tract for the study of probiotics*, International Journal of Food Microbiology **99** (2005), 287–296.

[167] E. Mann and M. D. Bellin, *Secretion of Insulin in Response to Diet and Hormones*, Pancreapedia (2016), no. 1.

[168] Jim I. Mann, *Nutrition recommendations for the treatment and prevention of type 2 diabetes and the metabolic syndrome: An evidenced-based review*, Nutrition Reviews **64** (2006), no. 9, 422–427.

[169] Thomas E. Marlin, *Process control: designing process and systems for dynamic performance*, 2nd ed., USA, 1995.

[170] O. Marsenic, *Glucose control by the kidney: an emerging target in diabetes*, American Journal of Kidney Diseases **53** (2009), 875–883.

[171] E. B. Mason, *Human physiology*, 1983.

[172] A. Mather and C. Pollock, *Glucose handling by the kidney*, International Society of Nephrology **79** (2011), s1–s6.

[173] P. G. McTernan, A. L. Harte, L. A. Anderson, A. Green, S. A. Smith, J. C. Holder, A. H. Barnett, M. C. Eggo, and S. Kumar, *Insulin and rosiglitazone regulation of lipolysis and lipogenesis in human adipose tissue in vitro*, Diabetes **51** (2002), 1493–1498.

[174] J. J. Meier, *Glp-1 receptor agonists for individualized treatment of type 2 diabetes mellitus*, Nat Rev Endocrinol **8** (2012), no. 12, 728–742.

[175] J. J. Meier, M. A. Nauck, W. E. Schmidt, and B. Gallwitz, *Gastric inhibitory polypeptide: the neglected incretin revisited*, Regulatory Peptides **107** (2002), no. 1, 1 – 13.

[176] P. Mergenthaler, U. Lindauer, G. A. Dienel, and A. Meisel, *Sugar for the brain: the role of glucose in physiological and pathological brain function*, Trends Neuroscience **36** (2014), no. 10, 587–597.

[177] C. Meyer, J. M. Dostou, and J. E. Gerich, *Role of the human kidney in glucose counterregulation*, Diabetes **48** (1999), 943–948.

[178] C. Meyer, J. M. Dostou, S. L. Welle, and J. E. Gerich, *Role of human liver, kidney, and skeletal muscle in postprandial glucose homeostasis*, American Journal of Physiology-Endocrinology and Metabolism **282** (2002), no. 2, E419–E427.

[179] T. Miller, *Explanation in Artificial Intelligence: Insights from the Social Sciences*, (2017).

[180] T. B. Miller and J. Larner, *Mechanism of control of hepatic glycogenesis by insulin*, Journal of Biological Chemistry **248** (1973), no. 10, 3483–3488.

[181] C. Molnar, *Interpretable machine learning a guide for making black box models explainable*, Creative Commons Attribution-NonCommercial-ShareAlike 4.0 International License., 2018.

[182] M. Monsalve V. and L. Jiménez G., *Modelo semifísico del rol del hígado en la homeostasis de la glucosa*, Memorias 26^o Congreso de la Asociación Argentina de Control Automático - AADECA. Buenos Aires (2018).

[183] K. Mori, M. Emoto, K. Motoyama, E. Lee, S. Yamada, T. Morioka, Y. Imanishi, T. Shoji, and M. Inaba, *Undercarboxylated osteocalcin does not correlate with insulin resistance as assessed by euglycemic hyperinsulinemic clamp technique in patients with type 2 diabetes mellitus*, Diabetology & Metabolic Syndrome **4** (2012), no. 1, 53.

[184] D. A. Muñoz, S. Taborda, and H. Alvarez, *A Phenomenological-Based Semiphysical Model for Hydrocyclones*, Proceedings of the World Congress on Mechanical, Chemical, and Material Engineering (MCM 2015) (2015), no. 348, 1–8.

[185] R. Muñoz-Tamayo, J. de Groot, E. Bakx, P. A. Wierenga, H. Gruppen, M. H. Zwietering, and L. Sijtsma, *Hydrolysis of β-casein by the cell-envelope-located PI-type protease of Lactococcus lactis: A modelling approach*, International Dairy Journal **21** (2011), no. 10, 755–762.

[186] R. Muñoz-Tamayo, L. Puillet, J. B. Daniel, D. Sauvant, O. Martin, M. Taghipoor, and P. Blavy, *Review: To be or not to be an identifiable model. Is this a relevant question in animal science modelling?*, Animal (2017), 1–12.

[187] R. Murphy, S. Ellard, and A.T. Hattersley, *Clinical implications of a molecular genetic classification of monogenic beta-cell diabetes*, Natur Clin Pract Endocrinol Metab **4** (2008), 200–213.

[188] D.N.P. Murthy and E.Y. Rodin, *A comparative evaluation of books on mathematical modelling*, Mathematical Modelling **9** (1987), no. 1, 17 – 28.

[189] M.A. Nauck, E. Homberger, E.G. Siegel, R.C. Allen, R.P. Eaton, R. Ebert, and W. Creutzfeldt, *Incretin effects of increasing glucose loads in man calculated from venous insulin and c-peptide responses**, The Journal of Clinical Endocrinology Metabolism **63** (1986), no. 2, 492–498.

[190] E. Nyman, *Hierarchical modeling of diabetes - a pilot study*, 2009.

[191] S. Ochoa, *Plantwide Optimizing Control for the continuous Bio-Ethanol Production Process*, 2010.

[192] F. A. Ortega Quintana, H. Alvarez, and H. Botero Castro, *Facing bioprocess modeling: a review of the methodologies of modeling*, ION, Investigación, Optimización y Nuevos procesos en Ingeniería **30** (2017), no. 1, 74.

[193] J. Ottesen, M. Olufsen, and J. Larsen, *Applied mathematical models in human physiology*, Society for Industrial and Applied Mathematics, 2004.

[194] M. J. Pagliassotti and A. D. Cherrington, *Regulation of net hepatic glucose uptake in vivo*, Annual Review of Physiology **54** (1992), no. 1, 847–860, PMID: 1562194.

[195] S. Pal and V. Elli, *The acute effects of four protein meals on insulin, glucose, appetite and energy intake in lean men*, British Journal of Nutrition **104** (2010), no. 8, 1241–1248.

[196] J. Parada and JM. Aguilera, *Food Microstructure Affects the Bioavailability of Several Nutrients*, Food Science **72** (2007), no. 2, 21–32.

[197] G. Pehling, P. Tessari, J. E. Gerich, M. W. Haymond, F. J. Service, and R. A. Rizza, *Abnormal meal carbohydrate disposition in insulin-dependent diabetes. Relative contributions of endogenous glucose production and initial splanchnic uptake and effect of intensive insulin therapy*, Journal of Clinical Investigation **74** (1984), no. 3, 985–991.

[198] M. J. Perley and D. M. Kipnis, *Plasma insulin responses to oral and intravenous glucose: Studies in normal and diabetic subjects*, The Journal of Clinical Investigation **46** (1967), no. 12, 1954–1962.

[199] M. C. Petersen, D. F. Vatner, and G. I. Shulman, *Regulation of hepatic glucose metabolism in health and disease*, Nature Reviews Endocrinology **13** (2017), no. 10, 572–587.

[200] A. G. Pittas, S. S. Harris, P. C. Stark, and B. Dawson-Hughes, *The effects of calcium and vitamin d supplementation on blood glucose and markers of inflammation in nondiabetic adults*, Diabetes Care **30** (2007), no. 4, 980–986.

[201] A.G. Pittas, J. Lau, F.B. Hu, and B. Dawson-Hughes, *The role of vitamin d and calcium in type 2 diabetes. a systematic review and meta-analysis*, Journal of Clinical Endocrinology Metabolism **92** (2007), 2017–2029.

[202] H. Pohjanpalo, *System identifiability based on the power series expansion of the solution*, Mathematical Biosciences **41** (1978), no. 1, 21 – 33.

[203] C. Postic, R. Dentin, and J. Girard, *Role of the liver in the control of carbohydrate and lipid homeostasis*, Diabetes & Metabolism **30** (2004), no. 5, 398 – 408.

[204] F. Poursabzi-Sangdeh, D. G. Goldstein, J. M. Hofman, J. Wortman Vaughan, and H. Wallach, *Manipulating and Measuring Model Interpretability*, 31st Conference on Neural Information Processing Systems - Nips (2018), 89–93.

[205] Cambridge University Press, *Cambridge Dictionary*, 4th ed., 2013.

[206] L. Pronzalo and E. Walter, *Identification of parametric models from experimental data*, Springer Berlin Heidelberg, Paris, Milan, Barcelona, 1997.

[207] E. Puertollano, S. Kolida, and P. Yaqoob, *Biological significance of short-chain fatty acid metabolism by the intestinal microbiome.*, Curr Opin Clin Nutr Metab Care **17** (2014), no. 2, 139–144.

[208] A. Quarteroni, A. Manzoni, and C. Vergara, *The Cardiovascular System: Mathematical Modeling, Numerical Algorithms, Clinical Applications*, MOX-Report (2016), no. 38, 213.

[209] I. Ramirez-Zuniga, J. E. Rubin, D. Swigon, and G. Clermont, *Mathematical modeling of energy consumption in the acute inflammatory response*, Journal of Theoretical Biology **460** (2019), 101–114.

[210] G. Pandu Rangaiah and V. Kariwala, *Plantwide control : recent developments and applications*, first ed., Wiley, 2012.

[211] M. B. Reddy, R. S. H. Yang, H. J. Clewell III, and M. E. Andersen, *Physiologically based pharmacokinetic modeling: Science and applications*, 2005.

[212] G.T. Reeves and S.E. Fraser, *Biological systems from an engineer's point of view*, PLOS Biology **7** (2009), no. 1, 32–35.

[213] M. T. Ribeiro, S. Singh, and C. Guestrin, *"Why Should I Trust You?": Explaining the Predictions of Any Classifier*, (2016).

[214] G. Ridgeway, D. Madigan, T. Richardson, and J. O'Kane, *Interpretable Boosted Naïve Bayes Classification*, the 4th International Conference on Knowledge Discovery and Data Mining (KDD-1998) (1998), 101–104.

[215] U. Risérus, W. C. Willett, and F. B. Hu, *Dietary fats and prevention of type 2 diabetes*, Progress in lipid research **48** (2010), no. 1, 44–51.

[216] R. Roche, R. Lamanna, M. Delgado, F. Rocaries, Y. Hamam, and F. Pecker, *Simulation of a cardiac cell. Part I: an electro-chemical model*, Revista de la Facultad de Ingeniería Universidad Central de Venezuela **24** (2009), no. 1, 71–87.

[217] P. V. Röder, K. E. Geillinger, T. S. Zietek, B. Thorens, and H. Koepsell, *The role of sglt1 and glut2 in intestinal glucose transport and sensing*, Plos One **9** (2014), e89977.

[218] P. V. Röder, B. Wu, Y. Liu, and W. Han, *Pancreatic regulation of glucose homeostasis*, Experimental & molecular medicine **48** (2016), no. November 2015, e219.

[219] M. P. Saccomani and C. Cobelli, *A minimal input-output configuration for a priori identifiability of a compartmental model of leucine metabolism*, IEEE Transactions Biomedical Engineering **40** (1993), 797–803.

[220] G. Sachs, N. Zeng, and C. Prinz, *Physiology of isolated gastric endocrine cells*, Annual Review of Physiology **59** (1997), no. 1, 243–256.

[221] K. S. Saladin, *Anatomy & physiology: The unity of form and function*, 2nd ed., 2001.

[222] H. Sato, T. Terasaki, H. Mizuguchi, K. Okumura, and A. Tsuji, *Receptor-recycling model of clearance and distribution of insulin in the perfused mouse liver*, Diabetologia **34** (1991), no. 9, 613–621.

[223] August-Wilhelm Scheer, *Aris - business process modeling*, 3 ed., Springer, 2000.

[224] A.C. Schoolwerth, B.C. Smith, and R.M. Culpepper, *Renal gluconeogenesis*, Mineral and Electrolyte Metabolism **14** (1988), 347–361.

[225] K. Schulze, *Imaging and modelling of digestion in the stomach and the duodenum*, Neurogastroenterology and Motility **18** (2006), no. 3, 172–183.

[226] L. Schwingshackl, B. Strasser, and G. Hoffmann, *Effects of monounsaturated fatty acids on glycaemic control in patients with abnormal glucose metabolism: A systematic review and meta-analysis*, Annals of Nutrition and Metabolism **58** (2011), no. 4, 290–296.

[227] I. Sgouralis and A. T. Layton, *HHS Public Access*, Mathematical Biosciences **264** (2015), 8–20.

[228] Muhammad Z. Shrayyef and J.E. Gerich, *Principles of diabetes mellitus*, ch. 2, pp. 19–35, Springer Verlag, 2010.

[229] A. P. Sinha and H. Zhao, *Incorporating domain knowledge into data mining classifiers: An application in indirect lending*, Decision Support Systems **46** (2008), no. 1, 287 – 299.

[230] Irwin W. Sizer, *Effects of temperature on enzyme kinetics*, ch. 2, pp. 35–62, John Wiley & Sons, Ltd, 2006.

[231] S. Skogestad, *Plantwide control: Towards a systematic procedure*, Computer Aided Chemical Engineering, vol. 10, Elsevier, 2002.

[232] Y. Song, K. He, E. B. Levitan, J. E. Manson, and S. Liu, *Effects of oral magnesium supplementation on glycaemic control in type 2 diabetes: a meta-analysis of randomized double-blind controlled trials*, Diabetic Medicine **23** (2006), no. 10, 1050–1056.

[233] J. T. Sorensen, *A Phisiologic Model of Glucose Metabolism in Man and its use to Design and Assess Improved Insulin Therapies for Diabetes*, 1985.

[234] M. Stumvoll, U. Chintalapudi, G. Perriello, S. Welle, O. Gutierrez, and J. Gerich, *Uptake and release of glucose by the human kidney. postabsorptive rates and responses to epinephrine.*, The Journal of Clinical Investigation **96** (1995), no. 5, 2528–2533.

[235] M. Stumvoll, C. Meyer, A. Mitrakou, V. Nadkarni, and J. E. Gerich, *Renal glucose production and utilization: New aspects in humans*, Diabetologia **40** (1997), no. 7, 749–757.

[236] William R. Swartout, *Rule-based expert systems: The mycin experiments of the stanford heuristic programming project: B.g. buchanan and e.h.*, Artificial Intelligence **26** (1985), no. 3, 364 – 366.

[237] N.A. Syed and R. L. Khandelwal, *Reciprocal regulation of glycogen phosphorylase and glycogen synthase by insulin involving phosphatidylinositol-3 kinase and protein phosphatase-1 in hepg2 cells*, Mol Cell Biochem **211** (2000), 123–136.

[238] A. K. Thompson, A. M. Minihane, and C. M. Williams, *Trans fatty acids, insulin resistance and diabetes*, European Journal of Clinical Nutrition **65** (2011), no. 5, 553–564.

[239] L.M.M. Tijskens, M.L.A.T.M. Hertog, and B.M. Nicolaï, *Food process modelling. front matter*, Woodhead Publishing Series in Food Science, Technology and Nutrition, Inglaterra, 2001.

[240] K. Tokuyama, S. Nagasaka, S. Mori, N. Takahashi, I. Kusaka, A. Kiyonaga, H. Tanaka, M. Shindo, and S. Ishibashi, *Hepatic Insulin Sensitivity Assessed by Integrated Model of Hepatic and Peripheral Glucose Regulation*, Diabetes technology & therapeutics **11** (2009), no. 8.

[241] G. J. Tortora and B. H. Derrickson, *Principles of anatomy and physiology*, 14th ed., 2013.

[242] C. L Triplitt, *Understanding the kidneys' role in blood glucose regulation*, Am J Manag Care **18** (2012), no. 1 Suppl, S11–6.

[243] C. Uluseker, C. Priami, A. Matone, G. Simoni, L. Marchetti, and M. Dauriz, *A closed-loop multi-level model of glucose homeostasis*, Plos One (2018), 1–23.

[244] S. Vajda, K. R. Godfrey, and H. Rabitz, *Similarity transformation approach to identifiability analysis of nonlinear compartmental models*, Mathematical Biosciences **93** (1989), no. 2, 217 – 248.

[245] L. M. Vargas-Villamil and Tedeschi L. O., *Potential integration of multi-fitting, inverse problem and mechanistic modelling approaches to applied research in animal science: a review*, Animal Production Science **54** (2014), 1905–1913.

[246] S. L. Volpe, *Magnesium, the metabolic syndrome, insulin resistance, and type 2 diabetes mellitus*, Critical Reviews in Food Science and Nutrition **48** (2008), no. 3, 293–300.

[247] E. Walter, I. Braems, L. Jaulin, and M. Kieffer, *Guaranteed numerical computation as an alternative to computer algebra for testing models for identifiability*, (1986).

[248] E. Walter and Y. Lecourtier, *Global approaches to identifiability testing for linear and nonlinear state space models*, Mathematics and Computers in Simulation **24** (1982), no. 6, 472 – 482.

[249] P.E. Walton and T.D. Etherton, *Stimulation of lipogenesis by insulin in swine adipose tissue: antagonism by porcine growth hormone*, Journal of Animal Science **62** (1986), 1584–1595.

[250] D. A. Waterman, *A guide to expert systems*, Teknowledge series in knowledge engineering, Addison-Wesley, 1986.

[251] D. I. Weiner and J. W. Verlander, *Renal ammonia metabolism and transport*, Comprehensive Physiology **3** (2013), 201–220.

[252] N. Wierup, H. Svensson, H Mulder, and F. Sundler, *The ghrelin cell: a novel developmentally regulated islet cell in the human pancreas*, Regul Pept. **107** (2002), no. 1-3, 63–69.

[253] John P.H. Wilding, *The role of the kidneys in glucose homeostasis in type 2 diabetes: Clinical implications and therapeutic significance through sodium glucose cotransporter 2 inhibitors*, Metabolism: Clinical and Experimental **63** (2014), no. 10, 1228–1237.

[254] G. Wirthensohn and W. G. Guder, *Renal Substrate Metabolism*, Physiological reviews **66** (1986), no. 2, 469–497.

[255] J. M. W. Wong and D. J. A. Jenkins, *Carbohydrate Digestibility and Metabolic Effects*, The Journal of Nutrition **137** (2007), no. 4, 2539S–2546S.

[256] H. A. Woods and J. K. Wilson, *An information hypothesis for the evolution of homeostasis*, Trends Ecology and Evolution **28** (2013), 283–289.

[257] R. L. Woods and K. L. Lawrence, *Modeling and simulation of dynamic systems*, 1st ed., USA, 1997.

[258] X. Xia and C. H. Moog, *Identifiability of nonlinear systems with application to hiv/aids models*, IEEE Transactions on Automatic Control **48** (2003), no. 2, 330–336.

[259] W. You and M. Henneberg, *Type 1 diabetes prevalence increasing globally and regionally: the role of natural selection and life expectancy at birth*, BMJ Open Diabetes Research and Care **4** (2016), no. 1.

[260] B. Zeigler, T. Kim, and H. Praehofer, *Theory of modeling and simulation*, Academic Press, 2000.

[261] M. Zhou, X. Ma, H. Li, X. Pan, J. Tang, Y. Gao, X. Hou, H. Lu, Y. Bao, and Jia W., *Serum osteocalcin concentrations in relation to glucose and lipid metabolism in chinese individuals*, European Journal of Endocrinology **161** (2009), no. 5, 723 – 729.

[262] M. Zimmerman and B. Snow, *An Introduction to Nutrition*, Creative Commons, 2012.

[263] A. Zisman, O.D. Peroni, E.D. Abel, M.D. Michael, F. Mauvais-Jarvis, B.B. Lowell, J.F. Wojtaszewski, M.F. Hirshman, A. Virkamaki, L.J. Goodyear, C.R. Kahn, and B.B. Kahn, *Targeted disruption of the glucose transporter 4 selectively in muscle causes insulin resistance and glucose intolerance*, Nat Med. **6** (2000), no. 8, 924–8.